71-23,709

BRENNER, Rolf Peter, 1937-
HYDROLOGIC MODEL STUDY OF A FORESTED AND A CUTOVER SLOPE.

The University of Michigan, Ph.D., 1971
Engineering, civil

University Microfilms, A XEROX Company, Ann Arbor, Michigan

THIS DISSERTATION HAS BEEN MICROFILMED EXACTLY AS RECEIVED

HYDROLOGIC MODEL STUDY OF A FORESTED AND A CUTOVER SLOPE

by

Rolf Peter Brenner

A dissertation submitted in partial fulfillment
of the requirements for the degree of
Doctor of Philosophy
(Civil Engineering)
in The University of Michigan
1971

Doctoral Committee:

Associate Professor Donald H. Gray, Chairman
Professor Ernest F. Brater
Professor Frank E. Richart, Jr.
Associate Professor Alan S. Wineman
Professor Robert Zahner

ABSTRACT

HYDROLOGIC MODEL STUDY OF A FORESTED
AND A CUTOVER SLOPE

by

Rolf Peter Brenner

Chairman: Donald H. Gray

The water potential in a slope is a key parameter in assessing the stability of natural slopes, since it directly influences the mechanical properties of the soil involved (i.e. shear strength and creep behavior). This work is an attempt to analyze and predict the effect of vegetation removal on the hydrologic regime or soil water potential in steep slopes. Vegetation in a watershed, in particular large forest trees, has a significant influence on the water regime in the soil mantle, since trees deplete soil moisture through the process of transpiration. It can therefore be postulated that a forest cover enhances slope stability by favorably affecting the soil water regime.

In view of the complexity of the problem, a considerable effort was devoted to a thorough screening and synthesizing of the available literature which usually deals only with limited aspects of the problem.

The problem was approached by an experimental model study, set up in a greenhouse. A tilting soil bin (12 feet long, 3 feet wide and with a soil depth of 10 inches) positioned at different slope angles, simulated a soil layer overlying impervious bedrock (no water table at the toe of the slope). A forest cover was modelled by a number of

small trees (Populus deltoides). The soil used was a clay loam. The response of the soil water potential to simulated rain storms was studied first for the forested- and later for the cutover slope at various slope angles. Transpiration in the greenhouse was measured by separately potted trees of the same kind.

The results showed that a forest cover accelerates the soil moisture depletion in a shallow soil mantle regardless of the steepness of the slope. For a storm of given intensity and duration; therefore, the recharge phase for the clear-cut slope was much shorter than for the forested one. The slope angle is only responsible for the distribution of recharge and the initial hydrologic conditions when drainage has ceased. During the drainage phase the flow in the slope is two-dimensional, whereas it is essentially one-dimensional (i.e. vertical upwards) after field capacity has been reached. At this point the matric suction increases exponentially with time for suctions within the tensiometer range. Within this same range water loss from any point in the soil took place at a constant rate. This result is consistent with field observations. The presence of vegetation contributes to an increase in the rate of depletion.

The measurement of the transpirative power in the greenhouse by means of phytometers yielded satisfactory results.

The model study proved to be suitable for qualitative investigations in forest microhydrology. It is, however, suggested that future studies should be carried out using larger models in order to obtain a better idea about the moisture

distribution in deeper soil profiles. It would also be desirable to extend the range of suction measurements.

The governing equations and boundary conditions of a mathematical model for the soil water potential in a forested slope are derived based on the flow equation and using information on evapotranspiration and water uptake by root systems.

To

MY MOTHER

ACKNOWLEDGMENTS

The author wishes to express his sincere gratitude to Professor Donald H. Gray, Chairman of the Doctoral Committee, under whose direction and guidance this thesis was completed. The writer also extends his appreciation to Professor Robert Zahner for his helpful suggestions and comments as well as to the other committee members for their interest in this work.

Special thanks are due to all the individuals who helped construct the experimental facilities, in particular to Harold G. (Bud) Chalmers. The author is also indebted to John Ludwig, Senior Research Gardener at The University of Michigan Botanical Gardens for his assistance in vegetation maintenance in the greenhouse.

This work was made possible by Research Grant No. GK-2377 from the National Science Foundation. The author is also grateful for the financial assistance he received during his studies from The University of Michigan.

CONTENTS

LIST OF APPENDICES . . . . . .

LIST OF TABLES . . . . . .

LIST OF FIGURES . . . . . .

NOTATION . . . . . .

Chapter Page

1. INTRODUCTION AND SCOPE OF STUDY 1

1. Reasons for Study 1

2. Some Alternative Approaches to Problem 6

3. Scope and Objectives of Present Study 9

2. THEORETICAL TOOLS AND DEFINITIONS 11

1. The State of Water in Soils 11

a. Some Properties of Water and the Chemical Potential 11
b. Units 15
c. Hysteresis 16
d. Field Capacity and Wilting Percentage 19

2. Flow of Water in Soils 20

3. The Influence of Vegetation 26

a. Basic Anatomy of Plants (in particular Woody Plants) 27
Roots 27
Stems 30
Leaves 31

Chapter | Page

b. Plant Water Potentials 32
c. Transport of Water through the Plant 34
Water Absorption by Roots. 34
Water Movement through the Vascular System in the Stem 36
Water Movement in the Leaf and Transpiration 38
The Overall Flow of Water from the Soil through the Plant 40

4. Influence of Climate 43

a. Solar Radiation and Energy Balance 43
b. Evapotranspiration 46

5. The Water Balance and the Hydrologic Cycle on a Forested Slope 51

3. REVIEW OF THE LITERATURE 54

1. Introduction 54

2. Effect of Clear-Cutting on Watershed Behavior . 55

a. Effect on Water Yield 56
b. Effect on Water Temperature 59
c. Effect on Nutrient Cycling 60
d. Effect on the Deep Seated Stability of Slopes 60

3. Studies of Flow through Porous Media without Considering the Influence of Vegetation 62

4. Studies of Soil-Water-Plant-Atmosphere Interactions 77

5. Field Measurements of Soil Moisture Regimes under Forested and Barren Areas 98

6. Soil Moisture and Water Outflow Measurements in a Sloping Soil Mass without Vegetation 114

7. Discussion and Summary 115

Chapter		Page
4.	AN EXPERIMENTAL MODEL STUDY OF A FORESTED AND A CLEAR-CUT SLOPE	118
	1. Experimental Set-up	118
	a. Model Slope and Soil Mantle	118
	b. Stability Check on Soil Mantle	127
	c. Rainfall Simulation	130
	2. Instrumentation and Equipment	130
	a. Tensiometers and Piezometers	130
	b. Determination of Rainfall	135
	c. Radiation, Temperature and Relative Humidity	137
	d. Vegetation Maintenance, Leaf Water Potential, and Transpiration Measurements	138
	3. Test Program	142
	4. In-situ Properties of Soil in Bin	148
	a. Density Tests	149
	b. Soil Moisture Retention	150
	c. Hydraulic Conductivity	155
5.	RESULTS FROM EXPERIMENTAL MODEL STUDY AND DISCUSSION	159
	1. Results from Test Series A (Test Nos. 1 to 18)	159
	2. Results of Transpiration Experiments	181
	3. Results from Test Series B (Test Nos. A, B, C, D)	195
	4. Discussion of the Results	198
	5. Conclusions from the Model Study and Suggestions for Further Research	203

Chapter

6 PROPOSAL FOR A MATHEMATICAL MODEL OF A FORESTED SLOPE 207

APPENDICES 220

REFERENCES 244

LIST OF APPENDICES

		Page
APPENDIX A	UNITS AND PHYSICAL DIMENSIONS OF WATER POTENTIALS AND OTHER RELEVANT QUANTITIES	220
APPENDIX B	FLOW THROUGH POROUS MEDIA	224
	1. Darcy's Law	224
	2. Equation of Continuity	225
	3. The Flow Equation	228
APPENDIX C	WATER CONTENT-DENSITY RELATIONS	231
	1. Relation Between Water Content by Weight and Water Content by Volume.	231
	2. Water Content-Density Relationships.	232
APPENDIX D	SOIL MOISTURE MEASUREMENTS WITH TENSIOMETERS	234
	1. Hydraulic Head Measurements with Tensiometers	234
	2. Response Time	239

LIST OF TABLES

Table		Page
3.1	Review of Treated Steady-State, Unsaturated Isothermal Flow Problems.	64
3.2	Review of Treated Unsteady, Unsaturated Flow Problems under a Hydraulic Gradient	66
3.3	Review of Some Problems on Soil-Water-Plant Relationships	80
4.1	Summary of Soil Properties	122
4.2	Relation between Tensiometer Reading and Moisture Content in Bin	152
5.1.a	Test Series A: Rain, Drainage + Runoff and Tensiometer Readings on a Forested Slope	160
5.1.b	Test Series A: Rain, Drainage + Runoff and Tensiometer Readings on a Clear-Cut Slope	161
5.2	Summary of Test Data, Test Series A	171
5.3	Water Balance for Test Series A	178
5.4	Tree Data at Time of Clear-Cutting (30/31 December, 1969)	182
5.5	Transpiration of Potted Trees I	183
5.6	Transpiration of Potted Trees II	184
5.7	Leaf Surface of Potted Trees	187
5.8	Pertinent Data of Potted Trees at the End of Test Series A	193
5.9	Relation between Surface Area and Weight of Leaves	194
A.1	Relation between Pressure Units	223

LIST OF FIGURES

Figure		Page
1.1	Interrelationships between the Major Components of a Watershed with Respect to Water	3
1.2	Idealized Representation of Soil Moisture Cycle in Forested and Clear-Cut Areas (after Bethlahmy, 1962 and Gray, 1971)	5
2.1	Schematic Representation of Suction Terms (from L. A. Richards, 1965)	17
2.2	Hysteresis of Soil Moisture	21
2.3	Water Retention Curves for Different Soils	21
2.4	Moving Boundary and Continuous Flow Theory	26
2.5	Diagrammatic Cross Section of a Leaf with Vein (after Northen, 1968)	28
2.6	Diagrammatic Cross Section of a Woody Stem	28
2.7	Diagram of a Portion of a Root as Seen in Cross Section in the Root Hair Region (after Esau, 1953)	29
2.8	Longitudinal Section through a Root Tip (after Kramer, 1969)	29
2.9	Pathways of Water from the Soil to the Atmosphere .	41
2.10	Daytime Radiation Balance	45
2.11	Energy Balance (after Tanner, 1968)	45
2.12	Idealized Slope and the Factors Affecting Its Water Regime	53

Figure		Page
3.1	Schematic Representation of the Relation between Transpiration Rate and Leaf Water Potential	91
3.2	Relation between Actual Daily Transpiration Rate and Soil Water Potential ψ_{soil} for Three Different Rates (Low, Intermediate and High) of Potential Transpiration with a Crop of Intermediate Root Density (after Cowan, 1965)	95
3.3	Relation between Actual Daily Transpiration Rate and Soil Water Potential ψ_{soil} for Different Root Densities (after Cowan, 1965)	95
3.4	Soil Moisture Regime in a Pine Plantation, a Barren Area, and a Broomsedge Field for the 0 to 66-Inch Depth of Soil (1952) (after Metz and Douglass, 1959)	102
3.5	Soil Moisture Depletion of the 30- to 66-Inch Zone of a Pine Plantation, a Broomsedge Field, and a Barren Plot (after Metz and Douglass, 1959)....	103
3.6	Soil Moisture Depletion of the 0 to 66-Inch Zone of a Pine Plantation, a Broomsedge Field, and a Barren Plot (after Metz and Douglass, 1959)	103
3.7	Average Matric Potential by Depth in Mountain and Piedmont Plots (after Patric et al., 1965)	106
3.8	Comparable Portions of Depletion Curves for Total Soil Moisture Content of Pinus coulteri Lysimeter Adjusted to the Same Initial Time (after Zinke, 1959)	111
3.9	Comparable Portions of Depletion Curves for Total Soil Moisture Content of Barren Lysimeter Adjusted to the Same Initial Time (from Data by Zinke, 1959)	111
3.10	Lysimeter Soil Moisture Depletion at Various Soil Depths under Pinus coulteri Beginning May 1, 1952 (after Zinke, 1959)	113

Figure		Page
3.11	Soil Moisture Depletion at Various Soil Depths in the Barren Lysimeter Beginning May 1, 1952 (after Zinke, 1959)	113
4.1	Side View of Tilting Soil Bin at a Slope of 30 Degrees	120
4.2	Rear View of Tilting Soil Bin at a Slope of 30 Degrees	121
4.3	Grain Size Distribution of Artificial Clay Loam	123
4.4	Tree Arrangement and Instrumentation	126
4.5	Longitudinal Soil Profile in Bin	127
4.6		
4.6	Sprinkler System	131
4.7	Bin Instrumentation: Tensiometers and Raingages	134
4.8	Tree Status Map	140
4.9	History of Test Series A (October 14, 1969 - February 26, 1970)	143
4.10	Arrangement of Tensiometers for Test Series B	147
4.11	Relation between Moisture Content and Tensiometer Reading	154
4.12	Soil Water Retention Curve, Determined from Pressure Plate Tests (Drying Cycle)	156
4.13	Relation between Water Content and the Logarithm of Matric Suction Determined from Pressure Plate Tests	157
5.1.a	Matric Suction during the Recharge and Depletion Phase for Tensiometer No. 10 and a Slope Angle of 10 Degrees	162
5.1.b	Matric Suction during the Recharge and Depletion Phase for Tensiometer No. 10 and a Slope Angle of 20 Degrees	163

Figure		Page
5.1.c	Matric Suction during the Recharge and Depletion Phase for Tensiometer No. 10 and a Slope Angle of 30 Degrees	164
5.2	Typical Storm Diagram Showing Rain, Drainage + Runoff (Test No. 14)	166
5.3.a	Matric Suction on a Slope of 10 Degrees, 165 Hours after End of Storm	168
5.3.b	Matric Suction on a Slope of 20 Degrees, 165 Hours after End of Storm	169
5.3.c	Matric Suction on a Slope of 30 Degrees, 165 Hours after End of Storm	170
5.4.a	Logarithm of Suction versus Time for a Slope of 10 Degrees	172
5.4.b	Logarithm of Suction versus Time for a Slope of 20 Degrees	173
5.4.c	Logarithm of Suction versus Time for a Slope of 30 Degrees	174
5.5	Determination of Evapotranspiration of the Bin by the Water Balance Method	177
5.6	Leaf Area and Weekly Transpiration from Potted Trees	186
5.7	Weekly Transpiration per Unit Leaf Area of Potted Trees and Hours of Sunshine	189
5.8	Daily and Weekly Averages of Temperature and Relative Humidity; Weekly Transpiration per Unit Leaf Area of Potted Trees, Test Series A	190
5.9	Logarithm of Suction versus Time for Tensiometers 9 to 15, Test Series B	196
5.10	Suction Gradients in a Slope as a Function of Time and Slope Angle	197

Figure		Page
5.11	Test Series B: Watertable, Positions 2, 3, 4 and 6 Hours after Beginning of Storm for a Slope of 10 Degrees and 30 Degrees	199
6 1	Model of a Vegetated Slope	209
B.1	Derivation of the Equation of Continuity	226
C.1	Idealized Three-phase Soil System	231
D.1	Essential Parts of a Tensiometer and Principles of Measuring Hydraulic Heads	235

NOTATION

(The expression within the square brackets indicates the dimension in the mks-system)

A	=	a constant (ordinate intercept of log suction vs. time relationship)
A_1	=	a constant
Ar_i	=	leaf area of pot no. i $[m^2]$
B	=	a constant (depending on the geometry of the root system) $[kg \cdot m^{-2} \cdot sec^{-2}]$
C	=	soil water capacity $[m^{-1}]$
CI	=	crown interception $[m]$
D	=	soil water diffusivity $[m^2 \cdot sec^{-1}]$
Dr	=	seepage outflow, drainage $[m]$ or $[m^3]$
E	=	evapotranspiration rate $[m \cdot sec^{-1}]$, also $[kg \cdot m^{-2} \cdot sec^{-1}]$
E'	=	evapotranspiration during a time t that includes interception $[m]$
E_a	=	actual evapotranspiration rate $[m \cdot sec^{-1}]$
E_I	=	evaporation of intercepted water $[m \cdot sec^{-1}]$
E_p	=	potential evapotranspiration rate $[m \cdot sec^{-1}]$
E_s	=	evaporation rate $[m \cdot sec^{-1}]$
E_s'	=	evaporation $[m]$
F	=	factor of safety

FI	=	forest floor interception [m]
G_F	=	sensible heat flux into ground $[kg \cdot sec^{-3}] = [Watt \cdot m^{-2}]$
G_s	=	specific gravity of soil solids
H	=	hydraulic head [m]
H_L	=	latent heat flux density $[kg \cdot sec^{-3}] = [Watt \cdot m^{-2}]$
H_S	=	sensible heat flux into air $[kg \cdot sec^{-3}] = [Watt \cdot m^{-2}]$
I	=	interception [m]
K	=	hydraulic conductivity $[m \cdot sec^{-1}]$
K_s	=	saturated hydraulic conductivity $[m \cdot sec^{-1}]$
K_c	=	cup conductance of a tensiometer $[kg^{-1} \cdot m^4 \cdot sec]$
K_p	=	coefficient in Darcy's equation when written in terms of volumetric potentials $[kg^{-1} \cdot m^3 \cdot sec]$
L	=	effective root density (effective length of root system per unit volume) $[m^{-2}]$
M	=	miscellaneous fluxes $[kg \cdot sec^{-3}]$
Ov	=	overland flow (surface runoff) [m] or $[m^3]$
P	=	pressure $[kg \cdot m^{-1} \cdot sec^{-2}]$
Pr	=	precipitation rate $[m \cdot sec^{-1}]$
Pr'	=	precipitation [m]
Q	=	total water uptake per unit cross-sectional area $[m \cdot sec^{-1}]$
$\overline{Q}$	=	outflow rate from a soil mass $[m^3 \cdot sec^{-1}]$
Q_f	=	flux through soil surface $[m \cdot sec^{-1}]$
Q_n	=	net precipitation on forest floor [m]
Q_s	=	stemflow [m]

Q_t = throughfall [m]

Q_i = infiltrating water [m]

Q_{sm} = total soil moisture in a soil profile [m]

R = gas constant $[kg \cdot m^2 \cdot sec^{-2} \cdot deg^{-1} \cdot mole^{-1}]$

R_L = net long wave flux $[kg \cdot sec^{-3}] = [Watt \cdot m^{-2}]$

R_N = net radiation flux $[kg \cdot sec^{-3}]$

R_s = direct and diffuse solar radiation $[kg \cdot sec^{-3}]$

R_t = thermal radiation $[kg \cdot sec^{-3}]$

S_g = gage sensitivity $[kg \cdot m^{-4} \cdot sec^{-2}]$

ST = soil texture

St = storage [m] or $[m^3]$ or [kg]

T = absolute temperature [deg]

Tr = transpiration rate $[m \cdot sec^{-1}]$ or $[kg \cdot m^{-2} \cdot sec^{-1}]$

Tr' = transpiration [m]

Tr_p = potential transpiration rate $[m \cdot sec^{-1}]$

Tr^o = maximum transpiration rate without wilting under wet conditions $[m \cdot sec^{-1}]$

Tr_{ti} = transpiration of pot no. i [kg]

$\overline{Tr}_t$ = transpiration per unit leaf area normalized

V = volume, bulk volume of soil $[m^3]$

V_i = volume of i^{th} section in bin $[m^3]$

V_w = volume of water in soil $[m^3]$

$\overline{V}_w$ = partial molal volume of water $[m^3 \cdot mole^{-1}]$

V_a = volume of air in soil $[m^3]$

V_s = volume of solids $[m^3]$

V_{tot} = total, bulk volume of soil $[m^3]$

V_v = volume of voids $[m^3]$

W_s = weight of solids $[kg \cdot m \cdot sec^{-2}]$

W_w = weight of water $[kg \cdot m \cdot sec^{-2}]$

W_{tot} = total water content of bin $[kg \cdot m \cdot sec^{-2}]$

a = a constant

a_1, a_1' = a distance

$\bar{a}$ = a constant

a_r = reflection coefficient (radiation), albedo

b = a constant

b_1, b_1' = a distance

$\bar{b}$ = a constant

b_B = width of bin $[m]$

c = water vapor concentration $[kg \cdot m^{-3}]$

c' = cohesion intercept $[kg \cdot m^{-1} \cdot sec^{-2}]$

c_p = specific heat of air $[m^2 \cdot sec^{-2} \cdot deg^{-1}]$ = $[Joule \cdot kg^{-1} \cdot deg^{-1}]$

d_1, d_2 = distance $[m]$

d_B = depth of soil in bin $[m]$

d_r = depth of root zone $[m]$

d_s = depth of soil $[m]$

d_z = zero plane displacement in air $[m]$

e = vapor pressure $[kg \cdot m^{-1} \cdot sec^{-2}]$

e' = void ratio

f_1 = function describing bedrock surface [m]

f_2 = function describing soil surface [m]

f_3 = function describing lower boundary of root zone [m]

g = acceleration of gravity $[m \cdot sec^{-2}]$

h = soil water head [m]

h_p = height of piezometric level in a slope [m]

j = impedance to water flow in soil and plant per unit volume of soil $[kg \cdot m^{-1} \cdot sec^{-1}]$

j_p = impedance to water movement in plant $[kg \cdot m^{-1} \cdot sec^{-1}]$

j_s = impedance to water movement in the soil $[kg \cdot m^{-1} \cdot sec^{-1}]$

k = permeability $[m^2]$ = [Darcy]

k_c = von Karman's constant

l_B = length of bin [m]

m = mass [kg]

$\overline{m}$ = unit mass of water

m_1, m_2 = constants

n = porosity

n_1 = a constant

q = rate of water extraction per unit volume of soil (source term) $[sec^{-1}]$

$\overline{q}$ = volume of water passing through a tensiometer cup $[m^3]$

q_o = surcharge per unit area on a slope $[kg \cdot m^{-1} \cdot sec^{-2}]$

q_w = supply function $[sec^{-1}]$

r	=	radial space coordinate [m]
r	=	resistance $[m^{-1} \cdot sec]$
r_c	=	radius of capillary [m]
s	=	degree of saturation
s_v	=	slope of saturation vapor pressure curve $[kg\ m^{-1} \cdot sec^{-2} deg^{-1}]$
t	=	time [sec]
t_I	=	time during which intercepted water evaporates
t_R	=	response time constant of a tensiometer [sec]
u	=	wind velocity $[m \cdot sec^{-1}]$
v	=	volume flux of water through soil $[m \cdot sec^{-1}]$
$\bar{v}$	=	specific volume of water $[kg^{-1} \cdot m^3]$
w	=	water content by weight
$\bar{w}_i$	=	average water content in a section i in bin
x	=	space coordinate [m]
x_g	=	intersection of upper edge of seepage zone with slope surface [m]
x_w	=	intersection of water level in river with slope surface [m]
y	=	space coordinate [m]
z	=	space coordinate, elevation [m]
$\bar{z}$	=	height above crop surface [m]
z_d	=	water level in a stream with respect to toe of slope [m]
z_s	=	upper end of seepage zone [m]

$\bar{z}_o$ = roughness length [m]

α = a constant (slope of log suction vs. time relationship) [sec^{-1}]

β = a constant

γ = unit weight of totally saturated soil [$kg \cdot m^{-2} \cdot sec^{-2}$]

γ_{dry} = unit weight of dry soil [$kg \cdot m^{-2} \cdot sec^{-2}$]

γ_w = unit weight of water [$kg \cdot m^{-2} \cdot sec^{-2}$]

θ = volumetric water content

κ = depletion coefficient [sec^{-1}]

λ = latent heat of vaporization [$kg \cdot m^{-1} \cdot sec^{-2}$] = [$Joule \cdot m^{-3}$] or [$Joule \cdot kg^{-1}$]

ν = viscosity [$kg \cdot m^{-1} \cdot sec^{-1}$]

ρ_a = density of air [$kg \cdot m^{-3}$]

ρ_v = density of water vapor [$kg \cdot m^{-3}$]

ρ_w = density of water [$kg \cdot m^{-3}$]

σ = surface tension [$kg \cdot sec^{-2}$]

τ = suction [$kg \cdot m^{-1} \cdot sec^{-2}$]

ϕ = angle of internal friction

χ = psychrometric constant [$kg \cdot m^{-1} \cdot sec^{-2} \cdot deg^{-1}$]

ψ = potential, soil water potential in particular [$kg \cdot m^{-1} \cdot sec^{-2}$] or [$m^2 \cdot sec^{-2}$]

ψ_g = gravitational potential [$kg \cdot m^{-1} \cdot sec^{-2}$] or [$m^2 \cdot sec^{-2}$]

ψ_m = matric potential [$kg \cdot m^{-1} \cdot sec^{-2}$] or [$m^2 \cdot sec^{-2}$]

ψ_a = adsorption potential $[kg \cdot m^{-1} \cdot sec^{-2}]$ or $[m^2 \cdot sec^{-2}]$

ψ_c = capillary potential $[kg \cdot m^{-1} \cdot sec^{-2}]$ or $[m^2 \cdot sec^{-2}]$

ψ_{tot} = total soil water potential $[kg \cdot m^{-1} \cdot sec^{-2}]$ or $[m^2 \cdot sec^{-2}]$

ψ_w = potential due to double layer effects $[kg \cdot m^{-1} \cdot sec^{-2}]$ or $[m^2 \cdot sec^{-2}]$

ψ_p = pressure potential $[kg \cdot m^{-1} \cdot sec^{-2}]$ or $[m^2 \cdot sec^{-2}]$

ψ_s = solute or osmotic potential $[kg \cdot m^{-1} \cdot sec^{-2}]$ or $[m^2 \cdot sec^{-2}]$

ψ_{pl} = average water potential in plant tissues $[kg \cdot m^{-1} \cdot sec^{-2}]$ or $[m^2 \cdot sec^{-2}]$

ψ_{leaf} = leaf water potential $[kg \cdot m^{-1} \cdot sec^{-2}]$ or $[m^2 \cdot sec^{-2}]$

$\psi_{leaf_{crit}}$ = critical leaf water potential $[kg \cdot m^{-1} \cdot sec^{-2}]$ or $[m^2 \cdot sec^{-2}]$

π = osmotic pressure $[kg \cdot m^{-1} \cdot sec^{-2}]$

CHAPTER I

INTRODUCTION AND SCOPE OF STUDY

1. Reasons for Study

A forested watershed is a valuable resource which has several important functions. In addition to providing a potential supply of commercial timber, it is also a regulator and source of water, a regulator of microclimate, a wildlife habitat, and a nutrient cycling system. Vegetation clearly plays an important role in all of these watershed functions. Too often vegetation removal proceeds without due consideration of its secondary and tertiary impacts. Commercial logging operations on steep slopes, for example, are likely to have considerable impact on water yield and mass wasting in a watershed. It is only recently, however, that these problems have received the attention of research workers in various disciplines. This thesis is an attempt to analyze and predict the effect of vegetation removal on the hydrological regime in steep slopes and, indirectly, on their stability as well.

A watershed represents a complex ecosystem whose main components are climate, topography, geology of the bedrock, soil profile

and biota (in particular, vegetation). All these components are interrelated and when one of them is altered by man's activities the others will be affected to some extent, which is often difficult to predict in advance. The principal agent connecting all these different components is water. Water occurs in several forms and is stored more or less temporarily at various locations in the hydrologic cycle, e.g., in the atmosphere, biomass, subsoil, and surface runoff. Transfer of water between these reservoirs is continuously occurring in a watershed. Man's activities in a watershed, such as vegetation removal, may shift the equilibrium in one direction or another. Figure 1.1 is an attempt to represent the interrelationships of the main components in a watershed with water as the central integrating agent.

One activity in particular is likely to significantly affect the hydrologic equilibrium of a watershed, viz., the practice of forest clear-cutting. Clear-cutting is a timber harvesting procedure widely employed in coniferous forests all over the world. In a commercial clear-cut all timber over a certain minimum diameter is felled and removed. If the forest in question consists of a mature, even age stand of timber, then all the trees in a selected area are likely to be removed. This practice, therefore, can result in a slope considerably denuded of all vegetation.

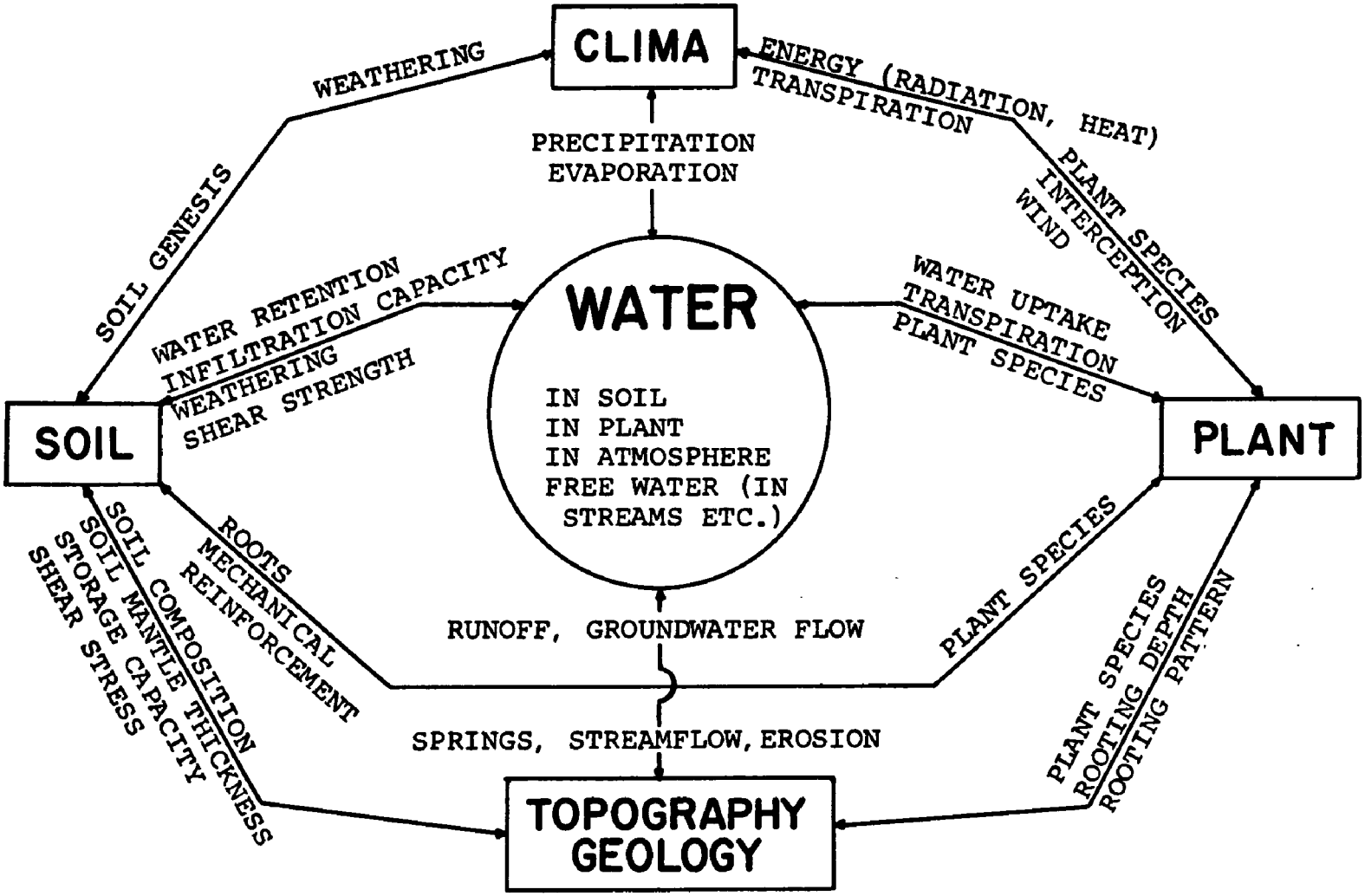


Figure 1.1 Interrelationships between the major components of a watershed with respect to water.

Forest trees are able to transpire large amounts of water during the growing season, approximately 3 to 30 inches, depending on species, depth of soil, and climate. When vegetation is removed in a clear-cutting operation the relative magnitude of the components in the water balance for the watershed will be considerably altered. Comparative field studies of soil moisture regimes under clear-cut plots and adjacent forested plots (Bethlahmy, 1962) clearly show the effect of soil water depletion by forest trees and therefore the considerably higher recharge time required to bring the soil profile back to field capacity. These trends are illustrated schematically in Figure 1.2. Some consequences of vegetation removal may be desirable, for example, a greater water yield; but unwanted side effects might also occur because of the change in the hydrologic regime in the soil mantle of a slope. For example, water in the soil pores strongly influences the mechanical and rheological properties of a given soil such as its shear strength and creep characteristics. Modification of the microhydrology in the soil mantle may lead to landslides, soil slips or slow but continuous creep of the soil mass.

In addition, removal of woody vegetation results in the loss of mechanical support by the root system. This interconnected root system which can extend down into fissures in the underlying bedrock helps to anchor a potentially unstable soil on steep slopes. In fact, landslides have been observed after heavy rains in areas which have been recently

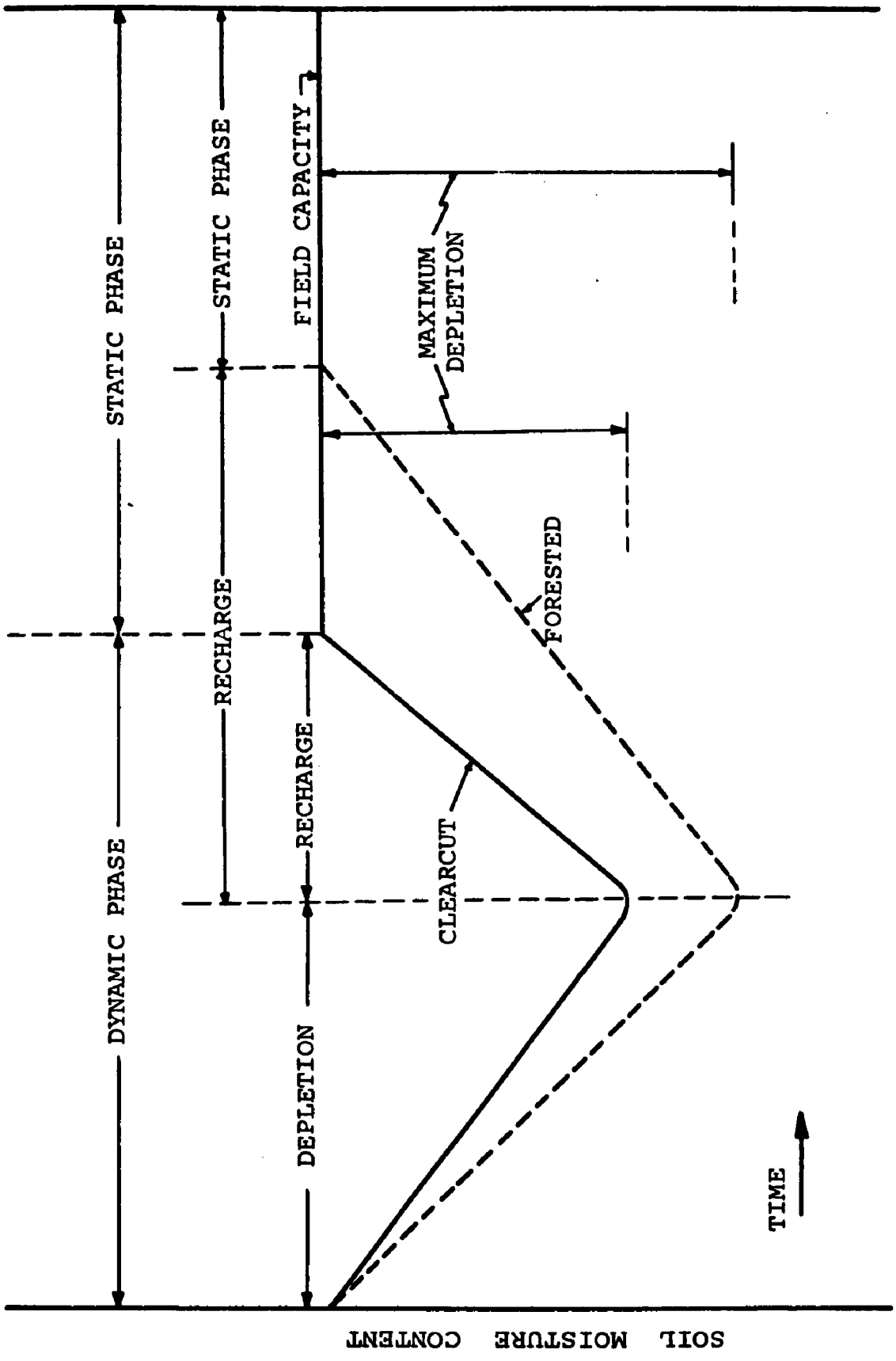


Figure 1.2 Idealized representation of soil moisture cycle in forested and clear-cut areas (after Bethlahmy 1962 and Gray 1971).

clear-cut or disturbed by road construction (Bishop and Stevens, 1964; Dyrness, 1967). It is therefore postulated that a forest cover enhances slope stability by favorably affecting or controlling soil moisture.

In order to support this hypothesis, it is necessary to study in a very broad sense the relationship between the vegetation and the soil mantle on a slope and take into account as many factors of the complex ecosystem as possible, such as climate, topography, geology, soils and vegetation. It has been emphasized that the hydrologic regime in the soil mantle is a crucial factor controlling the mechanical behavior of the soil mantle on a slope.

The movement of water in a slope, as affected by vegetation, has received little attention in a quantitative sense so far. It is the purpose of this study to present some first steps toward a better understanding of the complex relationship between removal of vegetation and the hydrologic regime in a slope.

2. Some Alternative Approaches to Problem

Basically, there are two ways of attacking forest hydrology problems--one is by means of field studies, the other by model studies. Both approaches are useful and can supplement each other. In a field study, data on the watershed characteristics (such as climate, topography, soil and vegetation) are gathered. A field study is indispensable

in this respect because these quantities are always needed, particularly as they govern the state of the water in the system. Usually a large amount of these data is required in order to account for the natural variation in watershed characteristics (such as varying soil depth).

In most cases the dependent variable of interest is the soil water potential; in addition, data on dependent quantities which influence the state of the water must be collected (for example, data on root density distribution, interception, water movement in slopes, etc.). The number of such quantities to be measured depends on how well the functional relationships between the different variables are already known. (For example, if the amount of rainfall reaching the forest floor is known as a function of the rainfall pattern above the tree crowns as well as the type and density of forest cover it is only necessary to determine the precipitation above the crowns. In other words, interception does not have to be measured in every case, and instead can be found from the known functional relationship.) Functional relationships can be obtained by comparing adequate physical models of a process (for example, the transpiration process or the process of water uptake by a root system), with collected data which have statistical validity. This makes it possible to find the necessary empirical coefficients in mathematical expressions describing such a functional relationship.

The disadvantage of a field study, however, is that the different variables cannot be controlled and therefore a large amount of data is

required to obtain a thorough picture of a process whose functional relationship is being investigated. Field studies are, therefore, usually time consuming and costly.

A model study can either be an experimental model where the actual object is scaled down a predetermined amount, or it can be a mathematical model which is based on the physical laws governing water flow through soils and plants under given boundary conditions. The experimental model will furnish useful qualitative information of the characteristics of its prototype (i.e., the watershed). Quantitative results, however, will be difficult to obtain since it is probably not possible to scale down complex processes of living systems, such as transpiration. To the author's knowledge, scaling parameters such as those used for model studies (for example, in structural mechanics or in river and harbor hydraulics) have not yet been found for complex processes in an ecosystem. Nevertheless, the qualitative results may serve as guidelines for setting up future field studies, they may yield information on the relative importance of certain variables affecting the state of the water in the soil, or they may be used to check results from mathematical models. The experimental model also requires less time for data acquisition than a field study. The environmental variables are easier to control or can be prescribed and the geometry of the model is made as simple as possible. This makes an interpretation of the data much easier than in a field experiment.

The final goal of a watershed study, however, should be a mathematical simulation model because this is the quickest way to evaluate the response of key parameters of interest to a change in other watershed variables. Once a generalized mathematical model is established and tested (which is the case when all major functional relationships are known), it can be applied to slopes in watersheds under various kinds of climatic, topographic and vegetative conditions.

3. Scope and Objectives of Present Study

An experimental model was chosen in this study. The broad purpose of the model was to study the spatial and time variation in soil water potential in a steep slope as a function of vegetation and slope angle. Such a slope can be idealized as a thin slab of soil overlying an inclined impermeable bedrock contact. A forest cover can be modeled by small trees planted in the slope. Clear-cutting can be simulated by cutting and removing the trees all at once. The response of the soil water potential to simulated rainstorms was studied first for a forested- and later for the cutover slope at various slope angles. The experiment was set up in a greenhouse in order to be less dependent on outdoor environmental conditions.

Specific objectives of this study were to answer qualitatively the following questions:

a. How suitable is such an idealized model for investigating the

impact of vegetation removal on the soil water regime in a slope?

b. How is the soil water potential at any point in a slope influenced as a function of slope angle and the presence or absence of vegetation?

c. Is there a significant downhill component of soil water flow in a steep slope or is water movement predominantly vertical due to water uptake by roots or evaporation, after drainage has ceased?

d. Is there a build-up of water table (saturated zone during and/or after a storm? If so, how is it affected by the slope angle?

In order to establish a basis for a better understanding of the factors governing soil water movement in vegetated slopes, the fundamentals of flow through porous media, water uptake by plants, and evapotranspiration each have been outlined in the next Chapter. This is followed in Chapter 3 by a review and synthesis of the relevant literature on the subject. This literature is contained in journals from a variety of disciplines which hitherto have only dealt with limited aspects of the total problem. Chapter 4 describes the experimental details and procedure of the hydrologic model study. This is followed in Chapter 5 by a presentation and discussion of results of the model study. The thesis ends with a proposed mathematical model for describing the hydrologic regime in a vegetated slope.

CHAPTER II

THEORETICAL TOOLS AND DEFINITIONS

In this chapter the theoretical basis for treating soil-water-plant relations is outlined. It contains definitions, physical principles and empirical equations used in problem of water movement in soils and plants, together with climatic influences. Longer derivations of equations are found in the Appendices. The material in this chapter has been compiled from numerous references.

1. The State of Water in Soils

a. Some Properties of Water and the Chemical Potential

Soil consists of three main fractions, the mineral solids, which constitute the soil matrix; water (or better, the soil solution); and air, which fills the voids. As a particular fraction one could also add non-living organic matter. The soil water is affected by two main mechanisms which influence its state relative to free bulk water. One mechanism involves the surface tension which develops when air enters the pore space of a saturated soil and curved air-water interfaces are created. This mechanism is important for non-swelling soils.

If on the other hand the soil matrix can shrink, water can be removed without air entering the pores. The particles (in this case

mostly clay particles) are brought into closer contact until their repulsive forces are then in equilibrium with the water extraction forces. In general both mechanisms occur together in most soils.

Osmotic forces caused by the presence of solutes in the soil water represent a third mechanism which lowers the free energy and increases the water retention. For most cases, however, osmotic effects may be neglected since they do not directly influence the amount of water retained against pressure or tension.

The state of water in a soil matrix is best described by energy considerations, i.e., one defines a soil water potential which is based on thermodynamic principles. The Gibbs free energy of water in a uniform multi-component system composed of solids, solutions and gases at a given location in space has proven to be the most useful term for expressing the condition of water in the soil and plant system at any given instant. The partial Gibbs free energy of water in such a system is then known as the chemical potential of water which is normally shortened to simply water potential ψ. A derivation of the water potential in soil using a thermodynamic approach has been presented for example by Babcock (1963) and also by Slatyer (1967).

The total soil water potential consists of four parts:

$$\psi_{tot} = \psi + \psi_g = \psi_p + \psi_s + \psi_m + \psi_g \qquad (2.1)$$

where: ψ = soil water potential

ψ_g = gravitational potential

ψ_p = pressure potential

ψ_s = solute or osmotic potential

ψ_m = matric potential

These individual terms are now briefly described.

Matric potential. The strong attractive forces between the surfaces of the soil particles and water molecules are responsible for lowering the potential energy of water in the soil, compared with water in bulk (free water). In theory, this potential energy may be further subdivided into several components, i.e.,

$$\psi_m = \psi_a + \psi_c + \psi_w \qquad (2.2)$$

ψ_a is the adsorption potential resulting from adsorption forces operative mainly in the first few molecular layers adjacent to the particle surface.

ψ_c is the capillary potential derived from the curved meniscus at the air-water interface and related to the radius of curvature r_c of this interface by the well-known relation

$$\psi_c = \frac{2 \cdot \sigma}{r_c} \cdot \frac{1}{\rho_w} \qquad (2.3)$$

where σ is the surface tension of the water (dynes/cm) (ψ_c is expressed in energy/mass). This term is important for coarse-textured soils

(i.e., sandy soils), particularly at water contents corresponding to relatively high potential energies, i.e., between 0 and 0.5 bar.

ψ_w is a potential due to the attraction between water molecules and ions in the electric double layer at the charged surfaces of the clay particles. This potential is most important in fine-textured soils which have a large surface area but it is difficult to separate from ψ_a and ψ_c.

In practice all three terms are normally lumped together since most methods of measuring matric potentials measure the sum of all. In saturated soils ψ_m is negligible.

Solute potential. This potential is the contribution to the potential energy due to the presence of salts in the soil water and is expressed by

$$\psi_s = \bar{v} \cdot \Delta \pi \qquad (2.4)$$

where $\bar{v}$ is the specific volume of water $\left(\bar{v} = \frac{1}{\rho_w} = 1 \frac{cm^3}{gr}\right.$

and $\Delta \pi$ is the osmotic pressure . (ρ_w = density of water)

Pressure potential. This potential is caused by the excess hydrostatic pressure, ΔP, i.e., due to the weight of a column of water above the point of measurement and is given by

$$\psi_p = \bar{v} \cdot \Delta P \qquad (2.5)$$

This potential is important for saturated conditions but negligible otherwise.

Gravitational potential. This potential is caused by the earth's gravitational field and is given by

$$\psi_g = g\Delta z \tag{2.6}$$

where Δz is the elevation above a reference level and g is the gravitational constant.

The water potential is normally a negative quantity since it represents the amount of work required to remove a unit mass of water from the system in the form of pure free water at the same elevation and temperature. This work is done on the system, and the potential is therefore negative.

b. Units

Potentials can be expressed in different units. A summary of possibilities of specifying potentials and their physical dimensions is given in Appendix A.

It has become customary to use "Bars" for pressure units.

$$1 \text{ Bar} = 10 \text{ Newton}/\text{cm}^2 = 14.5 \text{ psi} \tag{2.7}$$

When dealing with water flow in soils it is most convenient to use hydraulic head, which is simply the potential expressed in energy per unit mass divided by the acceleration of gravity g. Hence the hydraulic head is defined as

$$H = \frac{1}{g}(\psi_m + \psi_p + \psi_g) \tag{2.8}$$

where

$$\frac{\psi_m + \psi_p}{g} = h \qquad \text{soil water head}$$

and

$$\frac{\psi_g}{g} = z \qquad \text{elevation head} \tag{2.9}$$

The solute potential is generally neglected in most water flow problems.

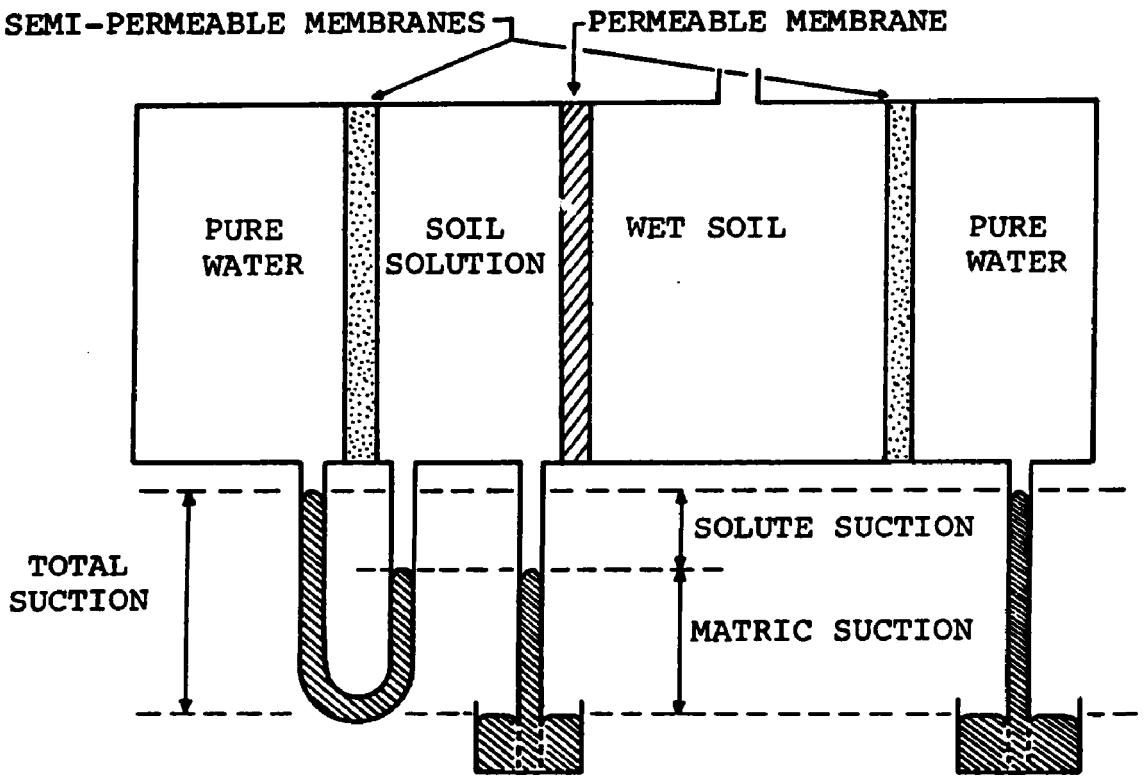
The negative of the matric potential has been traditionally called soil moisture tension or suction. It is usually expressed in bars or millibars.

Figure 2.1 shows schematically the relation between matric suction, solute suction, and total suction.

c. Hysteresis

The matric suction is a function of the water content of the soil. Unfortunately, the relation is not unique because of hysteresis phenomena. Hysteresis in this case refers to the variation in water content of the soil at any given suction, depending on whether the soil is being wetted or dried. This is shown schematically in Figure 2.2.

Hysteresis effects are particularly pronounced in coarse-textured, non-swelling soils where the pore space consists of "caverns" interconnected by "necks" consisting of narrower pores. As a wet soil dries the water-filled caverns tend to remain full until the suction rises to a value which causes the "necks" to drain. However, on rewetting a dry soil, each cavern tends to remain empty until the suction has



In an isothermal equilibrium system, matric suction is the pressure difference across a membrane separating soil solution (equilibrium dialyzate) in bulk from soil containing the solution, the membrane being permeable to solution, but not to matrix or mass flow of gas; solute suction is the pressure difference across a semipermeable membrane separating bulk phases of pure water and the soil solution; total suction is the sum of the matric suction and the solute suction and is the pressure difference across a semipermeable membrane separating pure water and soil that contains solution. An ideal semipermeable membrane is permeable to water only (from L.A. Richards 1965).

Figure 2.1 Schematic representation of suction terms.

fallen to that appropriate to the widest dimension of the cavern. Consequently, the water content at any one suction tends to be less when the soil is wetting than when it is drying (see Figure 2.2).

For fine-textured swelling soils, hysteresis is not so distinct and is thought to be due to reorientation of particles, which reduces porosity.

A theoretical relationship between the matric suction and the water content based upon soil properties has never been worked out. A number of empirical expressions or approximations have been worked out (Gardner, 1968; Cowan, 1965), for example:

$$h = h_o \cdot e^{\beta(\theta_o - \theta)} \tag{2.10}$$

where h_o and θ_o are the initial suction and moisture content respectively, and β is a constant.

and

$$h = \frac{A_1 (n - \theta)^{m_1}}{\theta^{m_2}} \tag{2.11}$$

The latter equation has been proposed by Visser (1966). A_1, m_1, m_2 are constants, and n is the porosity.

For low water contents the numerator is relatively constant and one may write

$$h \sim \theta^{-m_2} \tag{2.12}$$

m_1 varies between 0 and 10 and m_2 is normally somewhat below 3.

n is normally between 0.4 and 0.6.

θ is the volumetric water content.

d. Field Capacity and Wilting Percentage

Apart from the thermodynamic terminology for soil water, there exist some terms which are widely used to describe the state of water in soils and which are of particular significance to plant growth. The two most important of these are field capacity and permanent wilting percentages.

Field capacity. It can be defined as the water content of a soil at which drainage of gravitational water has virtually ceased. Such a situation exists one to three days after a soaking rain or irrigation. It is not a unique value for all soils because the hydraulic conductivity controls the rate of drainage. Neither is it a unique value for one soil since time and driving forces affect the drainage. During early drainage gravitational forces predominate as water drains from the large pores. Later capillary forces in the smaller pores predominate and water moves at a much slower rate. The water content at which gravity drainage ceases, i.e., at which capillary forces begin to predominate, is called field capacity. This definition might be meaningful for sands which have large pores, however, for clays with small pores it is difficult to determine at what water content gravitational forces become negligible.

Wilting percentage. This is the water content of a soil when plants growing in that soil can no longer maintain turgid leaves and permanent wilting occurs. It is generally considered to be the water content

at -15 bars of matric potential. The permanent wilting percentage is a fairly constant value for many plants on a particular soil.

The soil water retained between the field capacity and the permanent wilting percentage is the water available for the plant to extract from the soil. This range is therefore termed the available water. The amount of available water depends on the soil-water retention curve and hence upon the composition of the soil. Figure 2.3 represents these relationships.

The available water increases with finer texture and reaches a maximum for light clay-loams.

2. Flow of Water in Soils

The basic flow equation for describing water movement is derived by assuming a linear system in which the flux is proportional to the driving force, with the driving force being the gradient of the potential energy. The soil-water system is in equilibrium when the potential is everywhere the same. The osmotic component is ordinarily omitted in considering water movement, since the soluble ions generally move more readily than the water with respect to the soil system.

For water flow through a porous medium the relation between the flux and the driving force is described by Darcy's law, which is a phenomenological equation:

$$v = -K_p(x,y,z,\theta)\cdot\nabla \psi_{tot} \qquad (2.13)$$

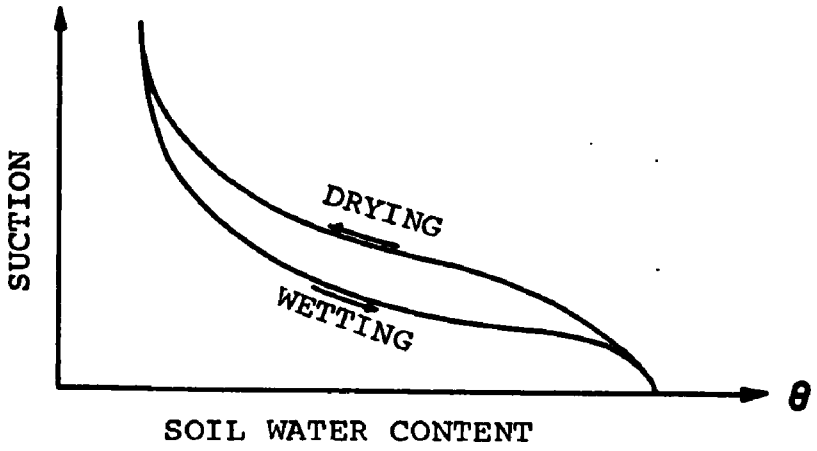


Figure 2.2 Hysteresis of soil moisture

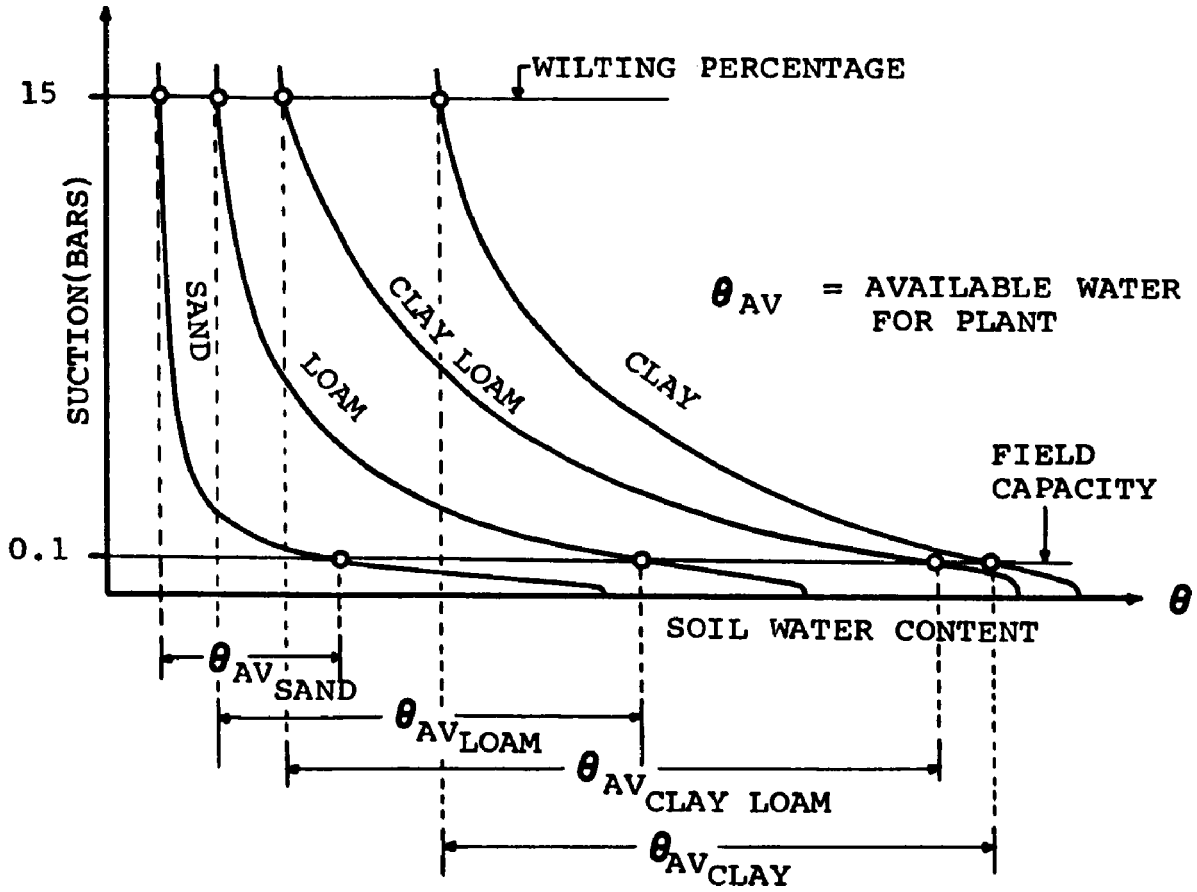


Figure 2.3 Water retention curves for different soils

where: $\nabla = \left(\frac{\partial}{x}, \frac{\partial}{y}, \frac{\partial}{z}\right)$ (vector)

All potentials will be subsequently expressed in terms of heads (see Equation 2.8). Hence we write for (2.13)

$$v = -K(x, y, z, \theta)\cdot\nabla H \tag{2.14}$$

x, y, and z are the space coordinates and θ is the volumetric water content.

$$\theta = \frac{\text{volume of water}}{\text{unit volume of soil}} = \frac{V_w}{V_{tot}} \tag{2.15}$$

v is the velocity or also the volume flux which is the volume of water through unit cross-sectional area of soil in unit time. K is called hydraulic conductivity and has the units of cm/sec. It is assumed to be a constant for a saturated soil whose structure does not change; however, for unsaturated conditions K depends on the water content of the soil and hence on the soil water head h. In the plant growth range of water content, K may vary many orders of magnitude. An empirical relation which has been found to hold for a number of soils is Gardner (1958a)

$$K = \frac{a}{(h^{n_1} + b)} \tag{2.16}$$

where a, b, and n_1 are constants. The ratio $\frac{a}{b}$ equals the saturated conductivity and n_1 varies from about 1.5 for clay soils to 4 or more for coarse-textured soils.

If Equation (2.14) is combined with the continuity equation, which represents the principle of the conservation of the matter, i.e.,

$$\frac{\partial \theta}{\partial t} = \nabla \cdot \mathbf{v} \tag{2.17}$$

one obtains the general isothermal flow equation:

$$\frac{\partial \theta}{\partial t} = \nabla \cdot \left[K(h) \cdot \nabla H \right] \tag{2.18a}$$

or in conventional notation:

$$\frac{\partial \theta}{\partial t} = \frac{\partial}{\partial x}\left[K(h) \frac{\partial H}{\partial x} \right] + \frac{\partial}{\partial y}\left[K(h) \frac{\partial H}{\partial y} \right] + \frac{\partial}{\partial z}\left[K(h) \frac{\partial H}{\partial z} \right] \tag{2.18b}$$

A more detailed derivation of Equation (2.18) is given in Appendix B, where other forms of this fundamental equation are also derived.

If we disregard hysteresis effects and consider θ to be a single-valued function of the suction h, $\theta(h)$, one may apply the chain rule to Equation (2.18) and express everything in terms of H. All subsequent derivations and analyses are restricted to two-dimensional flow, hence

$$C(h) \frac{\partial H}{\partial t} = \frac{\partial}{\partial x}\left[K(h) \frac{\partial H}{\partial x} \right] + \frac{\partial}{\partial z}\left[K(h) \frac{\partial H}{\partial z} \right] \tag{2.19}$$

where $C(h) = \frac{\partial \theta}{\partial h}$, i.e., the slope of the soil-water retention curve.

In deriving Equation (2.18) it has been assumed that Darcy's law is also valid for unsaturated conditions. However, K is now a

dependent variable or function of the water content. An analytical proof of this generalized form of the law depends on the assumption that the drag between the phases is negligibly small, Philip (1957f).

For saturated conditions $\frac{\partial \theta}{\partial t} = 0$ and $C = 0$ and Equation (2.18) or (2.19) becomes the Laplace equation.

$$K_s \cdot \nabla^2 H = 0 \qquad (2.20)$$

K_s represents the saturated hydraulic conductivity which is assumed to be constant.

For steady-state conditions $\frac{\partial \theta}{\partial t}$ is also zero, but K is still dependent on h.

The hydraulic head is given at any time and at any point by the solution of Equations (2.19) and (2.20) which satisfies the appropriate initial and boundary conditions. From the hydraulic head the water content and the rate of movement can then be determined.

Due to the dependence of K on h, Equation (2.19) is non-linear. A solution therefore has to be attempted by numerical techniques. A summary of solutions to both steady-state and transient flow problems has been compiled in Chapter 3.

For prediction of transient flow through a partly saturated porous medium, some additional difficulties arise (Hornberger and Remson, 1970). So far two theories exist that describe such kind of flow.

One theory postulates a fundamental difference between flow in the unsaturated zone and flow in the saturated zone. Water in the unsaturated zone is assumed to have relative compressibility. This theory assumes that positive changes in pressure correspond to increases in moisture content anywhere in the unsaturated zone; but, in the saturated region the moisture content is assumed to be constant. In other words, this means that the pore pressure should suddenly change at the boundary between saturation and unsaturation. Accepting such a discontinuity, the saturated-unsaturated boundary constitutes an internal moving boundary. Problems with internal moving boundaries have been solved for cases in the petroleum industry where the movement of the boundary between water and oil is considered.

The other theory assumes that the flow between saturated and unsaturated region possesses enough continuity so that it is not necessary mathematically to distinguish between the two zones. This latter concept has been put forward by Freeze (1969).

The difference between the two theories can be viewed by considering the soil-water retention curve in the neighborhood of zero suction (see Figure 2.4).

The moving boundary theory purports that the soil-water retention curve exhibits a first order discontinuity (a discontinuity in C) whereas the continuous flow theory suggests that no discontinuity exists.

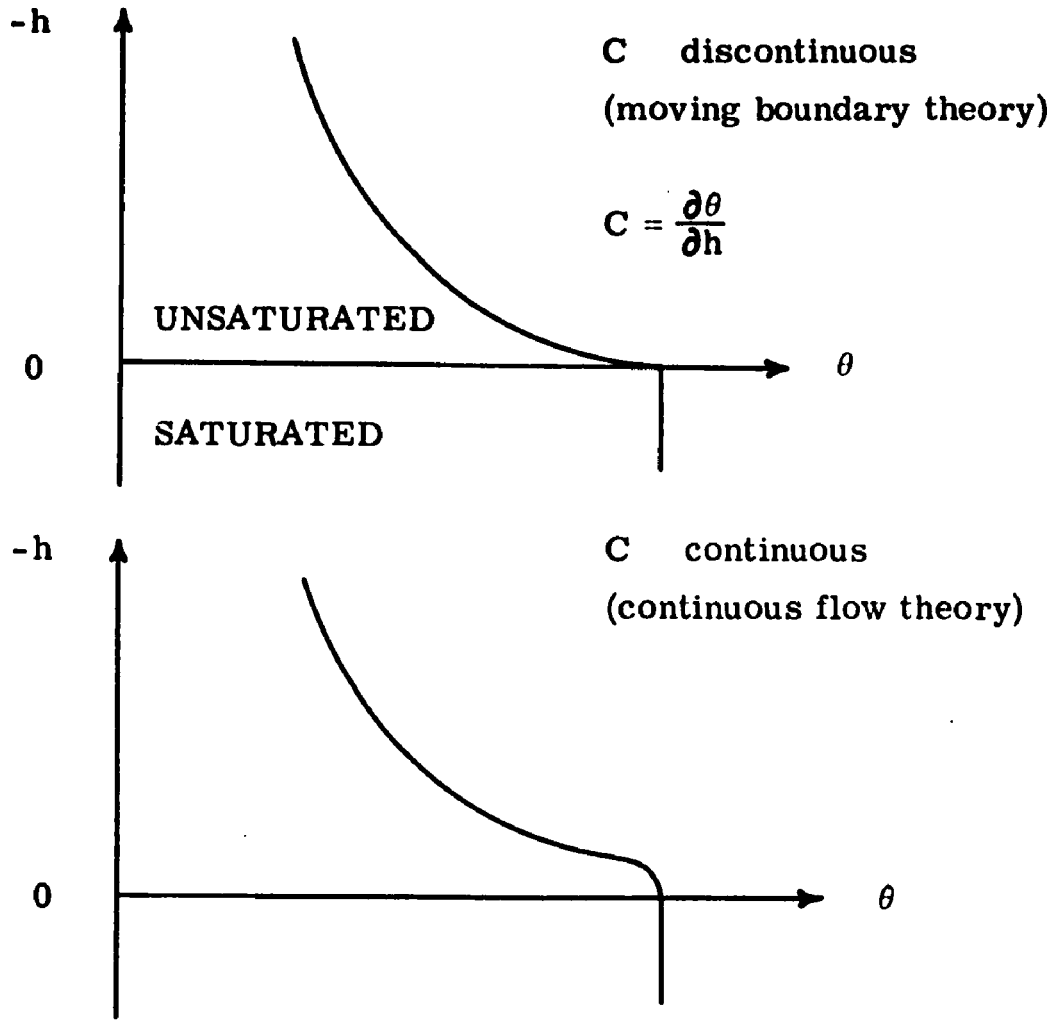


Figure 2.4. Moving boundary and continuous flow theory

3. The Influence of Vegetation

In this section the influence of plants on the soil water regime is outlined. After a brief description of the basic elements of the plant and their functions the state of the water in the plant tissues is reviewed and then subsequently the movement of water from the soil through the plant to the air.

If we talk about plants we should bear in mind that our attention is mostly directed towards large forest trees (woody plants).

a. Basic Anatomy of Plants (in particular woody plants)

Since the mechanism of water movement can scarcely be understood without some knowledge of the anatomy of the tissues through which it moves, a brief review is appropriate.

The description of the parts of a plant here is quite simplified but its only purpose is to create a reference for the later use of botanical terms.

All higher plants are vascular plants; that means that these plants have developed definite conducting tissues containing specialized cells of at least two types: the so-called xylem, or wood cells, which conduct water and mineral salts, and the phloem, which transport organic foodstuffs. These cells are organized into the conducting or vascular system of the plant which runs from the root through the stem into the leaf where it can be visualized as veins.

Cross-sections through a leaf, a stem and a root end showing the conducting tissues are shown in Figures 2.5, 2.6, and 2.7. Figure 2.8 shows a longitudinal section through the end of a root.

Roots. The root end consists of the root cap, the meristematic region which is the zone of maximum cell division, followed by the region of cell enlargement in which most increase in length of the

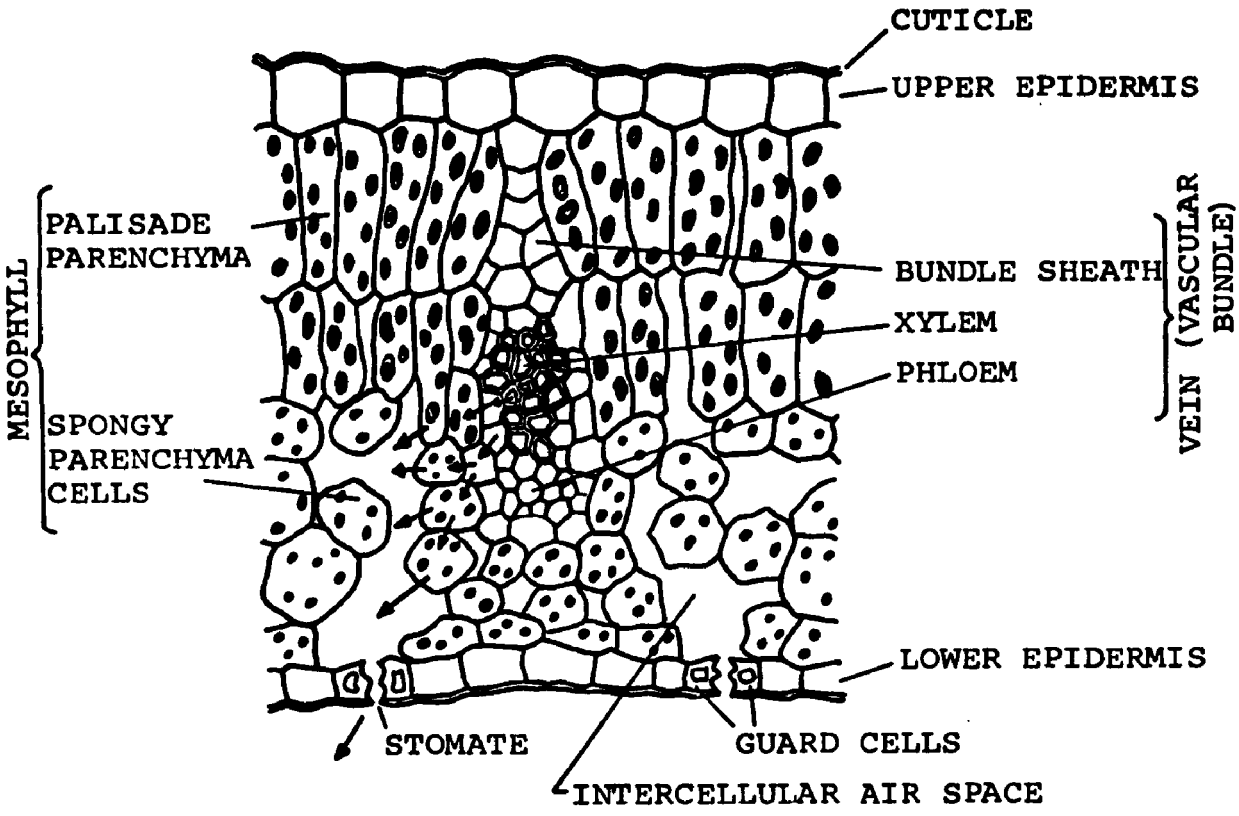


Figure 2.5 Diagrammatic cross section of a leaf with vein (after Northen 1968).

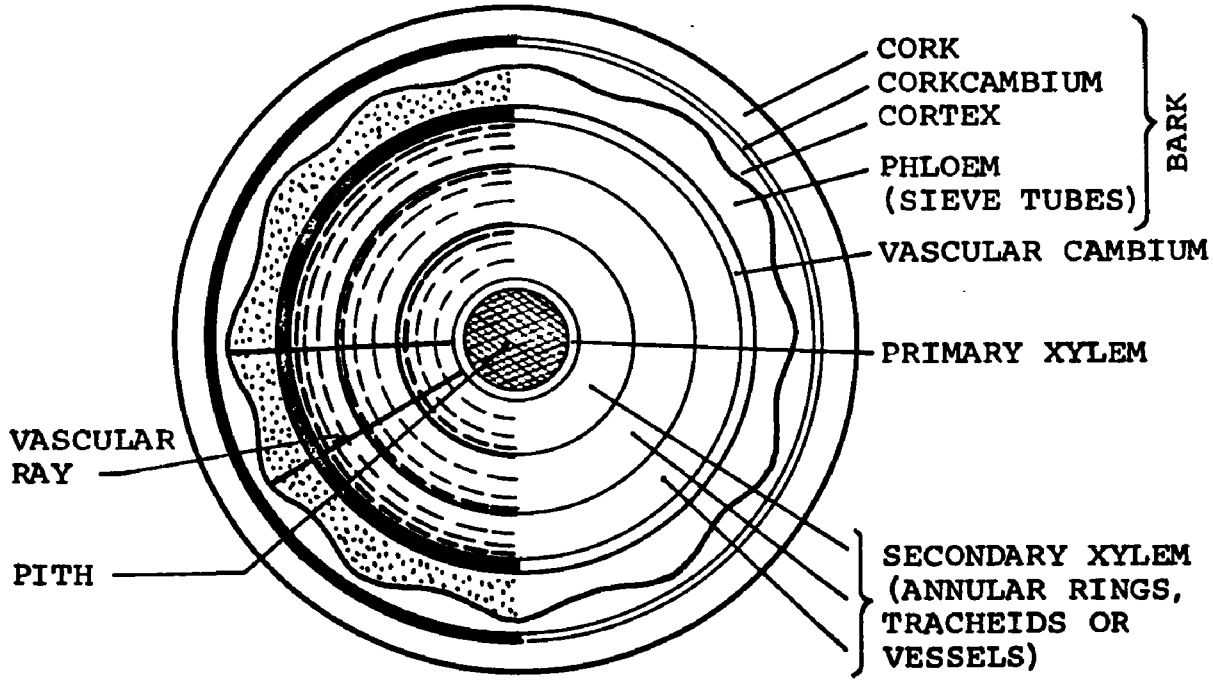


Figure 2.6 Diagrammatic cross section of a woody stem.

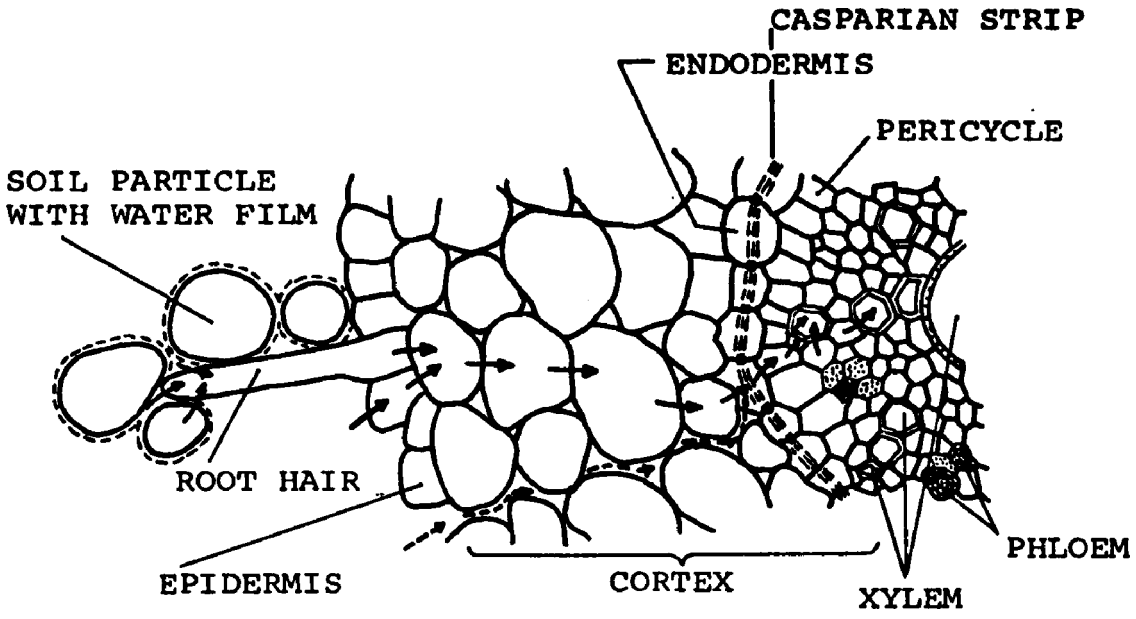


Figure 2.7 Diagram of a portion of a root as seen in cross section in the root hair region. The arrows show the pathways of water movement (after Esau 1953).

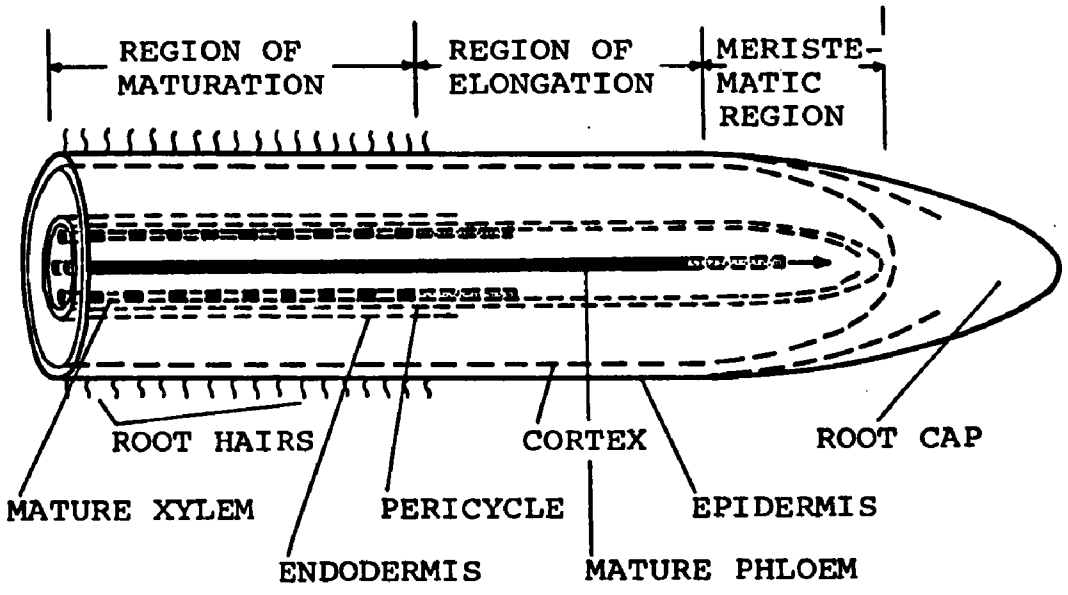


Figure 2.8 Longitudinal section through a root tip (after Kramer 1969).

root occurs. Above this region is the root hair zone, which is the zone of most of the water absorption. Beyond this zone the outer layers of the root become suberized or lignified and in older roots cork cambiums develop. In general, little absorption occurs through such regions of a root except through lenticels or other openings in the bark when the soil is very moist.

Root hairs are confined to the root hair zone. A root hair is an outgrowth of an epidermal cell. The root hairs are in intimate contact with the soil particles. In a rapidly growing root tip new hairs are continually developing just back of the zone of elongation. New root hairs are thus constantly developing in contact with different portions of the soil.

Stems. Stems vary greatly in their structure, every species possessing some anatomical features which are peculiar to itself. However, certain patterns of tissue arrangement can be found in most stems. Figure 2.6 is a diagrammatic sketch of these general arrangements.

Woody stems develop from primary tissue formed at the apical growing tip during growth of the stem in length. Stems, however, also grow in diameter, and this is a result of the development of secondary tissues from the vascular cambium. Additional layers of xylem (secondary xylem) are laid down on the inner face of the cambium and new layers of phloem (secondary phloem) on its outer face, during each

growing season. Thus the bulk of any woody stem is composed of secondary tissues.

In many woody species, as the xylem tissue increases in age, a change in composition and structure may result in a conversion from sapwood into heartwood by an increase in lignification and finally death of the sapwood cells. The function of this heartwood is then reduced to provide mechanical support rather than transport of water.

The xylem tissues of the wood of angiosperms are composed of vessels (long multi-cellular tubes), tracheids, fibers of several types, wood parenchyma and xylem ray cells. The wood of coniferous trees (gymnosperms) is simpler in its structure and the only cell types present are tracheids (short thick-walled cells) and wood ray cells.

Leaves. Leaves are constructed so as to present a large surface area to sunlight and since they are thin, every cell is relatively close to the outside atmosphere. The cross-section in Figure 2.5 shows that the bulk of the leaf tissue consists of two layers, the palisade tissue of elongated parenchyma cells in the upper half of the leaf and the spongy tissue of irregularly shaped parenchyma cells with large intercellular spaces in the lower half.

The palisade cells are crowded with chloroplasts and appear to be specialized for efficiency in photosynthesis. The spongy parenchyma cells normally possess fewer and smaller chloroplasts.

On both sides the leaf is covered by a layer of cells called the epidermis, whose cell walls fit tightly together without intercellular spaces. The outer cell walls of the epidermis are covered with a layer of wax, the cuticle, which is relatively impermeable to water.

The lower side of the epidermis bears numerous special openings called stomates. The stomatal pore is surrounded by two specialized epidermal cells, called guard cells, which regulate the amount of aperture. These stomatal pores constitute a very efficient pathway for gas exchange, i.e., intake of CO_2 for photosynthesis and output of water vapor. The latter process is termed transpiration.

The vascular bundles are usually enclosed by compactly arranged cells which form the bundle sheath. All this together forms a vein and is in intimate contact with the mesophyll cells. The veins also form the structural framework for the mechanical strength of the leaf. The vascular tissue in the leaf is continuous with that in the stem and on to the roots, thus forming a continuous passageway from the roots to the leaves, i.e., from the soil to the atmosphere.

b. Plant Water Potentials

There is an immense variation in size and forms of cells in the tissues of vascular plants. This variation in turn affects or controls water potentials in the plant.

In this section an attempt is made to present a generally valid expression for the water potential in the plant, ψ_{pl}, taking into account

all the various forces to which the water in the cell and tissues is subjected. Among these forces we may distinguish (analogous to water in the soil) three main groups; namely, forces associated with pressure on the water (for example, turgor), forces associated with osmotically active solutes, and forces associated with the tissue matrix. The water potential in the plant can be represented by different components (see Slatyer, 1967 for a more detailed treatment), namely

$$\psi_{pl} = \psi_p + \psi_m + \psi_s \qquad (2.21)$$

where

ψ_p = pressure potential (for example, turgor in a living cell)

ψ_m = matric potential

ψ_s = osmotic potential

which is analogous to Equation (2.1).

The component potentials ψ_p, ψ_m, and ψ_s are of different importance in the various regions of cells and tissues. In the vacuolar sap of the cell, ψ_m is probably unimportant, which means that Equation (2.21) reduces to $\psi_{pl} = \psi_p + \psi_s$. In cell walls, however, matric forces can be important due to electrical charges on the cell wall fibers, whereas the pressure component can generally be neglected due to the presence of air spaces which are in connection with the outside air.

In the vascular elements, the matric and pressure component are of greatest importance. The existence of high negative potentials (up

to -100 bars) which can develop in the xylem during the ascent of sap, has been explained by cohesion forces between the individual water molecules and the vessel or tracheid walls. They can therefore be attributed to a matric component.

c. Transport of Water Through the Plant

Water Absorption by Roots. Water flows to the surface of the plant root under the influence of a potential gradient of the soil water in the soil mass and at the root surface. Soil texture and hydraulic conductivity control water movement to root surfaces.

Water is absorbed by roots mainly in the region of the root hairs. This zone presents a large surface area in contact with water films surrounding soil particles (see Figure 2.7).

There appears also to be absorption of water through the suberized surfaces of older tree roots, which is particularly important in winter when young growing roots and root-hairs may be lacking.

The cell wall of the root-hair which is an enlarged epidermal cell appears to be highly permeable to water. From the epidermis the pathway of water to the root xylem occurs either through the protoplasts of successive rows of thin-walled cortex cells or outside the protoplasts via the cell walls. The innermost layer of cortex, however, contains suberin in a band-like layer in the radial and transversal walls, the so-called Casparian strips. Hence the cell wall pathway for water and ions

is effectively blocked and transport across the endodermal protoplasm is necessary. In the older parts of a root, the endodermal cells may become completely suberized, except for so-called passage cells through which water movement is presumed to occur. The endodermis, therefore, represents the main barrier to water flow.

The driving force for the transport of water across the root cortex is the gradient in water potential between the root surface and root xylem.

$$\text{Absorption} \sim \frac{\psi_{\text{root surface}} - \psi_{\text{root xylem}}}{r_{\text{root}}} \qquad (2.22)$$

where r is the resistance.

There are two mechanisms of water uptake which have to be distinguished. In rapidly transpiring plants, a negative pressure (negative pressure potential) develops in the xylem of the leaves and stem which is transmitted down to the root xylem, thus producing a difference in water potential in the root and in the soil at the root surface. Absorption due to this mechanism is called passive absorption and accounts for the intake of most of the water which enters the roots of plants.

In slowly transpiring plants (at night, for example), solutes are accumulated in the xylem and the solute potential is relatively low (-1 or -2 bars). The pressure potential is usually slightly positive (about 0.5 or 1 bar). If the soil water potential is high (for example when the soil is at field capacity), then there is still a gradient in water potential

causing water to move to the root xylem. This water absorption, caused by the low osmotic potential in the xylem, is called active absorption or root pressure.

Among the factors in the soil-root system affecting the absorption of water one may distinguish between those influencing the movement of water in the soil and those governing resistances to the transport through the root. The roots of many species are sensitive to temperature, soil aeration and suberization which modify the resistance to water movement in the root. In poorly aerated soils, oxygen concentration is low which for many species causes retarding the rate of water intake.

Water Movement Through the Vascular System in the Stem. Water from the root xylem is transported upwards through the stem in the nonliving xylem elements. Resistance to flow through dead cells is much lower than through living cells since the water does not have to pass through membranes. The pathway of water through the walls of the tracheids and vessels is established through pits. The conifers which only have tracheids offer a higher resistance to water flow along the stem than do angiosperms with large vessels. This difference in conductivity is also visualized in the velocity of water flow which in conifers is about 1 m/hr $\pm$ 0.5, in diffuse porous angiosperms 2-4 m/hr, and in ring porous angiosperms 20-50 m/hr.

The driving force for the water flow through the vascular elements of the stem is the pressure gradient between the leaves and the roots. The mechanism for the ascent of sap in tall trees has been explained by the so-called cohesion theory. According to this theory evaporation from the surfaces of mesophyll cell walls in the leaf causes a reduction in their water potential and this instigates withdrawal of water from the ends of the conducting elements with which they are in contact via water-filled cell walls. The water in the xylem is thus placed under a tension which is transmitted downwards because of cohesion between adjacent water molecules in continuous water columns and adhesion between the water molecules and the walls of the conducting tissue. The reduced pressure in the root xylem then causes entry of water and the whole column moves upwards by mass flow. One implication of this theory is that the pressure gradient in the xylary conducting system which develops as a result of transpiration is high enough to move water at the rates which have been observed in the field. (Zimmerman, 1964, postulates that a pressure gradient of about 0.15 bar/meter is required in an actively transpiring tree to overcome hydrostatic pressure and friction in the vessels.) This requires very high potential differences, but as a matter of interest, leaf water potentials of the order of -100 bars have been recorded.

Water Movement in the Leaf and Transpiration. There are three possible pathways for water from the leaf xylem to the outer atmosphere. The most important one leads through the cell walls of the parenchyma to the mesophyll liquid-air interfaces and then, in the gaseous phase, through the stomates to the outside air. A second path, parallel to the first one, leads to the epidermal interfaces and then, in the vapor phase via the cuticle, to the outside air. The third pathway is guttation, which is only operative when transpiration is minimal (e.g., at night) and only occurs where positive pressure builds up in the conducting system. This pathway involves liquid transfer right to the surface. However, it never occurs in tall trees.

Resistance to liquid flow in the cell walls of the leaf mesophyll is much less than through the cell vacuoles. Water again moves along potential gradients until it arrives at the evaporation sites. Cuticular transpiration, however, is not significant, due to the low hydraulic conductivity in the outer epidermal wall and cuticle.

Transpiration of deciduous trees can also occur through lenticels in the bark of the stems, particularly during winter.

Vaporization of water at the evaporation sites is made possible by the energy which comes from solar radiation. The rate of transpiration therefore depends on the supply of energy to vaporize water. The energy balance will be described in more detail in Section 2.4. The driving force for the vapor through the stomates is the concentration

gradient in water vapor. This can be described as

$$Tr = \frac{c_{leaf} - c_{air}}{r_{leaf} + r_{air}} = \frac{273}{PT} \cdot \rho_v \cdot \frac{e_{leaf} - e_{air}}{r_{leaf} + r_{air}} \qquad (2.23)$$

where:

$$r_{leaf} = r_{stomate} + r_{\substack{intercellular \\ space}} + r_{mesophyll\ cell\ wall}$$

c is the water vapor concentration in gr/cm^3 and r is the resistance in sec/cm. Tr is the evaporation (transpiration) in gr cm^{-2} sec^{-1}. e is the vapor pressure in mm Hg (corresponding to c), P is the atmospheric pressure in the same units as e, ρ_v is the density of water vapor, T is the absolute temperature, and $\frac{273}{PT} \cdot \rho_v$ is a conversion factor to change concentrations c to vapor pressures e $\left(\frac{273}{PT} \cdot \rho_v \approx 10^{-6}\right)$. The leaf resistance to vapor flow is largely governed by the stomatal behavior. On both sides of the stomates are the guard cells which contain chloroplasts unlike other epidermal cells. Stomatal aperture is regulated by the turgor in the guard cells which in turn is controlled by the leaf water potential and indirectly also by light.

Factors affecting transpiration are those influencing the vapor pressure gradient and the resistances according to Equation (2.23). Important environmental factors are light intensity, atmospheric vapor pressure (i.e., relative humidity), temperature, wind and water supply to the roots. Plant factors are the extent and efficiency of the root system in absorption, the leaf area, leaf arrangement and structure, and stomatal behavior.

In general, one of these factors will influence the vapor pressure as well as the resistance in the vapor pathway. Therefore, a change in one of the factors will not cause a proportional change in transpiration. Transpiration exhibits therefore also distinct diurnal variations.

The Overall Flow of Water from the Soil through the Plant.

Figure (2.9) shows schematically the pathway of the water from the soil to the atmosphere. The water passes either first through the plant to the free atmosphere or it leaves the soil directly by means of evaporation at the soil surface. In Figure 2.3 electrical analogs (resistances and capacitances) have been used to represent the resistances and storage locations in the pathway. Van den Honert (1948) applied this idea to express steady state flow through the plant in analogy to Ohm's law:

$$\text{Rate of water movement} \sim \frac{\psi_{soil} - \psi_{root\ surface}}{r_{soil}} = \frac{\psi_{root\ surface} - \psi_{xylem}}{r_{root}}$$

$$= \frac{\psi_{xylem} - \psi_{leaf}}{r_{xylem} + r_{leaf}} = \frac{\psi_{leaf} - \psi_{air}}{r_{leaf} + r_{air}} \qquad (2.24)$$

which means that the flow across each of these zones is proportional to the water potential difference. Such a model can be useful but is oversimplified for several reasons. First, the water movement through the soil-plant-atmosphere system is not a steady state process, and second, the resistances to water flow through the soil, the roots and

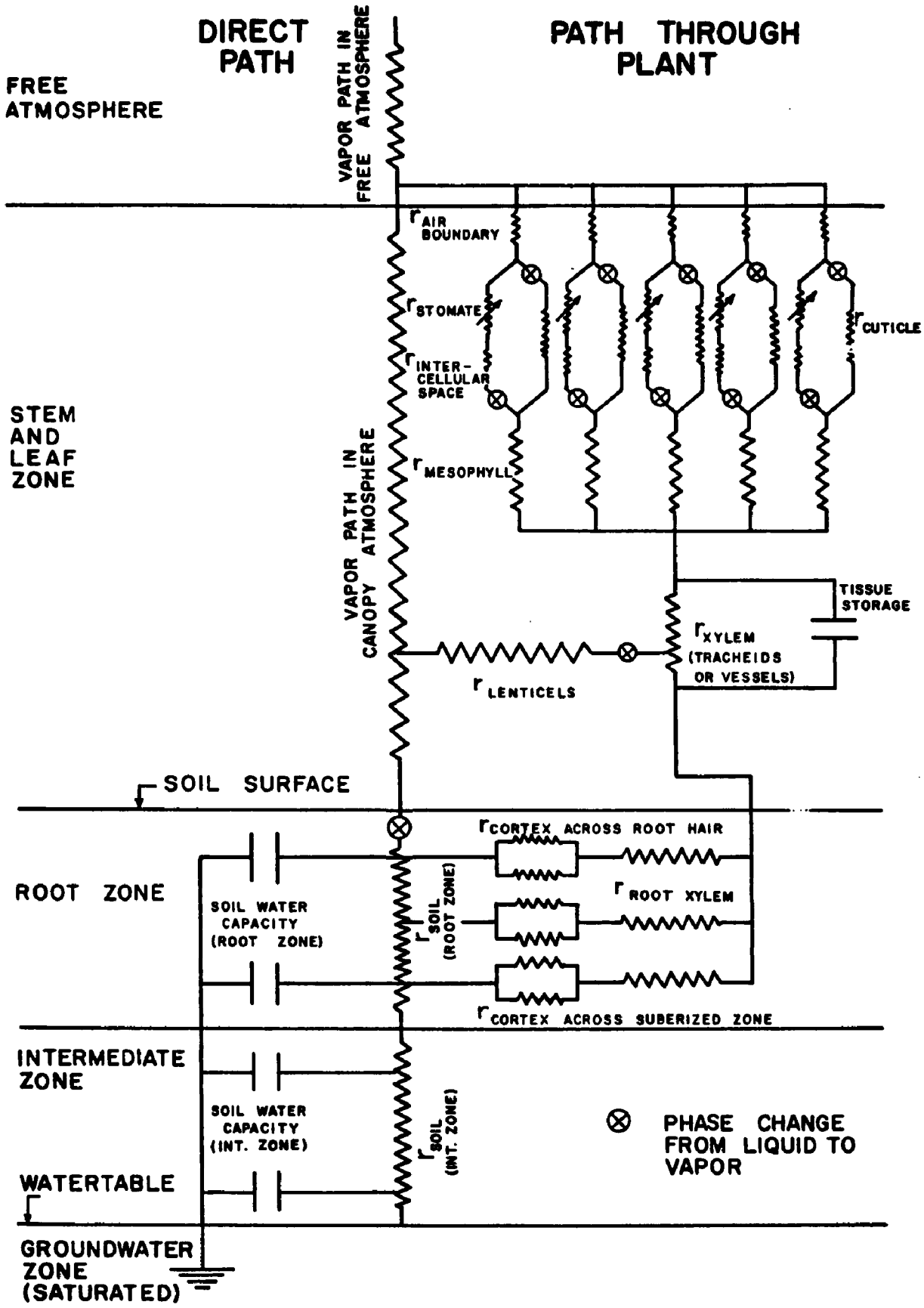


Figure 2.9 Pathways of water from the soil to the atmosphere.

the leaves vary with the rate of water flow. Third, there is a change in phase when liquid water is vaporized. Water vapor movement is not directly proportional to the water potential gradient but to the vapor pressure gradient. The vapor pressure and the water potential are related by a logarithmic function which is obtained from treating water vapor as an ideal gas.

$$\psi = \frac{RT}{\bar{V}_w} \ln\left(\frac{e}{e^o}\right) \qquad (2.25)$$

where: R = gas constant

$\bar{V}_w$ = partial molal volume of water

$\frac{e}{e^o}$ = relative vapor pressure

The largest resistance to overall flow occurs in the vapor phase from the evaporating sites to the free atmosphere. For the flow of liquid water, the largest resistance lies in the root cortex where the transport is through living cells. Resistance in the stem is low and in the leaves intermediate. $\psi_{cortex} - \psi_{xylem}$ might therefore be a reasonable estimate for $\psi_{root} - \psi_{leaf}$.

Flow from soil to the roots can be reasonably considered to be in the liquid phase along gradients of water potential. Flow from the root to the leaf can also be treated in this manner but only in very general and qualitative terms. Flow from the leaf to the air is in the vapor phase and along gradients of vapor concentration and should be treated as such.

Summarizing. One may say that total flow of water is controlled primarily in the vapor phase, because transpiration is governed by the gradient in vapor pressure and the stomates are the main regulators of water flow through the plant. An increase in resistance to flow somewhere in the system can reduce transpiration only indirectly by reducing the turgor in the leaf cells (and thus in the guard cells) to cause closure of stomates, which increases the stomatal resistance.

4. Influence of Climate

a. Solar Radiation and Energy Balance

In the previous section it was shown that the transpiration process depends on the amount of energy supplied, the vapor pressure gradient between the water at the evaporating surface and the bulk air, and the resistances in the vapor pathway.

All energy comes originally from solar radiation, and it should be emphasized that this is the only independent variable. Solar energy input not only provides the necessary thermal environment for the plants but also supplies the energy for photosynthesis.

In passing on and through the earth's atmosphere, solar radiation is influenced in a number of ways (Figure 2.10). Solar radiation is short-wave radiation. It comprises normally a direct and a diffuse component. On reaching the plant community, part of the already depleted radiation is reflected. The remainder is absorbed and changed into thermal energy of the absorbing materials. The reflection coefficient a_r for incoming

solar radiation is called the surface albedo and depends on the physical characteristics of the surface and the angle of incidence. The radiation absorbed by vegetation is emitted as long-wave radiation and is proportional to the fourth power of its absolute temperature and to its emission coefficient. The difference between the incoming and outgoing, short- and long-wave radiation fluxes, which represents the rate at which energy is being absorbed by the surface under study, is an important microclimatic parameter. It is usually called the net radiation R_N and can be expressed by

$$R_N = R_s (1 - a_r) - R_L \tag{2.26}$$

where: R_N = net radiation flux

R_s = direct and diffuse solar radiation incident on the earth's surface

$R_s(1-a_r)$ = net short-wave flux

a_r = reflection coefficient (albedo)

R_L = net long-wave flux

Part of the net radiation absorbed by plant and soil surface through energy exchange is dissipated as sensible heat and part as latent heat (by vaporization, which is transpiration). Another part is used for photosynthesis. One may write this energy balance as follows:

$$R_N = H_s + H_L + G_F + M \tag{2.27}$$

where: H_L = latent heat flux density ($Watt/cm^2$); $H_L = \lambda \cdot E$

E = evapotranspiration rate ($gr \cdot cm^{-2} \cdot sec^{-1}$) or ($cm^3 \cdot cm^{-2} \cdot sec^{-1}$)

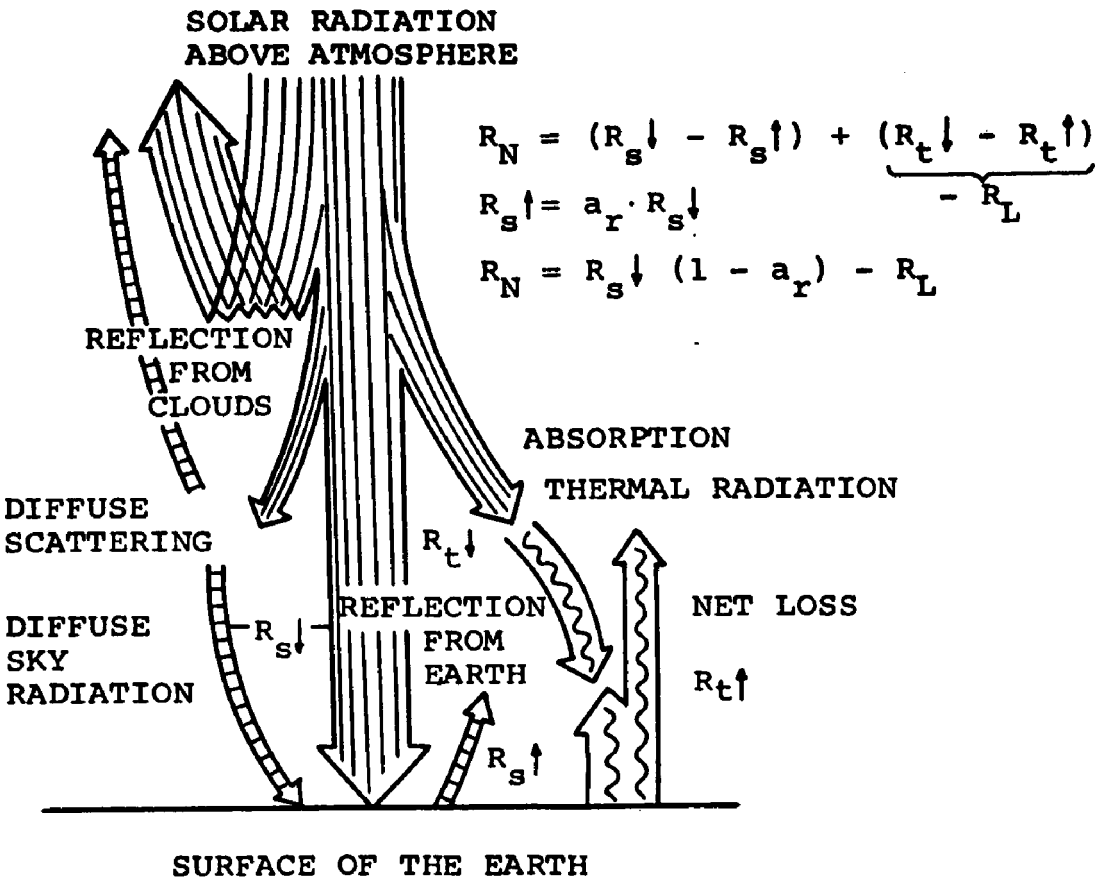


Figure 2.10 Daytime radiation balance

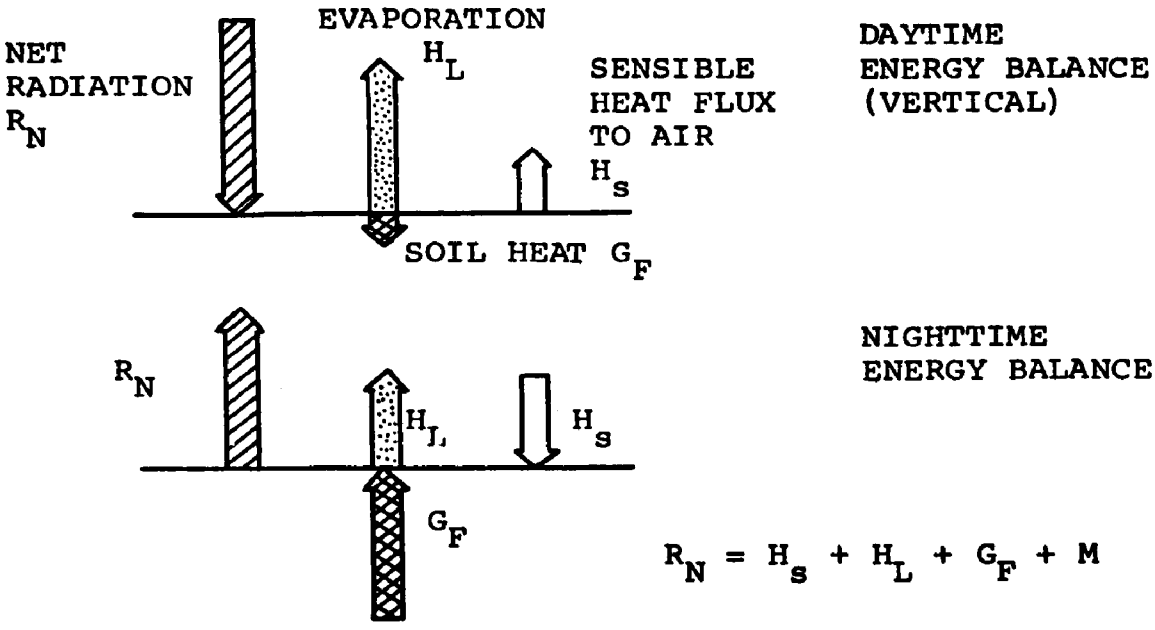


Figure 2.11 Energy balance (after Tanner 1968).

λ = latent heat of vaporization (Joule$\cdot$gr^{-1}) or (Joule$\cdot$cm^{-3})

H_s = sensible heat flux into air (Watt$\cdot$cm^{-2})

G_F = sensible heat flux into ground

M = miscellaneous fluxes, such as those involved in photosynthesis and respiration of the plant community and associated organisms.

M can generally be neglected and G_F is only important for short-term considerations, since net changes over the period of one day are relatively small (inward flux during the day and outward flux at night). Figure 2.11 illustrates the usual daytime and nighttime energy balance. The arrow of H_s during daytime can, however, become reversed due to the contribution of horizontally advected heat.

Both terms H_s and H_L are unknown. They represent the net exchanges of sensible and latent heat, respectively, between the vegetation surfaces and the atmosphere. This exchange occurs primarily by turbulent eddy movement and the partitioning of H_s and H_L requires the application of turbulent-transfer aerodynamic theory.

b. Evapotranspiration

Evaporation from plant community surfaces is frequently termed evapotranspiration. This expression combines the effect of transpiration of individual plants and evaporation from soil.

Potential evapotranspiration E_p is generally defined as the rate of evaporation which would take place if one were dealing with a small

area in the midst of a large unbroken, completely vegetated surface and if soil moisture were not limiting.

Actual evapotranspiration E_a is the rate of evaporation taking place under existing soil, vegetal and climatic factors. There are five general approaches to describe evapotranspiration (Tanner, 1968):

1) The hydrological or water balance approach (this is described in Section 2.5).
2) The eddy correlation approach which is based on turbulent vapor-transfer theory.
3) The energy balance approach, which measures the energy flow in the various pathways to the vapor source, and from this derives the energy used in vaporization, thus finding the latent heat term.
4) The aerodynamic or profile method which describes the vapor mass flux and requires an estimate of the turbulent diffusivity or transport coefficient and the vapor gradient. It uses wind profile information.
5) Combined approaches, using a combination of two or more of the above approaches.

In addition, also purely empirical ways have been developed to estimate evapotranspiration, for example, the Thornthwaite method, which gives the evapotranspiration in cm, based on the mean monthly temperature alone.

The following approach, however, is restricted to a method originally developed by Penman (1948) and modified by Monteith (1965). This method employs a combination of the energy balance and aerodynamic approach. Such a relation may prove to be most useful for a model of soil-plant-atmosphere relationships.

The transfer of water vapor to the bulk air occurs first inside the leaves, and then through a thin boundary layer outside the leaf, by molecular diffusion. Afterwards the transfer is by turbulent eddy movement. This can be idealized by writing

$$E = \frac{c_n - c_a}{r_n + r_a} \tag{2.28}$$

where c_n and c_a are the water vapor concentrations at the boundary layer and the bulk air, respectively and r_n and r_a are the resistances below and above this boundary layer (or effective crop surface). Based on this idea, and using Penman's approach, Monteith derived the following expression for potential evapotranspiration:

$$H_L = \lambda \cdot E_p = \frac{s_v \cdot R_N + \rho_a \cdot c_p [e^o(T) - e]/r_a}{s_v + \chi\left(1 + \frac{r_n}{r_a}\right)} \tag{2.29}$$

where E_p = potential evapotranspiration rate in $cm^3 \cdot cm^{-2} \cdot sec^{-1}$

λ = latent heat of vaporization of water = 590 cal/cm^3

R_N = net radiation intensity in $cal \cdot cm^{-2} \cdot sec^{-1}$

$e^o(T)-e$ = vapor pressure deficit in mbar of air at height z

r_n = internal resistance to diffusion of water vapor from leaves and soil over unit land area in $sec \cdot cm^{-1}$

r_a = external resistance to diffusion and transport of water from leaves and soil to the air at height z above the vegetation in $sec \cdot cm^{-1}$

$\rho_a \cdot c_p$ = product of density in $gr \cdot cm^{-3}$ and specific heat in $cal \cdot gr^{-1} \cdot {}^oC^{-1}$ of the air, taken as $2.9 \cdot 10^{-4}$ $cal \cdot cm^{-3} \cdot {}^oC^{-1}$

s_v = the slope of the saturation vapor pressure curve in $mbar \cdot {}^oC^{-1}$ at the bulk air temperature T, i.e., de^o/dT

χ = psychrometric constant = 0.66 $mbar \cdot {}^oC^{-1}$

The external resistance or air resistance r_a has been derived from wind profiles as follows:

$$r_a = \frac{\left[\ln\left(\frac{\bar{z} - d_z}{\bar{z}_o}\right)\right]^2}{k_c^2 \cdot u} \qquad (2.30)$$

where u = wind velocity in cm/sec at height $\bar{z}$

$\bar{z}_o$ = roughness length in cm

d_z = zero plane displacement in air in cm (for tall trees wind speed goes to zero at height $\bar{z}_o + d_z$, rather than $\bar{z}_o$)

k_c = von Karman's constant

More difficult to evaluate is r_n. However, all these quantities have been measured experimentally (or at least estimated) for different kinds of vegetation and net radiation values. Rutter (1968) has presented a summary of the available data.

Rutter (1968) also derives a relation taking into account evaporation of intercepted water for forests.

Equation (2.29) is an expression for the evapotranspiration rate E. If r_n, the internal diffusion resistance, is set equal to zero, the expression becomes an equation for the evaporation of intercepted water E_I. Hence, we may write:

$$\frac{E}{E_I} = \frac{s_v + \chi}{s_v + \chi \cdot \left(1 + \frac{r_n}{r_a}\right)} \tag{2.31}$$

The additional evaporation due to interception (assuming that there is no transpiration until all intercepted water is evaporated) is then:

$$I\frac{(E_I - E)}{E_I} = I \cdot \left(1 - \frac{E}{E_I}\right) = I \cdot \frac{\chi \cdot r_n / r_a}{s_v + \chi\left(\frac{r_n + r_a}{r_a}\right)} \tag{2.32}$$

where I = interception in cm

and $I \cdot \frac{E}{E_I}$ represents the transpiration that would occur during the time the intercepted water is evaporated.

The total evapotranspiration E', during a time t_I that includes interception I is then given by:

$$\lambda E' = \frac{s_v \cdot R_N \cdot t_I + \frac{1}{r_a} \rho_a \cdot c_p \cdot [e^o(T) - e] \cdot t_I}{s_v + \chi \cdot \left(\frac{r_a + r_n}{r_a}\right)} + \lambda \cdot I \left(1 - \frac{E}{E_I}\right)$$

$$\lambda E' = \frac{s_v \cdot R_N \cdot t_I + \frac{1}{r_a}\left\{\rho_a \cdot c_p \cdot [e^o(T) - e]t_I + \chi \cdot r_n \cdot I \cdot \lambda\right\}}{s_v + \chi \cdot \left(\frac{r_a + r_n}{r_a}\right)} \qquad (2.33)$$

The net interception loss depends very much on $\frac{r_n}{r_a}$ for a given s_v, and therefore on the type of vegetation.

5. The Water Balance and the Hydrologic Cycle on a Forested Slope

Figure 2.12 represents schematically the factors affecting the hydrologic regime in a forested slope.

During a rain storm, part of the water will infiltrate into the soil. The infiltration rate depends on the initial water content of the soil and the overall permeability of the soil profile. If the rain rate exceeds the infiltration capacity, water will be ponded on the surface or run off as overland flow (Ov). Another part of the precipitation will be intercepted by the crowns of the trees (CI). Part of this water may flow down the stem (Stemflow Q_s). The amount of gross precipitation falling through the crowns (Throughfall Q_t) might be intercepted by forest floor vegetation and litter (FI), before it infiltrates into the mineral soil (Q_i). The water intercepted by the tree crowns can be evaporated directly from there and represents a direct loss.

Hence, one may write for the total interception loss I:

$$I = CI + FI$$

$$I = (Pr' - Q_n) + FI \qquad (2.34)$$

where Q_n = net precipitation on forest floor

Pr' = precipitation above the crowns

$$Q_n = Q_t + Q_s \tag{2.35}$$

Q_t = throughfall

Q_s = stemflow

$$FI = Q_n - (Q_i + Ov) \tag{2.36}$$

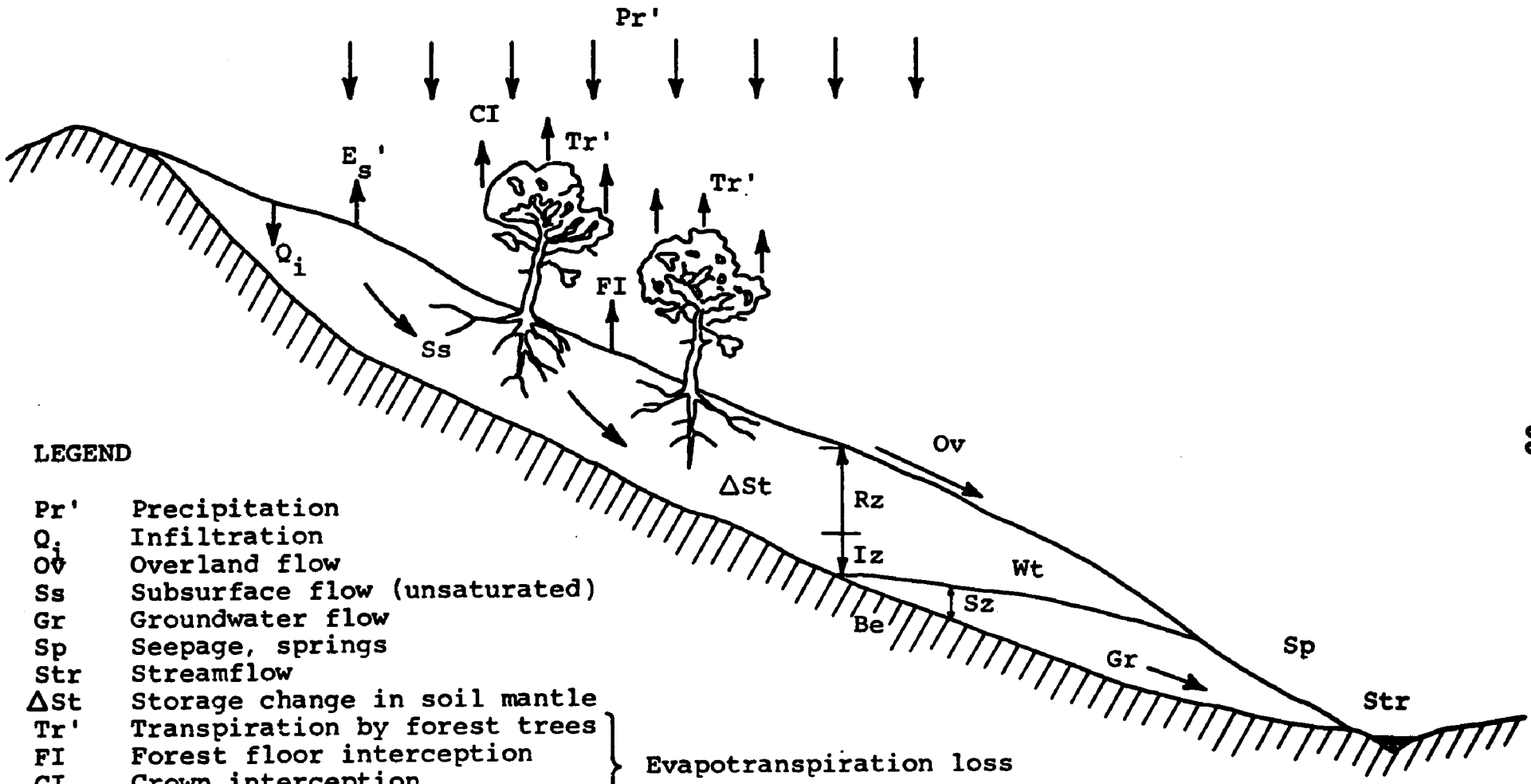
The water entering the soil (Ss) will change its storage ΔSt in the unsaturated region and may increase the saturated region (ground water storage). At the toe of the slope, the ground water will drain out through the seepage face (Dr). After the rain storm, trees will deplete water (Tr') and also the forest floor will lose water through evaporation (Es').

Combining all these effects, we may express this in a water balance for the slope over a given time interval. (All quantities in $\frac{cm^3}{cm^2}$ or in cm^3)

$$Pr' - \underbrace{(I + Tr' + Es')}_{E'} \pm \Delta St_{\text{soil moisture}} \pm \Delta St_{\text{ground water}} - \underbrace{(Dr + Ov)}_{\text{Stream Flow}} = 0 \tag{2.37}$$

E': Evapotranspiration

If all variables except E' can be measured, evapotranspiration can also be evaluated by the water balance method.



LEGEND

Pr'	Precipitation	
Q_i	Infiltration	
Ov	Overland flow	
Ss	Subsurface flow (unsaturated)	
Gr	Groundwater flow	
Sp	Seepage, springs	
Str	Streamflow	
ΔSt	Storage change in soil mantle	
Tr'	Transpiration by forest trees	} Evapotranspiration loss
FI	Forest floor interception	
CI	Crown interception	
E_s'	Forest floor evaporation	
Rz	Root zone	} Zone of aeration
Iz	Intermediate zone	
Sz	Saturated zone	
Wt	Water table	
Be	Bedrock (assumed impervious)	

Figure 2.12

Idealized slope and the factors affecting its water regime.

CHAPTER 3

REVIEW OF THE LITERATURE

1. Introduction

The literature on water flow in soils and plants, evapotranspiration, forest hydrology and watershed management is immense, and consequently it is not always easy to select the pertinent publications which relate to a specific problem. Attention is focused, in this review, on the problem of water flow in both barren and vegetated slopes.

This problem can be approached in several different ways. For example, one may study the change in subsurface stormflow and overland flow (which is reflected in the hydrograph response), caused by the removal of vegetation; or one may investigate the modification of the soil moisture regime in a forest soil on a water balance basis (by evaluating the available water as a function of time). This is directly related to tree growth, since severe water deficits are reflected in the plant growth rate. Finally, one might attempt to calculate the soil water potential as a function of location and time. This approach is perhaps of greatest interest to the soils engineer because this information would be useful for assessing the mechanical behavior and stability of a sloping soil mass.

A review of the salient literature has been organized in the following manner. First, a short survey on the effect of clear-cutting on the behavior of a watershed (in particular streamflow) is presented. Then, a theoretical investigation is given, followed by a presentation of available models for flow of water from the soil through the plant to the atmosphere. Finally, some experimental work on field measurements of soil moisture regimes as affected by vegetation and root distribution, as well as moisture conditions in a sloping soil mass is reviewed.

From such a presentation it should then be possible to recognize existing gaps of knowledge and needs for research, theoretical as well as experimental.

2. Effect of Clear-Cutting on Watershed Behavior

Clear-cutting is a practice of forest harvesting which is justified primarily on economic grounds and convenience. In this process all timber over a certain minimum diameter is felled and removed (see Chap. 1). Slash remaining on the slope, for which there is no immediate use, is frequently burned. A number of experimental watersheds in different parts of the United States have been treated this way in order to compare their behavior, either with their pre-cutover condition or with an adjacent undisturbed watershed of similar topographical and ecological features. These experimental watersheds were calibrated over a period of years prior to clearing so that it was possible to correlate climatic factors, such as precipitation with their hydrologic response. Regrowth

of vegetation in such experimental plots was usually prevented by spraying herbicides during the next several years following felling.

The effect of clear-cutting was investigated with respect to the following parameters:

- effect on stream flow, water yield, and flooding
- effect on water temperature
- effect on nutrient cycling
- effect on deep seated stability of slopes

a. Effect on Water Yield

Watershed managers and forest hydrologists are mostly concerned how the removal of vegetation might affect the water balance and streamflow of a whole watershed. Many experiments have been carried out in the Appalachian hardwood forests, in particular at Coweeta Hydrologic Laboratory in North Carolina, which is in a humid temperate climate (Hewlett and Hibbert, 1961; Hibbert, 1969; and Hewlett and Helvey, 1970).

Hewlett and Hibbert (1961) found an increased supply of water to the streams, which was greatest during the first year after cutting. It then diminished in following years regardless of whether cutting was repeated or not. Quantitative predictions of the increase due to forest cutting was not possible in advance.

Reinhart (1964) reports on a commercial clear-cut on an Appalachian hardwood forest where the slopes were severely disturbed by

bulldozed skidroads. (It must be emphasized that in experimental watersheds, which serve strictly research purposes, the forest floor remains as undisturbed as possible since the timber is not removed for commercial purposes.) He found that the skidroads increased overland-flow due to direct precipitation on these skidroads and due to interception of subsurface flow by the skidroads. (Overland flow before clear-cutting was negligible.) Outside the skidroads, where the disturbance was light, no overland flow was observed. He concluded that the removal of trees per se does not necessarily result in a drastic increase in overland flow and the associated side effects (such as erosion, gullying, floods and disappearance of streams during periods of drought), but that increased storm runoff in cut-over areas during the growing season was largely due to decreases in available storage rather than changes in the proportions of surface and subsurface flow.

Hibbert (1969) compares the amount of evapotranspiration by grass cover to which a watershed was converted,with the original forest. He found that the amount of evapotranspiration by the grass cover was closely related to the amount of grass produced. During years when grass production was high, the water yield from the catchment was about the same as from the original forest. Only where grass production declined did the annual water yield increase gradually.

Similar conclusions were reached by Rutter (1968) who compared the water consumption of forests with that of grassland as a function of the

water deficit. By reviewing results from different parts of the world, he states that in areas where water supply is unlimited, the ratio $\frac{\text{evapotranspiration (grassland)}}{\text{evapotranspiration (forest)}}$ is about 0.8 to 1.0. In semi-arid and arid regions, where severe water deficits exist, this ratio reaches a minimum because of the greater rooting depth of trees. The amount of water withdrawn from the soil is usually in similar proportion to the rooting depth.

Hewlett and Helvey (1970) report on additional, more complete results from the Coweeta laboratory. An increase in stormflow of 11 percent was found after clear-felling of a mature hardwood forest. No forest material was removed and no overland flow occurred. They noticed that the effect of forest evapotranspiration on flood water released by deep soil slopes persists throughout the year, a result explainable by the variable source area concept of runoff (Hewlett, 1961b; Hewlett and Hibbert, 1967). (Many authors pay attention only to changes in peak flow rates rather than storm flow volumes as affected by forest cover.) Cutting of forest trees and shrubs definitely increased the quick flow volume, i.e., direct runoff, whereas the peak flow rate increase was not so important. All streamflow was entirely subsurface flow. Thus they could draw the obvious conclusion that the tendency for forests to evapotranspire more water than cleared land can indeed decrease major floor peaks far downstream by withholding more storm water than the cleared land. In the southern Appalachians this reduction is limited to about 20 percent.

Peak discharges in the headwaters in the absence of overland flow are chiefly a matter of rainfall intensity and channel factors, whereas stormflow volumes which are the real cause of floods will be affected by any factor that controls the storage capacity of the entire basin (such as the antecedent moisture content). In this case, therefore, greater evapotranspiration by full forest cover appears to be the important difference in the storage factor.

Hornbeck et al. (1970) studied an experimental watershed in the White Mountains of New Hampshire. After the trees were felled, they were left in place and sprayed with herbicide and no soil disturbance occurred. They found that most of the increased annual water yield occurred during the growing season and mostly during the critical low flow periods in late summer and early fall. In addition they observed slight changes in the timing of spring flows due to the speed up in snow melt on the cleared watershed.

Lewis (1968) reports about a study in the western United States (Sierra Nevada) where oakwood land was converted to grassland in order to improve forage production. The streamflow increased 4.5 inches per year due to a decrease in consumptive use.

b. Effect on Water Temperature

The principle source of energy for warming streams is the sun. Clear-cutting may increase the amount of sunlight reaching the stream. In a study on a small watershed in Oregon's coastal range, Brown and

Krygier (1970) found that the average monthly temperature of the water was increased by 14°F and the annual maximum temperature increased from 57 to 85°F one year after clear-cut logging. Temperature is an important water quality parameter, since it strongly influences levels of oxygen and solids dissolved in the stream. This, in turn, can influence the life of aquatic organisms, such as algae and, in particular, fish.

c. Effect on Nutrient Cycling

Borman et al. (1968) studied the loss of nutrients in a clear-cut watershed in New Hampshire and observed that clear-cutting tends to deplete the nutrients of an ecosystem by

1) reducing the root system able to remove nutrients from the leaching waters.
2) increasing water flow through the system by decreasing evapotranspiration.
3) removal of nutrients in forest products.
4) adding to the organic substrate available for immediate mineralization.

Cation losses (NH_4^+, K^+, and Al^{3+}) were particularly high and were quantitatively balanced by the high level of nitrate anions in the stream runoff.

d. Effect on the Deep Seated Stability of Slopes

Relatively few studies have been carried out to evaluate the influence of logging on mass wasting or creep of steep slopes. Gray

(1971) has reviewed the present state of the art and found that in most publications there seems to be a cause and effect relationship between deforestation and mass-soil movement. However, rational approaches, based on principles of soil mechanics and soil physics, are lacking and it is necessary to determine in which way the different factors (e.g., hydrology, root-soil interaction, soil properties, etc.) affect the balance of forces in the slope soil mantle.

It has been stated that the emphasis in this review is placed upon water flow in slopes with and without vegetation. Studies on the effect of vegetation on streamflow, as presented under Section 3.1.a, may be of direct interest to watershed managers, and these studies do in fact confirm the hypothesis that forests decrease the total soil moisture storage in a slope. They consider, however, the entire watershed and they do not say anything about the modification of the soil water regime in the slope as a function of location and time; and they do not investigate the physical basis of this behavior, such as the soil water potential. It is, however, the soil water potential which influences the mechanical and rheological properties of the soil material which, in turn, are crucial factors in determining the stability of a sloping mass. It is, therefore, important to review those studies which deal with transient moisture flow through soil and ways in which vegetation can alter the moisture regime in a soil mantle.

3. Studies of Flow Through Porous Media Without Considering the Influence of Vegetation

Studies on the unsaturated flow of water in soils began as early as 1911 when Green and Ampt devised an empirical infiltration law which, although approximative, can even today give satisfactory answers to certain questions dealing with infiltration (Childs and Bybordi, 1969; Bybordi, 1969).

Truly quantitative approaches, however, did not start until 1952, when Klute applied the diffusion equation to the flow of soil moisture with variable diffusivity (see Equation B.19) and solved it by a numerical procedure. Since then, numerical, as well as analytical solutions to various problems, have become available. In particular, with the improvement of calculation aids, such as digital computers, it was possible to solve more and more complex problems. It has been mentioned in Chapter 2 that, due to the nonlinear functional relationship of K(h) or $D(\theta)$, the flow equation can be solved only numerically. Under special circumstances, however, in particular if the medium is considered as semi-infinite, analytical or semi-analytical solutions may be obtained by using special mathematical techniques (such as the Boltzmann transformation, perturbation methods, Delta function methods and linearization). Philip (1957, 1958 and 1969) has analyzed all these methods and applied them to infiltration (or to absorption and desorption if infiltration is horizontal).

Steady-state problems of unsaturated flow are much easier to solve than transient ones and with much less computational effort. They also can be treated by using an electrical analog.

Tables 3.1 and 3.2 are an attempt to present the state of the art in unsaturated soil water flow in a concise form. The table form is adopted from Freeze (1969) but is updated and extended.

Table 3.1 shows some steady-state cases, among which the last two ones are of particular interest to flow of water in slopes, since they study the water flow in a tilted soil slab. (Note that the paper by Klute et al. treats a saturated case. However, it has been incorporated into this table because of its special nature.)

Table 3.2 summarizes all major articles which were available to the writer and which are connected somehow with unsaturated, transient flow in soils.

Any transient problem is fully characterized by

1) the flow equation

2) the functional relationships of $h(\theta)$ and K(h) or $D(\theta)$

3) the initial conditions

4) the boundary conditions

It is in this sense that the headings of the different columns in Tables 3.1 and 3.2 have been chosen.

Water flow can be one-, two-, or three-dimensional, and the soil can be homogeneous or non-homogeneous (usually layered). The soil

Table 3.1: Review of Treated Steady-State, Unsaturated, Isothermal Flow Problems

No.	Name and Date		Dimension			Soil		Problem Type(Description)
			1	2	3	Homogeneous	Non-homogeneous or layered	
1	Luthin and Day	1955		x		x		Flow above a sloping water table
2	Gardner	1958a	x			x		Steady-state vertical flow, evaporation from a soil in presence of a water table (const. evaporation rate), effect of a surface mulch
3	Reisenauer	1963		x	x	x	x	Flow from a canal or circular pond to a static water table
4	Klute et al.	1965		x		x		Saturated flow in an inclined soil slab at different slope angles and different slope length to depth ratios
5	Whisler	1969		x		x		Saturated-unsaturated flow in an inclined soil slab with constant rainfall rate

Table 3.1 (continued)

No.	Soil Moisture Functions Used						Method of Solution				Form of Solution					Comparison with Experimental Data	
	h(θ)		K(θ)orK(h)		D(θ)			Numerical									
	F	E	F	E	F	E	Analytical	Finite Differences	Electrical Analog	Finite Element	Moisture Content θ(x, y, z, t)	Pressure Head h(x, y, z, t)	Total Head H(x, y, z, t)	Flux Calculations	Evaporation Rate	Yes	No
1		x		x				x					x			x	
2			x				x					x			x		x
3		x		x				x			x		x				x
4							x					x	x	x			x
5			x						x			x	x	x			x

F: Mathematical expression
E: Empirical data from experimental curve or table

Table 3.2: Review of Treated, Unsteady, Unsaturated Flow Problems Under a Hydraulic Gradient

No.	Name and Date	Dimension					Soil		Hysteresis		Problem Type				
		1D			2D	3D					Infiltration				
		Vertical-up	Vertical-down	Horizontal			Homogeneous	Non-homogeneous or Layered	Yes	No	Const. Moisture Content at UB	Const. Pressure Head at UB or Ponded Water	Const. Rainfall Rate at UB	Other BC
1	Green and Ampt 1911		x				x			x		x		
2	Klute 1952a, 1952b			x			x			x	x			
3	Day and Luthin 1956		x				x			x				
4	Youngs 1957, 1958a, 1958b		x	x			x			x	x			
5	Philip 1957, 1958, 1969	x	x	x	x	x	x			x	x	x		
6	Gardner and Mayhugh 1958			x			x				x			
7	Gardner 1959	x		x			x			x				
8	Gardner 1962a		x				x			x				
9	Gardner and Hillel 1962	x					x			x				
10	Hanks and Bowers 1962	x	x	x				x		x	x			
11	Scott and Hanks 1962			x			x			x	x			
12	Ashcroft et al. 1962			x			x			x	x			
13	Rubin and Steinhardt, 1963, 1964		x				x				x	x		

Table 3.2 (continued)

No.	Problem Type				Initial Condition				Water Table (saturated zone) Present or May Develop					Soil Moisture Functions Used					
														h(θ)		K(θ)orK(h)		D(θ)	
									No		Yes			F	E	F	E	F	E
	Gravity Drainage	Evaporation	Capillary Rise	Redistribution after Infiltration	Constant Moisture Content or Pressure Head or Total Head	Specified Moisture Content or Pressure Head or Total Head	Equilibrium	Steady-state Flow	Semi-Infinite	Finite	Static	Quasi-Dynamic	Dynamic						
1					x				x										
2					x				x						x		x		x
3	x				x						x				x		x		
4				x	x				x						x		x		x
5					x				x										
6					x				x									x	
7		x			x				x	x						x		x	
8	x					x					x							x	
9		x			x					x								x	
10					x				x						x				x
11					x				x									x	
12					x				x										x
13					x				x					x		x			

F: Mathematical expression
E: Empirical data from experimental curve or table

Table 3.2 (continued)

No.	Method of Solution		Form of Solution									Comparison with Experimental Data	
	Analytical	Numerical	Moisture Content $\theta(x,y,z,t)$	Pressure Head $h(x,y,z,t)$	Total Head $H(x,y,z,t)$	Flux Calculations	Cumulative Infiltration	Cumulative Evaporation	Cumulative Drainage	Hydraulic Conductivity Profile	Depth of Wetting Front as a Function of Time	Position of Water Table (Moving Boundary)	Yes / No
1	Exact or Approximative	Finite Differences	x			x	x						Yes
2		Finite Element	x	x		x							Yes
3		Other	x			x	x						Yes
4	Exact or Approximative	Finite Differences	x			x	x						Yes
5		Finite Element	x			x	x				x		Yes
6		Other	x			x	x						Yes
7	Exact or Approximative	Finite Differences	x					x					Yes
8		Finite Element	x						x				Yes
9		Other	x					x					Yes
10	Exact or Approximative	Finite Differences	x	x		x	x						No
11		Finite Element	x			x							No
12		Other	x			x							Yes
13	Exact or Approximative	Finite Differences	x			x							Yes
		Finite Element											
		Other											

Table 3.2: Review of Treated, Unsteady, Unsaturated Flow Problems Under a Hydraulic Gradient

No.	Name and Date	Dimension					Soil		Hysteresis		Problem Type			
		1D			2D	3D					Infiltration			
		Vertical-up	Vertical-down	Horizontal			Homogeneous	Non-homogeneous or Layered	Yes	No	Const. Moisture Content at UB	Const. Pressure Head at UB or Ponded Water	Const. Rainfall Rate at UB	Other BC
14	Wang et al. 1964		x				x			x	x			
15	Liakopoulos 1965a, 1965b	x	x				x			x	x			
16	Remson et al. 1965		x				x			x				
17	Klute et al. 1965			x			x			x	x			
18	Whisler and Klute 1965		x				x		x			x		
19	Staple 1966	x	x				x		x		x			
20	Biswas and Nielsen 1966		x				x							
21	Rubin 1966(1)		x				x			x	x		x	
22	Rubin 1967	x	x				x		x					
23	Remson et al. 1967		x				x		x					
24	Wang and Lakshminarayana 1968		x					x		x	x			
25	Rubin 1968				x		x			x				x(2)
26	Ibrahim and Brutsaert 1968		x				x		x		x			

(1) Review paper
(2) Equilibrium pressure head for horizontal infiltration

Table 3.2 (continued)

No	Problem Type				Initial Condition				Water Table (saturated zone) present or May Develop					Soil Moisture Functions Used					
									No		Yes			h(θ)		K(θ)orK(h)		D(θ)	
	Gravity Drainage	Evaporation	Capillary Rise	Redistribution after Infiltration	Constant Moisture Content or Pressure Head or Total Head	Specified Moisture Content or Pressure Head or Total Head	Equilibrium	Steady-State Flow	Semi-Infinite	Finite	Static	Quasi-Dynamic	Dynamic	F	E	F	E	F	E
14				x		x			x						x		x		
15	x	x	x	x	x	x			x		x				x		x		
16	x	x		x		x						x			x		x		x
17					x					x(1)								x	
18							x				x				x		x		
19				x	x				x						x		x		
20				x					x						x				
21					x	x			x										
22		x		x		x			x					x		x			
23	x	x				x					x				x		x		
24	x				x					x					x		x		
25	x				x	x			x		x			x		x			
26				x	x	x			x							x			

F: Mathematical expression
E: Empirical data from experimental curve or table
(1) Horizontal infiltration into column of finite length

Table 3.2 (continued)

No.	Method of Solution				Form of Solution										Comparison with Experimental Data	
	Analytical	Numerical														
	Exact or Approximative	Finite Differences	Finite Element	Other	Moisture Content $\theta(x,y,z,t)$	Pressure Head $h(x,y,z,t)$	Total Head $H(x,y,z,t)$	Flux Calculations	Cumulative Infiltration	Cumulative Evaporation	Cumulative Drainage	Hydraulic Conductivity Profile	Depth of Wetting Front as a Function of Time	Position of Water Table (Moving Boundary)	Yes	No
14				x	x											x
15		x			x	x	x	x							x	
16		x			x					x	x					x
17		x			x			x	x							x
18		x			x	x		x								x
19		x			x											x
20					x										x(1)	
21		x			x			x				x				x
22		x			x											x
23		x			x											x
24		x			x			x	x						x	
25		x			x		x	x								x
26		x			x			x	x							x

(1) Experiments only

Table 3.2: Review of Treated, Unsteady, Unsaturated Flow Problems under a Hydraulic Gradient

No.	Name and Date	Dimension					Soil		Hysteresis		Problem Type				
		1D			2D	3D					Infiltration				
		Vertical-up	Vertical-down	Horizontal			Homogeneous	Non-homogeneous or Layered	Yes	No	Const. Moisture Content at UB	Const. Pressure Head at UB or Ponded Water	Const. Rainfall Rate at UB	Other BC
27	Hanks et al. 1969	x	x				x		x(3)			x	x	
28	Bresler et al. 1969	x	x				x		x(3)			x	x	
29	Freeze 1969, 1970	x	x				x		x			x	x	
30	Staple 1969		x				x		x(3)					
31	Hornberger et al. 1969				x		x			x				
32	Childs and Bybordi 1969		x					x		x		x		
33	Bybordi 1969		x					x		x				
34	Whisler and Bouwer 1970(1)		x				x		x			x		
35	Green et al. 1970(2)		x				x	x	x			x		
36	Hornberger and Remson 1970		x				x			x				
37	Gardner and Hillel 1970a, 1970b	x	x				x			x				
38	Guymon 1970			x			x			x				

(1) Paper compares different methods
(2) Two-phase problem
(3) For $h(\theta)$ only

Table 3.2 (continued)

No.	Problem Type				Initial Condition				Water Table (saturated Zone) Present or May Develop					Soil Moisture Functions Used					
									No		Yes			h(θ)		K(θ)orK(h)		D(θ)	
	Gravity Drainage	Evaporation	Capillary Rise	Redistribution after Infiltration	Constant Moisture Content or Pressure Head or Total Head	Specified Moisture Content or Pressure Head or Total Head	Equilibrium	Steady-State Flow	Semi-Infinite	Finite	Static	Quasi-Dynamic	Dynamic	F	E	F	E	F	E
27	x	x		x	x	x			x		x				x		x		
28		x		x	x				x						x		x		
29		x		x		x	x	x					x		x		x		
30				x		x									x		x		x
31	x(1)				x								x		x		x		
32									x								x		
33	x				x						x						x		
34	x					x		x	x		x				x		x		
35				x			x			x					x		x		
36	x					x							x(2)		x		x		
37		x		x	x				x					x		x		x	
38						x				x									

F: Mathematical expression
E: Empirical data from experimental curve or table
(1) 2-Dimensional flow in response to a falling water table
(2) Moving watertable as boundary condition

Table 3.2 (continued)

No.	Method of Solution				Form of Solution										Comparison with Experimental Data	
	Analytical	Numerical														
	Exact or Approximative	Finite Differences	Finite Elements	Other	Moisture Content θ (x, y, x, t)	Pressure Head h(x, y, z, t)	Total Head H(x, y, z, t)	Flux Calculations	Cumulative Infiltration	Cumulative Evaporation	Cumulative Drainage	Hydraulic Conductivity Profile	Depth of Wetting Front as a Function of Time	Position of Water Table (Moving Boundary)	Yes	No
27		x			x			x		x	x				x	
28		x			x			x		x					x	
29		x			x	x	x	x							x	
30		x			x		x								x	
31		x			x		x									x(2)
32	x(1)							x	x			x	x		x	
33	x(1)										x				x	
34	x	x							x		x				x	
35		x			x										x	
36	x	x			x									x	x	
37	x				x					x	x				x	
38			x		x											x

(1) Method of Green and Ampt
(2) Comparison with 3 one-dimensional groundwater models

moisture functions $h(\theta)$, K(h) and $D(\theta)$ can either be obtained directly from empirical curves in the form of a table or a fitted equation, or some approximate function [for example, exponential behavior (see Equation B. 5 and B. 22)] can be assigned to them if appropriate for the type of soil under consideration. In addition, hysteresis in $h(\theta)$ and K(h) or $D(\theta)$ may be taken into account which might be given by a number of scanning curves within the hysteresis loop. The type of problem is characterized by its initial condition and its boundary conditions (upper and lower boundary for one-dimensional problems).

Many articles treat more than one problem but seldom combined problems, such as simultaneous redistribution of infiltrated soil water and evaporation. Of particular interest are those problems with a finite lower boundary and those with a saturated zone. Very few problems have been treated as composite (i. e., unsaturated-saturated) ones where the water table is dynamic and responds to an infiltration or evaporation by a rise or decline, respectively. Freeze (1969) was the first person to present a comprehensive treatment of an integrated saturated-unsaturated system with a dynamic groundwater table behavior.

A quasi-dynamic boundary condition is one where the movement of the water table is prescribed in advance. In all cases where the method of solution is indicated as analytical, only partial answers have been obtained, such as the cumulative infiltration or evaporation, or the depth to the wetting front. Alternatively, complete analytical solutions

must be based on simplified soil moisture functions. Many useful approaches in this sense have been worked out by Youngs (1957, 1958a, 1958b), Gardner (1959, 1962), Gardner and Mayhugh (1958), and Gardner and Hillel (1962, 1970a, 1970b), but whenever the moisture content or soil water potential distribution as a function of space and time is desired, a numerical solution is necessary. Most solutions are compared with experimental data. This is necessary since it is in general not possible to prove rigorously that the numerical solution for nonlinear partial differential equations converges to the correct answer. All numerical methods linearize the soil moisture functions by various techniques,and it is not always known to what extent this affects the final results.

Most numerical methods apply the finite difference technique. Only recently (Guymon, 1970) has the finite element method been applied to transient problems. This is possible by transforming the partial differential equation into a variational problem on which the finite element method then can be applied. This approach promises further progress in the study of complex problems, since it can account for a large variety of boundary conditions and can also save considerable computer time.

A look at Table 3.2 shows that only two 2-dimensional problems have been solved (Hornberger et al., 1969; Rubin, 1968) and only one of these shows a relatively generalized solution procedure. Two-dimensional problems require a large computational effort due to the nonlinearity of the soil-moisture parameters. Nonlinearities always require

iterative methods, and it is possible only by trial and error to find the optimal iteration parameters.

Infiltration has been treated in numerous articles by Rubin and Steinhardt (1963, 1964), Rubin (1966), Philip (1957, 1958, 1969), Whisler and Bouwer (1970) and others based on the flow equation and appropriate boundary conditions. Analytical considerations applied to this equation yield a qualitative description of the infiltration process as well as the necessary and sufficient conditions for the occurrence on ponding. Numerical solutions then furnish quantitative information on the moisture profiles and infiltration rates during non-ponding, preponding (rain controlled, and ponded (pressure controlled) rainfall infiltration, but the theory is not yet applicable where the soil exhibits soil-moisture parameter hysteresis which involves simultaneous wetting and drying of the soil. Also, no method exists today for analyzing one-dimensional rainfall infiltration into a finite profile (for example, a soil with impervious bedrock at its lower boundary) or rainfall into a layered soil. It should therefore be obvious that the mathematical treatment of microhydrology in soils and in particular slopes is still far from being complete.

4. Studies of Soil-Water-Plant-Atmosphere-Interactions

The anatomical and physical basis for water uptake and water flow through the plant and subsequent transpiration has been outlined in Chapter 2. In this section the models and methods which have been applied

to treat quantitatively water uptake in connection with transpiration and the water condition in the soil and in the conducting elements of the plant are reviewed.

Moisture flow to plant roots has been studied by a number of investigators. Basically there are two different approaches. Some studies are based on the radial flow of moisture to a single root (Gardner, 1960; Cowan, 1965; Molz et al., 1968). This can be considered as a microscopic approach. Other studies deal with the removal of moisture from the root zone as a whole, without considering explicitly the effects of individual roots. This then can be termed a macroscopic approach (Gardner and Ehlig, 1962a; Gardner, 1964; Whisler et al., 1968; and Molz and Remson, 1970).

In a microscopic study an individual root may be considered as a cylindrical sink of infinite length. The soil moisture flow equation is written in cylindrical coordinates (see Equation B. 23) and solved with appropriate boundary conditions at the root surface and at some distance r_{max} away from the root. At the root surface the moisture flux, moisture content, or a combination of both, may be specified as a boundary condition.

In a macroscopic approach, the flow to individual roots is ignored and the overall root system is assumed to extract moisture from each differential volume of the root zone at some rate q, where q is a function of space, moisture content, root density, etc. Because diffusivity may

be very small in the immediate vicinity of a root as compared to the surrounding soil, one may expect a tendency for uniform moisture extraction to occur even in moderately dense root systems (Molz et al., 1968).

The moisture removing roots may then be represented as an extraction (negative source term) q in the soil moisture flow equation (see Equation B. 13).

Table 3. 3 tries to summarize some of the published literature which may contribute to the development of a workable soil-water-plant-atmosphere model. In this review more emphasis is put on the description of macroscopic models.

The first quantitative approach to water uptake by roots was presented by Gardner (1960), based on a microscopic approach. He analyzed the variation of suction in a soil around an infinitely long, cylindrical root which had a prescribed rate of water uptake per unit length. The soil moisture parameters D and K were assumed to be constant and thus enabled an analytical treatment of the problem using the flow equation (B. 24). Initially the soil was at a uniform moisture content. The solution to this problem revealed that the distance at which any given suction occurs increases as the square root of time. This means that over a natural time period and for typical root radii and diffusivities, water can normally move only on the order of a few centimeters.

Table 3.3: Review of Some Problems on Soil-Water Plant Relationships

No.	Name and Date		Problem Type					Soil		Plant				Pot. Transpiration Rate		Dimension of Water Flow in Soil
			Steady-State	Unsteady	Water Uptake by Roots		Flow Through Plant	Transpiration	Homogeneous	Non-homogeneous or Layered	Constant ψ_{pl} Throughout Plant	Variable ψ_{pl}	Root System Uniform	Root System Non-uniform	Constant Rate	Fluctuating	
					M	S											
1	Gardner	1960	x	x		x		x	x		x		x				1 (1)
2	Gardner and Ehlig	1962a	x	x	x				x		x			x			1
3	Gardner and Ehlig	1962b	x		x				x		x				x		1
4	Gardner and Ehlig	1963	x	x	x			x	x		x		x		x		1
5	Gardner	1964		x	x				x		x			x			1

M: Macroscopic (root system)

S: Microscopic (single root)

(1) Radial flow

Table 3.3 (continued)

No.	Soil Moisture Functions Used						Hysteresis		Description of Problem
	h(θ)		K(θ)orK(h)		D(θ)		Yes	No	
	F	E	F	E	F	E			
1		x		x		x		x	Water availability to plants. Transient water uptake by an infinitely long cylindrical root. Steady-state solution for flow in a hollow cylinder. Distribution of water content and suction with distance from root. Effect of suction on transpiration rate. Uptake of water in a soil profile.
2				x				x	Steady-state and unsteady greenhouse experiments to determine relative magnitude of impedance to water movement in soil and plant. Experimental determination of fraction of water movement through the soil in the root zone.
3				x				x	Experimental determination of relative impedance to water movement in soil and plant, under a constant uptake rate.
4									Influence of suction on transpiration. Experimental determination of transpiration rate as a function of soil suction or water content. Transpiration rate is about proportional to θ, when soil water is limiting
5		x		x				x	Water uptake by a non-uniform root system as a function of root distribution and uptake rate. Neglects water movement in the soil.

F: Mathematical expression E: Empirical data from experimental curve or table

Table 3.3 (continued)

No.	Method of Solution		Form of Solution										Comparison with Experimental Data	
	Analytical	Numerical	Moisture Content $\theta(x, y, z, t)$	Pressure (suction) Distribution $\tau_{soil}(q, t)$; $\tau_{soil}(x, y, z, t)$	Flux Calculations	Potential at Root Surface	Potential in Plant ψ_{pl}	Water Uptake Rate q	Transpiration Rate as a Fct. of θ or ψ_{soil} or ψ_{pl} or Root Density	$\psi_{root\ surface} - \psi_{soil}$	Cumulative Transpiration	Impedance in Soil-Plant System	Other	Yes	No
1	x		x	x		x		x	x	x				x	
2			x	x	x				x					x	
3												x		x	
4	x								x		x			x	
5	x		x	x		x								x	

Table 3.3: Review of Some Problems on Soil-Water Plant Relationships

No.	Name and Date		Problem Type					Soil		Plant				Pot. Transpiration Rate		Dimension of Water Flow in Soil
			Steady-State	Unsteady	Water Uptake by Roots		Flow Through Plant	Transpiration	Homogeneous	Non-homogeneous or Layered	Constant ψ_{pl} Throughout Plant	Variable ψ_{pl}	Root System Uniform	Root System Non-uniform	Constant Rate	Fluctuating	
					M	S											
6	Ehlig and Gardner	1964		x				x	x		x				x		1
7	Slatyer and Gardner	1965(1)	x		x		x	x	x		x			x			1
8	Cowan	1965	x			x		x	x		x		x		x	x	1
9	Woo et al.	1966		x	x		x	x		x		x		x		x	1
10	Molz et al.	1968		x		x			x								1

M: Macroscopic (root system)

S: Microscopic (single root)

(1) Review paper

3.3: (continued)

No.	Soil Moisture Functions Used						Hysteresis		Description of Problem
	h(θ)		K(θ)orK(h)		D(θ)		Yes	No	
	F	E	F	E	F	E			
6									Experiments to determine transpiration rate as a function of the DPD in the leaves of different plants
7								x	Reviews general aspects of water flow from the soil to the leaves and from the leaves to the air and describes the governing factors.
8	x				x			x	Flow of water to a plant root and periodic extraction of soil water. Transpiration rate as a factor of potential rate $_{soil}$, critical leaf water potential and root density.
9		x		x				x	Simulation of transpiration process on an analog computer. Introduces storage factors and dynamic system gains by the method of computer-controlled adaptive control systems.
10					x			x	Radial flow of soil moisture to a single vertical root in an infinite soil mass, initially at uniform moisture content. Introduces concept of potential soil moisture availability.

F: Mathematical expression

E: Empirical data from experimental curve or table

Table 3.3 (continued)

No.	Method of Solution		Form of Solution											Comparison with Experimental Data	
	Analytical	Numerical	Moisture Content $\theta(x, y, z, t)$	Pressure (Suction) Distribution $\tau_{soil}(q, t)$; $\tau_{soil}(x, y, z, t)$	Flux Calculations	Potential at Root Surface	Potential in Plant ψ_{pl}	Water Uptake Rate q	Transpiration Rate as a Fct. of θ or ψ_{soil} or ψ_{pl} or Root Density	$\psi_{root\ surface} - \psi_{soil}$	Cumulative Transpiration	Impedance in Soil-Plant System	Other	Yes	No
6									x					x	
7															
8	x		x	x					x						x
9	x(1)			x		x	x		x						x
10		x	x		x										x

(1) Simulation on analog computer

Table 3.3: Review of Some Problems on Soil-Water Plant Relationships

No.	Name and Date		Problem Type						Soil		Plant				Pot. Transpiration Rate		Dimension of Water Flow in Soil
			Steady-State	Unsteady	Water Uptake by Roots		Flow Through Plant	Transpiration	Homogeneous	Non-homogeneous or Layered	Constant ψ_{pl} Throughout Plant	Variable ψ_{pl}	Root System Uniform	Root System Non-uniform	Constant Rate	Fluctuating	
					M	S											
11	Whisler et al.	1968	x		x			x	x		x		x		x		1
12	Whisler et al.	1970	x			x			x								1
13	Molz and Remson	1970	x	x	x				x					x	x		1

M: Macroscopic (root system)

S: Microscopic (single root)

Table 3.3 (continued)

No.	Soil Moisture Functions Used						Hysteresis		Description of Problem
	h(θ)		K(θ)orK(h)		D(θ)		Yes	No	
	F	E	F	E	F	E			
11			x					x	Steady-state evapotranspiration from a soil column using a negative source term in the flow equation. The lower boundary is a water table. Indicates shorting effect qualitatively.
12	x		x		x(1)			x	Radial steady-state flow of solution and solute to a single root, modelled as a hollow cylinder, which represents the soil shell. It is assumed that there is no interaction between the solute and solid phase, also no hydrodynamic dispersion.
13						x		x	Develops extraction terms depending on depth, transpiration rate and moisture content. Compares steady-state soil moisture flux with experiments and deduces from this an effective root density which is used for the unsteady case.

F: Mathematical expression E: Empirical data from experimental curve or table

(1) Solute dependent

Table 3.3 (continued)

No.	Method of Solution		Form of Solution											Comparison with Experimental Data	
	Analytical	Numerical	Moisture Content $\theta(x,y,z,t)$	Pressure (suction) Distribution $\tau_{soil}(q,t)$; $\tau_{soil}(x,y,z,t)$	Flux Calculations	Potential at Root Surface	Potential in Plant ψ_{pl}	Water Uptake Rate q	Transpiration Rate as a Fct. of θ or ψ_{soil} or ψ_{pl} or Root Density	$\psi_{root\ surface} - \psi_{soil}$	Cumulative Transpiration	Impedance in Soil-Plant System	Other	Yes	No
11		x	x	x	x								x(1)		x
12	x	x		x	x	x							x(2)		x
13		x	x		x									x	

(1) Source function profiles
(2) Concentration ratio profiles

The results of the analysis for a single root, in which the relationship between suction at the root surface, water uptake, water potential in the leaf, etc., were investigated were in turn generalized for water uptake in a soil profile, taking soil and plant factors into account. This can be stated in the following way: The rate of uptake from a given soil volume is proportional to the effective root length in that volume, the hydraulic conductivity of the soil, and the difference between the average soil water potential and the potential at the boundary between root and soil. Quantitatively, this can be expressed as

$$q \sim K \cdot L \left(\psi_{root} - \psi_{soil} \right) \tag{3.1}$$

where q = water uptake rate per unit volume (assumed to be equal to the transpiration rate) when integrated over the root depth

K = hydraulic conductivity of soil

L = effective length of root system per unit volume (effective root density)

ψ_{soil} = soil water potential at midway between two neighboring roots (energy/volume)

ψ_{root} = potential at root surface

If we take flux through the plant as proportional to the driving force, as we do in the soil, we may write:

$$q \sim \frac{d\theta}{dt} = \frac{\psi_{leaf} - \psi_{soil}}{j} \tag{3.2}$$

and

$$j = j_p + j_s = \frac{B \cdot r_{pl}}{L} + \frac{B}{KL} \tag{3.3}$$

where: j = sum of impedances to water movement in the soil and in the plant from a unit volume of soil to the leaves

r_{pl} = resistance to water movement in the plant from a root tip (independent of location in the soil) to the leaves

j_p, j_s = impedance to water movement in the plant and soil respectively

B = a geometric constant

Hence, one may write

$$q = \frac{\psi_{leaf} - \psi_{soil}}{\frac{B \cdot r_{pl}}{L} + \frac{B}{KL}} \qquad (3.4)$$

In a later publication, Gardner and Ehlig (1962a), and Gardner and Ehlig (1962b) try to evaluate the relative magnitude of the impedance j_p and j_s by experimental results. Data from transpiration experiments with birdsfoot trefoil, pepper and sorghum show that at sufficiently high suctions $j_s \gg j_p$ Under these circumstances, j is proportional to $\frac{1}{LK}$. It was also found that when the soil suction was below 0.6 bar, the impedance was largely in the plant and j_s is negligible. When the suction was greater than 1 or 2 bars, the soil became the limiting factor, which means that j_p is negligible in a first approximation.

Experiments were also carried out with nonunifirom root systems. Such a root system sets up suction gradients in the soil and causes water to move through the soil itself. In fact, considerable amounts of water moving through the soil directly were observed in steady-state (water table at the bottom) and nonsteady (initial saturation) greenhouse experiments.

The water movement within the root zone cannot be neglected even though the soil water content may be below the so-called field capacity. This water generally enters the root system at a higher elevation.

Gardner and Ehlig (1963) and Ehlig and Gardner (1964) investigated the influence of the soil water potential and the leaf water potential on the transpiration by plants. Starting with saturation, transpiration rates were determined as a function of suction or water content. The suction in the leaves was determined by thermocouple psychrometer measurements. Thus a functional relationship between the transpiration rate and the leaf suction could be determined experimentally (see Figure 3.1).

$$Tr = \int_{\substack{\text{root}\\\text{zone}}} q \, dz = f\,(\psi_{leaf}) \qquad (3.5)$$

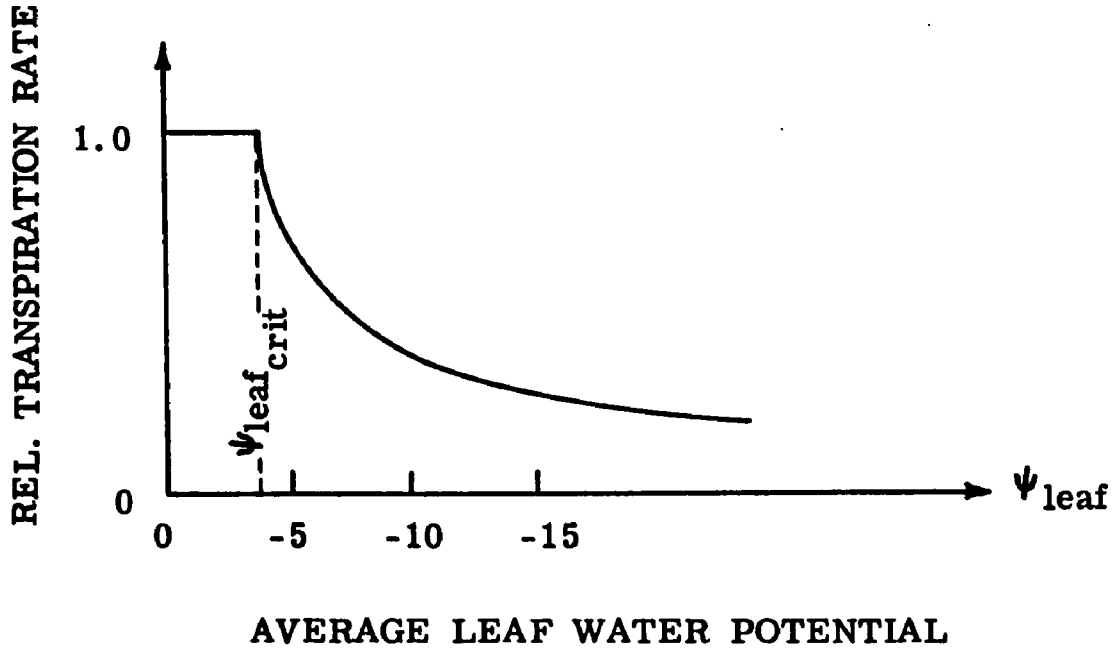


Figure 3.1. Schematic representation of the relation between transpiration rate and leaf water potential.

Results showed that above a characteristic value of ψ_{leaf} for each plant, the transpiration rate was equal to the potential transpiration rate. Below this value, the transpiration rate tended to decrease, rapidly at first, and then more slowly with decreasing ψ_{leaf}. Thus it was possible by combining Equation (3.5) with Equation (3.4) to determine directly a relationship between transpiration and soil water potential or soil water content.

The analysis showed that similar relationships or graphical plots are obtained between transpiration rate and leaf water potential on the one hand and between transpiration rate and soil water potential on the other. This is because the difference between ψ_{leaf} and ψ_{soil} tends to assume a more or less constant value when the plant starts wilting; the value depends on the plant type.

The authors also demonstrated that the lower limit of water available for transpiration is well beyond the -15 bar value. They estimate that -30 to -50 bars would be more realistic values. This may not be important in sandy soils but it can make a real difference in clay soils.

Cowan (1965) developed a model which uses three main functions. The first describes soil water flow to the roots in terms of the water potential of the soil mass, ψ_{soil}, the water potential at the root surface ψ_{root}, the hydraulic conductivity K and the root density and yields similar results to those of Gardner (1960), discussed earlier.

The other functions describe the influence of leaf water potential, and resistance to liquid flow in the plant, on stomatal aperture and hence on the capacity of the plant to transpire at the potential rate. It is assumed that the rate of water flow, and hence of transpiration, is proportional to $(\psi_{root} - \psi_{leaf})$ and also that the sum of the internal plant resistances j_p be effectively constant. A critical value of ψ_{leaf} $(= \psi_{leaf_{crit}})$ is adopted at which stomatal closure reduces transpiration to a degree which prevents further decline in ψ_{leaf}. At ψ_{leaf} values higher than $\psi_{leaf_{crit}}$, it is assumed that transpiration proceeds at the potential rate. A so-called supply function q_w is introduced which is defined by

$$q_w = \frac{\psi_{leaf_{crit}} - \psi_{root\ surface}}{j_p}$$

and

$$Tr = \int_{\substack{root \\ zone}} q_w \cdot dz \qquad (3.6)$$

In an unwilted plant then, transpiration takes place at the potential rate $Tr = Tr_p$, whereas in a wilting plant the uptake rate is equal to the supply function $q = q_w$, which is a function of $\psi_{leaf_{crit}}$, the soil water potential ψ_{soil}, the root density and the internal impedance of the plant. The value of the plant resistance r_{pl} is obtained from the rate of transpiration Tr^o, at which

$$\psi_{leaf} = \psi_{leaf_{crit}} \quad \text{and} \quad \psi_{\substack{root \\ surface}} = 0, \text{ i.e.}$$

$$Tr^{o} = \int \frac{\psi_{leaf_{crit}}}{\frac{B}{L(z)} \cdot r_{pl}} \cdot dz \quad \text{and} \quad r_{pl} = \frac{\psi_{leaf_{crit}}}{Tr^{o}} \frac{\int L(z) \cdot dz}{B} \qquad (3.7)$$

Tr^{o} signifies the maximum possible rate of transpiration the plant can sustain without wilting, and hence without stomatal closure. It may be determined experimentally. Typical results of Cowan's analysis are shown in Figures 3.2 and 3.3. The expected relationship between transpiration and soil water potential is given for three different levels of potential transpiration. The figures show that as the soil dries, there is initially no effect on transpiration, but when K falls to a level at which stomatal closure commences $\psi_{leaf} = \psi_{leaf_{crit}}$, because of decreasing ψ_{soil}, a progressive decline in transpiration occurs. This stage is reached at higher values of ψ_{soil} with higher rates of potential transpiration, since steeper gradients of ψ_{soil} are required to sustain flow, resulting in lower levels of ψ_{root} and hence of ψ_{leaf} at any given value of ψ_{soil}. It can be seen that when very high potential transpiration rates occur, the actual daily transpiration might not at any stage equal the potential daily transpiration.

In Figure 3.3 the effect of the root density on the relationship between transpiration and ψ_{soil} is depicted. In this case this is done for an intermediate level of potential transpiration. It can be seen as root density increases, higher potential rates of transpiration can be sustained until much lower values of ψ_{soil} exist, smaller values of $\psi_{soil} - \psi_{root}$ being adequate to sustain flow at the desired rate.

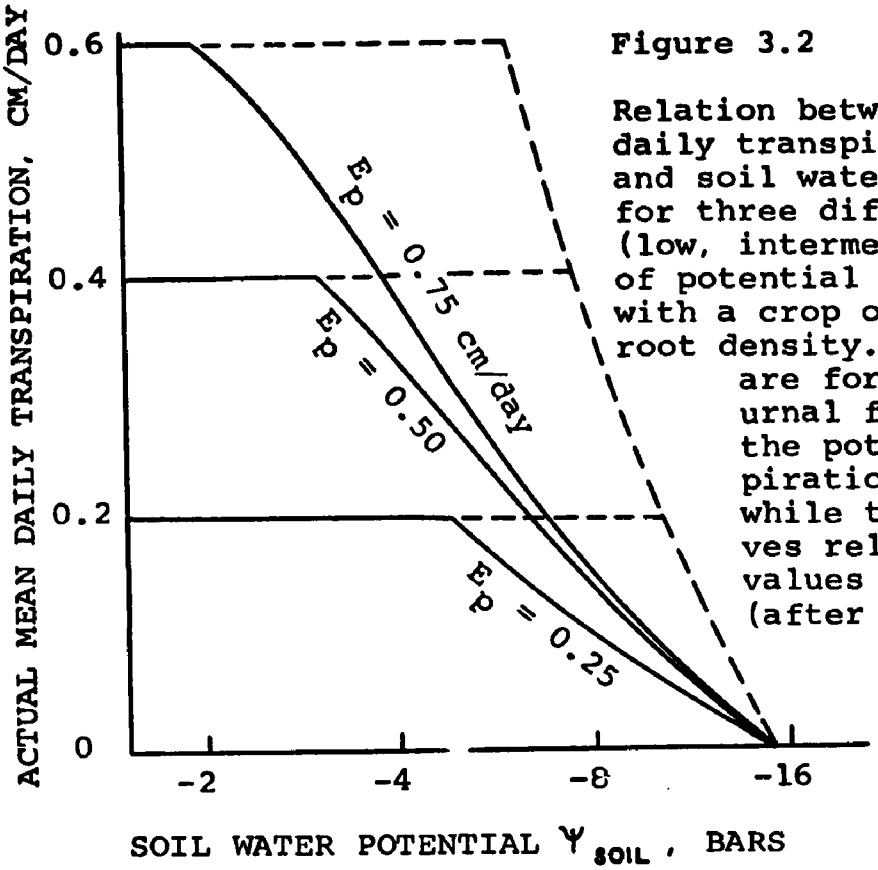


Figure 3.2

Relation between actual daily transpiration rate and soil water potential Ψ_{soil} for three different rates (low, intermediate and high) of potential transpiration with a crop of intermediate root density. The full curves are for periodic diurnal fluctuations of the potential transpiration rate E_p, while the broken curves relate to steady values of E_p (after Cowan 1965).

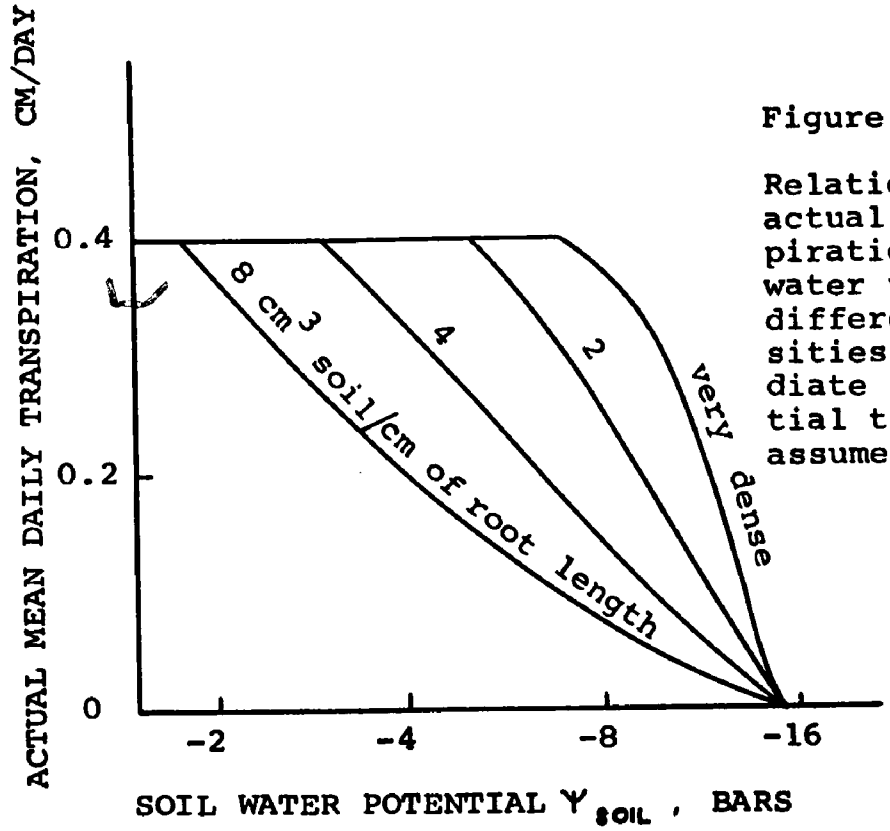


Figure 3.3

Relation between actual daily transpiration rate and soil water potential Ψ_{soil} for different root densities. An intermediate rate of potential transpiration is assumed (after Cowan 1965).

A quite different approach to a transpiration model was presented by Woo et al. (1966). This model starts out from the van den Honert concept (see p. 40) which treats the water movement through the plant as a catenary process. But this assumes a steady-state movement and does not account for dynamic system characteristics. In order to describe the transient, dynamic nature of the transpiration process, storage factors must be included. This is achieved by including gain constants into the model, defined for each part of the system. The systems gain is a function of both the transpiration rate and the soil water conditions. Thus diurnal and seasonal fluctuations in temperature, humidity, light, etc., can be described by including the system gain in the dynamic equation for water transport. The dynamic equations express the time response lag of the water suction in the plant system with respect to the leaf transpiration.

These equations are then simulated on an analog computer which then yields the resulting dynamic characteristics of water transfer through the soil-plant-atmosphere system in response to changes in environmental conditions.

Whisler et al. (1968) presented the first numerical treatment of an integrated soil-water plant system by a macroscopic approach, using the flow equation with a negative source term. The problem treats steady-state evapotranspiration from a soil column with a static water table at the lower boundary. The top boundary condition is specified by

the constant evapotranspiration rate and its partitioning between plant transpiration and soil evaporation. The source term is given by

$$q(z) = L(z) \cdot K(h) \, (h_{pl} - h) \qquad (3.8)$$

where:

$L(z)$ = root density distribution (length of root per unit volume)

K = hydraulic conductivity of the soil

h_{pl} = water head in the root tissue (assumed constant throughout plant)

h = soil water head

The results, although not verified by independent experiments, show that the source term approach is feasible. The analysis presents pressure head profiles, flux profiles, effects of rooting depth on the flow and investigates also the shorting effect. The latter refers to the transfer of water via the root system from the lower part of the rooting zone to the upper, where it flows out into the soil again, because the pressure head of the water in the root is greater than the pressure head of the soil water. It is possible to predict such a phenomena, at least qualitatively, by this model.

In both Cowan's and Whisler's model, the extraction term depends directly or indirectly on the water potential in the plant. This is reasonable since the transpiration rate is not an independent variable, it is determined by climatic conditions and soil water availability. Therefore, a source term should not contain the actual transpiration rate as a

prescribed variable, as was done for example by Molz and Remson (1970), but rather as a boundary condition.

5. Field Measurements of Soil Moisture Regimes under Forested and Barren Areas

The knowledge of soil moisture depletion during various seasons is important for evaluating moisture stresses in vegetation and for the management of land under various cover types.

Some of these studies show interesting results or conclusions with respect to the influence of vegetation on the moisture regime, such as the water extraction pattern and the influence of root distribution.

Hoover et al. (1953), working in the South Carolina Piedmont, measured the soil moisture under a young (10 years old) loblolly pine plantation, using fiberglass electrodes, down to a depth of 66 inches. They report that an average of 86 percent of the rainfall measured in the open reached the ground under the pines. About one-fifth of this amount could be attributed to stem flow. They observed that water was withdrawn most rapidly from the zone where it was most readily available regardless of depth and despite the greater concentration of roots in the surface layer. Roots in the surface layer grow abundantly

there only because conditions are favorable to root growth (aeration) and not because a large mass of roots is needed there to extract water. Pine roots were found to a depth of 8 feet and removal from depths of 5 feet occurred at a rapid rate.

Metz and Douglass (1959) measured soil moisture regimes under several Piedmont cover types near Union, South Carolina over a period of 5 years. The plots were located on nearly level ridges and upper slope positions. The soil type was a heavy red clay of 3 to 6 feet in thickness. The 3 major cover types considered were a forest cover (loblolly pine plantation and shortleaf pine-hardwood stand), a broomsedge field, and a barren plot. Soil moisture measurements were made down to a depth of 66 inches.

Precipitation in this area is fairly uniform throughout the year but the character of the rainfall is different. Whereas winter rains are gentle and of long duration, which makes infiltration and therefore recharge of the soil profile possible, summer rains are short and of high intensity so that most of the precipitation is lost by runoff. Thus droughts during the late summer months are not unusual.

The soil moisture variation was studied at different depths by dividing the profile arbitrarily into different zones. The loss of water from the vegetated plots in the upper regions was due to the

combined effect of evaporation from the soil and transpiration by the plants (and was similar for all the vegetated areas). On the nonvegetated plot all upward moisture loss was due to evaporation. In the upper 15 inches the water losses from the barren soil were less than from either one of the other plots. This was probably due to the much smaller infiltration rate of the barren soil which limited the recharge. In the next lower zone (15 to 30 inches), more roots were present in the pine plot than in the broomsedge plot. As a consequence, a lower moisture content could be observed for the pine plot than for the broomsedge plot. Similar patterns could be observed at succeeding depths. Effects of recharges (unless under very heavy rains) were small at greater depths and almost non-existent for the barren plot. In the deepest zone (54 to 66 inches) recharge in general did not occur until early spring and then depletion began throughout the summer without interruptions under the pine plot. For the barren and the broomsedge plot there was almost no change in soil moisture at this depth during the whole growing season.

It is apparent from these observations that the roots by their withdrawal of moisture have a pronounced effect on the water content in the 66 inches deep zone studied. The authors concluded, based on their observations, that the rate of soil moisture loss is dependent on depth

of the soil. The root concentration at the surface is greatest and causes the top soil layer to lose moisture at a much faster rate than the lower layers. The rate of depletion decreases with depth, and the wilting point is reached first at the top if no recharge occurs.

Figure 3.4 shows the moisture condition (total available water) for the entire 0 to 66 inches profile during the year of 1952 for the pine plantation, the broomsedge field, and the barren area. Recharge of the soil beneath the pine cover did not occur until March. The high moisture content under the broomsedge plot compared to the one under the barren area is due to the greater infiltration capacity of the first one, which facilitated recharge during summer storms in late summer.

Using a special technique to derive curves of soil moisture loss from drying periods during the growing season for a given period of time, the authors were able to plot depletion curves versus time of drying. Figures 3.5 and 3.6 show such curves for the 30 to 66 inches zone and the 0 to 66 inches zone for all three types of plots. The curves for the 30 to 66 inches zone clearly indicate the difference in root concentration in that zone. The rate of moisture loss from the pine plantation (Figure 3.5) is constant throughout the 40-day period; the same can be said for the other two plots although they tend to level off a bit. It seems that moisture at greater depth where no broomsedge roots were present did have almost no influence on the depletion rate for this type of cover. The decrease in moisture at this depth from the barren plot is

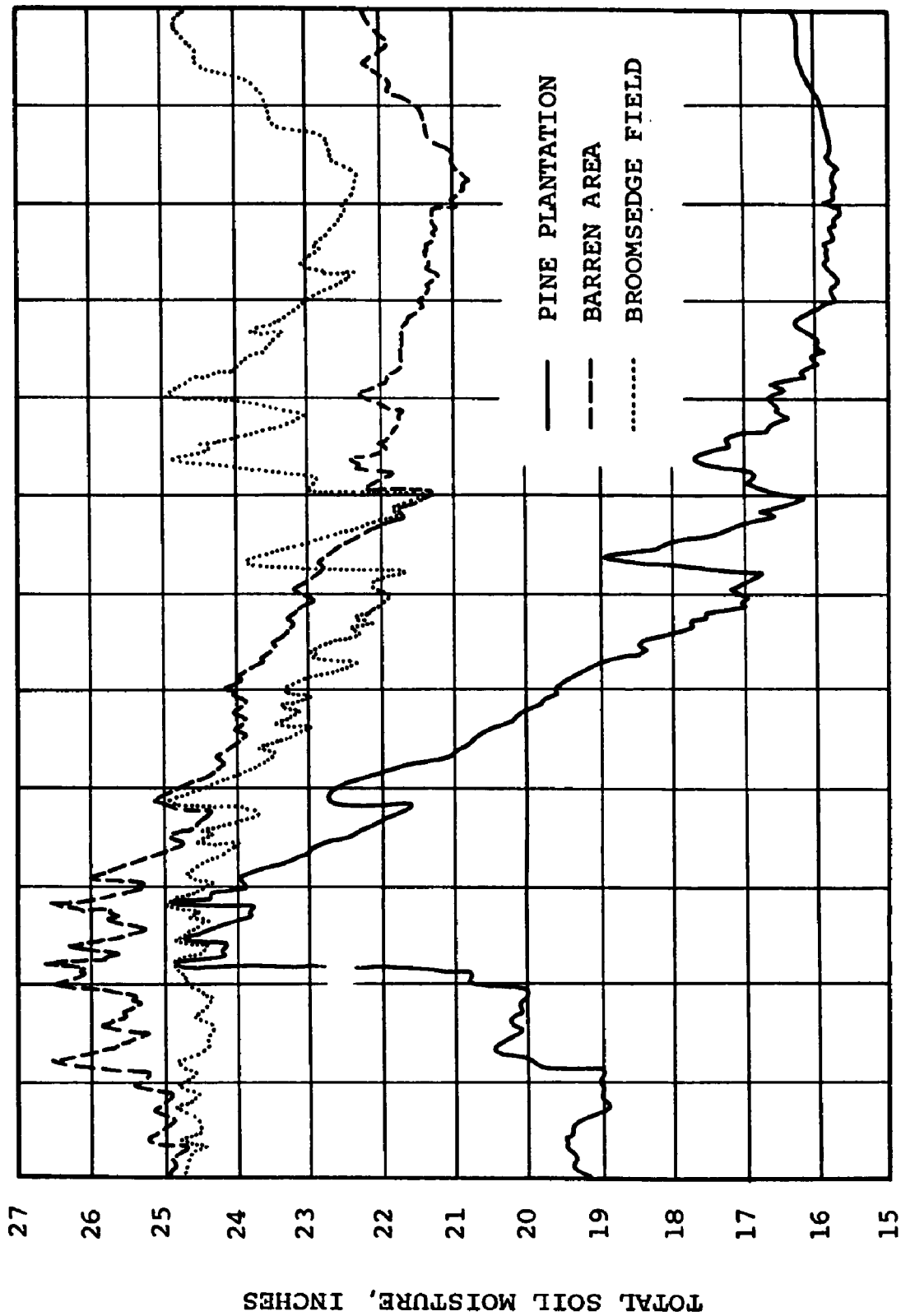


Figure 3.4 Soil moisture regime in a pine plantation, a barren area, and a broomsedge field for the 0 to 66-inch depth of soil (1952) (after Metz and Douglass 1959).

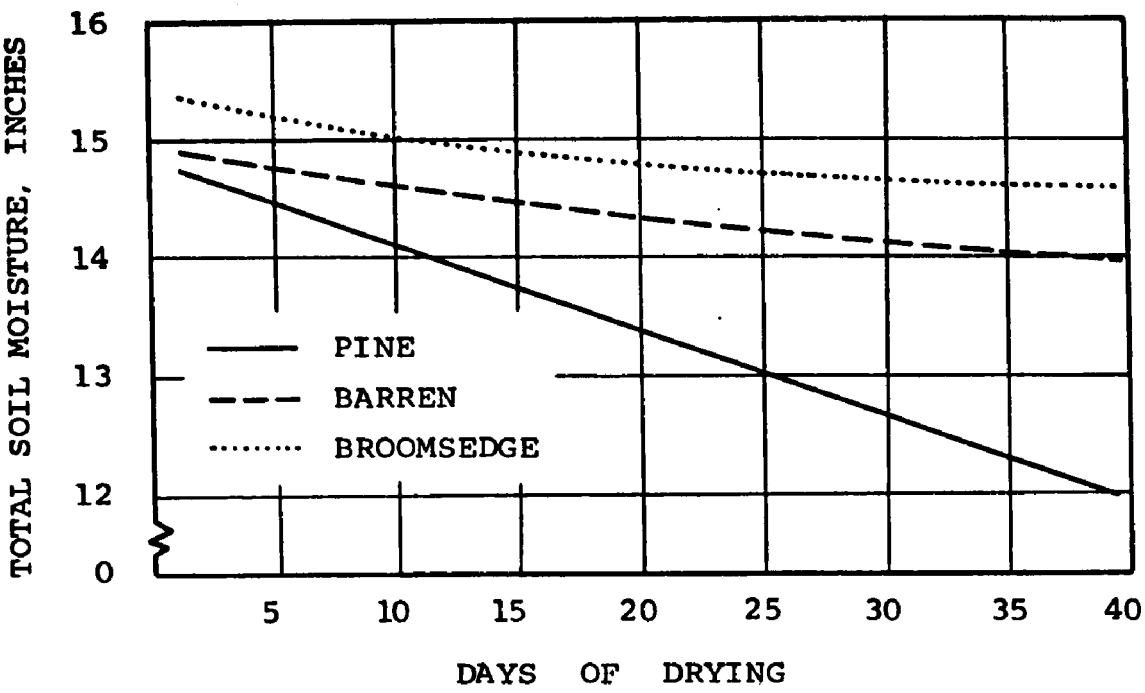


Figure 3.5 Soil moisture depletion of the 30- to 66-inch zone of a pine plantation, a broomsedge field, and a barren plot (after Metz and Douglass 1959)

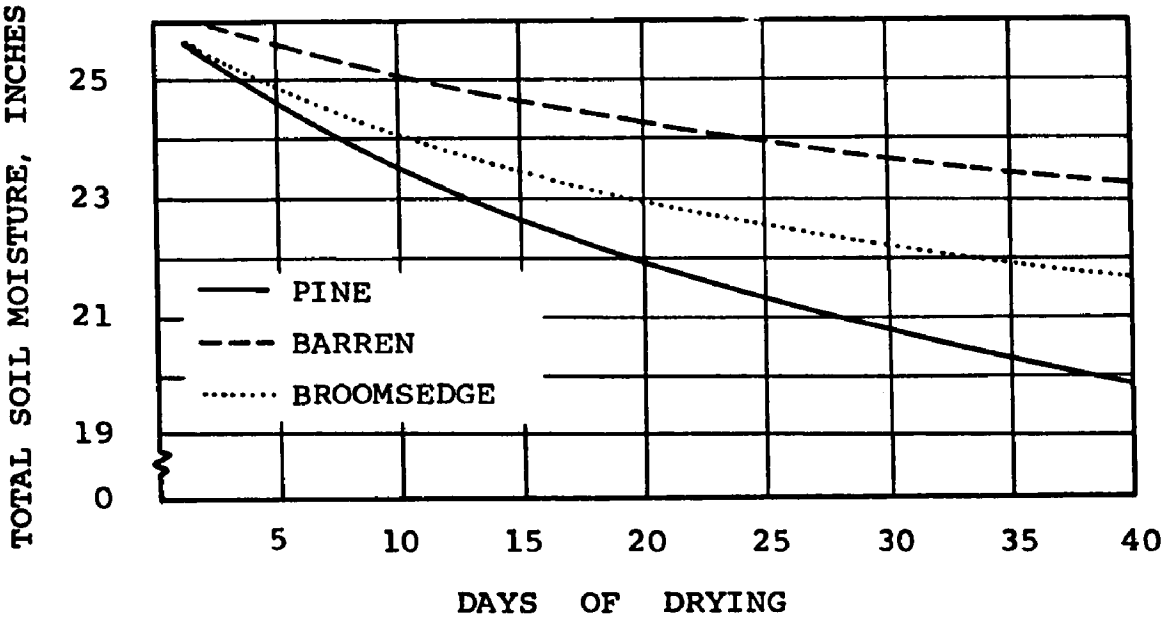


Figure 3.6 Soil moisture depletion of the 0 to 66-inch zone of a pine plantation, a broomsedge field, and a barren plot (after Metz and Douglass 1959).

probably due to capillary action and upwards movement of water to dryer zones.

For moisture depletion of the total soil profile (Figure 3.6), the same tendency is recognized again. Deep roots of the pine stand were able to extract water at greater depths relative to the broomsedge. The low permeability of this clay soil accentuated this difference by hindering upward migration of water beneath the broomsedge roots.

Summarizing, the authors conclude that their study supports the assumption that deep-rooted species such as trees can transpire more water than shallow-rooted species and thereby create a maximum storage for winter precipitation.

In another study, Patric et al. (1965) tried to separate absorption of water under forest from other factors. They compared transpiration by forest stands from plastic-covered plots (50 x 50 feet in size) in two contrasting soil types and climates. Recharge and evaporation was thus eliminated. Trenches 3.5 feet deep surrounding the plots isolated the root system within the plot from the outside. Most of the roots below 3 feet were vertically oriented.

The two sites were a mountain site in North Carolina and a Piedmont site in South Carolina. The mountain site was stocked with an oak-hickory stand and the soil profile was relatively homogeneous; a 3-foot sandy clay-loam was overlying a sandy loam extending beyond 20 feet in depth.

The Piedmont site was vegetated with a 21-year old loblolly pine (Pinus taeda) plantation. The soil profile was less uniform--a slowly permeable clay loam of 8 feet thickness overlaid a sandy loam which extended down to more than 20 feet. Roots could be found at depths of 20 feet.

For both plots the rainfall was evenly distributed throughout the year and calculated potential evapotranspiration (after Penman) was also similar. The plots were located on ridge sites in order to eliminate surface and subsurface movement from higher areas.

Figure 3.7 presents some of the results of this study. Winter rains had wet the entire 20-foot profile of the mountain plot and by April the matric potential was below 0.1 bar throughout the profile. In the piedmont soil, however, only the upper 8 feet were fully wetted and the soil beneath entered the growing season with matric potentials already above 3 bars. This is probably due to the low permeability in this horizon. In the mountain plot some drainage also occurred simultaneously with absorption until about the end of May, i.e., until the suction reached about 0.2 bar. However, the water involved in drainage is estimated to be small; a precise separation is quite difficult. Initial soil water absorption rates were high in the upper zones of the profile and almost no water was absorbed from the lower regions. The roots decreased more or less exponentially with depth as determined from a root count. Later in the season, however, the extraction rates tended

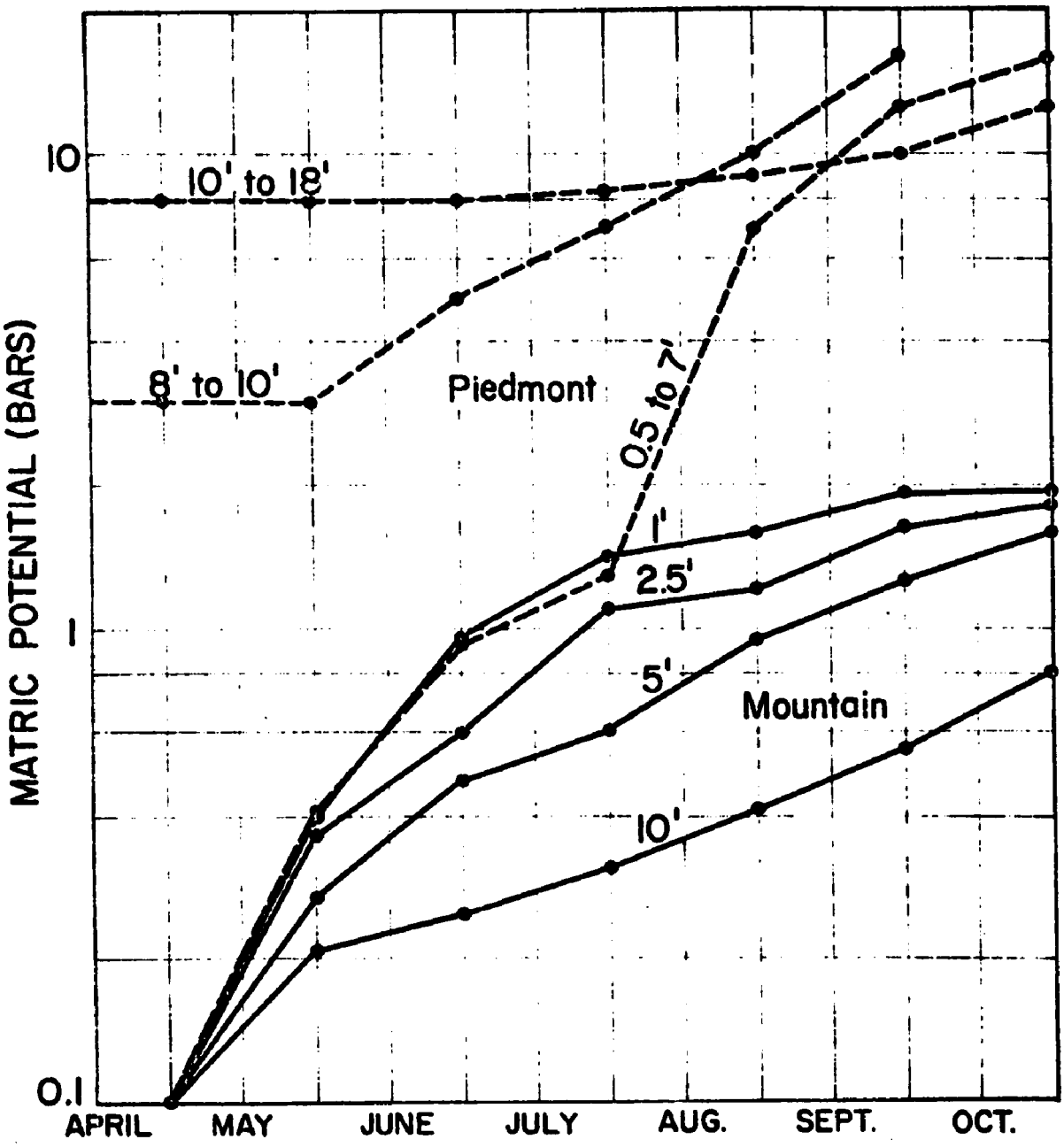


Figure 3.7 Average matric potential by depth in mountain and piedmont plots (after Patric et al., 1965).

to become more and more uniform with depth for the entire profile. The loss at lower depth can be the result of both local absorption and upwards movement through the soil, as was observed by Gardner and Ehlig (1962a) in laboratory studies with a nonuniform root system (see p. 90). Reduction in root density seems to be compensated by increasing soil water conductivity resulting in equal absorption from all depths.

Vazquez and Taylor (1958) arrived at a similar conclusion from a laboratory experiment. In this experiment water uptake by a nonuniform root system was simulated by porous cups with an applied suction in a soil column. The number of cups decreased with depth. From the results they postulated that for a steady-state extraction, a suction gradient would be established at any point in the soil, such that equal amounts of water would be taken up from each volume of soil, regardless of the root density.

Another way of stating the results of these two investigations is as follows: If the entire soil is depleting from field capacity, each zone contributes to the total transpiration in proportion to its root density. However, if a dry soil is wetted by a summer storm, this moisture will be depleted rapidly from the surface zone because of the high root concentration there before it has time to infiltrate into deeper layers (Zahner, 1965). The data by Patric et al. verify on a large scale the theory that early absorption from a uniformly wet soil is mostly related to root concentration and that later absorption tends toward equal extraction

with depth, even down to 20 feet. Nonhomogeneous profiles cause uneven moisture distribution and lead to somewhat irregular early extraction; nevertheless, early extraction is related primarily to root concentration. The experiment of Patric et al. also shows that if matric suction is kept low, because of frequent rains, most of the transpiration water will come from densely rooted zones near the surface. In humid areas, therefore, the later phases of uniform absorption from all depth would seldom occur and we can expect little change in soil moisture in the bedrock zone in such climates. Only during long periods of drought, i.e., in semi-arid climates, will soil water beyond the rooting depth return to the surface.

Soil moisture regimes under forest cover in terms of available water can be predicted with surprising accuracy for different soils. This has been demonstrated by Zahner (1965) who employed special depletion functions dependent on the soil moisture tension for different soils. As long as the soil moisture tension was less than 2 bars, depletion took place at the potential rate. The 2 bar limit occurs at different percentages of available moisture, depending on the texture of the soil (see Figure 2.3). When the soil became drier than 2 bars, daily withdrawal rates were equal to some fraction of the potential evapotranspiration. Surface recharge (recharge storage) resulting from summer storms was always assumed to be depleted first before the remaining water in the profile (main storage) was further depleted. Only when the

recharge of the two storage accounts exceeded the field capacity of the total soil profile was the excess credited to a surplus moisture account, the main storage account set to field capacity and the recharge account set to zero. At this point depletion started again from field capacity. Potential evapotranspiration was calculated according to the Thornthwaite method, i.e., from temperature data alone. This method gave very good results for loam and sandy soils. In the case of clay soils, such as the one encountered in the work by Douglass and Metz (1959) (see Figure 3.4), it is more difficult to use because the amount of storm runoff in this heavy soil is often difficult to estimate. Also in soils with low permeability some of the stored water in the lower zones is not available for transpiration. Such soils also may not even be at field capacity at the beginning of the growing season. The method works only for areas of uniformly stocked forest stands and is not suitable for sparsely stocked areas or range lands. It also cannot take into account lateral movement of soil moisture as it may occur in steep slopes.

Zinke (1959) presented the data of a study of soil moisture regime in a semi-arid climate (San Dimas Experimental Forest in Southern California) on a forested and a barren lysimeter plot. The lysimeters were 20.8 x 10.5 feet in area and 6 feet deep. The soil was a sandy clay loam. The moisture content was recorded at various depths down to 66 inches by means of electric fiberglass soil moisture units. The vegetated lysimeter was stocked with 12-year-old (in 1957) Pinus coulteri. There were 19 trees approximately 12 feet in height on the lysimeter.

The runoff from the barren lysimeter was almost twice as much as from the pine covered one, which means that there were significant differences in the quantities of precipitation entering the soil.

During the winter rainfall period, the lysimeter profiles were wetted to field capacity (28 percent by volume) or even above. Then during the summer dry period, the soil under the pine dried out over its full depth to the wilting percentage (about 11 percent by volume), whereas the soil in the barren lysimeter only dried to a depth of about 12 inches. Soil moisture depletion of the total profile for the vegetated and the barren lysimeter are shown in Figures 3.8 and 3.9 as a function of time. In these figures all of the dates are adjusted to the same initial conditions of soil moisture. In reality this is not the case, since the drying season (or occurrence of the last rainfall) may start at a different date each year. The curves indicate that depletion is linear with time initially and tends then to level off. Zinke fitted an exponential function with empirical coefficients

$$Q_{sm} = Q_{sm_o} \cdot e^{-\kappa \cdot t} \tag{3.9}$$

where:

Q_{sm_o} = initial soil moisture

Q_{sm} = actual soil moisture

t = time

The constant κ was 0.0097 for the pine covered lysimeter and 0.0069

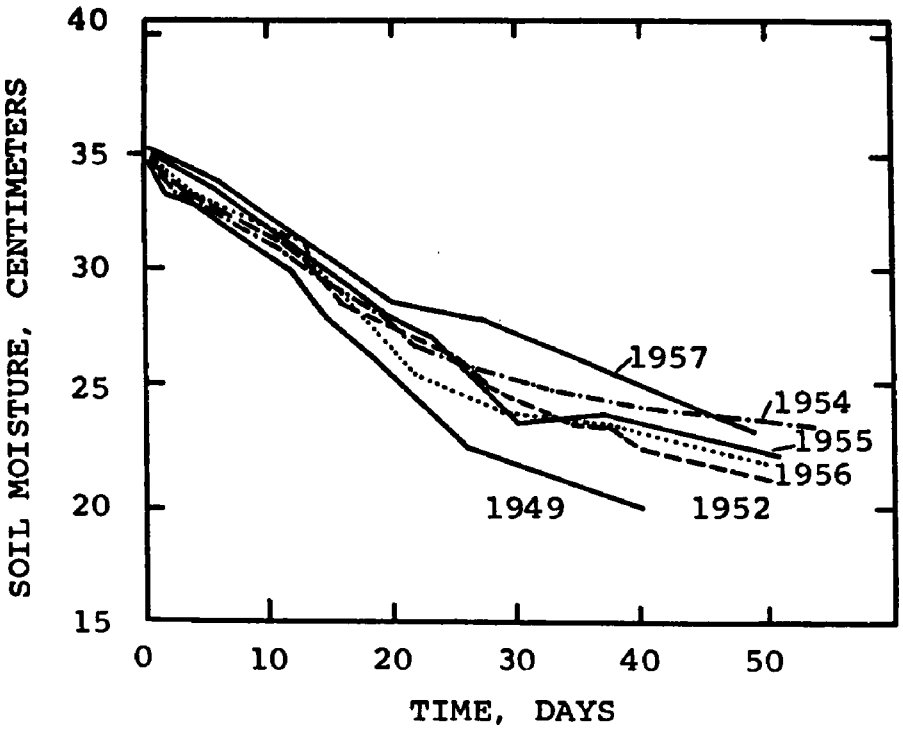


Figure 3.8 Comparable portions of depletion curves for total soil moisture content of Pinus coulteri lysimeter adjusted to the same initial time (after Zinke 1959).

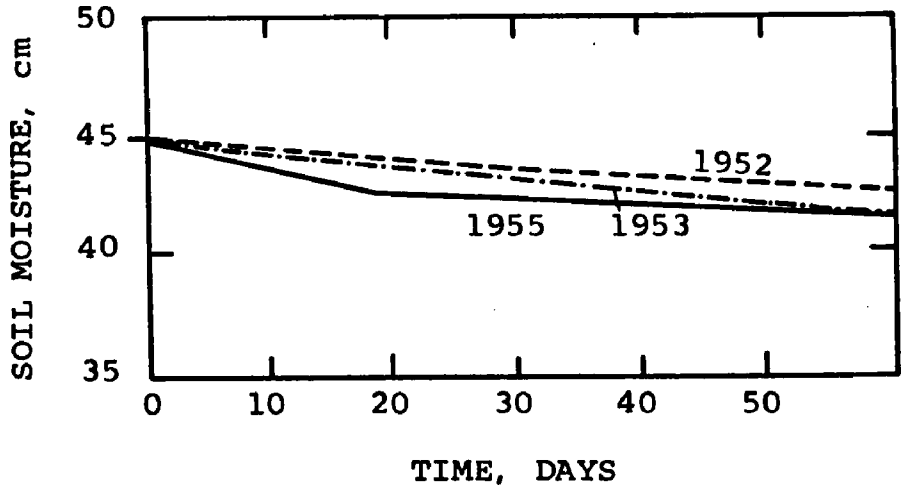


Figure 3.9 Comparable portions of depletion curves for total soil moisture content of barren lysimeter adjusted to the same initial time (from data by Zinke 1959).

for the barren one. For small times Equation (3.9) can easily be approximated by

$$Q_{sm} = Q_{sm_o} \cdot (1 - \kappa t) \qquad (3.10)$$

since the second term in the series expansion $\frac{\kappa^2 t^2}{2!}$ is small. Equation (3.10) represents a linear relationship, as mentioned previously.

The soil moisture depletion of various depth horizons of the lysimeters took place in the following pattern. Each soil layer was successively drained beginning with the uppermost layer. After the desiccation of that layer had reached a certain point, the next lower layer began to lose moisture. This is pictured in Figure 3.10. One may see that each layer dries approximately at the same rate (the soil is homogeneous) and the depletion rate $\frac{d\theta}{dt}$ is approximately constant until moisture becomes limiting and all curves converge at the wilting percentage. Moisture extraction does not reach uniformity as postulated by Vazquez and Taylor (1958) or Patric et al. (1965), but this is because the available water at the top is exhausted before water can move up from deeper layers in response to the moisture gradient. Water is then absorbed while it is moving upwards. As can be seen from Figure 3.10, there is always a region of more or less uniform absorption. If water can move only slowly and root density is low, there will always be such a lag in absorption.

The bare soil dried according to a quite different pattern as seen from Figure 3.11. The drying rate decreased with depth and reached

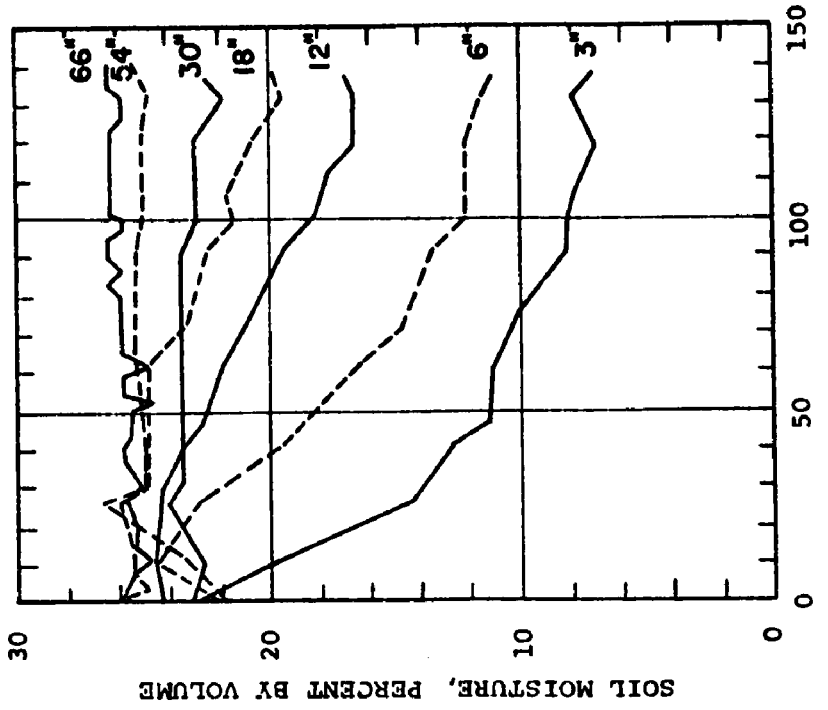


Figure 3.11 Soil moisture depletion at various soil depths in the barren lysimeter beginning May 1, 1952. (after Zinke, 1959.)

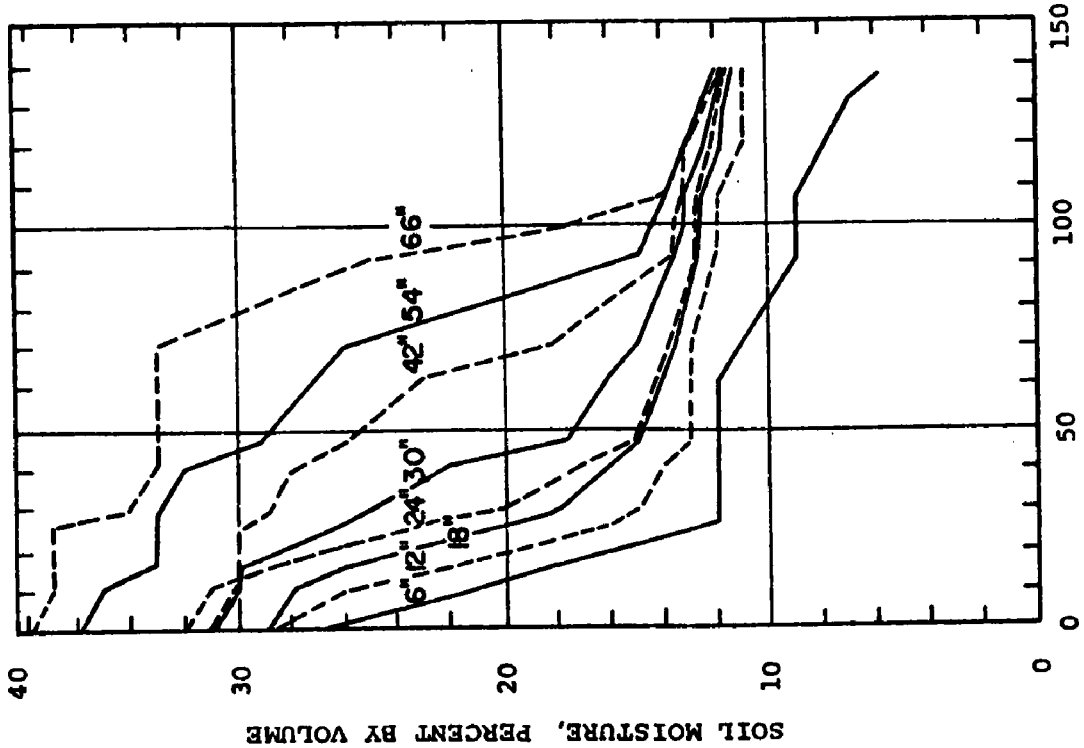


Figure 3.10 Lysimeter soil moisture depletion at various soil depths under Pinus coulteri beginning May 1, 1952. (after Zinke, 1959.)

finally zero at about 30 inches depth. Depletion in this profile is due to evaporation only and upwards movement of water can only occur in response to a soil water potential gradient.

6. Soil Moisture and Water Outflow Measurements in a Sloping Soil Mass without Vegetation

Hewlett (1961a) and Hewlett and Hibbert (1963) report on experiments with a sloping bin. The concrete trough measured 3 x 3 x 45 feet and was constructed on a 40 percent slope. The soil used was a natural sandy loam. At its lower end the bin drained to a static water table. After initial saturation by a sprinkler system, the structure was covered with plastic film to prevent evaporation and allowed to drain for several months until the outflow was negligible. This represents a two-dimensional gravity drainage problem with simple boundary conditions and should be accessible to mathematical analysis. Soil moisture tension was determined by tensiometers and by the nuclear moisture probe. Three phases of outflow could be observed and all were of the form

$$\overline{Q} = \overline{a} \cdot t^{-\overline{b}} \qquad (3.11)$$

where $\overline{Q}$ is the outflow rate (m^3/sec) and t is the time.

$\overline{a}$ and $\overline{b}$ are constants whose magnitude depends on the drainage phase.

The first phase was characterized by the drainage of the saturated portion, the second phase was a transition phase during which the larger pores of the soil drained (field capacity) and the last phase, which

lasted until the end of the test, represented the outflow from the unsaturated zone below field capacity.

The soil moisture tension at each point tended to approach an equilibrium value which is equivalent to the height above the static water table. They also found that the logarithm of moisture content decreased linearly with the logarithm of time. The rate of decrease seemed to be higher for points farther above the water table than for points at a lower elevation with respect to the outflow level.

From this study the authors conclude that the unsaturated zone in a slope can be considered as dynamic storage and should not be overlooked as an important contribution to sustained baseflow in mountain streams.

7. Discussion and Summary

The survey of the literature shows that neither experimental nor mathematical model studies have been made to investigate the hydrological regime of planar slopes with vegetation.

A few one-dimensional soil-water-plant models have been proposed among which Cowan's model is probably the most complete one. An attempt to model two-dimensional water flow in a sloping soil mass subjected simultaneously to evaporation and transpiration has never been made.

Field studies on soil moisture regimes were usually made at more or less level spots in order to avoid lateral flow which is difficult to

account for in water balance methods, but the studies clearly show the influence of a deeper rooted forest on total depletion in contrast to a shallow rooted grass cover or a barren plot. The influence of vegetation on the infiltration capacity is difficult to estimate and should be evaluated directly from field data.

Lysimeter experiments are useful because of the homogeneity of the soil profile which facilitates data interpretation. Unfortunately, Zinke (1959) does not give the water retention properties of the soil used. It would be desirable to perform a lysimeter experiment with soil water potential measurements at many points. This would make possible the computation of hydraulic heads and, assuming K(h) is also known, fluxes within the soil as well.

Models should also allow for a variety of boundary conditions which may occur in nature. For example, if the slope ends at its lower boundary in a water table, the soil water regime will be quite different than the case in which the lower boundary is exposed to air only. This again speaks in favor of mathematical models, since results for changes in boundary conditions are more readily available and less time consuming than in experimental models.

Gardner and Ehlig's laboratory investigations on the water uptake by roots and on the transpiration rate provide very useful guidelines for constructing mathematical models and are necessary for the fundamental understanding of the physical processes taking place. However, a massive

screening and synthesizing effort is still required before all this information can be effectively incorporated into a useful and generally applicable model for predicting the soil water regime under a variety of field conditions.

CHAPTER 4

A HYDROLOGIC MODEL STUDY OF A FORESTED AND A CLEAR-CUT SLOPE

In view of the lack of adequate experiments a model study was undertaken at The University of Michigan Botanical Gardens. The aim of the study was to investigate the unsaturated flow of water in steep slopes under known but realistic boundary conditions and to evaluate the influence of vegetation on the soil moisture regime. The experiment was carried out in a greenhouse in order to avoid problems caused by seasonal variations in climate out-of-doors. The experimental set-up, instrumentation and the test program are described in subsequent sections of this chapter.

1. Experimental Set-Up

a. Model Slope and Soil Mantle

In order to model a slope, a 12-foot long, 3-foot wide, and 11-inch deep wooden trough was constructed. Three, 4x6-inch beams to which the trough was attached served as carrying elements. A requirement of the study was a variable tilt angle in the model slope. Accordingly, a steel frame built out of iron pipes and I-beams was erected in order to support one end of the trough in a raised position. The frame

had to be designed in such a way that it could be assembled inside the greenhouse. Hence, the size of the components was limited by the clearance of the doors to the greenhouse. By means of a chain hoist hooked to the top of the frame it was then possible to lift and lower the bin and thus bring it into the desired positions. The bin rested on specially designed supports at each end. Three interchangeable supports, each of different height, were built for the upper end, and this made it possible to position the bin at three different slope angles, namely, 10, 20 and 30 degrees. Sliding of the bin was prevented by angle irons bolted across the wooden beams at the bottom of the bin. Figures 4.1 and 4.2 show the bin at an angle of 30 degrees from the side and from the back, respectively. (In this picture, the support built to produce a 30-degree angle was not used. Instead the necessary height was achieved by putting concrete blocks underneath the support for 20 degrees until the required elevation was reached.)

The soil used to fill the trough was an artificial mixture, consisting of 30 percent per weight AGSCO #16 fine sand, 40 percent AGSCO #140 silica flour, and 30 percent ball clay. Ball clay is a Kaolinite clay ($Al_2O_3 \cdot 2SiO_2 \cdot 2H_2O$) containing traces of α-Quartz, as revealed by an X-ray analysis. Approximately 0.5 percent lime was added to this mixture in order to reduce the soil acidity. The pertinent soil properties of this soil are summarized in Table 4.1. A grain size analysis curve is presented in Figure 4.3. This artificial mixture can

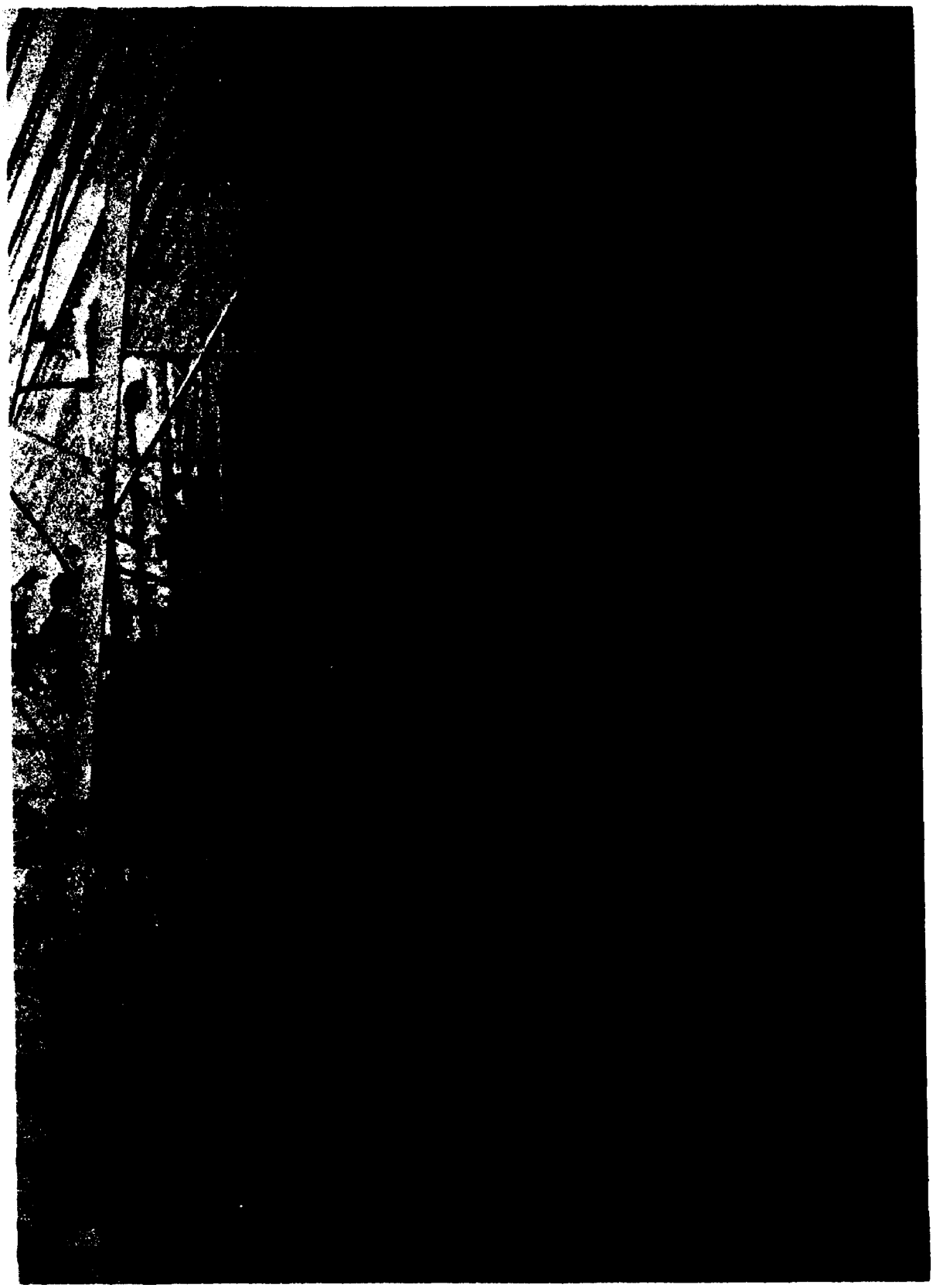


Figure 4.1 Side view of tilting soil bin at a slope of 30°.

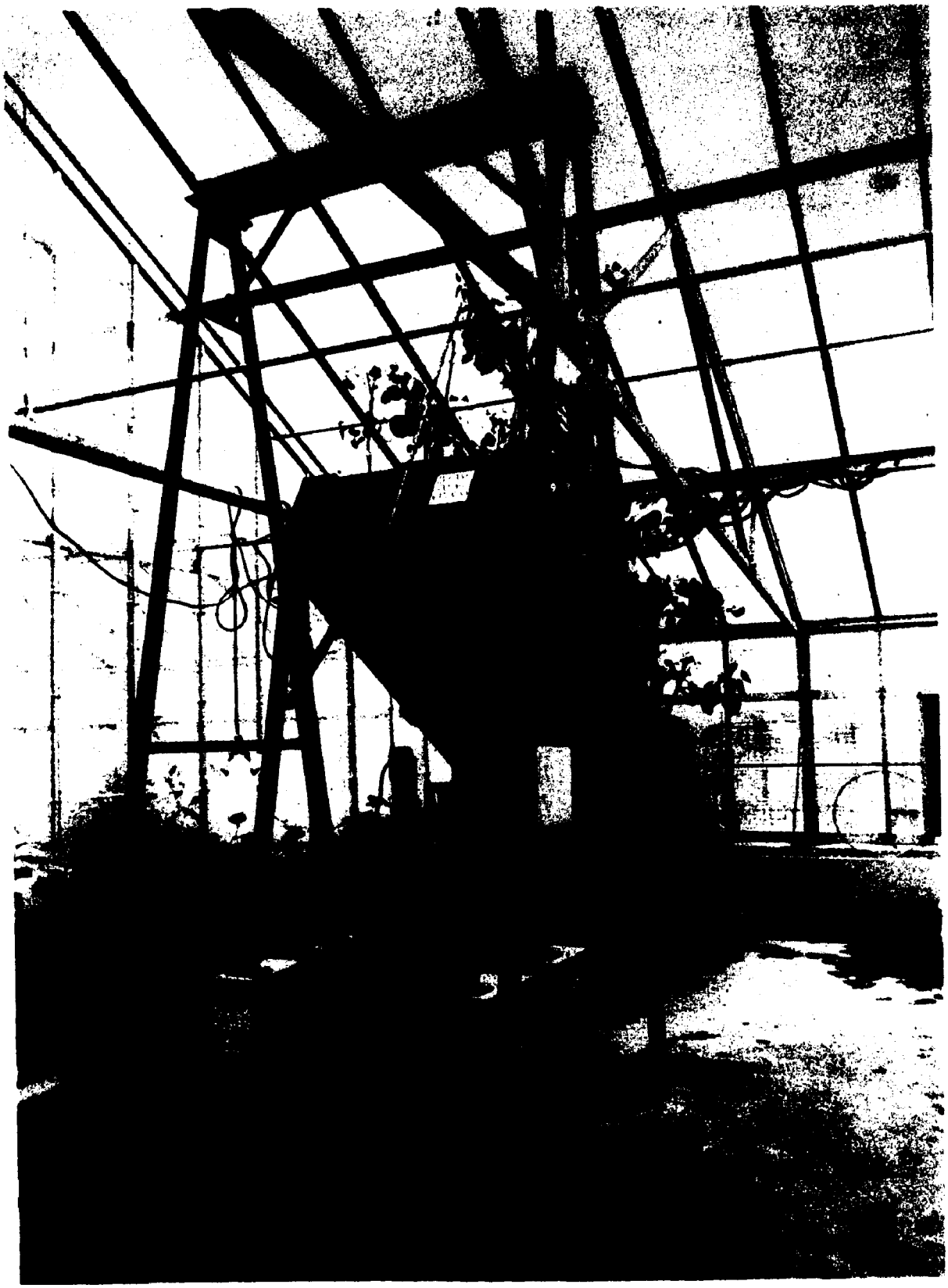


Figure 4.2 Rear view of tilting soil bin at a slope of 30 degrees. The frame, fitted between the greenhouse trusses, serves to lift or lower the bin.

Table 4.1: Summary of Soil Properties

Soil Composition:	30% AGSCO #16 Fine Sand 40% AGSCO #140 Silica Flour 30% Ball Clay (Kaolinite)
Specific Gravity:	2.64
Liquid Limit:	28.0%
Plastic Limit:	17.4%
Compaction: (Harvard Miniature Compaction Test)	$w_{opt} = 13.5\%$; $\gamma_{dry_{max}} = 121$ lb/ft^3
Bulk Density:	Soil in Bin: 89.7 ± 2.5 lb/ft^3 1.438 ± 0.040 gr/cm^3 Extruded Soil: 106 lb/ft^3 = 1.700 gr/cm^3
Hydraulic Conductivity of Saturated Soil in Bin:	$2-4 \cdot 10^{-6}$ cm/sec
Water Retention of Soil in Bin:	Field Capacity (approx. 60 cm), w≈25% (by weight) Wilting Percentage (-15 bar), w = 12.5% (by weight)
Strength of Extruded Soil:	$c' = 0.1 - 0.2$ kg/cm^2; $\phi' = 9^o$

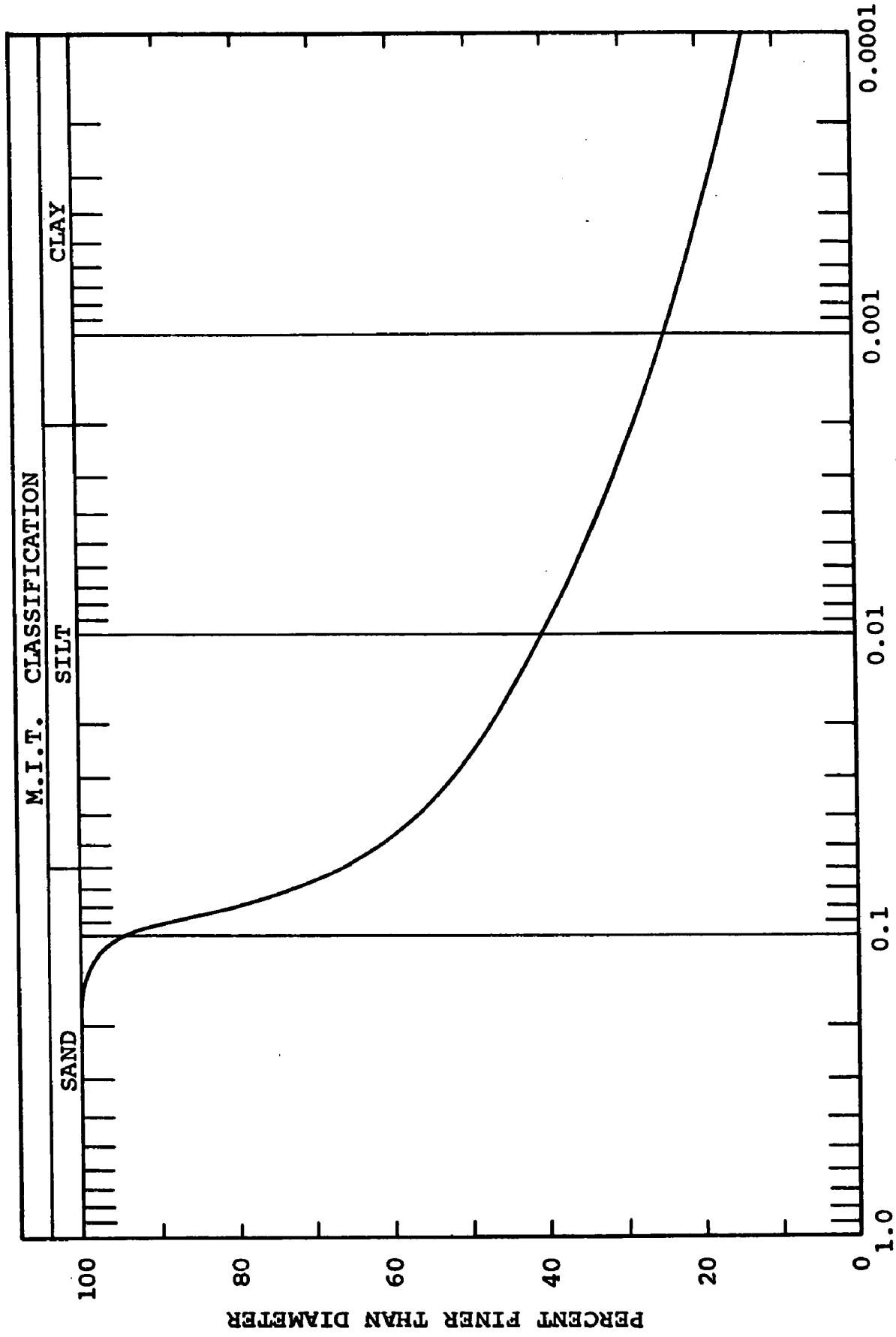


Figure 4.3 Grain size distribution of artificial clay loam.

be classified as a clay loam (after the U. S. Bureau of Soils Textural Classification Chart). It was chosen because it satisfied the following requirements: On the one hand the material exhibited rheological properties required for later creep studies on this same material. On the other hand, the permeability was not so low as to make drainage and infiltration impossible, tensiometer response too slow, and plant growth unsatisfactory. Had montmorillonite been chosen as the clay component the second requirement would not have been met. An artificial mixture also has the advantage that it is reproducible at any time, which is more difficult in the case of a natural soil. Mixing of the dry soil components was performed by a meat grinder.

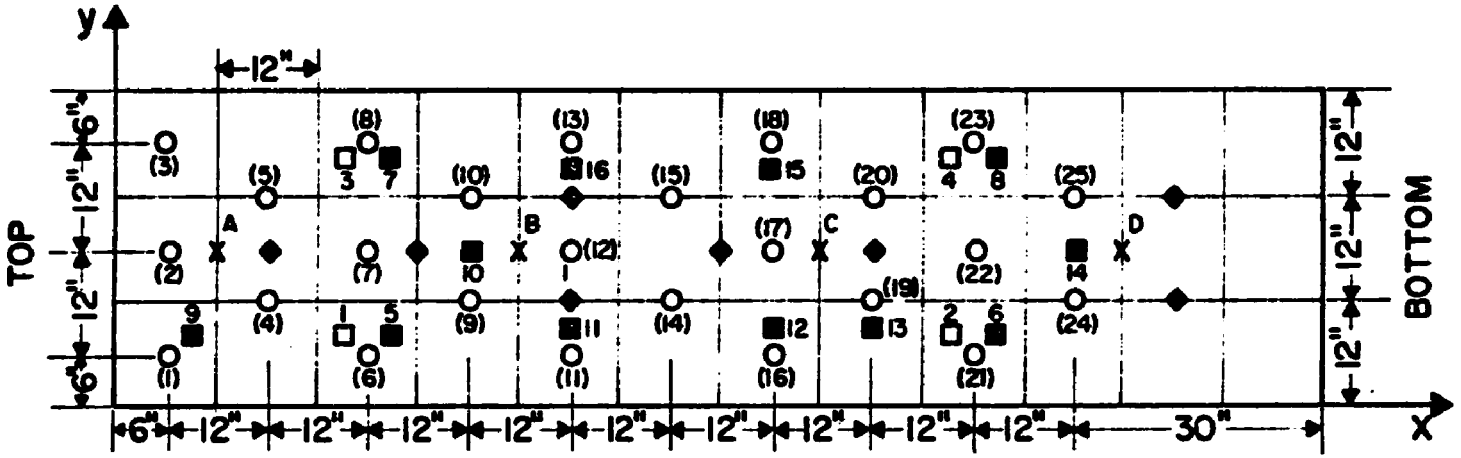
Before the soil was placed into the bin, a thin layer of epoxy glue was poured over the bottom inside the trough. Then a very coarse sand was spread over the glue until the whole surface was covered. After the glue was dry, the excess sand was brushed off. The purpose of this sand layer was to produce a rough surface in order to prevent the soil slab from sliding down the trough.

The soil in a dry condition was placed into the bin in lifts of about 3/4 to 1 inch in thickness. Over each lift, water containing some fertilizer was sprinkled until the lift was thoroughly soaked. About a total of 1,600 pounds of dry soil was needed, and the water used for wetting the soil profile amounted to 65 gallons.

Previous to filling the bin with soil, cottonwood tree seedlings (Populus deltoides) were planted in 8-inch diameter pots in the same type of clay loam as used for filling the bin. These trees were selected because of their ability to develop an extensive root system even in poor soils and in a relatively short time. Former attempts to grow lombardy poplar (Populus nigra) in this soil failed. About two months after potting, approximately 50 percent of the trees had developed leaves, or at least open buds; these were chosen for transplanting into the bin.

In order not to disturb the root system of the potted trees, the following procedure for transplanting the tree from the pot into the bin was devised: An aluminum mold, having the size of the inside dimensions of an 8-inch pot was shaped,and pushed into the soil of the bin at locations where a tree was supposed to be planted. The trees were planted in such a way that their stems would be vertical when the bin was elevated to a 20-degree slope. This means that the axis of the cone-shaped mold had to make an angle of 70 degrees with the soil surface when pushed in. The soil inside the mold was then excavated. After removing the mold, the trees, together with the soil, were removed from their pots and fitted into the holes. A total of 25 trees were planted in this way. Their arrangement is shown in Figure 4.4.

After all trees were planted, one inch of organic soil was placed on top of the clay-loam in order to facilitate the growth of grass roots. A mixture of four kinds of perennial grass seeds was spread over the



LEGEND:

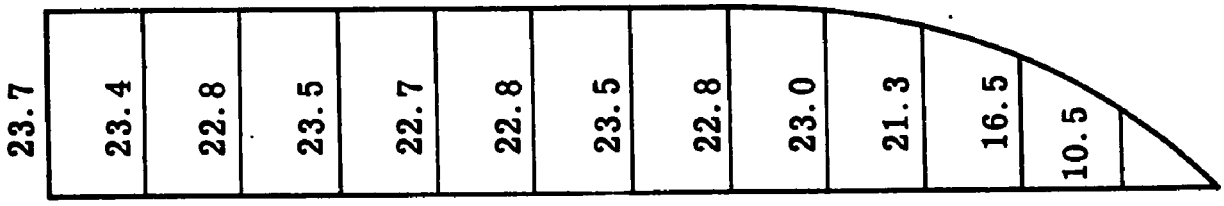
- O(5) TREE WITH CORRESPONDING NUMBER
- ■ TENSIOMETER 9½" DEEP
  NOS. 5 TO 8 HAVE BOURDON GAGE
  NOS. 9 TO 16 HAVE MERCURY MANOMETER
- □ TENSIOMETER 5" DEEP
- X PIEZOMETER TUBE
- ◆ RAINGAGE

(NOTE: DEPTH OF TENSIOMETER NO. 10: ~7.5")

TENSIOMETER LOCATIONS:					
NO.	x(INCHES)	y(INCHES)	z(INCHES), MEASURED FROM THE TOE OF THE SLOPE TO THE CENTER OF THE POROUS CUP		
			10°	20°	30°
1	26	9			
2	98	8			
3	27	28.5			
4	99	30			
5	30	8.5	21.0	40.2	58.2
6	102	9	8.5	15.6	22.2
7	31	27.5	20.8	39.9	57.7
8	103	28	8.3	15.2	21.7
9	13	6	23.9	46.0	66.7
10	39	17	20.9	38.6	55.2
11	56	7.5	16.5	31.3	45.2
12	75	7.5	13.2	24.8	35.7
13	87	9	11.1	20.7	29.7
14	114	19.5	6.4	11.7	16.2
15	76	30.5	13.0	24.5	35.2
16	55	29.5	16.7	31.7	45.7

Figure 4.4 Tree arrangement and instrumentation.

surface of the organic soil in order to produce a grass cover which served as a protection against erosion. Finally, about 1/8 inch of fine natural sand was employed to cover the grass seeds. The whole surface then was lightly pressed with a wooden plate in order to smooth out uneven spots and the sand was moistened. The total soil depth in the bin was then about 9 to 9 1/2 inches. This depth gradually tapered to zero at the bottom end of the trough, where a V-shaped gutter was attached to collect drainage and runoff water. The longitudinal soil profile is shown in Figure 4.5.



30.5 30.5 30.5 30.5 30.5 30.5 30.5 30.5 30.5 30.5 30.5 30.5

All dimensions in centimeters

Thickness of top soil + sand ≈ 2.5 - 3 cm = 1 - 1 1/4"

Total volume of soil = 0.686 m^3 = 24.2 $ft.^3$

Figure 4.5 Longitudinal soil profile in bin

b. Stability Check on Soil Mantle

In order to make sure that the soil mantle did not slide when tilted to steep angles, it was necessary to perform a stability check. However, this required the knowledge of the strength properties of this

artificial soil mixture, which in turn made it necessary to produce representative soil samples for use in the strength testing equipment. Samples for this purpose were fabricated from the same clay loam mixture in a soil extruder (Vac-Aire "experimental" extrusion machine, International Process Equipment Co., East Liverpool, Ohio). In such a machine the soil is kneaded by an auger mechanism and extruded under a vacuum. The samples are then virtually saturated. The cylindrical specimens obtained this way had a water content of 21.0 percent and were used to estimate the strength parameters of this soil. Consolidated, undrained triaxial tests and unconfined compression tests gave a cohesion intercept between 0.1 and 0.2 kg/cm^2 and an angle of internal friction of $\phi' = 9^o$. These values were used to calculate the factor of safety of the sloping soil mass when the bin was tilted.

Ter Stepanian (1963) has presented a stability analysis for an infinitely long planar slope. He defined the factor of safety F as the ratio of total shear strength to the mobilized shear strength. This is given by

$$F = \frac{\tan \phi'}{(q_o + \gamma d_s)\cdot \tan \omega}\left(\frac{c'}{\tan \phi' \cdot \cos^2 \omega} + q_o + \gamma d_s - \gamma_w \cdot h_p\right) \qquad (4.1)$$

where: ϕ' = angle of internal friction of the soil material

ω = slope angle

q_o = surcharge on slope per unit area

$d_s \cdot \cos \omega$ = thickness of soil layer (measured perpendicular to the surface)

$h_p \cdot \cos\omega$ = height of piezometric level (measured perpendicular to the surface)

γ = unit weight of totally saturated soil

γ_w = unit weight of water

c' = cohesion intercept

The most unfavorable case (smallest F) occurs when $h_p = d_s$, i.e., the piezometric level reaches the surface of the planar slope. Then

$$F = \frac{\tan\phi'}{(q_o + \gamma \cdot d_s)\tan\omega} \cdot \left[\frac{c'}{\tan\phi' \cdot \cos^2\omega} + q_o + d_s(\gamma - \gamma_w)\right] \qquad (4.2)$$

Although the bin does not represent an infinitely long slope, Equation (4.2) may be applied to it as a reasonable approximation. q_o is zero, since there is no surcharge and F is calculated for the steepest angle $\omega = 30^o$. The other quantities have the values (see also Table 4.1): $d_s = 27$ cm, $\phi' = 9^o$, $c' = 0.1$ kg/cm^2, $(\gamma - \gamma_w) = \gamma_w \cdot \left[\frac{G_s - 1}{1 + e'}\right] = \gamma_{dry} \cdot \frac{(G_s - 1)}{G_s} = 0.932$ $(G_s = 2.64;\ \gamma_{dry} \sim 1.5$ gr/cm$^3)$

Using these values in Equation (4.2), one obtains a factor of safety of 4.5. This value looks rather large, however, the analysis is very sensitive to a variation in c', because the soil slab is very thin. The cohesion of the bin soil is probably considerably smaller than the one of the extruded soil, which has a higher bulk density. For a factor of safety of 1.0, i.e., just on the vergy of sliding, the cohesion may be as low as 0.020 kg/cm^2.

c. Rainfall Simulation

In order to simulate a rainstorm over the sloping bin, a sprinkler system was installed, consisting of four wide spray hydraulic atomizing nozzles 1/4 LN 2W (available from Spraying Systems Company, Bellwood, Illinois 60104). These nozzles were arranged in a line downslope and parallel to the slope surface and with a spacing that provided as uniform as possible a distribution of rain over the bin. For steeper slope angles, the distance between the uppermost nozzle and the line passing through the upper end of the bin had to be shortened in order to secure a proper distribution (see Figure 4.6). The distance between the nozzles and the soil surface was held at 38 inches. It was assumed that frequent rains would leach the soil considerably. By incorporating a cell containing solid fertilizer, it was possible, however, to provide the soil with nutrients during a rain storm. The fertilizer salt slowly dissolved and was used up by the time the storm was over. The cell can be seen at the lower right hand corner of Figure 4.1.

2. Instrumentation and Equipment

a. Tensiometers and Piezometers

About four months after planting the trees into the bin, tensiometers were installed in order to start preliminary measurements of

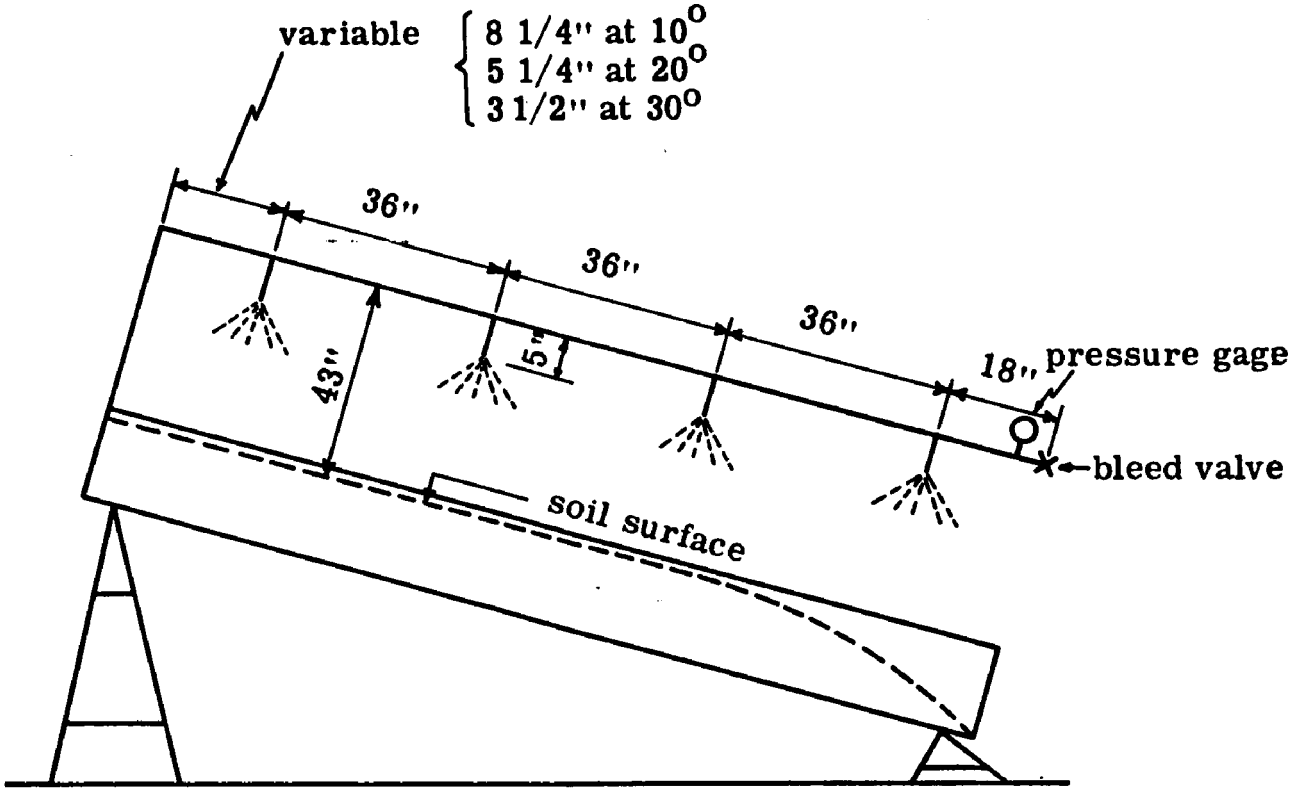


Figure 4.6 Sprinkler System

the soil moisture regime. A total of 16 tensiometers were inserted in the slope. The spatial distribution of these tensiometers is shown in Figure 4.4. Tensiometers are soil moisture gages and are able to measure the matric component of the soil water potential up to values of about 0.85 bar. The instrument consists essentially of a tube,

sealed at one end by a porous ceramic cup which is in contact with the soil particles and soil solution. The other end of the tube is above ground and is connected to a vacuum gage or to a mercury manometer. The porous cup is permeable to soil solution but not to the soil matrix or mass flow of gas (see Figure 2.1). If the pore water in the soil is under tension, water is imbibed through the porous cup until equilibrium is reached between the soil water and the water in the tensiometer tube. The resulting negative pressure in the tube is then registered on the attached Bourdon dial gage or by a mercury manometer. Since pressures are measured with respect to the outside atmospheric pressure, the theoretical limit of the tensiometer range is 1 bar, however, it was found (Richards, 1949) that the reliable range goes only as far as about 0.8 or 0.85 bar, because at this suction the porous cup starts losing water and soil air enters. Further details about measuring soil moisture tension with tensiometers are given in Appendix D.

Three different types of tensiometers were employed. (All of them are available from Soil Moisture Equipment Corporation, Box 30025, Santa Barbara, California 93105). Four soil moisture gages (Nos. 5 to 8) were provided with a Bourdon dial gage, graduated 0 - 100 centibars; 8 other tensiometers (Nos. 9 to 16) were connected with a mercury manometer which had a scale allowing readings directly in millibars.

These 12 tensiometers had an outside diameter of 7/8" and were inserted such that the tip of the porous cup was very close (approx.

1/4") to the bottom of the bin. This is because the water potential in this region of the soil profile is crucial if one is concerned about stability problems. Equation (4.1) states that the factor of safety in a planar slope is proportional to the soil water head h_p which can be negative or positive. Of course, in order to obtain a more complete picture of the soil moisture flow in steep slopes, tensiometers at various distances from the bedrock surface should be installed.

The third kind of tensiometers (Nos. 1 to 4) were soil moisture probes. These are miniature porous cups, 1/4" in diameter and 1" long, which are connected by two coaxial nylon tubes to the sight tube assembly with the Bourdon dial gage. The sight tube assembly was mounted to the side wall of the bin. All three types of tensiometers can be seen in Figure 4.7. The soil moisture probes were inserted to a depth of 5 inches below the soil surface. Since the point of measurement and the Bourdon gage were usually at different elevations, the readings had to be corrected for the corresponding head. The Bourdon dial gages were not very accurate below 10 centibars.

Before installment, the tensiometer units had to be degassed carefully in order to remove all air from the porous cups. A detailed procedure for degassing is given by the manufacturer.

Tensiometers can also be used for measuring small positive soil water heads (see Appendix D). However, readings thus obtained were unreliable due to the slow response on rewetting, which is caused by

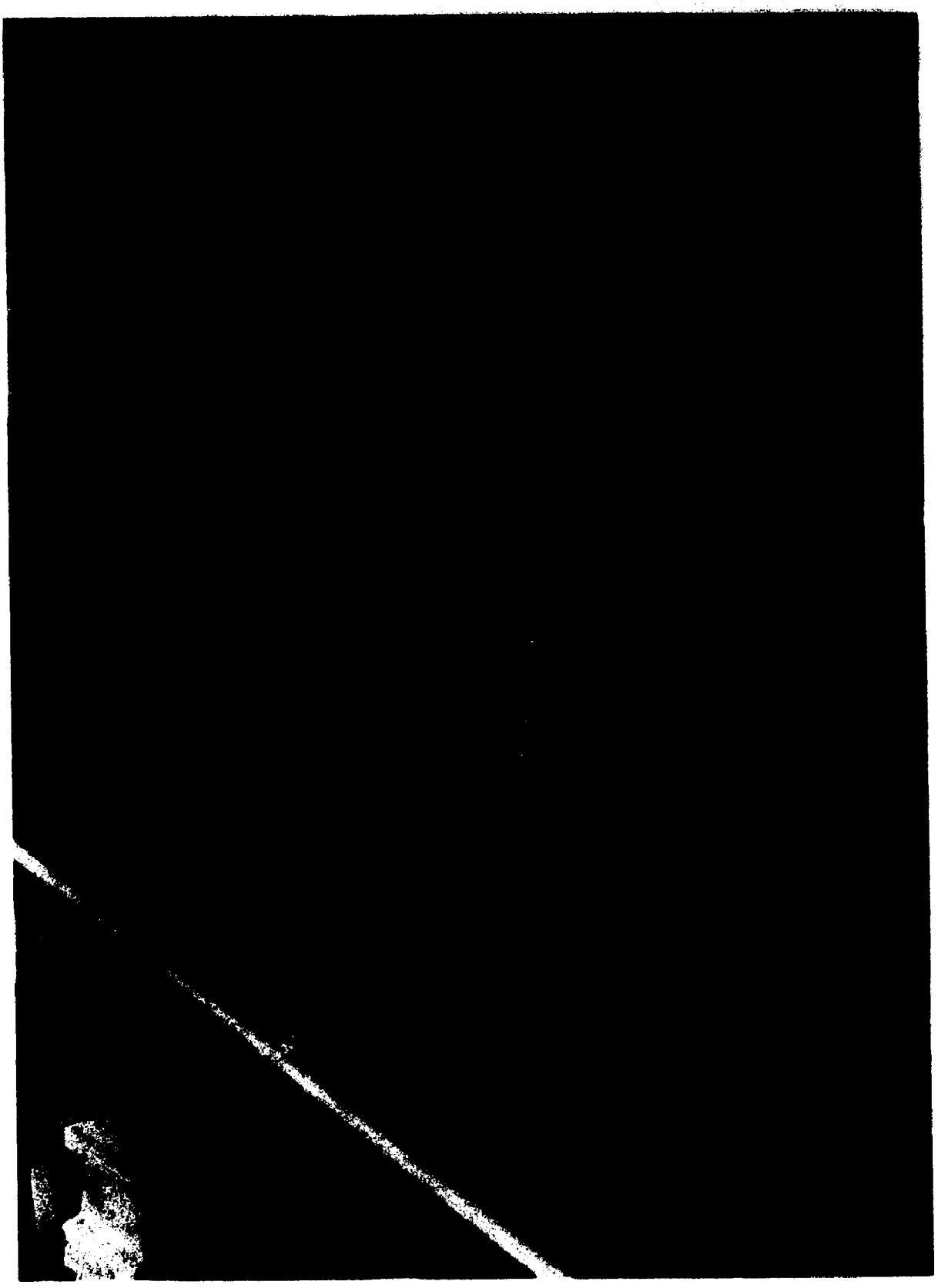


Figure 4.7 Bin instrumentation: Tensiometers and raingages. The tubing connects the soil moisture probes with the sight tube assembly mounted on the bin wall.

the low hydraulic conductivity or by the presence of air in the porous cups. Accordingly, in a later test series, four piezometer tubes were installed in order to study or get some idea about the rise and fall of a ground water table during and after a rain storm, respectively. The piezometer tubes consisted of 3/16" diameter, 12" long thin-walled brass tubes perforated at the bottom for a length of 1.5 inches. The perforated part of the tube was wrapped with a layer of glass wool. Then the tubes were inserted into one-inch diameter holes drilled into the soil which in turn were backfilled with a coarse sand in the lower part. A bentonite plug (to prevent direct infiltration along the tube) was placed at the top. Piezometric levels then could be determined by inserting a thin-walled piece of plastic tubing into the brass tube, temporarily plugging up the top end, and withdrawing it.

b. Determination of Rainfall

Rain on the bin was originally intended to be measured by miniature rain gages, i.e., small funnels of 6.8 cm in diameter which collected the water in small bottles embedded in the soil. These rain gages were placed in such a way that dripping of water from leaves was more or less avoided (see Figure 4.4). However, an unusually large scatter in the measurements was observed, so that the data could not be used to evaluate the amount of rain on the bin. A more accurate but very laborious method was then devised to estimate the amount of rainfall on the bin: It was noticed that the water pressure in the line fluctuated,

which of course affected the output of the nozzles. Therefore, a pressure gage was installed at the lower end of the nozzle line. During a rain storm line pressure was recorded every 5 minutes and the timed output of each nozzle was measured under various pressures by means of a beaker or graduated cylinder. Unfortunately, this had to be done for every storm, since the relation between pressure and nozzle output was different for every rain storm, despite cleaning the nozzles with hydrochloric acid before each storm.

For each storm a relation was obtained between the pressure and the output for each nozzle. This was done by fitting a straight line through the data points (usually 6 points per nozzle). Then by interpolation and summation, the total water output could be found for any of the recorded line pressures. This total water output was then plotted versus time for the duration of the storm. The total area under this curve represented the total rain output.

Next it was necessary to determine the percentage of this total output falling on the bin surface. This had to be accomplished later in the test series, after the trees had been removed. The soil surface of the bin was covered with a sheet of plastic. A one-hour storm was then initiated during which the line pressure was recorded every minute, and the nozzle output was measured at various line pressures in order to obtain again the total water output. The runoff from the plastic was collected in the gutter at the lower end of the bin and drained into a pail

as was done previously for the test storms. Every 15 minutes the run-off was weighed. The ratios of collected runoff over total output for every 15 minutes of the one-hour storm gave four independent values in excellent agreement with one another. The mean value was then used as the factor by which the total rain output had to be multiplied in order to obtain the rain actually falling on the bin. This factor had to be determined for each of the three slope angles of 10, 20 and 30 degrees respectively. The rate of water application on the bin corresponded to a rainfall of about 0.25 inches per hour. This intensity with respect to its duration reasonably approximates a real live storm, although such a storm is usually not of uniform intensity.

c. Radiation, Temperature and Relative Humidity

Since the tests were run during the winter months (October through March) (see Figure 4.9), it was necessary to illuminate the trees continuously in order to prevent them from going dormant. This was achieved by hanging first 6, and then later as the days became shorter, 8 and 10, 150-Watt light bulbs about 10 inches above the crowns of the trees.

Temperature and relative humidity were recorded with a hygro-thermograph. The calibration of this instrument was checked daily by a thermometer and an aspirating psychrometer. Differences in temperature between the top and the bottom part of the slope never exceeded $3^{o}F$.

d. Vegetation Maintenance, Leaf Water Potential and Transpiration Measurements

In order to estimate the water potential in the leaves of the trees, numerous measurements were made with the pressure chamber method. This method was first described by Scholander (1965), and later by Waring and Cleary (1967), Boyer (1967), and Kaufmann (1968).

In the vascular system of a plant, the water column is generally under tension (see Chapter 2). When a twig or a leaf is severed, the water column is broken and water withdraws into the xylem capillary a short distance. In order to measure the original tension, the leaf is placed into a pressure bomb with the cut end (cut made with a razor blade) protruding through a seal. Then a pressure is applied on the leaf and the sap moves suddenly back to the surface where it bubbles vigorously as it spills over. This can be observed easily through a lens. This pressure, with a negative sign, ideally equals that which existed in the leaf stem xylem before it was severed from the tree and is called the xylem sap pressure. It does not equal the leaf potential in the mesophyll cells where transpiration takes place but does approximate it reasonably well.

Kaufmann (1968) compared this method with the thermocouple psychrometer method which is regarded as the most accurate method for determining leaf water potentials. He performed his experiments on different forest tree species. In most cases a good agreement was found; however, for a few species large discrepancies were obtained. He

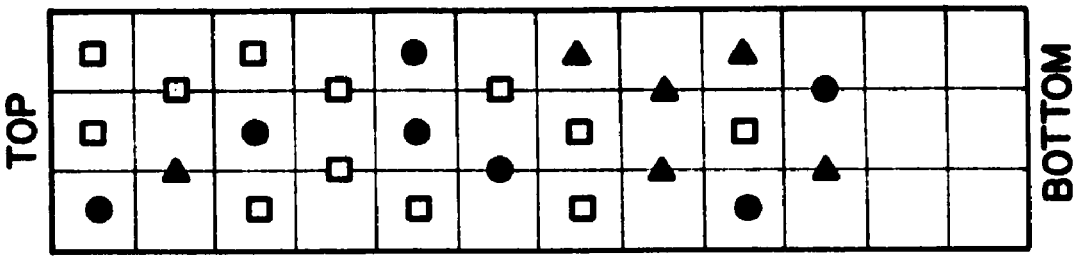
concluded therefore, that the best procedure for using the pressure chamber technique as direct estimates of leaf water potentials is first to determine a calibration curve for each species, relating the estimate of xylem pressure potential to known leaf water potentials, determined by thermocouple psychrometer measurements.

The pressures measured in the present study varied with the time of the day at which the measurement was made, the environmental conditions (sunlight), the quality, age and size of the leaf (young or old) and on the position of the leaf on the tree. A total of 55 leaves were measured. The pressure was usually between 50 and 90 psi and never exceeded 130 psi (about 9 bars). Matric potentials in the soil water were always below 1 bar, so that soil water was never limiting.

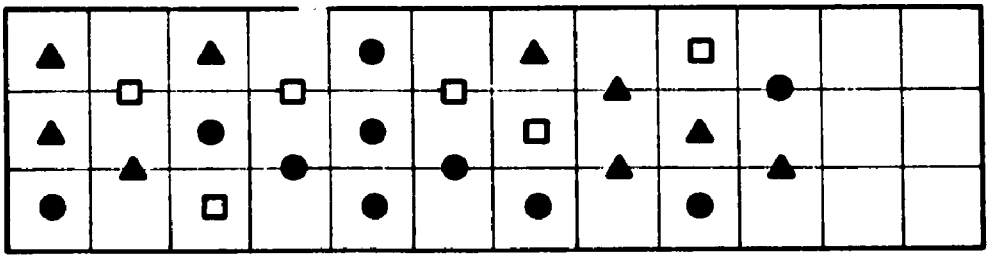
The height of the trees was kept between 3 and 4 feet by trimming the crowns when necessary. The grass on the slope surface was also kept very short by frequent cutting.

Unfortunately, during the course of the test series, the trees were attacked by various greenhouse insects, such as millibug and red spider. This caused some trees to lose almost all of their leaves which in turn had a marked effect on soil water depletion. The condition of the trees was recorded on a tree status plot every month, as shown in Figure 4.8.

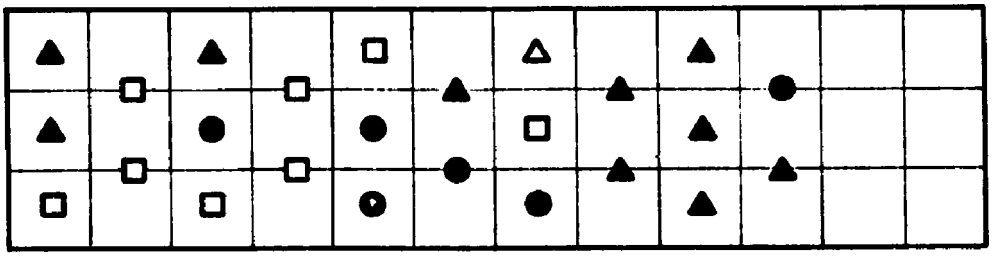
The environmental factors affecting transpiration in the greenhouse, such as temperature, relative humidity and solar radiation varied



OCT. 20, 1969



NOV. 19, 1969



DEC. 18, 1969

LEGEND:

● GOOD (BIG, HEALTHY TREE WITH MANY LEAVES)

□ MEDIUM

▲ POOR (TREE HAS ALMOST NO LEAVES)

Figure 4.8 Tree status map

considerably and it was therefore necessary to establish some kind of a scale in order to evaluate the evapotranspirative power in the greenhouse. This was achieved by devising a phytometer experiment. Four good specimens were selected from among the surplus potted trees. One of these trees (pot no. 4) was cut at its base. The surface of the soil in the pots was also covered with grass. The pots were then double wrapped with plastic so that no moisture was lost through the pot walls. The soil in the pots was brought to near field capacity so that soil water would never be limiting and the plants could then transpire at the potential rate. The loss of water from all four pots was then determined daily. After the weighing the water lost was replaced very slowly. By subtracting the loss of pot no. 4 from the loss of each of the other 3 pots, it was possible to eliminate surface evaporation and grass transpiration and thus obtain the net transpiration for each of the three trees.

From time to time the height of the trees was measured and the total leaf surface was determined by tracing the shape of each leaf on paper and then finding the area by means of a planimeter. This was necessary because, during the five months test period, the trees were growing considerably and therefore were transpiring more than at the beginning under the same conditions. These potted trees were never trimmed. The transpiration per unit leaf area should thus provide a measure of the transpiration power in the greenhouse.

It was found, as a result of these experiments, that the major factor influencing transpiration was solar radiation (amount of sunshine).

A detailed discussion of these pot experiments is presented later in Chapter 5. During the entire duration of the experiment, these pots were illuminated by two 150-Watt light bulbs, in addition to the daylight. When the first test series on the bin was completed (February 27) (see Figure 4.9), the trees in the pots were cut and both the leaf area and the leaf weight were determined. Thus it was possible to find an average value for the leaf area per gram of leaf weight. This value was then used to estimate the total leaf area of the trees in the bin. This is described in more details in the following section and in Chapter 5.

3. Test Program

Test series A consisted of 18 tests which were performed to evaluate the influence of vegetation and slope angle on the soil water potential. Preliminary tests were started in September, i.e., about 4 1/2 months after planting the trees into the bin. By that time the trees had developed a considerable amount of leaves and a well established root system. The test series began on October 14. Figure 4.9 represents the history of the 18 tests of series A.

The tests were started with a slope angle of 10 degrees, then the bin was tilted to 20 degrees, and finally to 30 degrees. Next the trees were cut at their base, and the tests were repeated on the denuded slope in a reversed sequence of slope angles.

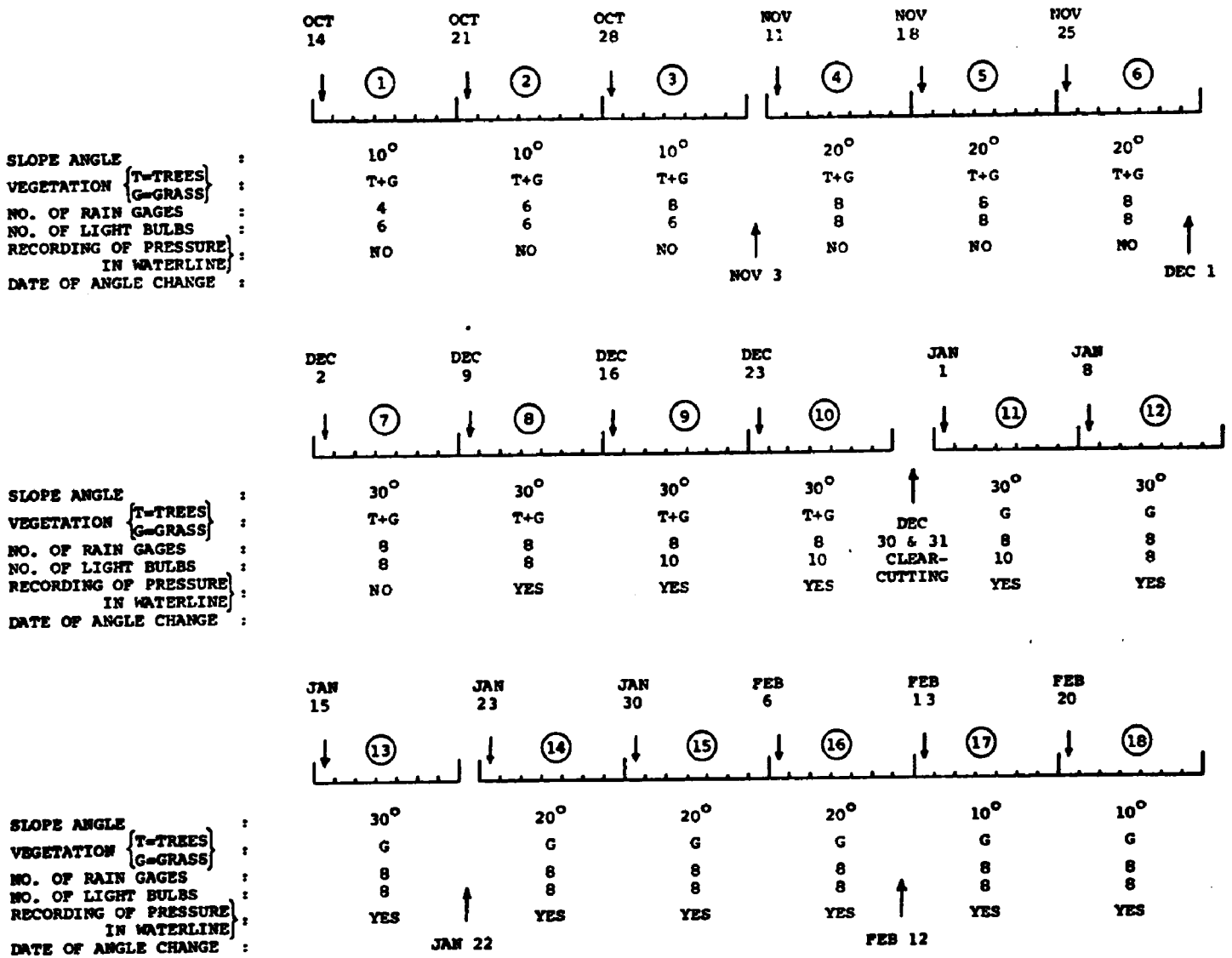


Figure 4.9 History of Test Series A (Oct. 14, 1969 - Feb. 26, 1970)

It should be noted that the time of clear-cutting (see Figure 4.9) almost coincided with the shortest day, so that the tests were symmetrically distributed with respect to day length.

Each test consisted of a 3-hour rainstorm produced by the sprinkler nozzles. During the storm, runoff + drainage (stormflow + baseflow)were recorded by periodic weighing of the collector pail. Soil water potential decrease was indicated by the tensiometers. These readings, however, have to be used with caution because of the finite response time of the tensiometer-soil system. Precipitation on the bin was first determined from raingage measurements and later, when this method was found to be unsatisfactory, by the procedure described in Section 4.2.b. For a 3-hour storm, it was estimated that interception must be very small compared to the total precipitation on the bin, especially in later tests when leaf density decreased due to the tree diseases.

After the rain stopped, the soil was allowed to drain freely and slowly dry out for a period of 165 hours. During this time water loss or redistribution could occur by gravity flow, transpiration by the trees and the grass, and by evaporation. The tensiometers were read periodically. About 4 hours after every storm, just after a reading had been taken, the tensiometers were serviced. This was necessary, since each time soil suction falls in response to rewetting, small amounts of air-filled water from the soil enters the gage through the porous cup. This air collects below the filler cap and tends to slow down the response of the gage.

Servicing consisted of removing the filler cap and replacing the air with air-free water. Mercury manometers were flushed by forcing water through the tubing in order to remove all the air. This was accomplished by means of a special applicator bottle. Equilibrium with the soil suction was established again well before the next reading (approximately 20 hours later). After an elapsed time period of 168 hours following initiation of a storm, a new test started with another 3-hour storm. The interval of 1 week (168 hours) was chosen because it was found that after this period and under favorable evaporative conditions, suction in the upper part of the slope with trees reached approximately one bar. Since tensiometers are limited to a range of 0.85 bar, it was useless to carry the experiments beyond this time period.

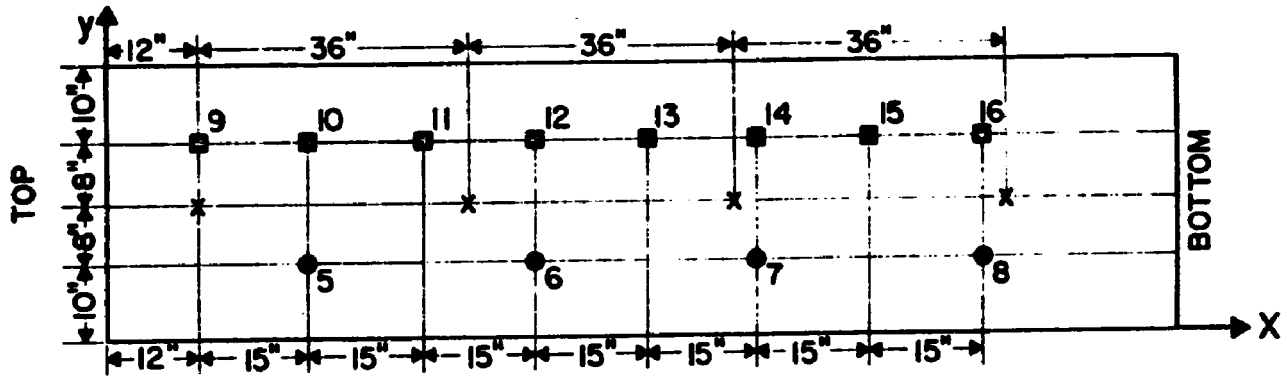
In an attempt to reproduce the test data, three tests were usually run at each slope angle. Completely reproducible sets of data were not obtained, however, because of the changing environmental conditions (i.e., cloudy and clear days, and photoperiod), and because of the decrease in leaf area of the trees caused by the aforementioned leaf diseases.

The daily transpiration rates of the potted trees were recorded during the entire testing period, as mentioned in section 4.2.d. This information made it possible to compare results from the clear-cut slope as opposed to the forested slope in the bin. After the trees in the bin were cut, each tree was stripped of its leaves. The leaves then were weighed which gave an indication on the total leaf area by using the relation found

from the potted trees between leaf area and weight. The basal diameter of each stem was also determined which made it possible to calculate the total basal area of this miniforest at the time of clear-cutting. These results are presented in Chapter 5.

A few weeks after test series A, which is schematically diagrammed in Figure 4.9, was completed, another series (series B) was started whose purpose was to observe the rise and fall of a water table and subsequent change of soil moisture for slopes of 10 degrees and 30 degrees. During test series A, it had been observed that a water table must exist during the last hour of each storm, because some mercury tensiometers showed a negative reading. However, this reading was not reliable with respect to its magnitude, as mentioned earlier. Whereas negative tensiometer readings in the case of the denuded slope could be definitely correlated with the development of a water table in the slope, this was not the case for the forested slope where some slightly negative readings may have simply been caused by a small shift in the zero reading of the tensiometer.

In order to resolve this question, 4 piezometers were installed as described in Section 4.2. The tensiometers were arranged differently, i.e., in equidistant positions, as shown in Figure 4.10. Since only the mercury tensiometers furnish precise readings, the 4 tensiometers with Bourdon gages were used only as a check. The soil moisture probes were not employed.



■ MERCURY TENSIOMETER

● BOURDON GAGE TENSIOMETER

X PIEZOMETER

DEPTH OF TENSIOMETER TIP:

8.3" FOR NOS. 9 TO 14; 5, 6, 7
7.9" FOR NO. 15
5.9" FOR NO. 16; 8

} TIP IS APPROX. 0.79" ABOVE BOTTOM FOR ALL TENSIOMETERS

TENSIOMETER LOCATIONS:				
NO.	x(INCHES)	y(INCHES)	z(INCHES), MEASURED FROM THE TOE OF THE SLOPE TO THE CENTER OF THE POROUS CUP	
			10^{o}	30^{o}
9	12	26	24.1	67.2
10	27	26	21.5	59.7
11	42	26	18.9	52.2
12	57	26	16.3	44.7
13	72	26	13.7	37.2
14	87	26	11.1	29.7
15	102	26	8.5	22.2
16	117	26	5.9	14.7

Figure 4.10 Arrangement of tensiometers for Test Series B.

Test series B consisted of 4 more storms of 3 hours, i.e., two runs with slopes of 10 degrees and two at 30 degrees. The same measurements were performed as in series A, only the drying period after the storm was extended to 333 hours (i.e., two weeks from start of storm. Transpiration measurements, as well as temperature and humidity recordings, were not made during this test series. The data were not reproducible due to different evaporative conditions during every test period; however, the same tendency could be observed for both tests at each angle, i.e., the tensiometer readings were more or less proportional to each other. The piezometers made it possible to observe the build-up of a water table during the wetting cycle (storm) and its decline following the cessation of rain.

4. In-Situ Properties of Soil in Bin

With a clayey soil it is very different to obtain homogeneous conditions in a bin of this size. It was therefore necessary to determine some soil properties which are relevant for future evaluation of the test results, in-situ, or from undisturbed samples taken from the bin. Three such properties are of importance:

- The bulk density or dry density γ_{dry}, since it is related to the water content (see Appendix C)
- The soil water retention characteristics (in particular in the range between 0 and 1 bar), since this information is necessary

in order to correlate tensiometer readings with actual water contents in the bin.

- The saturated hydraulic conductivity, which is required for approximate calculations of soil water movement.

All these tests had to be performed after the two test series were terminated, since sampling implied severe disturbance of the soil in the bin.

a. Density Tests

Two kinds of density tests were performed. The first type was the sand cone method as described by ASTM-Specification D1556-64 (re-approved 1968), Vol. 11, 1970. Three such tests were taken. The second type was a method by which a thin-walled sampling tube, 4" in diameter and 4" long, was forced into the ground by a driving hammer having a 10-pound dropping weight. The tube was then carefully dug out and both ends were trimmed level by a spatula and straight-edge. Such a sample can be considered as fairly undisturbed. Since the volume of the tube was known, the dry density could be obtained from weighing the sample dried at 105°C. Fourteen such tests were performed. The following results were obtained:

Sand cone method (average from 3 tests) = 90.5 lb/ft^3

Thin-walled tube method (average from 14 tests) = 89.7 ± 2.5 lb/ft^3
= 1.438 ± 0.040 g/cm^3

According to Equation (C.7), 90 lb/ft^3 corresponds to a saturated water content of 31.4 percent by weight.

The non-homogeneity of the soil in the bin is reflected in the large standard deviation.

The dry density of the artificially extruded soil on which strength tests were performed was 106 lb/ft^3 or 1.700 g/cm^3.

b. Soil Moisture Retention

It was difficult to establish a well-fitted relation between suction and water contents from experimental data in the low suction range due to the scatter in bulk density. In other words, for a given suction the corresponding water content is also sensitive to the bulk density.

Tension table tests were performed according to the method described by Hoover et al. (1954). Water contents at very small (usually 20 cm and 60 cm) negative heads can be determined in this method by putting a sample in a brass core on a table with blotter paper. However, this method was not well suited in this case; first, because of the relatively low permeability of the soil, which requires long times for equilibration; and second, because of the size of the cores (69 cm^3) which is too small when the bulk density varies considerably.

Another method was then tried. Soil cores of 4" diameter and 4" length were sampled by the thin-walled tubes used also for density determinations. Sampling took place when the soil in the bin was at a low suction. A tensiometer was then inserted into the center of the core

and the sample was allowed to dry out slowly. Tensiometer readings and weighings of the core made it possible to determine a relation between water content and suction for each core sample. Each sample had a different dry density within the range encountered during density testing. Although smooth curves were obtained from the data, it was not possible to determine a unique relation between suction, water content and dry density.

A very simple method was then used to correlate tensiometer readings with the moisture content in a nearby soil profile. Two-inch shelby tubes were driven into the soil close to tensiometers. The sample was ejected and cut into four equal parts. Then the moisture content of these portions was determined gravimetrically. Twenty-two shelby tube samples were taken at different tensiometer readings, each sample furnishing four moisture values. These results are presented in Table 4.2. The mean value for each profile was then evaluated and plotted against the tensiometer reading. Then a curve was fitted through the data points, using a method described by Rabinowicz (1970). This curve is shown in Figure 4.11.

From this curve the total water content of the bin could be estimated at any time from a set of tensiometer data obtained along the slope. This information was used for water balance calculations later in Chapter 5.

Table 4.2: Relation Between Tensiometer Reading and Moisture Content in Bin

Sample No.	Water Content by Weight from Top to Bottom	Avg. %	Corresponding Tensiometer Reading (millibar)	Sample No.	Water Content by Weight from Top to Bottom	Avg. %	Corresponding Tensiometer Reading (millibar)
1	25.8 21.6 22.8 25.5	23.8	30	7	20.1 20.7 22.0 23.7	21.9	180
2	21.9 22.4 24.4 25.0	23.5	40	8	20.4 23.2 24.9 24.6	23.2	210
3	20.8 22.0 24.8 25.5	23.2	60	9	20.4 22.4 23.1 23.7	22.5	210
4	21.1 24.6 25.7 25.2	24.1	140	10	20.4 21.5 23.9 24.4	22.6	250
5	21.5 23.8 25.8 25.4	24.0	150	11	20.0 21.4 22.6 23.4	21.8	295
6	19.7 20.0 23.2 25.0	21.9	150	12	19.6 20.3 21.4 22.3	20.7	320

Table 4.2: (continued)

Sample No.	Water Content by Weight from Top to Bottom	Avg. %	Corresponding Tensiometer Reading (millibar)	Sample No.	Water Content by Weight from Top to Bottom	Avg. %	Corresponding Tensiometer Reading (millibar)
13	21.6 22.1 22.2 22.8	22.3	320	19	17.1 18.5 18.8 18.4	18.2	700
14	20.4 20.5 22.9 22.7	21.7	390	20	16.7 18.2 18.2 18.2	17.8	750
15	19.3 19.3 20.4 19.7	19.6	470	21	17.0 17.3 17.7 18.2	17.6	830
16	19.7 20.3 21.0 20.3	20.3	~ 500	22	16.6 17.6 18.7 18.4	17.9	830
17	19.2 19.7 20.5 19.2	19.7	570				
18	18.7 19.1 20.1 19.6	19.4	650				

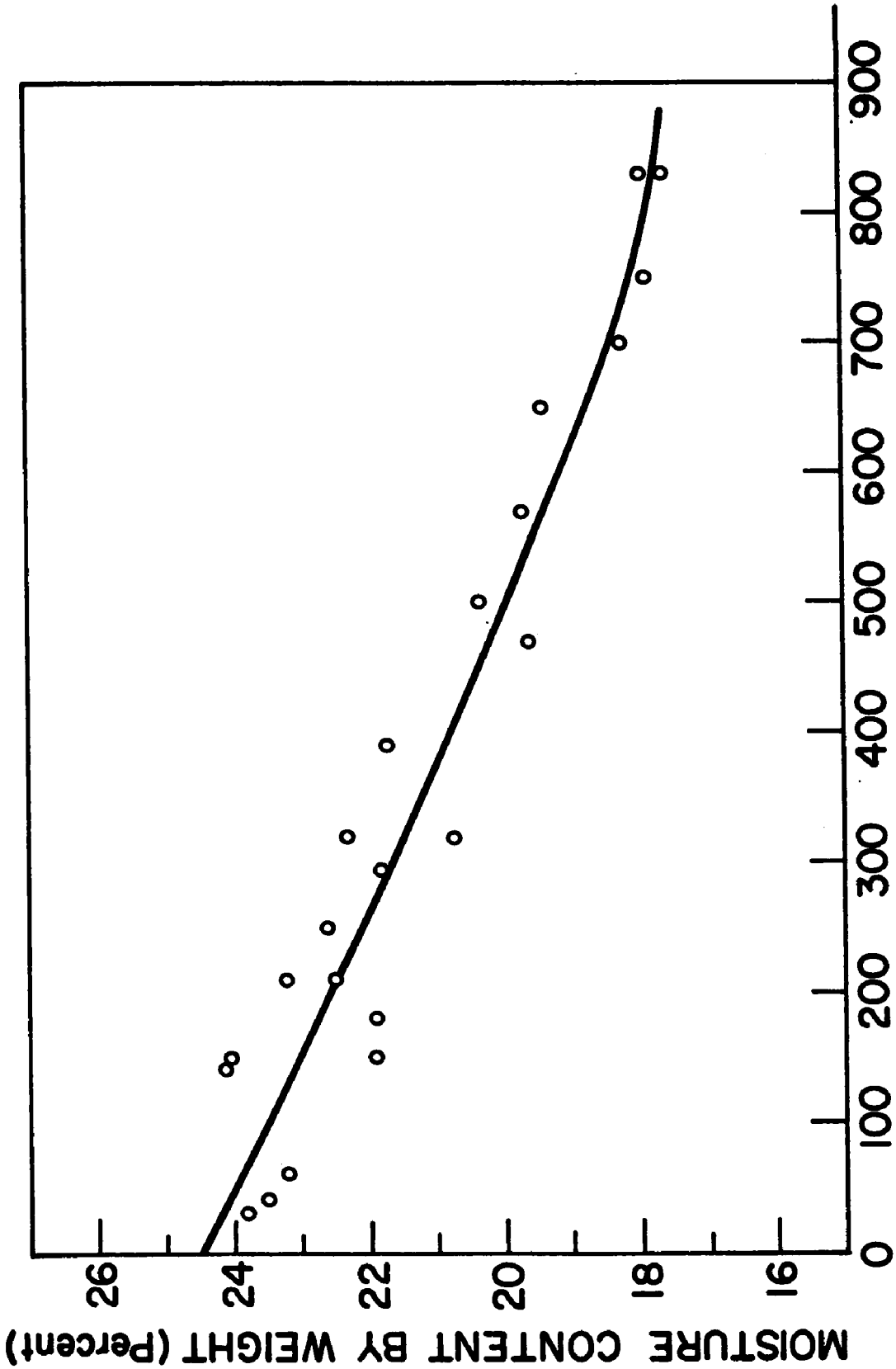


Figure 4.11 Relation between moisture content and tensiometer reading.

Finally, soil moisture retention was also determined by making use of a pressure plate extractor (available from soil moisture equipment Corporation, Santa Barbara, California 93105). Two extractors were employed, one working in the 0-2 bar range, the other one working in the 2-15 bar range. Soil from the bin as well as extruded samples was used. The results are plotted in Figure 4.12 on a linear scale and in Figure 4.13 on a semi-logarithmic scale. Each plotted point represents the average of 3 or more samples of the respective soil. Only the drying cycle was evaluated, but for clays hysteresis effects are usually small. It can be seen from Figure 4.12 that the available soil moisture is about 12.5 percent for the soil in the bin, and that the range between 0 and 1 bar contains only about 40 percent of this available moisture.

The influence of soil structure which is reflected in porosity and dry density, on the water retention of a soil is clearly seen in the difference of the two curves. The straight line relationship of Figure 4.13 suggests that the relation between suction and water content for this soil be expressed by

$$\tau = \tau_o \cdot e^{\beta(\theta_o - \theta)} \qquad (4.3)$$

where β is a constant and θ_o is the initial water content. Such a relationship has also been employed, for example, by Cowan (1965).

c. Hydraulic Conductivity

A falling head permeameter similar to the one described by Klute (1965) was constructed. This permeameter was able to accommodate

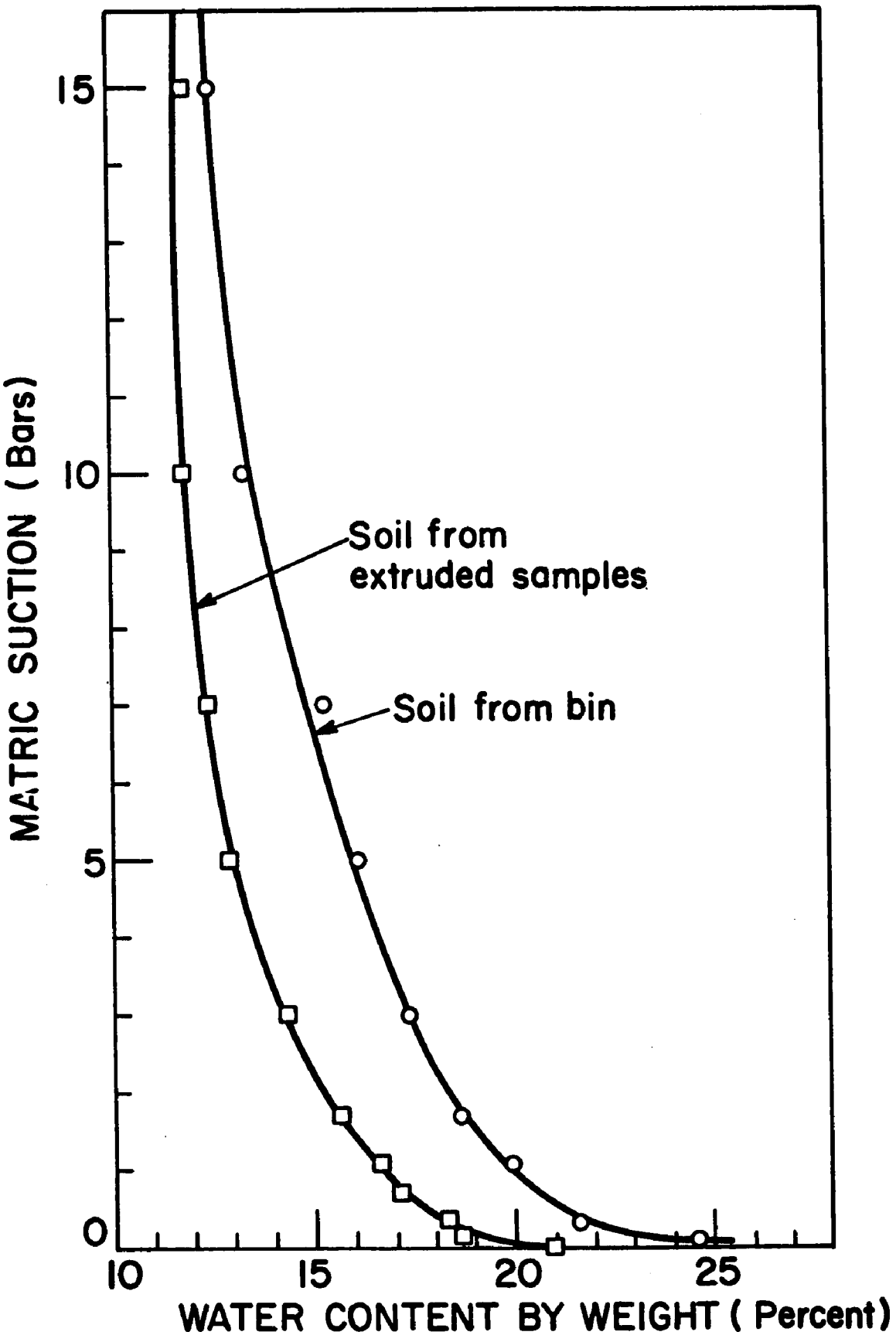


Figure 4.12 Soil water retention curve determined from pressure plate tests (drying cycle).

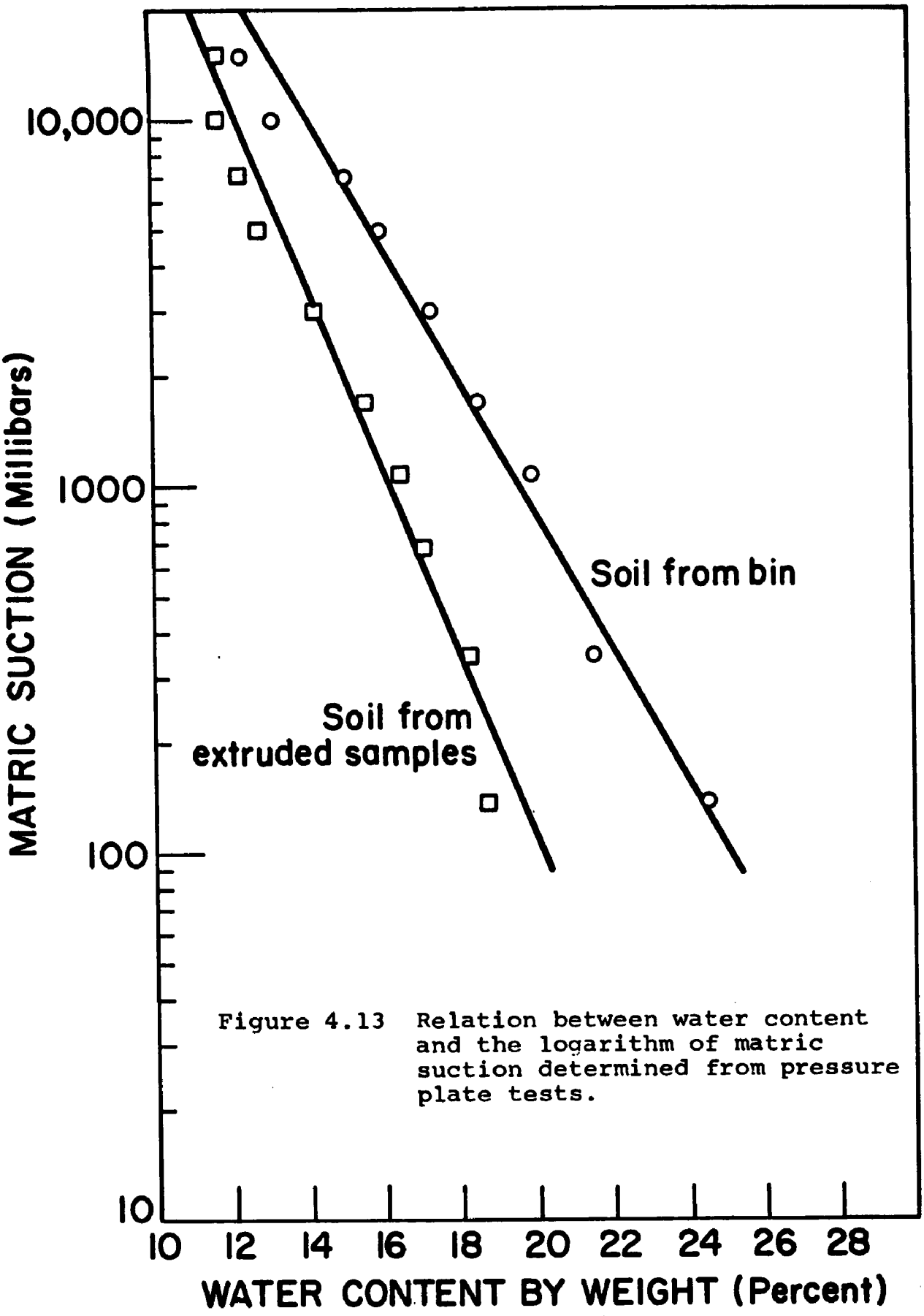


Figure 4.13 Relation between water content and the logarithm of matric suction determined from pressure plate tests.

the 4" diameter, 4" long thin-walled tubes used for density determination. Large undisturbed samples could therefore be taken from the bin soil. On each sample several measurements of K_s were made. A total of three different samples was used in the permeameter. The value for the saturated hydraulic conductivity K_s varied between $2 \cdot 10^{-6}$ and $4 \cdot 10^{-6}$ cm/sec.

CHAPTER 5

RESULTS FROM HYDROLOGIC MODEL STUDY AND DISCUSSION

1. Results from Test Series A (Test Nos. 1 to 18)

Tables 5.1a and 5.1b show typical results of two tests (nos. 9 and 13) of test series A. All data of the 18 tests show the same trend. The initial runoff is caused by the rain falling on the gutter at the end of the bin. However, the contribution of this area is very small compared with the total area of the bin ($\sim$ 2 percent) and has not been subtracted from the total runoff and drainage.

Test no. 9 was performed on a slope of 30 degrees with trees, whereas test no. 13 is a test on the clear-cut slope under similar environmental conditions. From these data alone, it can be seen at once, that recharge takes place much faster in the cut over slope, because of its higher initial moisture content at the beginning of the storm. This trend is also clearly visible from Figures 5.1a, 5.1b and 5.1c, where the matric suction reading of tensiometer no. 10, which is located in the upper third of the slope, is plotted versus time during a 168-hour test period. This was done for all three slope angles of 10, 20 and 30 degrees. Note that different time scales were chosen for the recharge

Table 5.1.a: Test Series A: Rain, Drainage + Runoff and Tensiometer Readings on a Forested Slope

Test No. 9 Slope Angle: 30° Vegetation: Trees + Grass

Elapsed Time since Storm Began	Rain on Bin			Drainage + Runoff		Tensiometer Readings (Reduced) in Centibars														
	Cumulative		Rate	Cumulative	Avg. Rate															
Hrs Min	Liter	cm	Liter/Min	Liter	Liter/Min	9	1	3	5	7	10	11	16	12	15	13	2	4	6	8	14
00:00	0.00	0.000		0.00		75.0	61	50	55	37	32.4	24.8	26.4	18.8	17.4	13.8	9	8	9	8	7.2
			0.383		0.015	-	-	-	-	-	-	-	-	-	-	-	-	-	-	-	-
00:15	5.75			0.23		76.8	61	52	52	36	33.4	24.8	27.2	18.8	17.5	13.8	10	8	8	7	7.2
			0.378		0.033	-	-	-	-	-	-	-	-	-	-	-	-	-	-	-	-
00:30	11.42			0.73		76.4	59	50	2	36	31.6	21.0	26.5	4.2	17.4	10.0	0	8	1	7	4.4
			0.348		0.038	-	-	-	-	-	-	-	-	-	-	-	-	-	-	-	-
00:45	16.64			1.30		74.5	46	46	0	35	18.5	14.3	25.0	0.8	9.6	2.2	0	7	0	7	1.0
			0.292		0.044	-	-	-	-	-	-	-	-	-	-	-	-	-	-	-	-
01:00	21.02	0.628		1.96		71.5	17	26	9	33	7.0	3.3	14.2	-0.2	4.0	1.2	0	0	0	0	0.4
			0.287		0.057	-	-	-	-	-	-	-	-	-	-	-	-	-	-	-	-
01:10	23.89			2.53		-	0	14	0	32	5.0	1.1	9.3	-0.4	1.2	0.6	0	0	0	0	0.0
			0.394		0.077	-	-	-	-	-	-	-	-	-	-	-	--	--	--	--	-
01:20	27.83			3.30		-	-	-	-	-	-	-	-	-	-	-	-	-	-	-	-
			0.373		0.097	-	-	-	-	-	-	-	-	-	-	-	-	-	-	-	-
01:30	31.56			4.27		-	0	3	0	4	2.0	0.6	5.0	-0.4	0.2	0.2	0	0	0	0	0.0
			0.337		0.104	-	-	-	-	-	-	-	-	-	-	-	-	-	-	-	-
01:40	34.93			5.31		-	-	-	-	-	-	-	-	-	-	-	-	-	-	-	-
			0.335		0.139	-	-	-	-	-	-	-	-	-	-	-	-	-	-	-	-
01:50	38.28			6.70		-	-	-	-	-	-	-	--	-	-	-	-	-	-	-	-
			0.314		0.156	-	-	-	-	-	-	-	-	-	-	--	-	-	-	-	--
02:00	41.42	1.236		8.26		36.8	0	0	0	4	1.5	0.5	2.8	-0.2	0.2	0.0	0	0	0	0	0.0
			0.324		0.186	27.2	0	5	0	7	2.4	0.8	2.5	0.8	1.4	0.8	0	0	0	0	0.6
02:10	44.66			10.12		15.2	4	6	8	8	4.2	2.5	4.0	2.3	2.4	2.1	0	0	0	0	2.0
			0.326		0.192	15.0	10	10	11	9	6.4	5.1	5.6	3.6	3.4	3.2	1	1	0	0	2.3
02:20	47.92			12.04		19.0	13	13	14	10	9.2	7.0	7.7	5.0	5.1	4.4	2	-	1	2	2.8
			0.320		0.204	26.2	19	18	18	15	13.2	9.8	10.6	7.4	7.3	6.2	2	1	1	2	3.7
02:30	51.12			14.08		36.8	28	25	25	21	17.6	13.0	14.4	10.0	9.8	8.0	5	5	4	5	4.5
			0.322		0.218	55.5	41	36	37	27	24.4	17.4	19.7	13.4	13.2	10.4	7	6	7	7	5.8
02:40	54.34			16.26		76.5	63	53	57	38	32.5	23.8	26.4	17.4	16.8	13.5	10	9	10	9	7.3
			0.309		0.224																
02.50	57.43			18.50																	
			0.285		0.209																
03:00	60.28	1.800		20.59																	
			0.000		0.145																
03:10				22.04																	
					0.081																
03:20				22.85																	
					0.058																
03:30				23.43																	
					0.045																
04:00				24.79																	
					0.0187																
08:00				29.29																	
					0.0020																
29:00				31.82																	
					0.0001																
52:00				31.96																	
					0.000																
76:00																					
101:30																					
124:30																					
148:00			0.000		0.000																
168:00	60.28			31.96																	

Table 5.1.b: Test Series A: Rain, Drainage + Runoff and Tensiometer Readings on a Clear Cut Slope

Test No: 13 Slope Angle: 30° Vegetation: Grass

Elapsed Time since Storm Began	Rain on Bin			Drainage + Runoff		Tensiometer Readings (Reduced) in Centibars														
	Cumulative		Rate	Cumulative	Avg. Rate															
Hrs Min	Liter	cm	Liter/Min	Liter	Liter/Min	9	1	3	5	7	10	11	16	12	15	13	2	4	6	8	14
00:00	00.00	0.00	0.417	0.00	0.017	14.4	14	12	12	10	10.8	8.4	10.5	6.8	8.0	6.1	5	3	3	3	3.8
00:15	6.26		0.398	0.254	0.024	-	-	-	-	-	-	-	-	-	-	-	-	-	-	-	-
00:30	12.23		0.383	0.61	0.029	14.4	13	13	9	9	10.5	8.5	10.1	5.0	7.8	6.0	4	2	3	3	3.6
00:45	17.98		0.370	1.05	0.038	-	-	-	-	-	-	-	-	-	-	-	-	-	-	-	-
01:00	23.53	0.702	0.363	1.62	0.048	14.5	12	1	9	0	2.2	8.1	9.7	1.4	6.9	3.8	0	0	0	0	1.8
01:10	27.16		0.350	2.10	0.072	-	-	-	-	-	-	-	-	-	-	-	-	-	-	-	-
01:20	30.66		0.331	2.82	0.114	-	-	-	-	-	-	-	-	-	-	-	-	-	-	-	-
01:30	33.97		0.309	3.96	0.141	14.5	7	0	0	0	0.0	1.7	5.7	0.0	2.9	0.6	0	0	0	0	0.2
01:40	37.06		0.350	5.37	0.193	-	-	-	-	-	-	-	-	-	-	-	-	-	-	-	-
01:50	40.56		0.418	7.30	0.275	-	-	-	-	-	-	-	-	-	-	-	--	-	-	-	-
02:00	44.74	1.335	0.403	10.05	0.303	14.5	0	0	0	0	-0.2	0.3	2.0	-0.4	0.0	0.0	0	0	0	0	0.0
02:10	48.77		0.399	13.08	0.348	-	-	-	-	-	-	-	-	-	-	-	-	-	-	-	-
02:20	52.76		0.383	16.56	0.309	-	-	-	-	-	-	-	-	-	-	-	-	-	-	-	-
02:30	56.59		0.371	19.65	0.355	14.4	0	0	0	0	-0.2	0.2	1.0	-0.4	0.0	0.0	0	0	0	0	-0.2
02:40	60.30		0.364	23.20	0.328	-	-	-	-	-	-	-	-	-	-	-	-	-	-	-	-
02:50	63.94		0.360	26.48	0.343	-	-	-	-	-	-	-	-	-	-	-	-	-	-	-	-
03:00	67.54	2.015	0.000	29.91	0.215	14.0	0	0	0	0	-0.2	0.2	0.7	-0.5	0.0	-0.2	0	0	0	0	-0.2
03:10	|	|	|	32.06	0.104	-	-	-	-	-	-	-	-	-	-	-	-	-	-	-	-
03:20	|	|	|	33.10	0.081	-	-	-	-	-	-	-	-	-	-	-	-	-	-	-	-
03:30	|	|	|	33.91	0.058	-	-	-	-	-	-	-	-	-	-	-	-	-	-	-	-
04:00	|	|	|	35.64	0.0181	10.6	0	0	0	0	-0.1	0.1	0.8	-0.5	0.0	-0.2	0	0	0	0	-0.2
09:00	|	|	|	41.08	0.0024	6.7	0	0	0	0	1.0	1.1	1.5	0.5	1.1	0.4	0	0	0	0	0.1
29:00	|	|	|	43.94	0.0004	5.4	0	0	2	2	1.5	1.9	1.6	0.8	1.3	1.0	0	0	0	0	0.9
52:30	|	|	|	44.48	0.0000	4.9	1	2	4	2	2.6	2.7	2.4	1.4	1.8	1.4	0	0	0	0	1.5
77:00	|	|	|	44.54	0.000	5.8	4	3	5	4	3.6	2.9	3.2	1.8	2.4	2.0	0	0	0	1	1.8
99:00	|	|	|	|	|	7.5	6	5	6	5	4.9	4.0	4.6	2.5	3.5	2.8	1	1	1	2	2.2
125:00	|	|	|	|	|	9.3	8	6	8	7	6.5	5.7	6.6	3.2	5.1	3.7	1	1	2	2	2.7
148.30	|	|	0.000	|	0.000	11.6	10	9	9	8	8.8	7.3	8.7	5.7	6.9	5.3	2	2	2	3	3.3
170:00	67.54			44.54		14.5	14	11	12	10	10.7	9.3	11.0	7.3	8.7	6.7	5	4	4	4	3.8

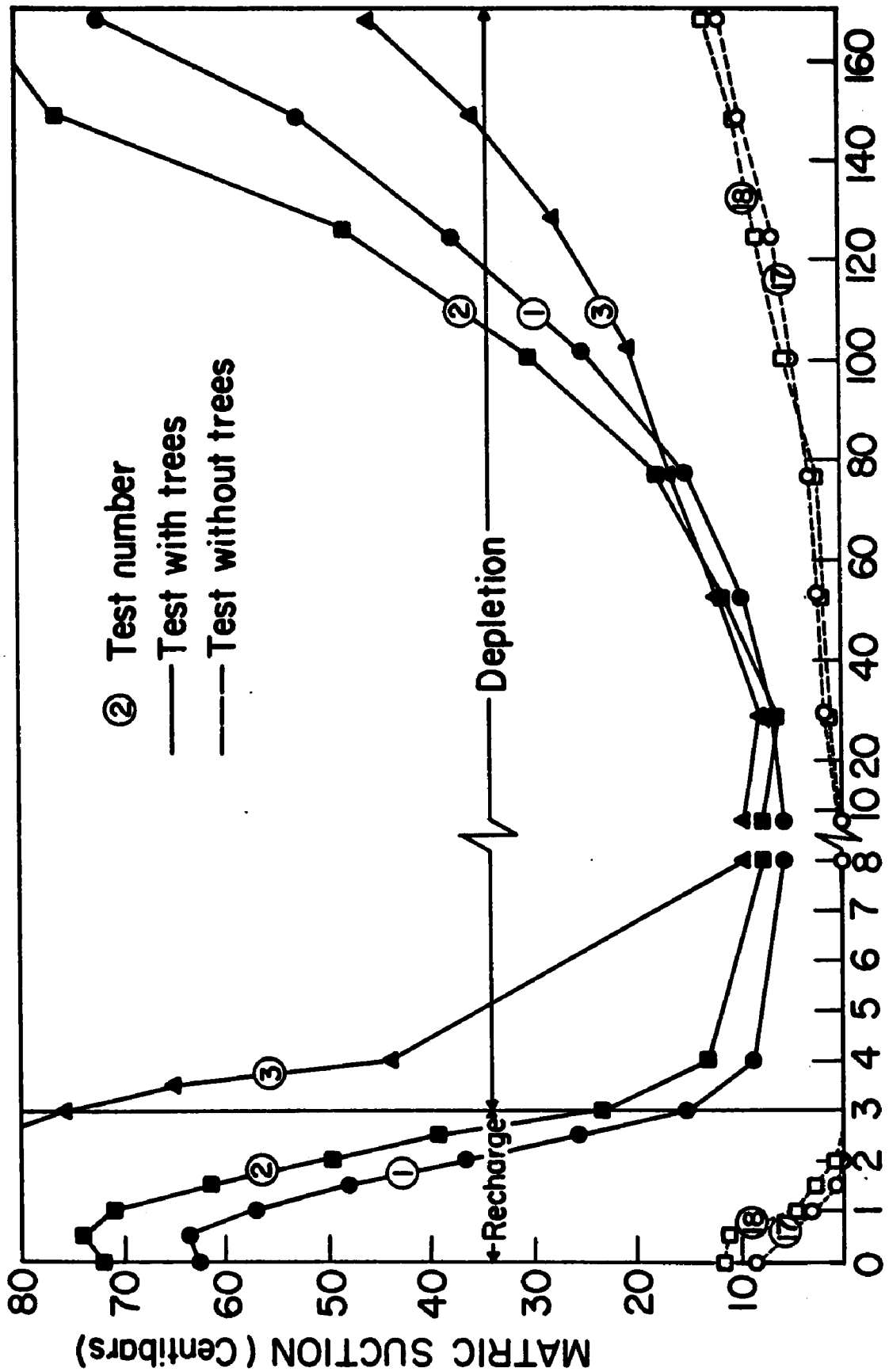


Figure 5.1.a Matric suction during the recharge and depletion phase for tensiometer no. 10 and a slope angle of 10 degrees.

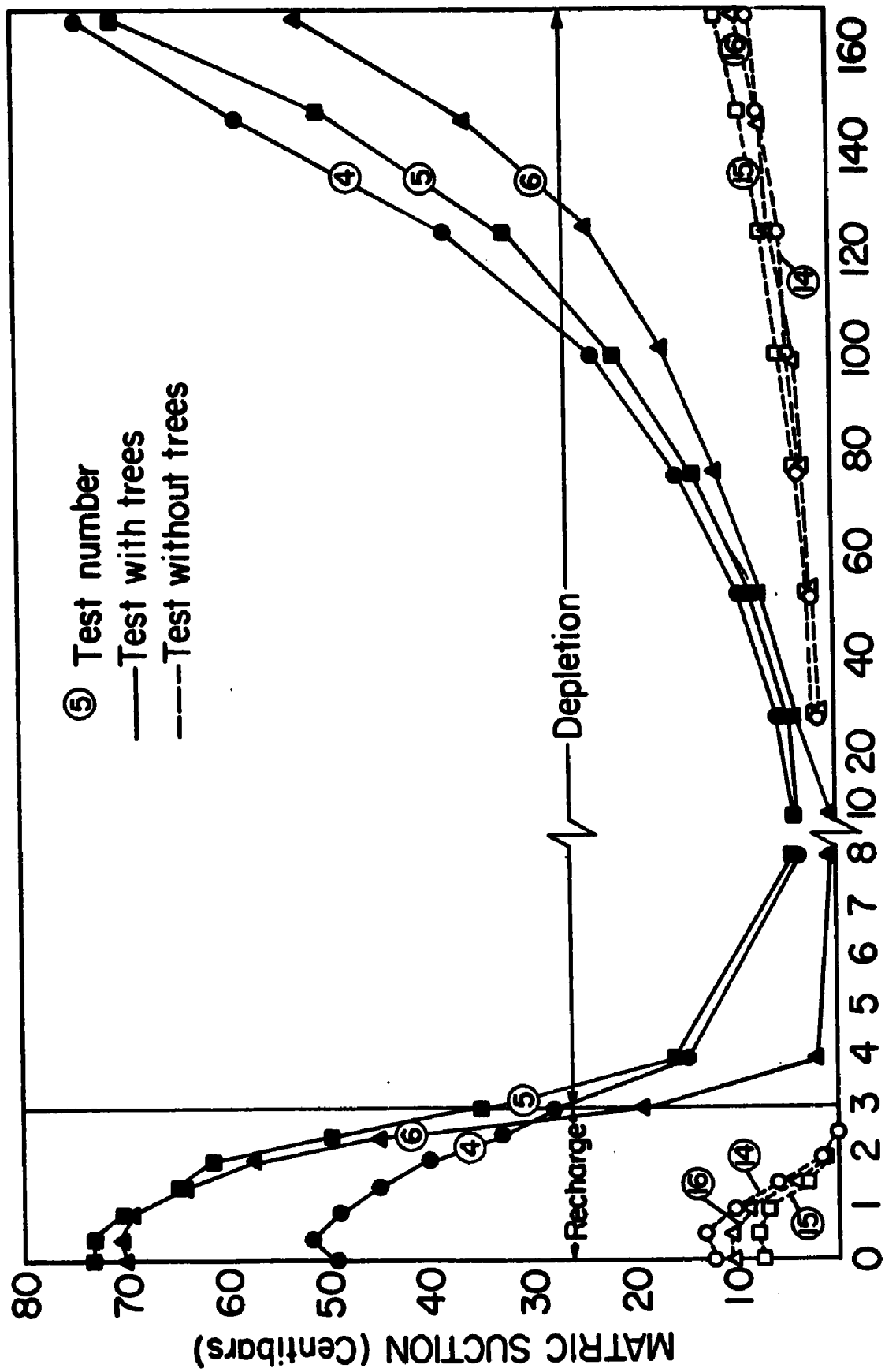


Figure 5.1.b Matric suction during the recharge and depletion phase for tensiometer no. 10 and a slope angle of 20 degrees.

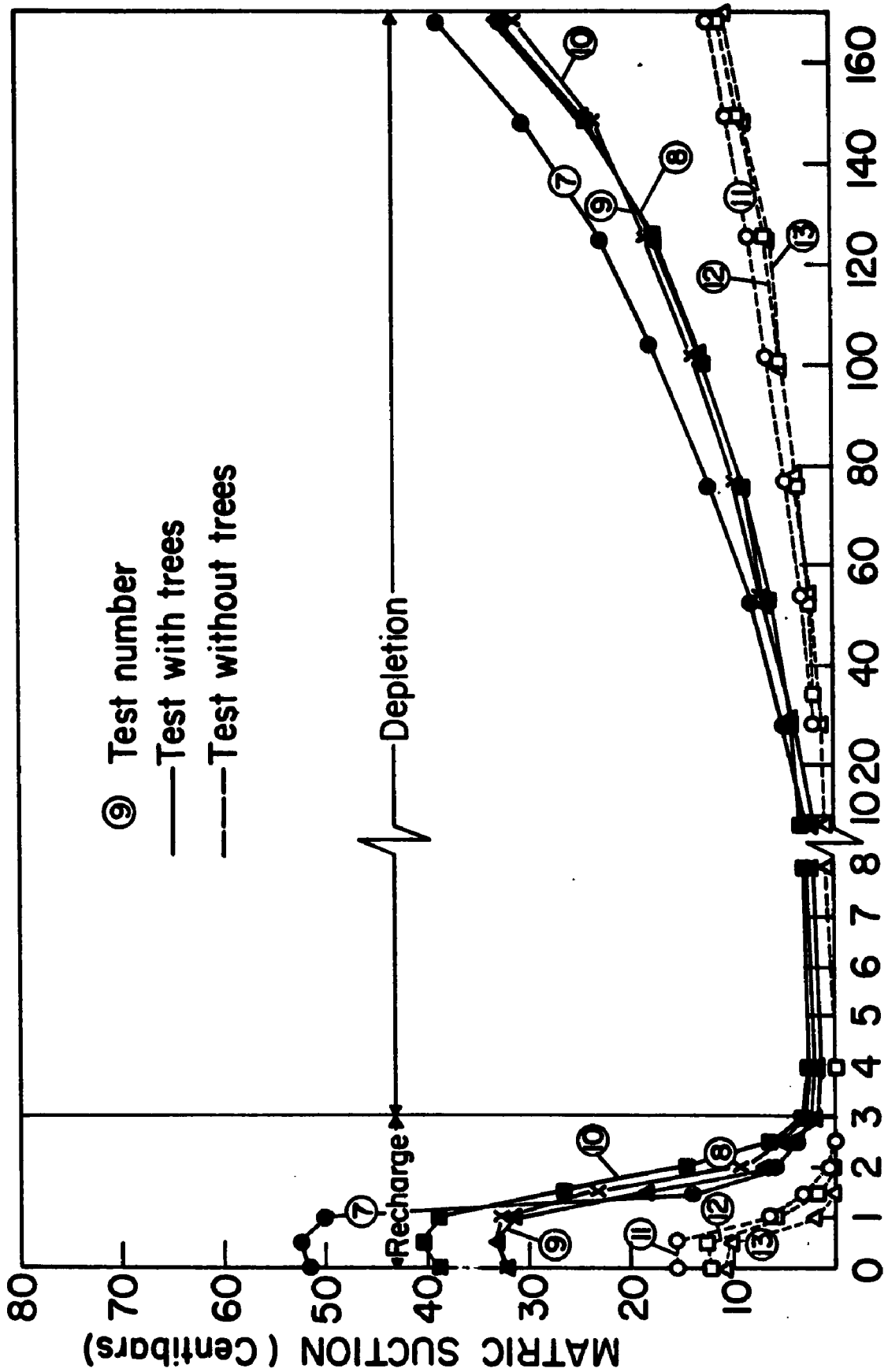


Figure 5.1.c Matric suction during the recharge and depletion phase for tensiometer no. 10 and a slope angle of 30 degrees.

and the depletion phase. Due to the time lag in tensiometer response, the plotted tensiometer readings from the recharge phase are probably somewhat distorted. But the curves clearly show the trend postulated in Figure 1.2, namely, the slope without trees reaching saturation much sooner than the one with trees. The difference in soil moisture tension at the end of one week is also significant and is consistent with the fact that soil moisture is depleted much faster on a forested slope after the recharge period than on a denuded one.

The relatively low values at the end of tests nos. 7, 8, 9 and 10 are due to the decreasing number of healthy trees caused by the tree diseases (insects). The same is also true for tests nos. 4, 5 and 6 during which the evaporative conditions were similar and the difference in suction is a result solely of the tree diseases. The first three tests, nos. 1. 2 and 3, are the only ones which truly reflect changing environmental conditions in their tensiometer readings from one test to the next. During test no. 3, sunlight was very scarce and humidity was high, which resulted in a low amount of depletion. On the other hand, test no. 2 took place during a very sunny period.

It can also be seen from these figures that the forested slope tended to retain at least some soil moisture tension during the recharge period, whereas the cut-over slope always reached saturation.

Figure 5.2 shows a typical storm diagram in which the rainfall and subsequent drainage (baseflow + direct runoff) are plotted versus

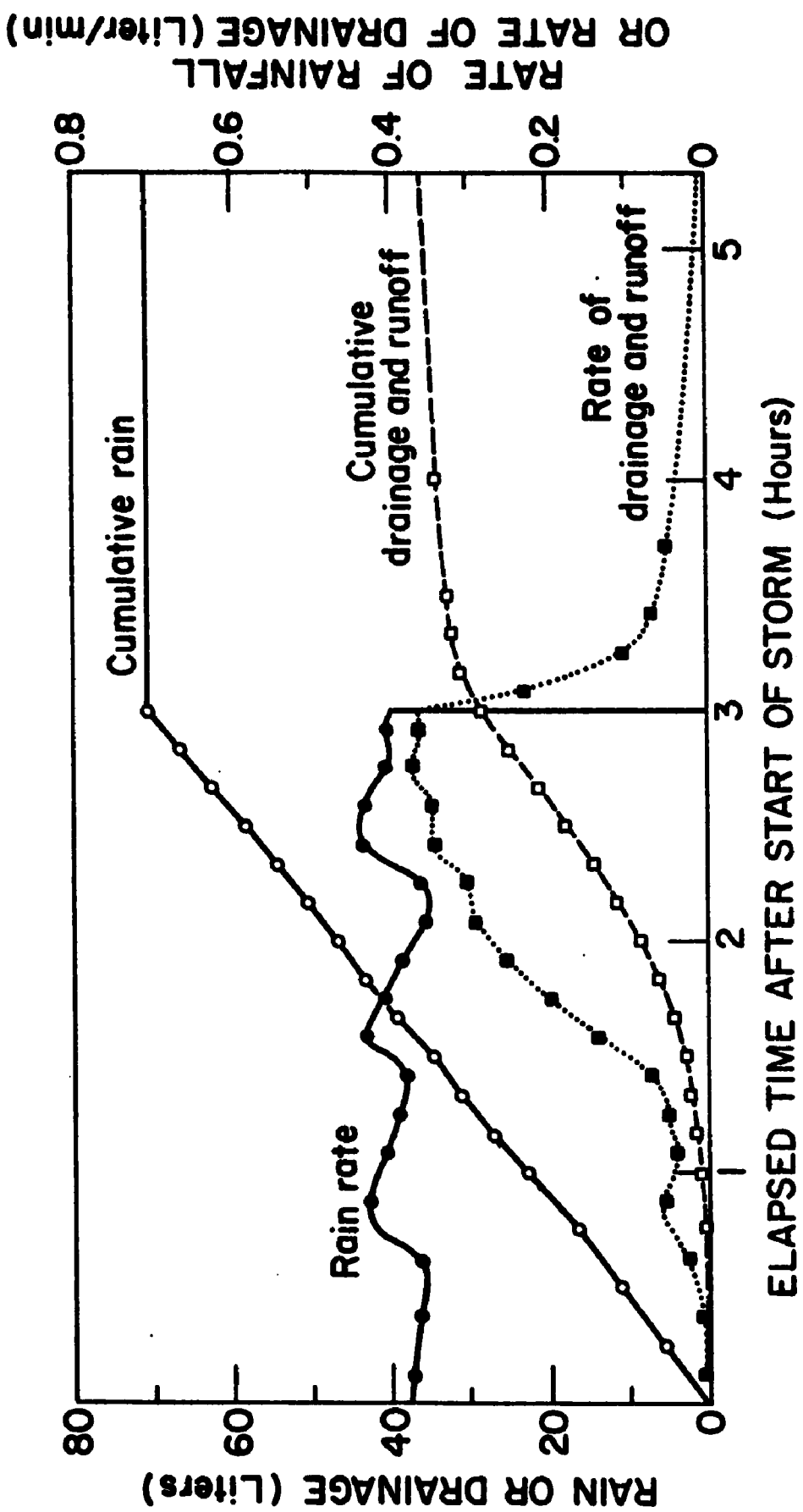


Figure 5.2 Typical storm diagram showing rain, drainage and runoff (Test no. 14).

time. Although the rate of precipitation fluctuates somewhat, the curves for the cumulative rainfall and drainage are quite smooth.

Figures 5.3a, 5.3b and 5.3c show the tensiometer readings at the end of each test period as a function of tensiometer location for the three slope angles. Again the difference in suction between the forested and the clear-cut slope is clearly visible, but also the effect of the slope angle. Whereas on the 10 degree slope the curves are almost horizontal, i.e., only a small difference in tension between the top and the bottom of the slope, this difference becomes greater with increasing slope angle. Unfortunately, this trend is again somewhat masked for the 30 degree slope (Figure 5.3c) because of the poor condition of the trees at the time this test sequence was run, particularly in the lower part of the slope. That is why such a sharp bend occurs at the location of tensiometer no. 10. In view of the fact that the measuring tips of tensiometers nos. 1 through 4 are at different depth relative to the other tensiometers, no attempt was made to fit the plotted curves to these points.

Table 5.2 summarizes all the pertinent data of the 18 tests of test series A, i.e., the total rainfall on the bin, the total drainage + runoff collected, and the tensiometer readings at the end of each test period.

In Figures 5.4a, 5.4b and 5.4c, the logarithm of suction is plotted versus the elapsed time after the end of a storm for tensiometers

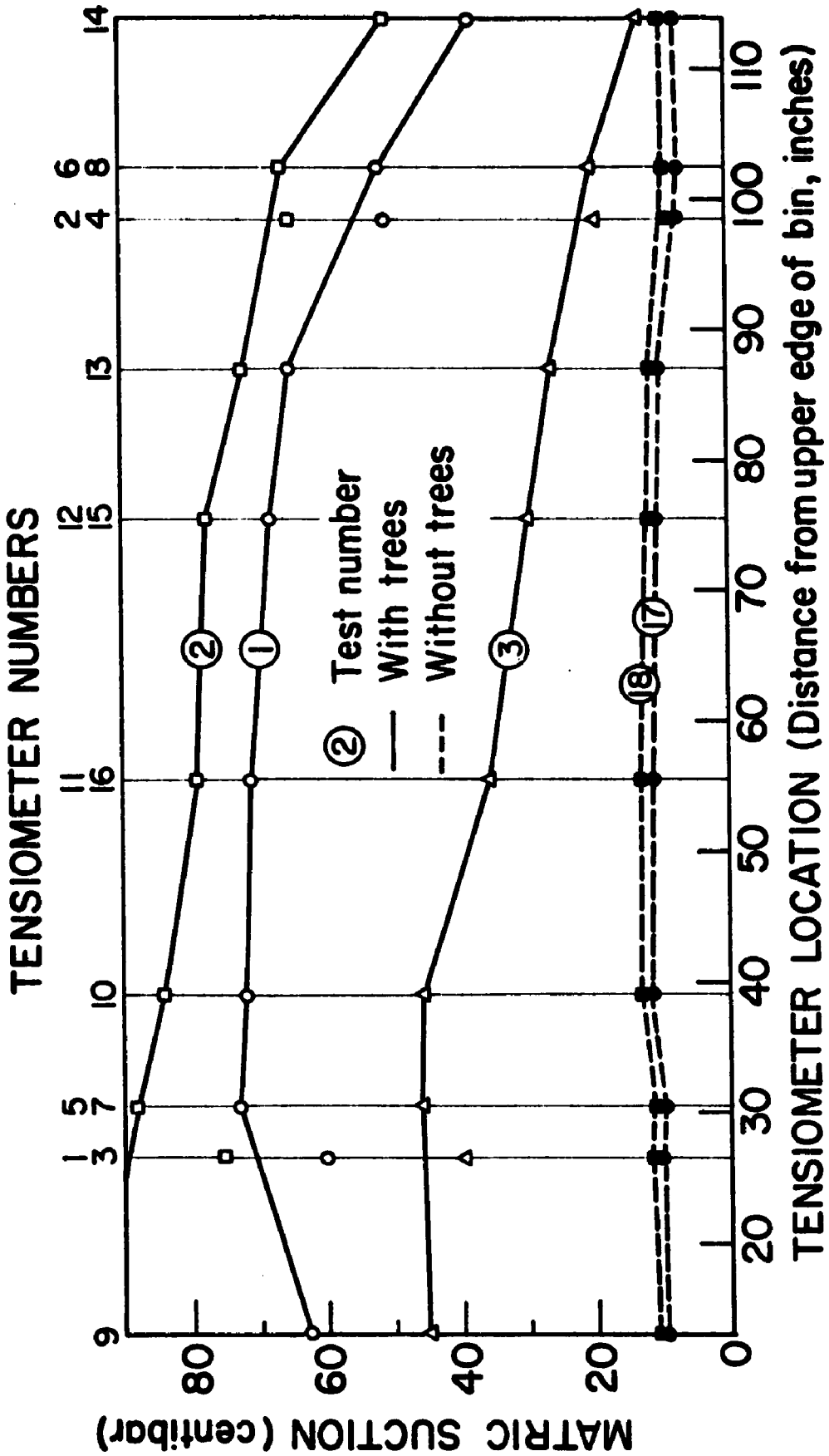


Figure 5.3.a Matric suction on a slope of 10^{o}, 165 hours after end of storm.

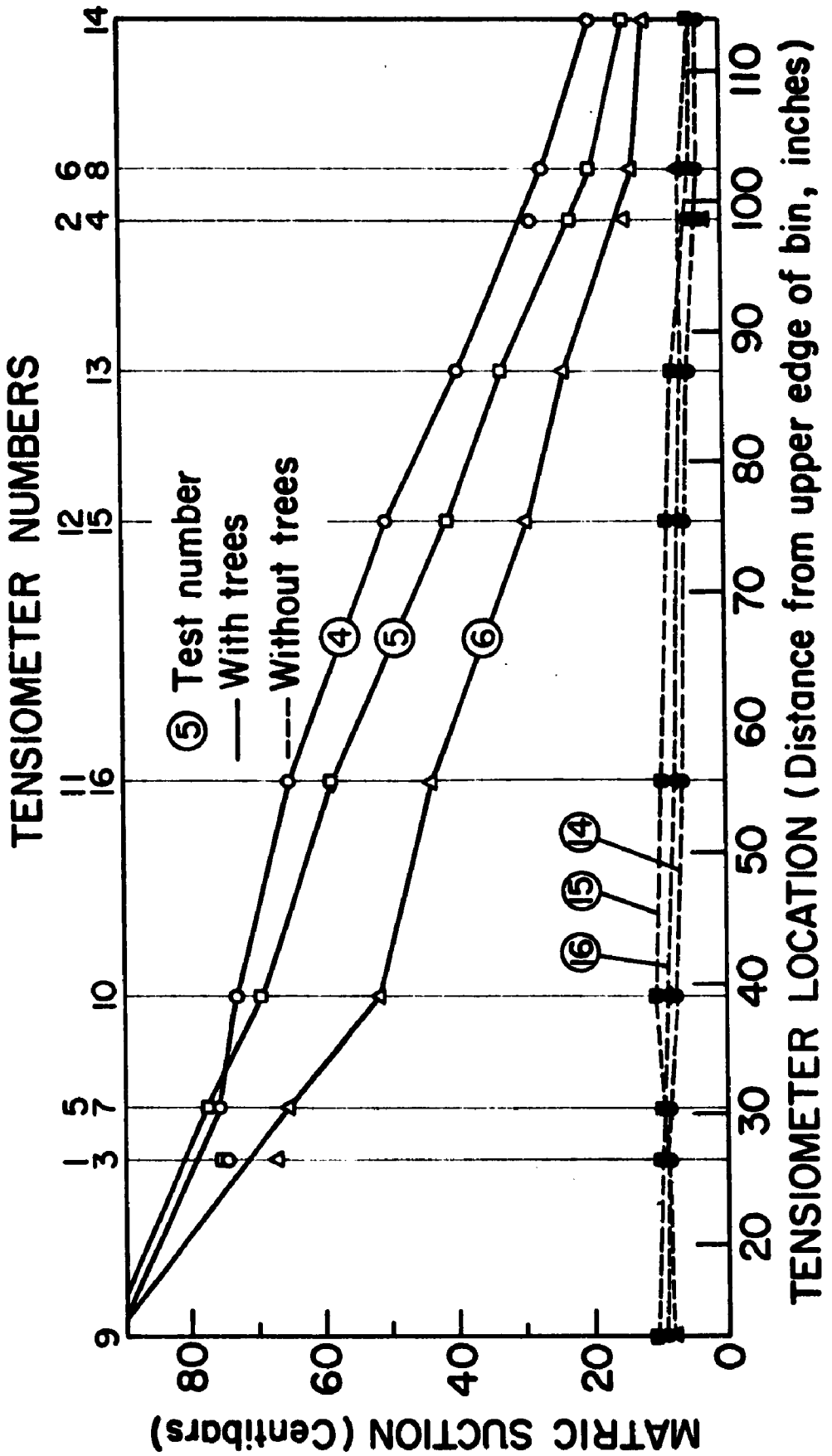


Figure 5.3.b Matric suction on a slope of 20^{o}, 165 hours after end of storm.

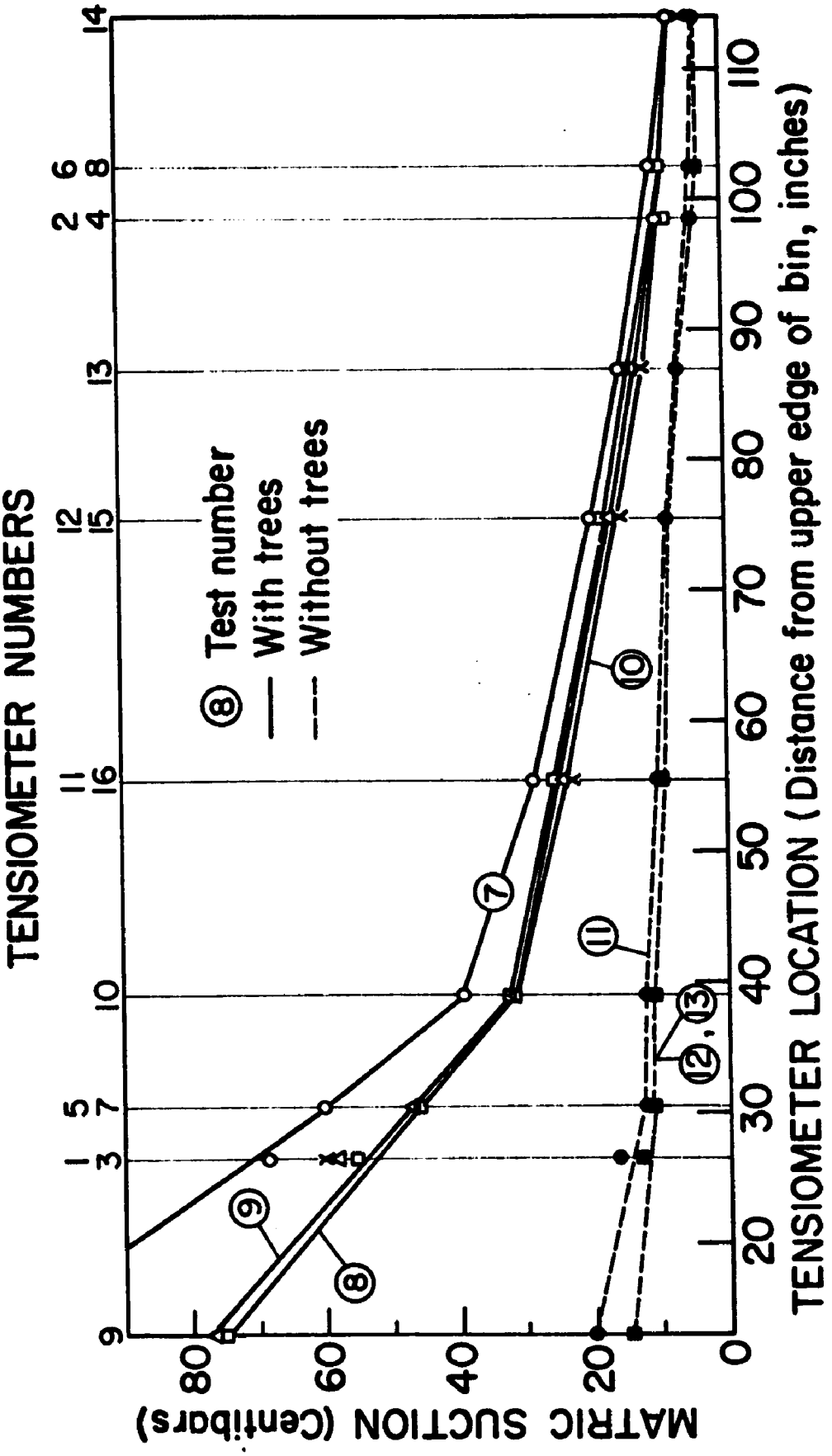


Figure 5.3.c Matric suction on a slope of 30^{o}, 165 hours after end of storm.

Table 5.2: Summary of Test Data, Test Series A

Test No.	Slope Angle in Degrees	Total Rainfall (liter) Pr'	Total Drainage + Runoff (liter) Dr	Tensiometer Reading at End of Test (168 Hrs.) in Centibars														
				9	1	3	5	7	10	11	16	12	15	13	2	4	6	8	14
1	10	57	14.84	62.5	65	56	74	72	72.0	73.6	68.5	73.5	62.1	65.2	58	43	60	43	38.0
2	10	61	15.91	>85.0	76	74	88	88	84.1	80.0	78.2	80.2	75.1	72.2	69	61	72	61	51.0
3	10	64	11.17	45.2	43	37	47	45	45.6	35.2	35.8	29.8	29.8	26.5	23	16	23	17	13.6
4	20	55	22.21	>85.0	76	72	83	69	72.8	64.4	65.0	49.7	50.9	39.1	29	27	28	25	18.8
5	20	60	23.24	>85.0	76	73	82	73	69.4	57.7	59.0	43.5	38.9	32.7	24	20	21	17	14.0
6	20	63	25.89	>85.0	69	65	74	55	51.5	43.5	43.3	32.2	26.1	23.3	15	13	14	12	10.8
7	30	62	28.55	>85.0	70	67	70	50	38.8	27.2	29.0	19.8	17.8	14.8	10	9	11	9	7.4
8	30	64.11	36.20	75.0	61	50	55	37	32.4	24.8	26.4	18.8	17.4	13.8	9	8	9	8	7.2
9	30	60.28	31.96	76.5	63	53	57	38	32.5	23.8	26.4	17.4	16.8	13.5	10	9	10	9	7.3
10	30	59.63	27.60	76.4	61	57	55	39	30.8	22.0	24.2	15.7	15.7	12.0	8	8	8	8	6.5
11	30	61.18	35.47	20.1	16	17	13	12	12.0	9.2	11.4	7.3	8.6	6.7	4	4	4	4	4.0
12	30	66.63	40.35	14.4	14	12	12	10	10.8	8.4	10.5	6.8	8.0	6.1	5	3	3	3	3.8
13	30	67.54	44.54	14.5	14	11	12	10	10.7	9.3	11.0	7.3	8.7	6.7	5	4	4	4	3.8
14	20	70.60	43.25	9.2	9	8	9	8	7.4	6.2	6.4	5.4	5.3	5.0	4	2	4	3	3.0
15	20	70.10	48.39	10.5	10	9	9	9	10.4	9.1	9.4	7.8	7.8	7.0	4	3	4	4	4.6
16	20	71.28	47.28	9.0	10	9	9	9	8.7	7.6	8.7	6.7	7.2	6.6	3	3	7	4	4.4
17	10	73.73	43.25	9.5	12	11	10	10	11.7	10.9	11.7	10.3	10.8	10.2	7	7	8	6	7.6
18	10	73.42	38.85	9.9	12	11	12	10	12.8	12.2	12.9	11.7	12.5	11.4	8	9	10	9	9.3

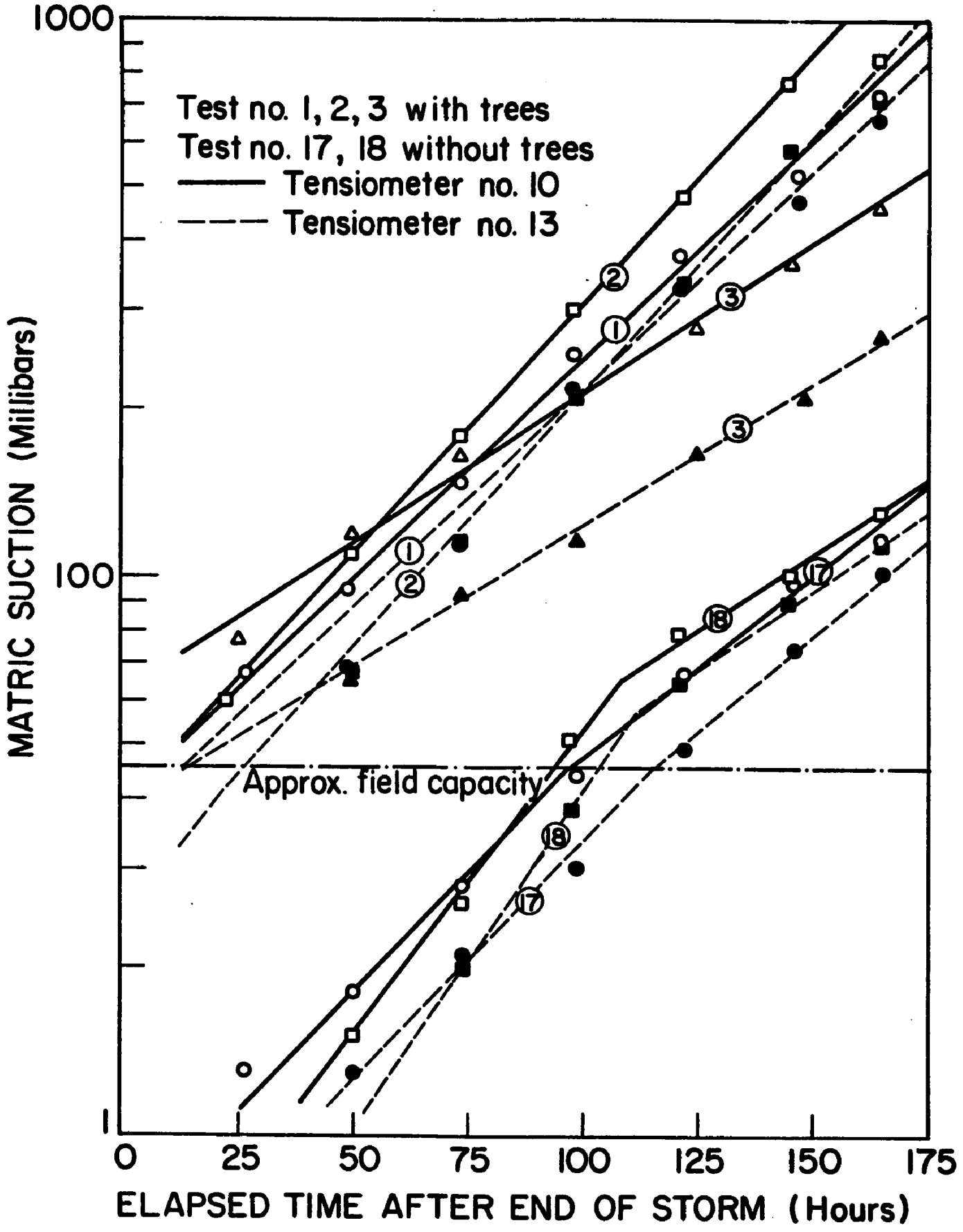


Figure 5.4.a Logarithm of suction versus time for a slope of 10 degrees.

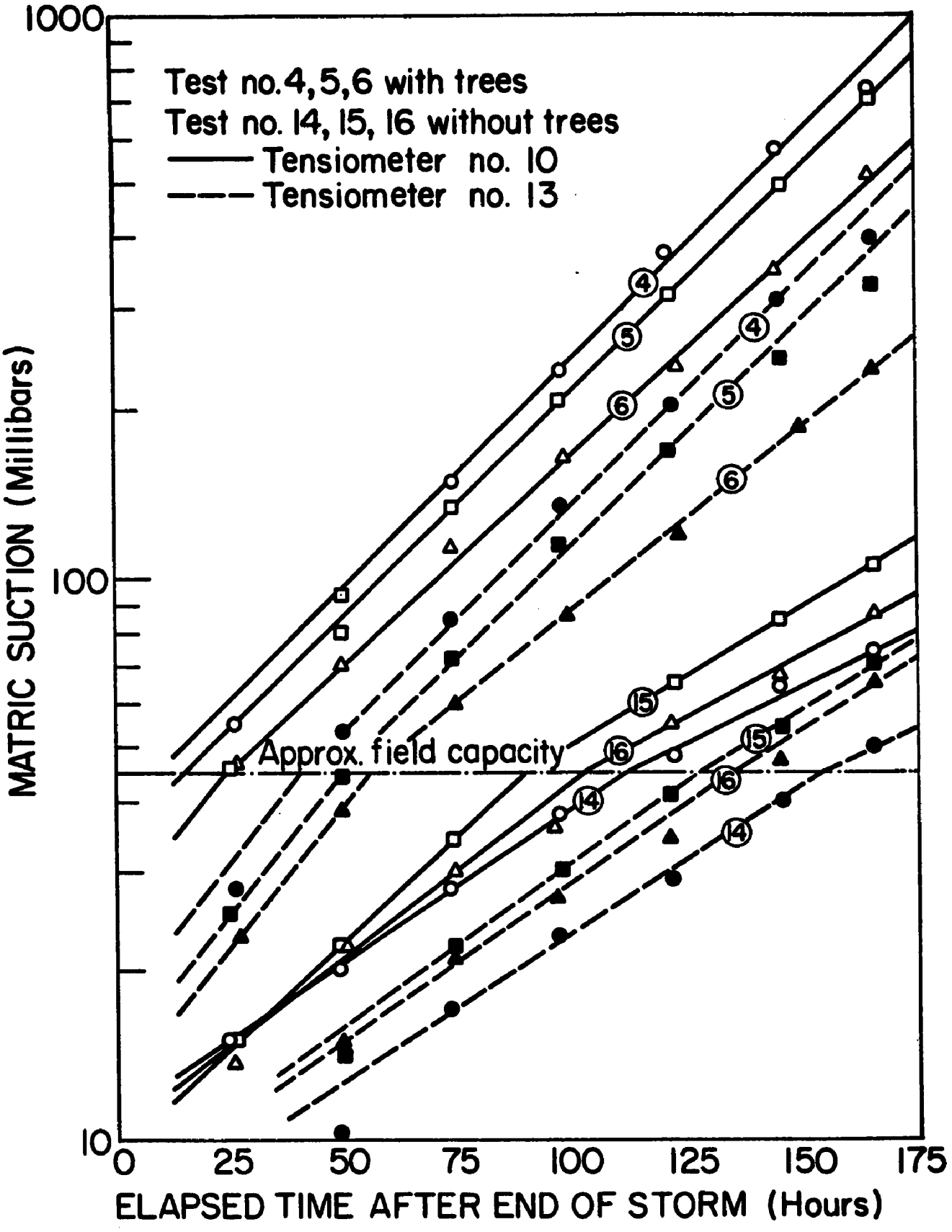


Figure 5.4.b Logarithm of suction versus time for a slope of 20 degrees.

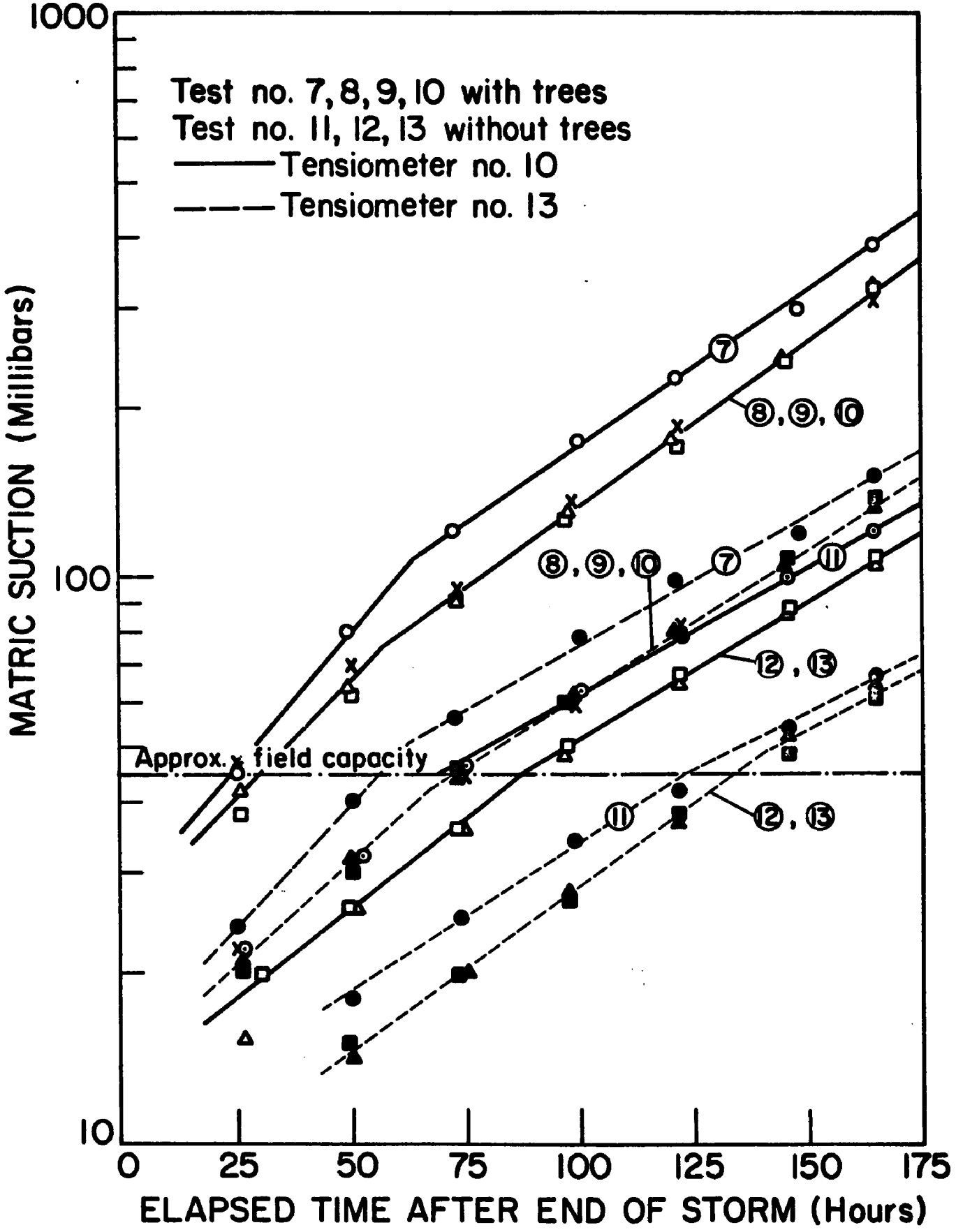


Figure 5.4.c Logarithm of suction versus time for a slope of 30 degrees.

no. 10 and no. 13. Tensiometer no. 10 represents a point in the upper third of the slope, whereas tensiometer no. 13 is located in the lower third. For each slope angle, the test results of the forested as well as the cleared slope are plotted. The matric suctions at higher elevations are always higher than at lower elevations for a given time, that is why the curves for tensiometer no. 10 always lie above those of tensiometer no. 13. This pattern could be observed for all tests and appeared to be influenced only by transpiration factors, i.e., climate and leaf area. Note also that the curves for tensiometer nos. 10 and 13 of the same test are more or less parallel at suctions above field capacity, which means that the slope of the curves is independent of the location of the tensiometers along the length of the soil bin.

The fitted straight-line relationship in these figures can be expressed by

$$\tau(t) = A\, e^{\alpha t} \qquad (5.1)$$

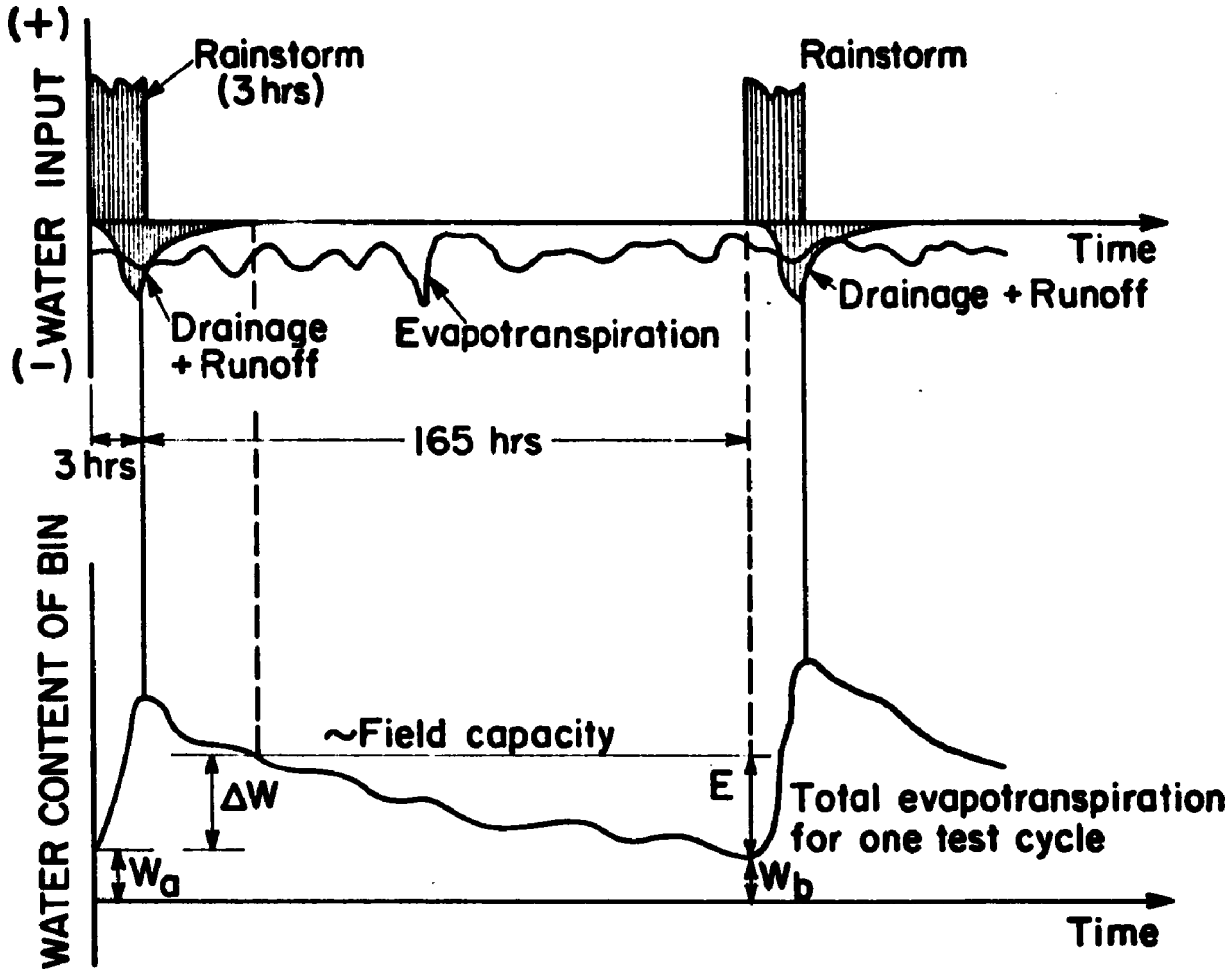
where τ is the matric suction, A is the ordinate intercept and α is the slope.

α seems to be mainly a function of soil water uptake or evaporation, and therefore, of the environmental conditions. The bend in the straight lines, occurring somewhere between 40 and 100 millibars, probably represents field capacity and means that below this value the soil water content decrease is governed mainly by gravity drainage. Above this value, matric forces appear to dominate soil moisture

movement and redistribution. As mentioned in Chapter 2, the point at which this happens is not very distinct in clayey soils.

In order to evaluate the total evapotranspiration occurring during each test, the water balance method was used. This is shown schematically in Figure 5.5 and the results are summarized in Table 5.3. Evapotranspiration in this simple case could be obtained from the difference in water content of the bin at the beginning and end of each test period, plus the amount of recharge. The recharge is simply the difference between precipitation and runoff + drainage. The main difficulty in this case was to determine the total water content of the bin. This was done from tensiometer readings along the longitudinal profile. These readings were converted to water contents using the empirical relationship found in Figure 4.11. Hence, it was possible to draw a longitudinal water content profile, assuming that the average water content was the same everywhere in the y-direction (along the strike of the slope) for a given x (along the dip of the slope). Taking into account that the volume (soil depth) in the longitudinal sense is changing according to Figure 4.5, the profile was divided into 12-inch sections and the total water content was then obtained from

$$W_{tot} = \sum_{i=1}^{n} \frac{\overline{w}_i}{100} \cdot V_i \cdot \frac{\gamma_{dry}}{\gamma_w} \qquad (5.2)$$



Pr' = TOTAL RAINFALL ON BIN

Dr = TOTAL RUNOFF + DRAINAGE

$\Delta W = Pr' - Dr$ = CHANGE IN STORAGE

$$W_a + \Delta W = W_b + E$$

$$W_a - W_b - E + Pr' - Dr = 0$$

$$E = W_a - W_b + (Pr' - Dr)$$

Figure 5.5 Determination of evapotranspiration of the bin by the water balance method.

Table 5.3: Water Balance for Test Series A

Test Number	Water Content of Bin at Start of Test W_a (liter)	Water Content of Bin at End of Test W_b (liter)	Total Rainfall on Bin Pr'(liter)	Total Drainage + Runoff Dr (liter)	Evapotranspiration $E = W_a - W_b + (Pr' - Dr)$	Evapotranspiration $E = W_{FC} - W_b$
1	193.8	188.4	~57	14.84	47.6	48.6
2	188.4	179.2	~61	15.91	54.3	57.8
3	179.2	211.2	~64	11.17	20.8	25.8
4	205.8	194.6	~55	22.21	44.0	42.4
5	194.6	197.6	~60	23.24	33.8	39.4
6	197.6	204.4	~63	25.89	30.3	32.0
7	204.4	210.2	~62	28.55	27.6	26.8
8	210.2	213.0	64.11	36.20	25.1	24.0
9	213.0	213.2	60.28	31.96	28.1	23.8
10	213.2	214.1	59.63	27.60	31.1	22.9
11	225.7	231.2	61.18	35.47	20.2	5.8
12	231.2	232.7	66.63	40.35	24.8	4.3
13	232.7	232.2	67.54	44.54	23.5	4.8
14	230.3	234.5	70.60	43.25	23.2	2.5
15	234.5	232.8	70.10	48.39	23.4	4.2
16	232.8	233.4	71.28	47.28	23.4	3.6
17	233.4	231.6	73.73	43.25	32.3	5.4
18	231.6	230.1	73.42	38.85	36.1	6.9

W_{FC} = Water content of bin at 45 cm tension (~ field capacity)
= 237.0 liter

which is an approximation to:

$$W_{tot} = \int_0^{l_B} \frac{w(x)}{100} \cdot d_B(x) \cdot b_B \cdot \frac{\gamma_{dry}}{\gamma_w} \cdot dx \qquad (5.3)$$

where $\bar{w}_i$ is the average water content in the section i of length 12 inches and volume V_i; $d_B(x)$ is the soil depth and b_B is the width of the bin.

Unfortunately the results of this procedure are affected by the uncertainties of the quantities involved such as w(x) as a function of matric suction (Figure 4.11) and the scatter in the bulk density γ_{dry}. The standard deviation of 0.040 gram/cm^3 in bulk density alone produces variations in total water content of ± 6 liters. This is almost on the same order of magnitude as the transpiration of the trees alone. It is therefore not surprising that the values for evapotranspiration in the water balance do not show a very distinct influence of the vegetation. In addition, precipitation values of the first 7 tests were estimated from raingage measurements which are much less accurate than those determined later by techniques described in Section 4.2.b. Nevertheless, the evapotranspiration calculated by this procedure for a slope with vegetation was usually higher than that on the same slope without vegetation inspite of uncertainties in the precipitation and soil water content measurements.

Evapotranspiration can also be determined from the difference of the water content after drainage has ceased, i.e., when the bin is

approximately at field capacity and the water content at the end of the drying cycle. However, at no time will all points of the bin be at field capacity simultaneously; the upper parts of the slope are always at a smaller moisture content than the downslope locations. Nevertheless, a fictitious water content W_{FC} was computed in which the whole bin was assumed to be under 45 cm tension. (This tension represents approximately field capacity, as shown in Figure 5.4.) The water content at the end of the test was subtracted from this fictitious water content and the difference recorded in the last column of Table 5.3. Reasonably good agreement with the values computed by the first procedure was obtained for the forested slope; however, large discrepancies occurred for the clear-cut slope. This might be explained as follows: While the slope was forested, the grass cover was very thin (grass did not grow very well under the trees). After the trees were cut, the grass cover became very dense. Its roots were mostly concentrated in the organic soil layer and in the top inch of the clay-loam. When recharge took place during a simulated storm, most of the water was probably stored in this top zone and was then depleted rapidly by the dense root system while the rest of the soil profile remained at a high water content, which then still exhibited a high average moisture content. This, however, can account only for part (about 10 liters) of the recharge water that is used. The unaccounted remainder (approximately 10 liters) must be due to inaccuracies in the water content determinations W_a and W_b.

Inaccuracies in calculated water contents are much more significant in this case near saturated conditions. The test results suggest the computed water contents in the soil, W_a and W_b, at low suctions, were too high.

The second method for determining evapotranspiration is therefore only useful when the water content at the end of the test is considerably different from field capacity, as was the case for the forested slope.

Summarizing: These data suggests that transpiration by the trees alone amounted to about 15 to 25 liters when the trees were in good condition and to about 5 to 10 liters when the trees were severely affected by the insects, i.e., at the time of clear-cutting. This means that under normal conditions the forested slope could absorb about 60 to 100 percent more water than the denuded slope after a one-week depletion period.

Table 5.4 shows the size and quality (amount of leaves) of the trees at the time of clear-cutting. The total basal area of the trees was 42.4 cm^2 which, with respect to the bin surface, corresponds to 55 ft^2 per acre. From this table it can be seen that only about 10 trees with a reasonable amount of leaves were present at the time of clear-cutting. Eleven trees had lost their leaves completely.

2. Results of Transpiration Experiments

The data obtained from the transpiration measurements with potted trees are shown in Tables 5.5 and 5.6. Table 5.5 also gives the weekly averages of temperature and relative humidity obtained from

Table 5.4: Tree Data at Time of Clear-Cutting (30/31 December 1969)

Tree No.	Weight of Leaves (grams)				Approx. Total Leaf Surface (Total x 54.1) (cm^2)	Average Stem Diameter at Base (cm)	Weight of Tree without Leaves (gr)	Length of Cut Tree (cm)	Remarks
	Large	Medium	Small	Total					
1	0	19.45	13.30	32.75	1772	1.485	150.9	124	
2	0	0	0	0	0	1.219	36.9	97	Tree dead
3	0	0	0	0	0	1.579	91.9	86	Leaves dry
4	0	0	11.33	11.33	613	1.079	46.2	71	
5	0	0	6.88	6.88	372	1.290	93.0	79	
6	0	0	0	0	0	1.611	104.5	92	Leaves dry
7	10.01	73.93	23.66	107.60	5821	1.840	195.7	109	
8	0	0	0	0	0	1.168	48.1	64	
9	0	6.41	9.38	15.79	854	1.138	57.7	74	
10	3.92	13.64	10.52	28.08	1519	1.353	103.3	89	
11	2.17	29.92	8.92	41.01	2219	1.160	77.4	94	
12	21.56	17.54	22.56	61.66	3336	1.600	201.1	145	
13	2.92	19.57	18.19	40.68	2201	1.261	91.7	86	
14	0	6.12	14.91	21.03	1138	1.575	129.5	84	
15	0	0	0	0	0	1.180	57.6	107	
16	9.10	18.74	30.10	57.94	3135	1.472	139.6	107	
17	0	0	4.71	4.71	255	1.359	92.5	102	
18	0	0	0	0	0	1.311	71.0	76	
19	0	0	0	0	0	1.630	96.0	79	
20	0	0	0	0	0	1.273	68.8	84	
21	0	0	0	0	0	1.778	154.9	122	
22	0	0	0	0	0	1.765	127.4	89	
23	0	0	2.05	2.05	111	1.595	110.4	94	
24	0	0	0	0	0	1.630	69.4	84	
25	28.26	38.17	27.47	93.90	5080	1.930	230.6	145	
	77.94	243.49	203.98	525.41	28426	Total Basal Area: 42.42 cm^2			

Table 5.5: Transpiration of Potted Trees I

Test No.	Time Period	Avg. Temp.		Avg. Rel. Humidity %	Total Evaporation (liter)							$\sum_{1}^{3} -3 \times (4)$ Tr_{tot} (liter)
					Pot 1		Pot 2		Pot 3		Pot 4	
		^{o}F	^{o}C		Tot	(1-4)	Tot	(2-4)	Tot	(3-4)		
1	Oct 14-Oct 21	67.9	19.9	60.2	1.36	1.02	1.23	0.89	1.36	1.02	0.34	2.93
2	Oct 21-Oct 28	69.9	21.1	45.2	1.67	1.18	1.63	1.14	2.04	1.55	0.49	3.87
3	Oct 28-Nov 4	68.6	20.3	65.0	1.48	1.11	1.08	0.71	1.44	1.07	0.37	2.89
4	Nov 11-Nov 18	66.7	19.3	51.2	1.70	1.28	1.53	1.11	1.89	1.47	0.42	3.86
5	Nov 18-Nov 25	65.5	18.6	49.2	1.82	1.41	1.78	1.37	2.03	1.62	0.41	4.40
6	Nov 25-Dec 2	64.8	18.2	49.0	1.86	1.52	1.94	1.60	2.07	1.73	0.34	4.85
7	Dec 2-Dec 9	65.2	18.4	56.8	1.58	1.27	1.77	1.46	1.99	1.68	0.31	4.41
8	Dec 9-Dec 16	64.9	18.3	55.7	1.81	1.57	1.97	1.73	2.12	1.88	0.24	5.18
9	Dec 16-Dec 23	64.5	18.1	54.0	1.88	1.62	2.12	1.86	2.34	2.08	0.26	5.56
10	Dec 23-Dec 30	65.7	18.7	57.9	1.77	1.53	1.84	1.60	2.36	2.12	0.24	5.25
11	Jan 1-Jan 8	65.8	18.8	51.8	1.97	1.71	2.09	1.83	2.62	2.36	0.26	5.90
12	Jan 8-Jan 15	65.0	18.3	55.8	2.20	1.94	1.90	1.64	2.50	2.24	0.26	5.82
13	Jan 15-Jan 22	66.3	19.1	52.0	2.16	1.88	1.78	1.50	2.52	2.24	0.28	5.62
14	Jan 23-Jan 30	67.7	19.8	63.0	1.79	1.59	1.34	1.14	2.16	1.96	0.20	4.69
15	Jan 30-Feb 6	67.8	19.9	55.0	2.22	1.95	1.70	1.43	2.56	2.29	0.27	5.67
16	Feb 6-Feb 13	67.0	19.4	61.9	2.18	1.94	1.44	1.20	2.53	2.29	0.24	5.43
17	Feb 13-Feb 20	67.2	19.6	63.0	2.91	2.56	1.93	1.58	3.16	2.81	0.35	6.95
18	Feb 20-Feb 27	67.8	19.9	72.2	2.77	2.43	2.12	1.78	3.01	2.67	0.34	6.88

Table 5.6: Transpiration of Potted Trees II

Test No.	Transp. Pot 1 (liter) Tr_{t1}	Leaf Surface Pot 1 (m^2) Ar_1	Transp. Pot 2 (liter) Tr_{t2}	Leaf Surface Pot 2 (m^2) Ar_2	Transp. Pot 3 (liter) Tr_{t3}	Leaf Surface Pot 3 (m^2) Ar_3	$\frac{Tr_{t1}}{Ar_1}$ $\left(\frac{liter}{m^2}\right)$	$\frac{Tr_{t2}}{Ar_2}$ $\left(\frac{liter}{m^2}\right)$	$\frac{Tr_{t3}}{Ar_3}$ $\left(\frac{liter}{m^2}\right)$	$\frac{Tr_{t1}+Tr_{t2}+Tr_{t3}}{Ar_1+Ar_2+Ar_3}$ $\left(\frac{liter}{m^2}\right)$	$\bar{Tr}_t$ Normalized for Test No. 10	Hours of Sunshine	Open Sky (Percent)
1	1.02	0.275	0.89	0.240	1.02	0.275	3.71	3.70	3.71	3.71	0.995	28.5	40.4
2	1.18	0.315	1.14	0.290	1.55	0.325	3.75	3.93	4.77	4.16	1.110	38.7	38.6
3	1.11	0.330	0.71	0.300	1.07	0.350	3.37	2.37	3.05	2.95	0.790	12.6	22.6
4	1.28	0.335	1.11	0.310	1.47	0.365	3.83	3.58	4.02	3.82	1.024	19.0	18.4
5	1.41	0.350	1.37	0.350	1.62	0.410	4.02	3.92	3.95	3.96	1.061	23.8	24.4
6	1.52	0.360	1.60	0.380	1.73	0.450	4.22	4.21	3.85	4.08	1.096	29.7	26.9
7	1.27	0.375	1.46	0.410	1.68	0.490	3.39	3.56	3.43	3.46	0.922	21.0	26.6
8	1.57	0.390	1.73	0.425	1.88	0.515	4.02	4.07	3.65	3.90	1.045	11.8	18.1
9	1.62	0.415	1.86	0.430	2.08	0.525	3.90	4.32	3.97	4.06	1.089	19.4	19.0
10	1.53	0.430	1.60	0.435	2.12	0.535	3.56	3.68	3.96	3.75	1.000	17.2	25.2
11	1.71	0.460	1.83	0.420	2.36	0.550	3.72	4.36	4.29	4.12	1.098	24.7	25.6
12	1.94	0.475	1.64	0.405	2.24	0.555	4.08	4.05	4.03	4.05	1.086	25.3	27.4
13	1.88	0.490	1.50	0.375	2.24	0.565	3.84	4.00	3.97	3.93	1.053	35.0	42.2
14	1.59	0.495	1.14	0.360	1.96	0.570	3.22	3.17	3.44	3.29	0.881	4.9	11.4
15	1.95	0.495	1.43	0.350	2.29	0.570	3.94	4.38	4.02	4.00	1.072	30.9	42.6
16	1.94	0.495	1.20	0.335	2.29	0.570	3.92	3.59	4.02	3.88	1.040	15.6	19.6
17	2.56	0.490	1.58	0.330	2.81	0.570	5.23	4.80	4.93	5.00	1.335	58.9	39.1
18	2.43	0.475	1.78	0.360	2.67	0.570	5.12	4.95	4.68	4.90	1.308	50.6	58.5

hygrothermograph recordings for all 18 tests. The evaporation of pot no. 4 (with a cut tree) was subtracted from the other three pots in order to obtain the net transpiration. The weekly net transpiration of each pot is plotted in Figure 5.6. The leaf area of the potted trees was determined three times and the results are given in Table 5.7 and plotted for each tree in Figure 5.6. The quality of the leaves was divided into several categories, because it was assumed that there might be a marked effect of leaf condition on transpiration; however, this did not seem to be the case. Therefore, the total leaf area was always used regardless of the conditions of the leaves.

It should also be mentioned that the trees in the pots were in a much healthier state than those in the bin. Whenever they were attacked by insects, the leaves were washed individually, which was an effective countermeasure. But this time-consuming treatment was only possible because the number of leaves was limited.

It is reasonable to assume that for individual plants the transpiration is more or less proportional to the total leaf area. (Other factors may be important too, such as the density and position of the leaves or the extent of the root system. However, it was observed that when such a plant was stripped of half of its leaf surface at the end of test series A, daily transpiration also decreased about one-half.)

Accordingly, the transpiration of each pot was divided by its total leaf area. The leaf area at each test was obtained from the curves in

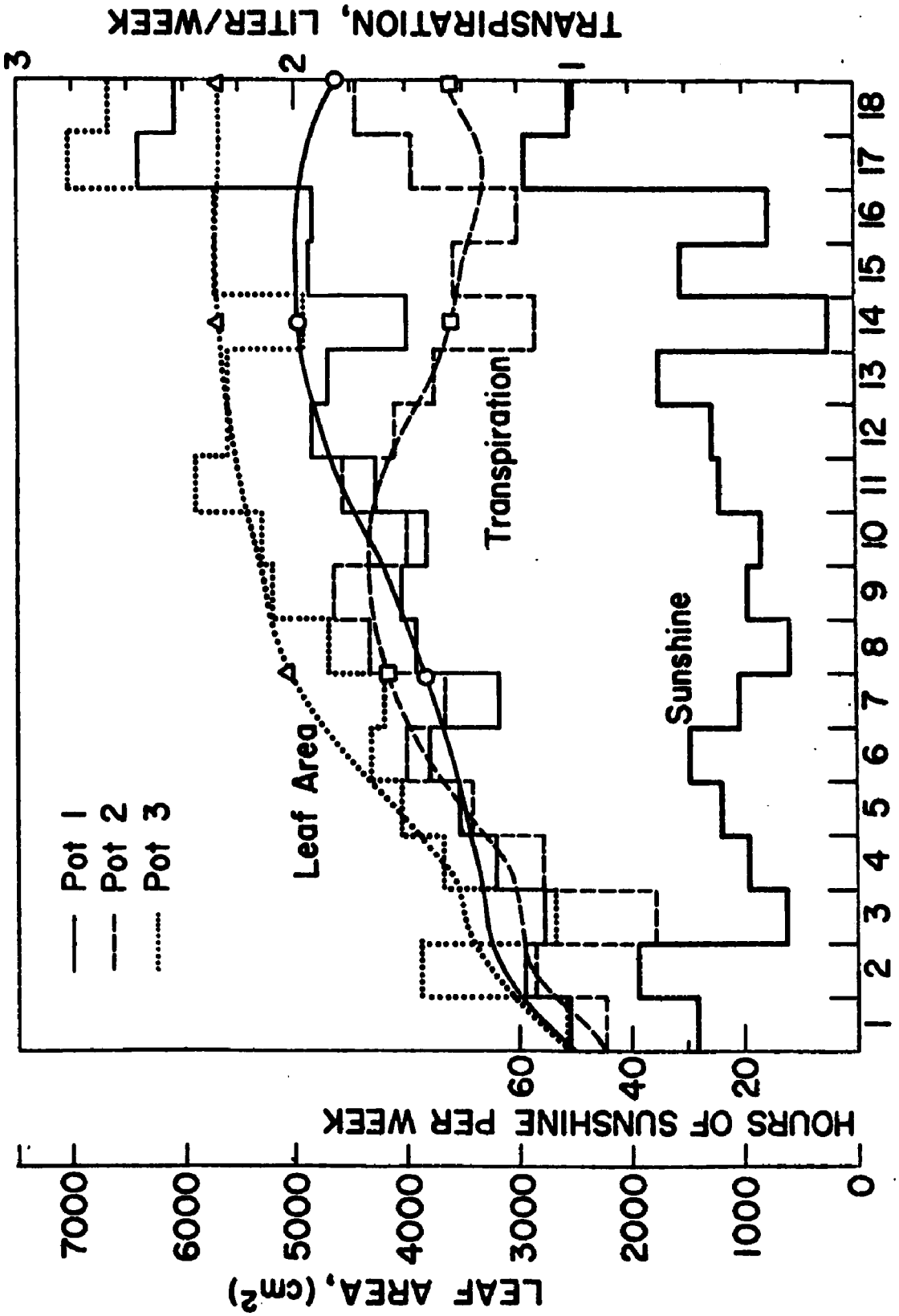


Figure 5.6 Leaf area and weekly transpiration of potted trees.

Table 5.7: Leaf Surface of Potted Trees

Date	Pot No.	Leaf Size	Leaf Area (cm^2)					
			Leaf Quality					
			Good	Yellowish	> 50% Brown	Old	Old + Br. Rim	$\sum$
Dec. 7, 1969	1		2480	1379	-	-	-	3859
Dec. 9, 1969	2		3783	364	-	-	-	4147
Dec. 8, 1969	3		5100	-	-	-	-	5100
	1 +2 +3		11363	1743	-	-	-	13106
Jan. 26, 1970	1		4750	185	-	-	-	4935
Jan. 27, 1970	2		3390	236	-	-	-	3626
Jan. 29, 1970	3		5690	-	-	-	-	5690
	1 +2 +3		13830	421	-	-	-	14251
Feb. 28, 1970	1	Small	594	-	-	-	-	594
March 3, 1970		Medium	776	-	-	-	-	776
		Large	3265	-	-	-	-	3265
		Total	4635	-	-	-	-	4635
Feb. 28, 1970	2	Small	339	-	-	70	-	409
		Medium	263	-	63	325	101	752
		Large	243	-	510	605	1105	2463
		Total	845	-	573	1000	1206	3624
Feb. 28, 1970	3	Small	440	-	-	-	-	440
March 3, 1970		Medium	842	-	-	-	-	842
		Large	4430	-	-	-	-	4430
		Total	5712	-	-	-	-	5712
	1 +2 +3		11192		573	1000	1206	13971

Figure 5.6. These curves are a best fit of actual data points and indirect data based on climatic and tree growth conditions in the greenhouse. The transpiration per unit leaf area of each pot is plotted in Figure 5.7 and the total transpiration of all three pots divided by the total leaf area $\frac{Tr_{t1} + Tr_{t2} + Tr_{t3}}{Ar_1 + Ar_2 + Ar_3}$ in Figure 5.8. This figure also contains the daily averages of temperature and humidity and the weekly averages. It can be seen from this graph that temperature and humidity variations in the greenhouse do not significantly affect transpiration. On the other hand the hours of sunshine during each test period appear to dominate the magnitude of transpiration. In Figure 5.7 the variations in transpiration per unit leaf area of all three pots are reflected quite closely by the variations in the hours of sunshine. The hours of sunshine were obtained from local climatological data sheets for Detroit Metropolitan Airport, published by the U.S. Department of Commerce, Environmental Science Services Administration. The sunshine record at The University of Michigan Botanical Gardens is probably similar, but not necessarily always identical to these data. This weather record also furnished sky cover data. The last column in Table 5.6 gives the percentage of uncovered sky per week between sunrise and sunset. It is obvious that this also influences the fluctuations in transpiration, since sky cover governs the amount of radiation reaching the earth's surface.

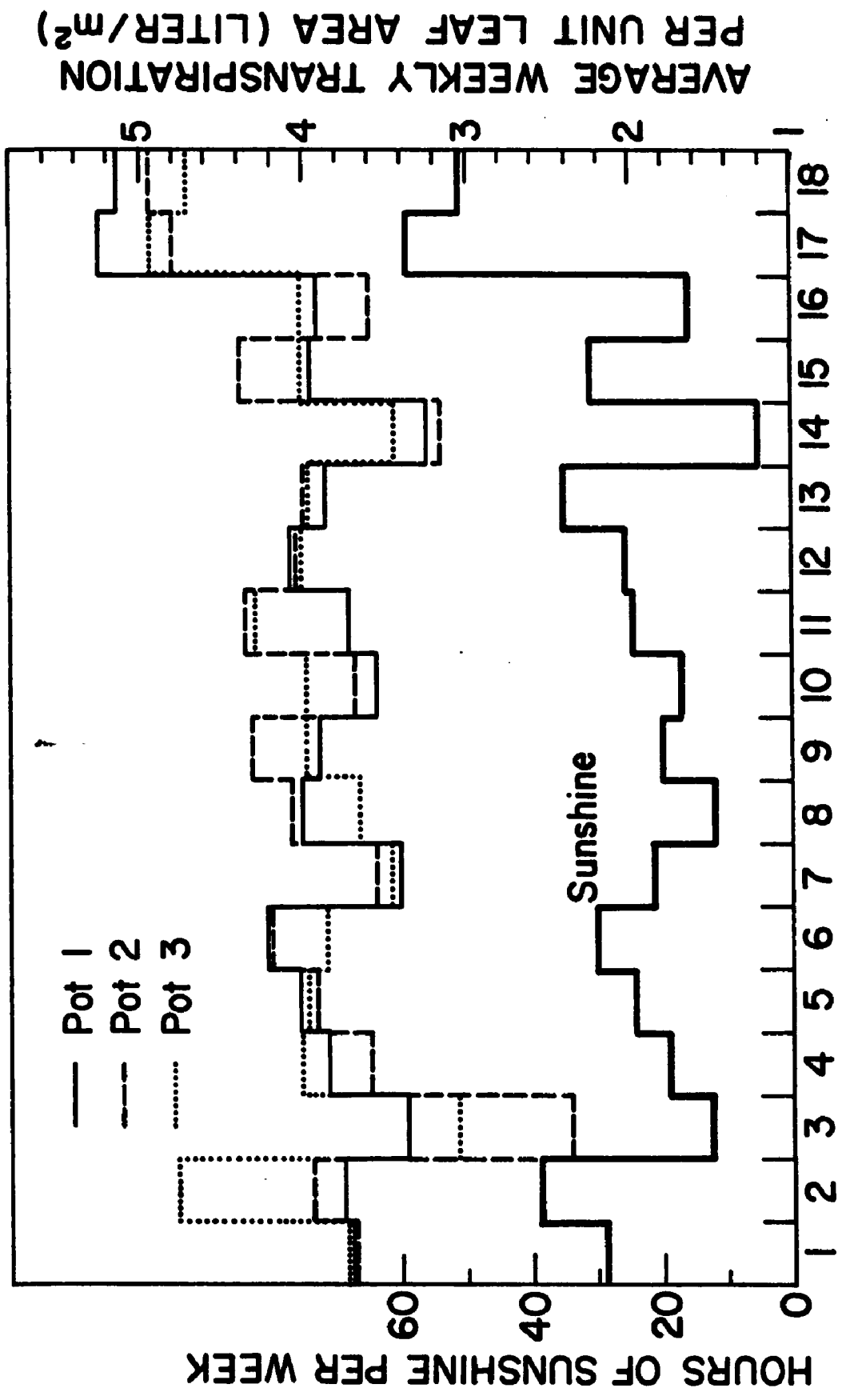


Figure 5.7 Weekly transpiration per unit leaf area of potted trees and hours of sunshine.

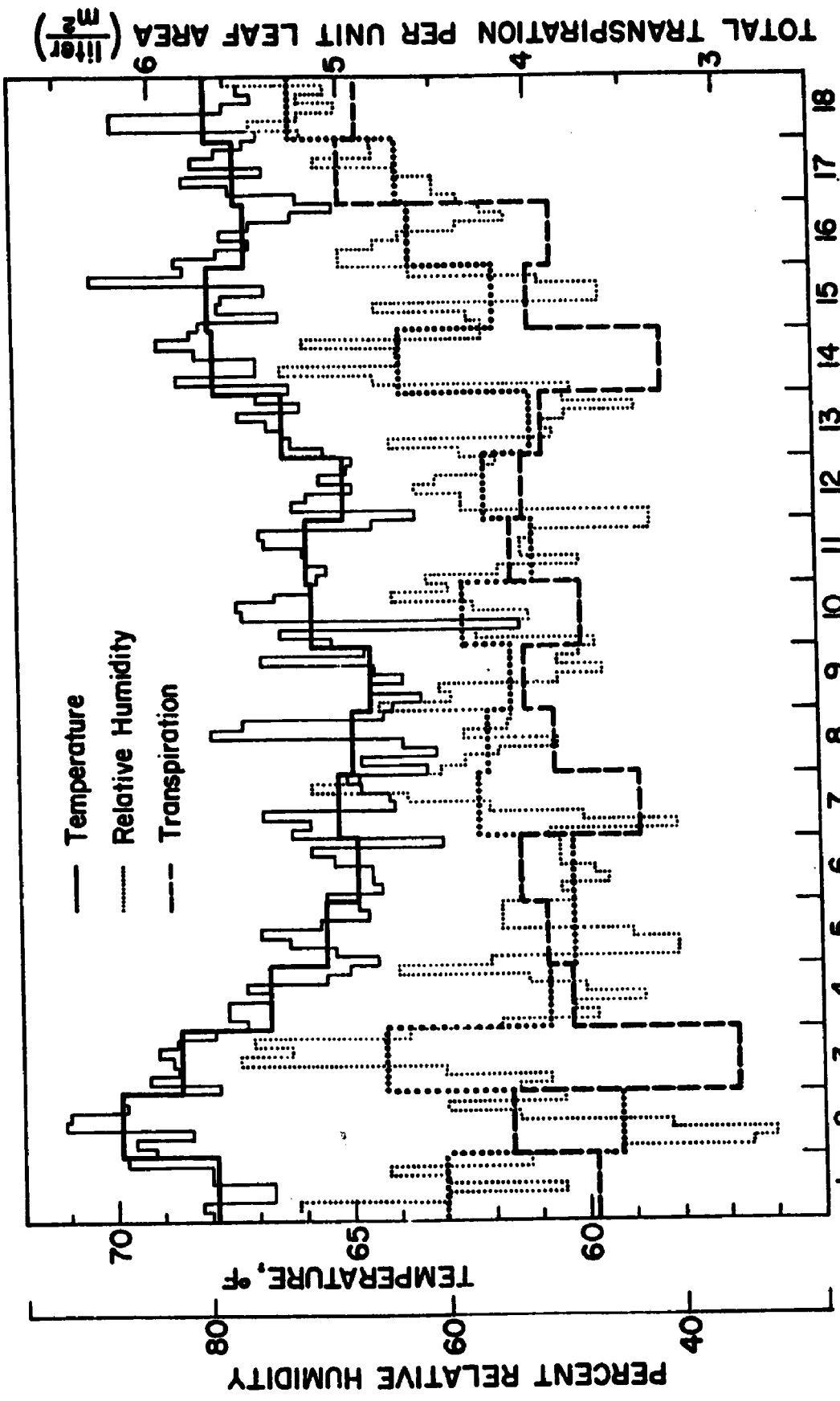


Figure 5.8 Daily and weekly averages of temperature and relative humidity; weekly transpiration per unit leaf area of potted trees, Test Series A.

The transpiration per unit leaf area is an indication of the transpirative power in the greenhouse and its variation depends, as mentioned above, mainly on the variation in sunshine. Of course, there is also transpiration on days without sunshine, since radiation is always present. The hypothetical total transpiration during a 168-hour test period without sunshine was determined; this fictitious value was then subtracted from the actual, measured transpiration readings. This then would give the additional transpiration due to bright, direct sunshine. This attempt, however, was not very successful, partially because the effect is probably not linear.

Finally, the total transpiration per unit leaf area was normalized for test no. 10 ($\overline{T}r_t = 1.00$). This made it possible to compare the transpirative power in the greenhouse during the entire period of test series A. Normalizing results on this basis makes it possible to conclude that despite the higher transpiration power during test nos. 17 and 18 (slope angle 10 degrees, barren slope), depletion was much less than during the counterpart tests nos. 1, 2 and 3 (slope angle 10 degrees, vegetated slope), which proves that the additional depletion is due to the presence of trees. The lower depletion of test no. 3 (relative to nos. 1 and 2) is also readily explainable from the low value of $\overline{T}$ for this test.

Unfortunately, during later tests the variation in depletion does not correspond anymore to the variation in these $\overline{T}$-values (compare, for example, tests nos. 4, 5 and 6), since the response to the environmental conditions alone is masked by the decreasing leaf area of the trees in the

bin. Otherwise it would have been possible to establish some kind of standard environmental conditions, for example, those prevailing during test no. 10. It would then be possible to predict a change in depletion in the bin due to a change in environmental conditions based on such reference conditions and measurement of the transpirative power with potted trees.

All pertinent data of the potted trees are summarized in Table 5.8. The bulk density of the soil in the pots is considerably less than for the soil in the bin. Also the average volume of soil per tree in the bin is about 25,000 cm^3, i.e., about seven times more than in the pots. The distribution of the root system will therefore be quite different.

In Table 5.9, the relation between leaf area and leaf weight was evaluated. These leaves were taken from the potted trees at the end of test series A. The influence of leaf size does not show a regular pattern and therefore an overall average was determined which was used to estimate the total leaf surface of the trees in the bin at the time of clear-cutting. The leaf area of the trees in the bin is about twice that of the area of the 3 potted trees together. The net transpiration of the 3 potted trees during test no. 10 was 5.25 liters (Table 5.5). Hence the trees in the bin should deplete about 10 liters of water. This is in quite good agreement with the values found from water balance calculations (Table 5.3), although the distribution of the roots in the pots and in the bin might have been quite different.

Table 5.8: Pertinent Data of Potted Trees at the End of Test Series A

	Pot 1	Pot 2	Pot 3	Pot 4
Total leaf surface (cm^2)	4,635	3,624	5,712	---
Length of stem (cm)	162	147	165	---
Average diameter of stem at base (cm)	1.34	---	1.22	---
Weight of stem without leaves (gr)	126.2	91.2	170.9	---
Approx. volume of soil in pot V(cm^3)	3,590	3,350	3,620	3,290
Wet weight of soil at field capacity (kg)	5.505	5.059	5.506	5.120
Dry weight of soil W_s (kg)	4.170	3.854	4.246	3.960
Weight of water (kg)	1.335	1.205	1.260	1.160
Water content by weight w(%)	32.1	31.3	29.7	29.3
Volume of solids $V_s = \frac{W_s}{G_s}$ ($G_s \sim 2.60$) (cm^3)	1,600	1,480	1,635	1,525
Bulk density $\gamma_{dry} = \frac{W_s}{V}$ (gr/cm^3)	1.16	1.15	1.17	1.20
Water content by volume $\theta = w \cdot \gamma_{dry}$ (%)	37.3	36.0	34.8	35.2
Volume of voids V_v (cm^3)	1,990	1,870	1,985	1,765
Void ratio $e = V_v/V_s$	1.24	1.26	1.21	1.16
Growth of trees — Length of stem on Nov. 26 (cm)	112	119	135	---
" " " " Dec. 29	135	142	160	---
" " " " Feb. 19	162	147	165	---

Table 5.9. Relation Between Surface Area and Weight of Leaves

Pot No.	Leaf Size	Surface (cm^2)	Weight (grams)	Surface Weight (cm^2/gram)
1	small	594	13.03	45.6
	medium	776	13.54	57.3
	large	3,265	57.50	56.8
	Total	4,635	84.07	55.1
2	small	409	10.20	40.1
	medium	752	19.06	38.3
	large	2,463	35.88	68.7
	Total	3,624	65.68	55.2
3	small	440	10.80	40.7
	medium	842	15.78	53.2
	large	4,430	83.31	53.2
	Total	5,712	109.89	52.0

Average surface per 1.0 gram weight:

$$1/3\ (55.1 + 55.2 + 52.0) = \underline{54.1\ cm^2/gr}$$

3. Results from Test Series B (Test Nos. A, B, C, D)

In Figure 5.9 the logarithm of the matric suction is again plotted versus time. Since in this test series the tensiometers are equally spaced, a more or less regular pattern should be expected. Again the functional relationship appears to be quite close to a straight line, according to Equation (5.1), and a family of straight lines was fitted through the data points. The slope angle (10 or 30 degrees) does not seem to influence the slope of these straight lines; however, it does influence the spacing between them, i.e., the ordinate intercept A. It was mentioned earlier that the difference in matric suction between an upper and a lower point in the slope does increase with increasing angles of tilt. This was exactly verified by these tests. Another verification of this fact is shown in Figure 5.10, where the variation in soil suction with time has been compared for both the 10 and 30 degree slope for all tensiometers. The increased suction gradient for the 30 degree slope is clearly visible. All these can be explained by the fact that initially gravitational flow tends to deplete soil moisture at the top to a greater extent than it does at the bottom, since water coming from the upper portion of a slope has to flow first through the lower portions before it can seep out at the toe of the slope.

The irregularity of tensiometer 16 is caused by the reduced soil depth of that location. The high readings of tensiometer no. 9 are likewise caused by its close promixity to the upper edge of the bin.

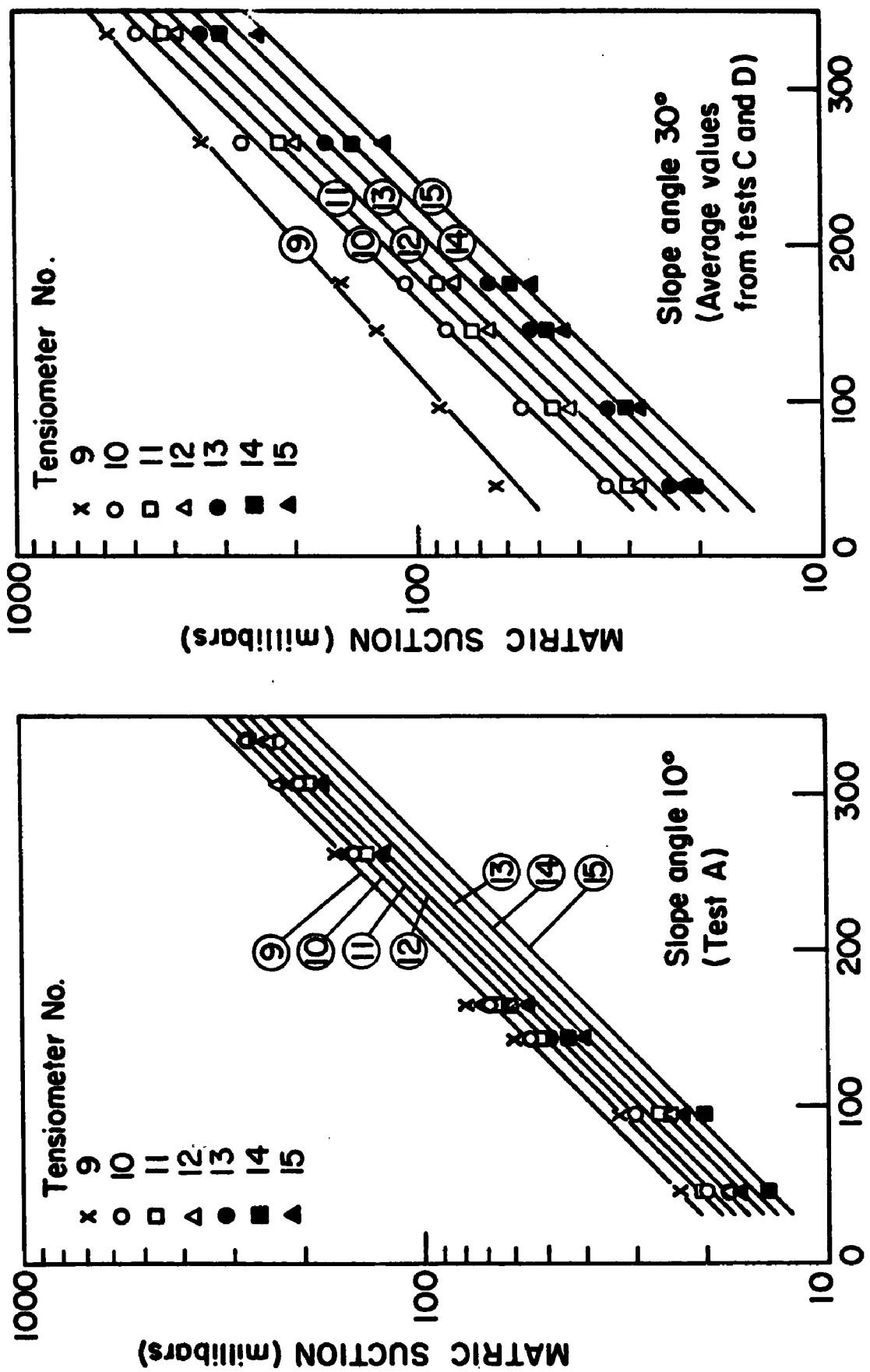


Figure 5.9 Logarithm of suction versus time for tensiometers 9 to 15, Test Series B.

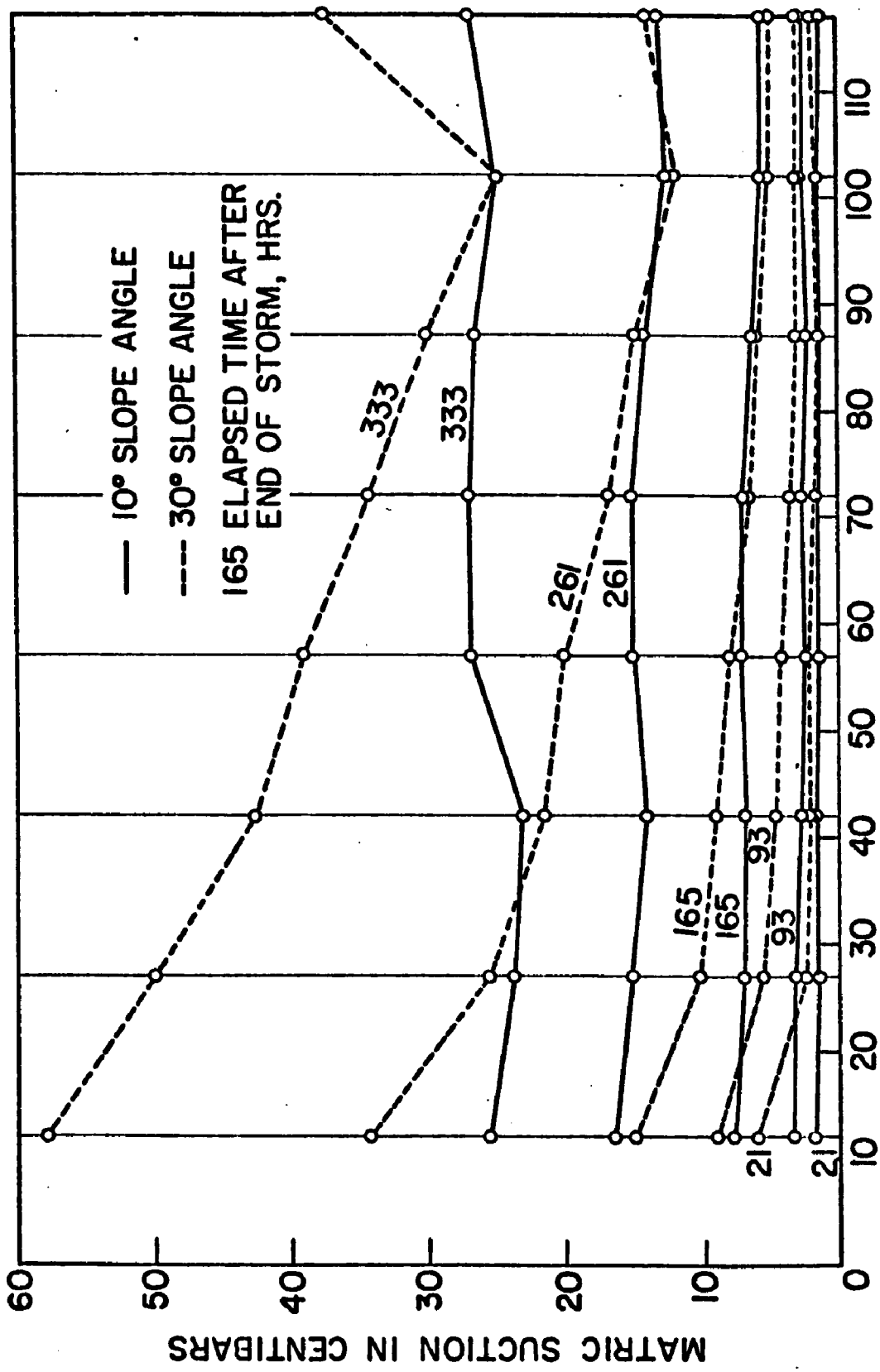


Figure 5.10 Suction gradients in a slope as a function of time and slope angle.

Finally, Figure 5.11 shows the water table rise and decrease during and after a rain storm, respectively, as recorded from the readings of the four piezometers. The highest water table is always reached after 3 hours, i.e., when the rain stops. From these measurements one may conclude that in a steep slope the uppermost part never reaches saturation and that the zone with the highest piezometric level occurs around the center portion of a slope.

4. Discussion of the Results

The straight-line relationship between the logarithm of the matric suction and the time after drainage stopped (i.e., field capacity was reached), Equation (5.1), is consistent with the flow equation (Equation 2.19), however, the existence of such a relationship is best explained by the fact that a given point in this shallow soil profile water is being lost at a constant rate q per unit volume. The summation of all these losses over the whole depth of the soil mantle is equal to the potential evapotranspiration. For moderate evaporation the loss might even be equal for all points in the profile (Gardner and Hillel ,1962). This rate of water loss can be expressed by the following relationship

$$\frac{d\theta}{dt} = -q \tag{5.4}$$

$$\text{and} \quad \int q \cdot dz = E_p \tag{5.5}$$

where E_p is the potential evapotranspiration (water loss per unit surface area per unit time), and the integration is over the whole soil mantle

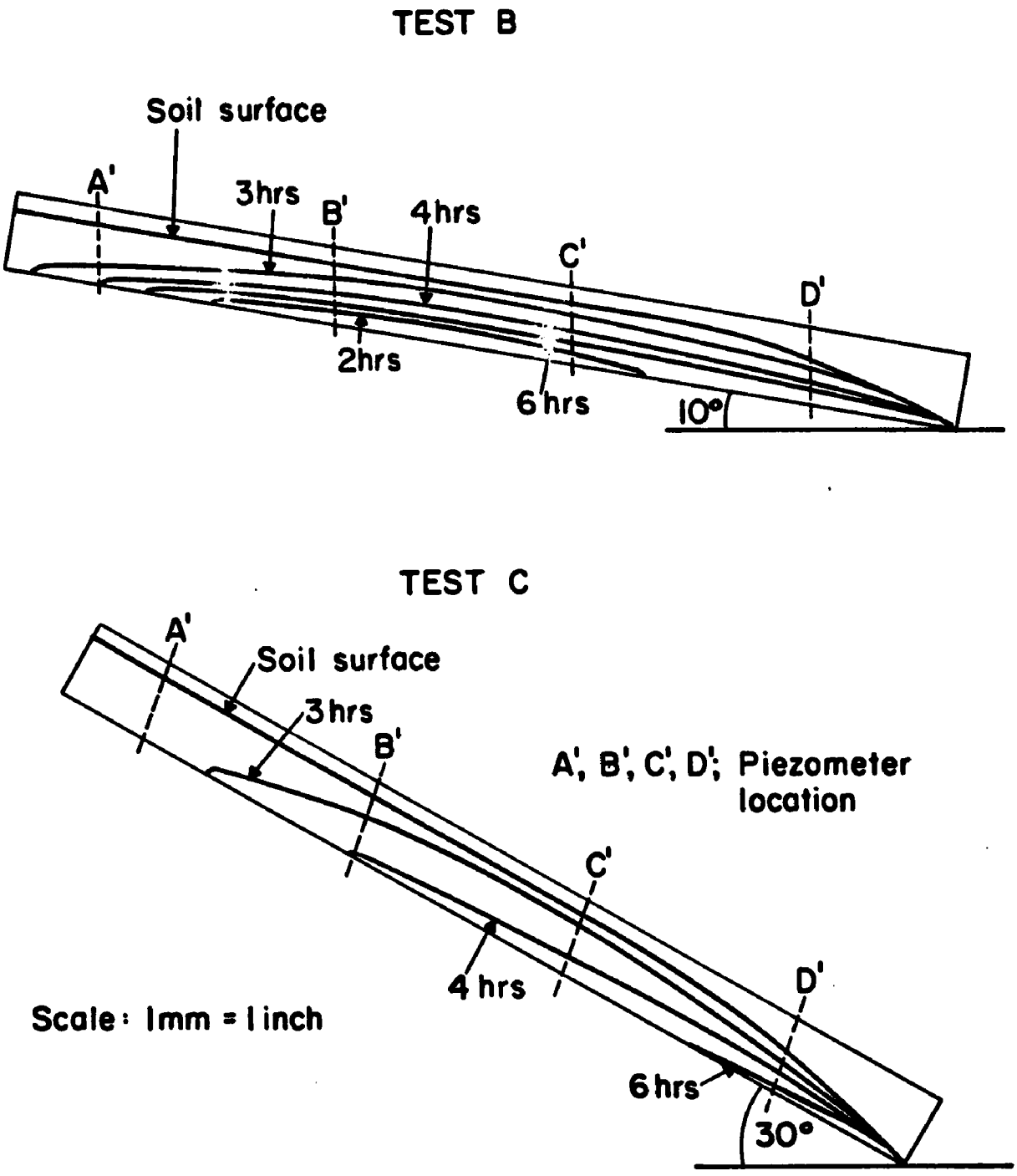


Figure 5.11 Test Series B: Watertable positions after 2, 3, 4 and 6 hours after beginning of storm for a slope of 10° and 30°.

depth. Once gravity drainage has ceased, the gravitational influence on soil water movement becomes negligible compared with the evaporative movement. Thus the movement of water will be predominantly upwards. The "constant" q actually depends on the potential evapotranspiration rate and will be larger when plants help to deplete water than on a denuded slope with no plants.

A constant water uptake rate, independent of depth, by a non-uniform root system was also postulated by Vasquez and Taylor (1958) and Patric et al. (1965) as mentioned in Chapter 3. Also Zinke's data (1959) from a forested lysimeter (Figure 3.11) show a more or less constant $\frac{d\theta}{dt}$ for all depths as long as the moisture content was well above the wilting percentage. It also applied for the upper 12 inches of the barren lysimeter. Zinke also obtained an approximate linear relationship for the total water content decrease (Equation 3.10) which can also be obtained when Equation (5.4) is integrated and q is constant throughout the depth d_s of the soil profile, i.e., $q \cdot d_s = E_p$. Then

$$\theta \cdot d_s = Q_{sm} = - E_p \cdot t + Q_{sm_o} \tag{5.6}$$

If E_p is replaced by $Q_{sm_o} \cdot \kappa$ then

$$Q_{sm} = Q_{sm_o} (1 - \kappa t) \tag{5.7}$$

where Q_{sm_o} is the initial, total soil moisture content.

The data reported by Metz and Douglass (1959) (Figures 3.6 and 3.7) can also be approximated by the same relationship (Equation 5.7). It thus appears that for a shallow soil profile the influences of evaporation dominates completely and the influence of the water uptake by the roots is just an additional contribution to the loss q. Deeper soil profiles are necessary to separate clearly water uptake by roots and losses due to evaporation only. In a deeper soil profile the moisture content at greater depths in a denuded slope would then be practically unaffected by external evaporative conditions, as shown by Zinke (1959) and Metz and Douglass (1959).

Assuming the relationship between the soil moisture tension and the volumetric water content θ is exponential (or approximately so), i.e.,

$$\tau = \tau_o \cdot e^{\beta(\theta_o - \theta)} \tag{5.8}$$

which is the case for many soils and which also applied to the soil used in this study (see Figure 4.13 and Equation 4.3), one may combine Equation (5.4) with the relation (5.8) and obtain

$$\tau(t) = A \cdot e^{\beta \cdot q \cdot t} \tag{5.9}$$

which is equivalent to Equation (5.1).

One realizes at once that a larger q (e.g., increased water uptake by the presence of roots) results in a steeper slope of the straight line relationship between the logarithm of the matric suction and the time. The results of the present study support this finding, i.e., the

slopes of the curves in Figures 5.4.a, 5.4.b and 5.4.c are always greater for the forested slope than for the clear-cut one. Only when the environmental conditions for the forested slope are much less favorable to depletion than those for the clear-cut one will the slopes of the suction vs. time curves be nearly equal. This was the case, for example, for test no. 3 in comparison with tests nos. 17 and 18.

The linear relationship (Equation 5.1) can only be maintained as long as soil water is not limiting, which certainly is the case at least for suctions up to 1 bar.

It should be noted that the depletion curves presented by Patric et al. (1965) (Figure 3.8) can be approximated fairly well by straight lines within the range 0 to 1 bar. Unfortunately the authors do not present data on the soil water retention properties of soils from their experimental plots. But if their water retention behavior can also be represented by Equation (5.8), it would mean that the water uptake at a given depth is constant up to about 1 bar. At higher suctions, as the curves tend toward equal slopes, this implies that the extraction rate is constant throughout the soil profile. Accordingly, if the mechanism of depletion takes place as postulated, these field results which are due to transpiration only, seem to be consistent with the results from the model experiment.

5. Conclusions from the Model Study and Suggestions for Further Research

From the previous discussion, we now summarize the mechanism of water depletion in a thin soil mantle on steep slopes in so far as this is possible from the data obtained with this simple model.

After a storm, and during the drainage period which we shall call phase (1), flow in the slope will be two-dimensional, and the difference in water content between an upper and a lower point in the slope at a given time depends on the slope angle. When the field capacity is reached, which will happen earlier in the upper part of the slope (it may not be completely recharged at all), water movement is essentially one-dimensional and independent of the slope angle; we shall refer to this as phase (2). During this phase the matric suction increases exponentially with time for suctions within the tensiometer range. The slope angle in this case simply determines the initial conditions (ordinate intercept A) for phase (2), whereas the rate of water uptake (in turn influenced by the presence of slope vegetation) determines the slope α of the suction-time relationship.

Some useful conclusions to be drawn from this model study are therefore the following:

1) It could be shown that a forest cover accelerates the soil moisture depletion in a shallow soil mantle as compared to evaporation alone regardless of the steepness of the

slope. The slope angle is only responsible for th distribution of recharge and the initial conditions when drainage has ceased.

2) There is no significant downhill component of soil water flow in phase (2) in a steep slope with a thin soil mantle under the given boundary conditions (i.e., no water table at the toe of the slope).

3) A water table build-up during a storm could be verified. In a steep slope the upper part may never reach saturation. The region with the highest piezometric level appears to occur around the center portion of a slope.

4) The experiments with the pots showed that phytometer measurements may be used successfully as a scale for the environmental conditions in a greenhouse. The increase in leaf area due to the growth of the plant has to be taken into account. Transpiration in the greenhouse appeared to be mainly a function of solar radiation rather than of temperature and relative humidity.

The model has proven its suitability for qualitative investigations of the influence of vegetation on the soil water regime in a slope.

However, the model definitely has its limitations in several aspects (for example, with respect to scaling problems or to the instrumentation used). But the experience gathered from this model can be

used for the design of future experiments which avoid the limitations encountered in the present study and thus extend the range of useful data. One of the shortcomings of the present study was the shallow soil depth and also the limited range of suction that could be measured with the tensiometers.

It is proposed here that a future study should have a soil depth of at least 5 feet and the length of the slope should exceed 50 feet. A model of this size of course cannot be set up in a greenhouse and, due to the enormous weight, it cannot be lifted or lowered to an arbitrary angle of tilt. The experiment has therefore to be established outdoors and the slope of the bin must be fixed. A concrete trough built in place, similar to the one constructed by Hewlett and Hibbert (1963), would probably be most appropriate. A series of bins at different but fixed angles of tilt would then replace the bin with variable angle of tilt as used in the present study. Parallel studies, i.e., studies where observations on a forested as well as on a clear-cut slope, are made simultaneously (this requires twice the number of bins used for a sequential study) would facilitate the interpretation of the data, since the environmental conditions are then the same for both types of slope, and climate would not mask the influence of vegetation. The whole test area should be covered by a clear roof in order to prevent natural precipitation from falling on the surface of the bins. A sprinkler system in which the pressure can be controlled and which is so designed that it can simulate uniform rainfall as closely as

possible would serve as source of rain. Such experiments could be set up in regions of various climates (temperature, relative humidity, radiation and wind) with different kinds of vegetation (for example, shallow and deep rooted species) and with a variety of soils. Soil water potential determinations would probably be made most economically by using soil psychrometers[1] which are capable of measuring water potentials between -1 and -50 bars, supplemented by tensiometers. Such experiments will be much more time consuming (they will extend over several years) and costly than the present smaller scale greenhouse study. However, it is felt that they would represent a really valuable supplement to the present large scale watershed studies as outlined in Section 3.2 or to the small scale water uptake studies by plant roots described in Section 3.4. In addition, they would help to verify and test mathematical models.

---

[1] Available for example from WESCOR, Inc., Logan, Utah 84321

CHAPTER 6

PROPOSAL FOR A MATHEMATICAL MODEL OF A FORESTED SLOPE

In Chapter 1 it was mentioned that a desirable goal in the study of watershed behavior would be a mathematical simulation model. Such a model would enable us to predict quantitatively the response of the watershed system to a change in one of its parameters (for example, the change in soil water potential due to a change in the vegetal cover when a slope is clear-cut).

In this chapter, an attempt is made to construct a two-dimensional model for a slope (i.e., a slope of unit width) based on the flow equation and using the information on water uptake and transpiration as was outlined in Chapters 2 and 3. The purpose of this model is to calculate the soil water potential at any point and at any time in the slope as a function of climate (precipitation, potential evapotranspiration), vegetation, topography, and soil characteristics. The formulation of the problem is quite general and some of the functional relationships used (for example, the root density distribution for a given type of vegetation cover) are not yet well established. Some special cases of this generalized model are discussed at the end of this chapter. For a given

site we may consider topography, soil characteristics and vegetation as fixed (the latter implies that vegetation growth can be neglected over a limited interval of time). This would leave climatic factors (precipitation, and potential evapotranspiration) as the only significant independent variables determining the soil water potential. The model also permits one to examine the effect of changing topography, i.e., slope angle and soil mantle thickness, and also the effect of vegetal cover, i.e., converting from a forested to a bare slope. Thus, a variety of questions can be studied relating the effects of slope geometry, soil type and vegetation cover to the soil water potential for a given climatic regime. This in turn is then a useful information in predicting the stability of a sloping mass.

The soil water potential is determined by the flow equation (Equation 2.19), the boundary conditions (topography and climate) and the initial conditions. The influence of vegetation can be taken into account by adding a source term q to the flow equation (see Equation B.13) which in turn is a function of climatic influences (potential transpiration). The main problem is to find relations which satisfactorily represent the source term in a mathematical model. Figure 6.1 illustrates an idealized slope and shows the principal quantities involved in the proposed model.

Bedrock and soil surface of the slope are characterized by functions $f_1(x)$ and $f_2(x)$, respectively in a (x-z)-coordinate system.

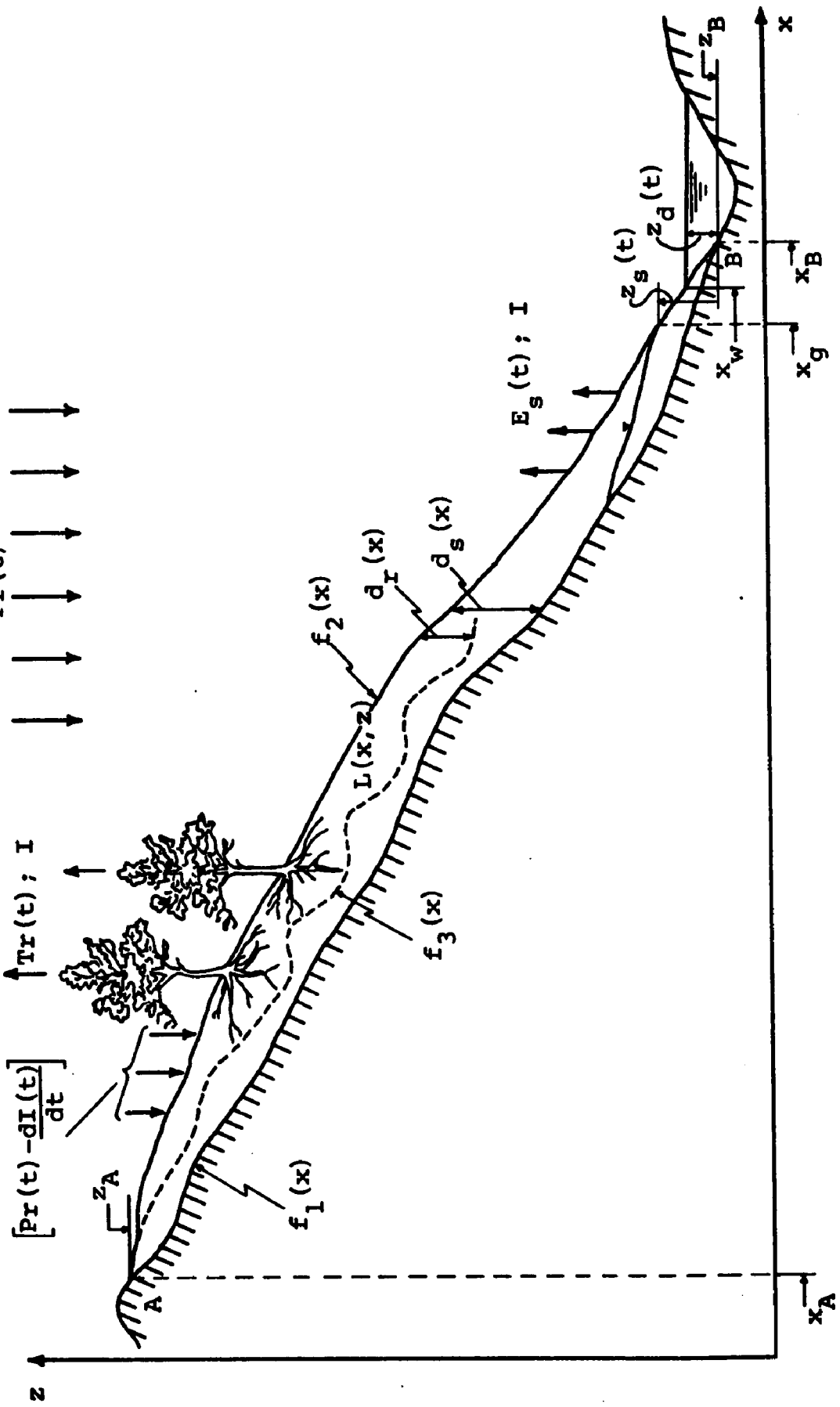


Figure 6.1 Model of a vegetated slope.

At the toe of the slope there may be a ground water table draining into a stream with a water level somewhere above point B. (The water level of this stream can also lie below point B.)

The soil type is characterized by the soil water retention properties $h(\theta)$ and the hydraulic conductivity $K(h)$.

Climatic influences are represented by a rain intensity $Pr(t)$, a total interception loss $I(t)$, an evaporation rate E_s from the soil surface and a potential transpiration rate Tr_p. It is assumed that the net difference between rainfall and interception $[Pr(t) - \frac{dI(t)}{dt}]$ infiltrates into the ground and that this difference is less or equal to the saturated hydraulic conductivity. If this assumption is not met, the infiltration capacity would be exceeded sooner or later during the progress of a storm and result in ponding or surface runoff. This would complicate the problem significantly. It is further assumed that during a rainstorm there is no transpiration and that after the storm has ceased, the intercepted water is evaporated first before transpiration Tr and evaporation flux E_s through the ground surface resumes. The time during which intercepted water evaporates is t_I (see p. 50) and the evaporation rate is E_I ($E_I = E_p$ ($r_n = 0$), see Equation 2.29.)

The influence of vegetation is characterized by a root system which is responsible for water uptake; the latter in turn is a function of potential transpiration, the water potential in the soil and in the plant. It is assumed that the water uptake equals the actual transpiration of the

plant at any instant of time. In reality, however, there is usually a lag in absorption with respect to transpiration because of the resistance in the plant, particularly in the roots. The plant suffers a water deficit during the day which is finally balanced out during the night when transpiration ceases whereas root absorption still continues. The roots are assumed to be distributed continuously, i.e., macroscopic approach, see p. 78) in a region bounded by the soil surface function $f_2(x)$ and a function $f_3(x)$. Outside this region, i.e., for $z(x) < f_3(x)$, it is assumed that there are no roots. $f_3(x)$ depends on the type of vegetation, i.e., on the rooting depth and distribution of the roots. The effective root density is characterized by a function $L(x, z)$.

An expression for a source term is now constructed following the approaches of Gardner (1960), Gardner and Ehlig (1962a), (1962b), (1963), and Cowan (1965) (see Chapter 3). Gardner and Ehlig proposed a water uptake term of the form (Equation 3.4):

$$q = \frac{\psi_{leaf} - \psi_{soil}(x, z)}{j_p + \frac{B}{K(h) \cdot L(x, z)}} \qquad (6.1)$$

where j_p is the impedance to water movement in the plant and B is a constant. If j_p is neglected, Equation (6.1) reverts to the expression used by Whisler et al. (1968) (see Equation 3.8). (The relative importance of the impedances in the plant and in the soil was discussed on p.90)

Cowan (1965) assumes that the impedance to water flow in the plant remains virtually constant over periods which are short compared with the growth cycle of the plant. He further adopts a critical leaf water potential $\psi_{leaf_{crit}}$ at which stomatal closure begins. This prevents the leaf water potential from decreasing any further. This assumption is consistent with the experiments conducted by Gardner and Ehlig (1963) in which it was shown that closure of stomata due to water stress occurs within a rather narrow range. As long as the stomata are fully open (i.e., $\psi_{leaf} \geq \psi_{leaf_{crit}}$), the plant transpires at the potential rate Tr_p. The value of the internal resistance in the plant r_{pl} is obtained from (see Equation 3.7)

$$r_{pl} = \frac{\psi_{leaf_{crit}}}{Tr^o} \cdot \frac{\int L(x, z)dz}{B}$$

where Tr^o represents the maximum possible rate of transpiration a plant can sustain without wilting, i.e., $\psi_{leaf} = \psi_{leaf_{crit}}$ and $\psi_{soil} = 0$. It was mentioned in Chapter 3, p. 90 that under these circumstances the magnitude of the term $\frac{B}{K \cdot L}$ is small compared to j_p. When the soil water potential reaches -15 bars (wilting percentage), it is assumed that water absorption ceases. The potential transpiration rate is given by the difference between the potential evapotranspiration E_p and the evaporation flux through the soil surface E_s.

The approach followed here will produce curves similar in shape to those in Figures 3.2 and 3.3 According to these figures, the

transpiration is reduced as a result of either one of the two following causes:

- the soil water potential is so low that $\int q dz < Tr_p$ when $\psi_{leaf} = \psi_{leaf_{crit}}$, i.e., the potential rate cannot be met anymore, or;
- the potential transpiration rate is so high that even in a moist soil and with $\psi_{leaf} = \psi_{leaf_{crit}}$ it cannot be satisfied because of the impedance to flow in the plant.

Before the governing equations of the model are presented, all the quantities involved are summarized again.

The quantities which are known, i.e., determine the problem, are:

(1) Quantities characterizing <u>topography</u>

$f_1(x)$: function describing bedrock surface between points A and B

$f_2(x)$: function describing soil surface

$d_s(x)$: soil depth $d_s(x) = f_2(x) - f_1(x)$
(note that $f_1(x_A) \equiv f_2(x_A) \equiv f_3(x_A) = z_A$
and $f_1(x_B) \equiv f_2(x_B) \equiv f_3(x_B) = z_B$)

$z_d(t)$: water level in a stream with respect to point B

x_w : intersection of water level in stream with slope surface $f_2(x_w) - f_2(x_B) = z_d$

$z_s(t)$: upper end of seepage zone

x_g : intersection of upper end of seepage zone with slope surface $f_2(x_g) - f_2(x_B) = z_s$

(2) Quantities characterizing soil properties

$ST(x, z)$: soil texture

$h(\theta, ST)$: soil water retention (with hysteresis)

$K(h, ST)$: hydraulic conductivity (with hysteresis)

$C(h, ST)$: soil water capacity

(3) Quantities characterizing climate

$Pr(t)$: precipitation

$E_p(t)$: potential evapotranspiration (can be assumed constant or diurnal, i.e., zero at night and fluctuating during a 12-hour photoperiod)

$E_s(t)$: evaporation flux through the soil surface

$Tr_p(t)$: potential transpiration = $E_p - E_s$

(4) Quantities characterizing vegetation

$I(t)$: total interception; $I = I(Pr)$

$L(x, z)$: effective root density (i.e., that part of the roots which is responsible for water uptake)

B : geometrical factor for root system

$f_3(x)$: function describing lower boundary of root zone

$\psi_{leaf_{crit}}$: critical leaf potential at which closure of stomata starts

Tr^o : max. possible transpiration rate without wilting

r_{pl} : resistance to water flow in the plant

The unknown quantities for which the model has to be solved are:

ψ_{soil} : soil water potential = $\psi_m + \psi_p$

$H(x, z, t)$: hydraulic head

Tr : actual transpiration rate, which is equal to the water uptake rate integrated over the root depth

One may now write down the governing equations:

Flow equation (in terms of hydraulic head):

$$C(h) \cdot \frac{\partial H}{\partial t} = \frac{\partial}{x} [K(h) \cdot \frac{\partial H}{\partial x}] + \frac{\partial}{\partial z} [K(h) \cdot \frac{\partial H}{\partial z}] + q(x, z, t) \quad (6.2)$$

where: $H = h + z; \quad h = \frac{\psi}{g \cdot \rho_w}$

and (from Equation 3.4)

$$q(x, z) = \frac{h_{leaf}(x) - h_{soil}(x, z)}{\frac{B \cdot r_{pl}}{L(x, z)} + \frac{B}{K(h) \cdot L(x, z)}} \cdot (\rho_w \cdot g) \quad (6.3)$$

$$r_{pl} = \frac{\psi_{leaf_{crit}}}{Tr^o} \cdot \int_{\text{root zone}} \frac{L(x, z)dz}{B} \quad (6.4)$$

$$\int_{f_3(x)}^{f_2(x)} q(x, z)dz = Tr(x, t) \quad (6.5)$$

For $\left.\begin{array}{l} \psi_{leaf} > \psi_{leaf_{crit}} \\ \psi_{soil} \geq -15 \text{ bars} \end{array}\right\} \quad Tr(x, t) = Tr_p(t)$

and $$\psi_{leaf} = \frac{Tr_p(t) + \int_{f_1}^{f_2} \left[\frac{B \cdot r_{pl}}{L} + \frac{B}{K \cdot L}\right] \cdot \psi_{soil} \cdot dz}{\int_{f_3}^{f_2} \left[\frac{B \cdot r_{pl}}{L} + \frac{B}{K \cdot L}\right] \cdot dz} \qquad (6.6)$$

If ψ_{leaf} turns out to be less than $\psi_{leaf_{crit}}$ in order to satisfy Equation (6.6), then

$$\psi_{leaf} = \psi_{leaf_{crit}}$$

and

$$q(x, z) = \frac{h_{leaf_{crit}} - h_{soil}}{\frac{B \cdot r_{pl}}{L(x, z)} + \frac{B}{K(h) \cdot L(x, z)}} \cdot \rho_w \cdot g \quad ; \quad \psi_{soil} \geqslant -15 \text{ bars} \qquad (6.7)$$

$$Tr_p(t) = E_p(t) - E_s(t)$$

E_p can be obtained from climatic data using Equation (2.29)

For $\psi_{soil} < -15$ bars, $q = 0$

After a rainstorm: $Tr = 0$; i.e., $q = 0$

$E_s = 0$

$\Big\}\ 0 \leq t \leq t_I$

where $t = 0$ is the time when the rainstorm ends

$$t_I = \frac{I}{E_I} = \frac{I}{E_p(r_n = 0)}$$

Boundary Conditions

(1) no flow through impervious boundary (bedrock)

$$\text{grad } H \cdot \vec{n} = 0, \quad (\vec{n} : \text{vector normal to boundary})$$

$$\text{i.e.:} \quad \frac{\partial H}{\partial x} \cdot \frac{df_1(x)}{dx} + \frac{\partial H}{\partial z} = 0 \quad \begin{cases} x_A \leq x \leq x_B \\ f_1(x_A) \geq z \geq f_1(x_B) \end{cases} \tag{6.8}$$

(2) rain infiltration or evaporation at boundary in contact with air, except seepage face

$$\underbrace{K(h) \cdot \frac{\partial H}{\partial z}}_{\text{flux through surface of unit area}} = Q_f(t)$$

$$Q_f(t) = Pr(t) - \frac{dI(t)}{dt} \qquad \text{rainfall or}$$

$$= -E_s(t) \qquad \text{evaporation after intercepted water has evaporated, i.e., } t > t_I \tag{6.9}$$

$$x_A \leq x \leq x_g$$

$$f_2(x_A) \geq z \geq f_2(x_g) = z_s(t)$$

(3) atmospheric pressure in the pore water at the seepage face (between z_s and z_d)

$$H = z \tag{6.10}$$

$$x_g \leq x \leq x_w$$

$$z_s \geq z \geq z_d$$

(4) outflow into stream

$$H = z_d \tag{6.11}$$

$$x_w \leq x \leq x_B$$

$$z_d \geq z \geq f(x_B)$$

Initial Conditions

Usually the soil water head h or the moisture content θ is given at the initial time, i.e.:

$$h(x, z, 0) = h_o(x, z) \tag{6.12}$$

or $$\theta(x, z, 0) = \theta_o(x, z)$$

Equations (6.2) through (6.12) fully describe the hydraulic regime in a vegetated slope. A solution of the system is possible only numerically on a large computer.

It might be rewarding to consider first some simplified versions of the model by holding certain variables constant. For example, the following case might be of interest and furnish useful information:

Consider a slope of simple geometry such as a rectangular slab. The soil conditions are homogeneous. Vegetation is uniform, i.e., the root density is constant throughout the soil profile (independent of x and z). Interception is neglected as a first approximation, and the precipitation rate and potential evapotranspiration are constant.

These assumptions considerably simplify the solution of the system of equations (Equations 6.2 to 6.12).

A further simplification would be to lump all the influences of vegetation and climate into a constant source term q. Equation (6.2) could then be solved either for a given value of q, thus representing the presence of vegetation, or for $q = 0$, which would signify its absence. As initial conditions one may prescribe the whole soil slab to be at field capacity. Then the soil water potential during a depletion phase and a subsequent recharge phase could be simulated for both cases. This procedure should yield results similar to those found from the experimental study in the previous chapter.

APPENDIX A

UNITS AND PHYSICAL DIMENSIONS OF WATER POTENTIALS AND OTHER RELEVANT QUANTITIES

Term	Dimensions	
	c g s system	m k s system
Length	cm	m
Mass	gram	kg
Time	sec	sec
Force	dyne = $\frac{gr \cdot cm}{sec^2}$	Newton = $\frac{kg \cdot m}{sec^2}$
Pressure	———	Pascal = $\frac{N}{m^2} = \frac{kg}{m \cdot sec^2}$, 1 Bar = $10^5 \cdot \frac{N}{m^2} = 10 \cdot \frac{N}{cm^2}$
Energy (work)	erg = $\frac{gr \cdot cm^2}{sec^2}$	Joule = (Newton · m) = $\frac{kg \cdot m^2}{sec^2}$

Table A. 1 gives the relation between different units used for pressure.

Potentials are expressed in:

a. Energy per unit mass = specific potential = $\frac{Joules}{kg} = \frac{m^2}{sec^2}$

b. Energy per mole = molar potential = $\frac{\text{Joules}}{\text{mole}}$

c. Energy per unit volume = volumetric potential = $\frac{\text{Joules}}{\text{m}^3}$

$= \frac{\text{kg}}{\text{m} \cdot \text{sec}^2}$ = Pressure

d. Energy per unit weight of water = $\frac{\text{Joules}}{\text{Force}}$

$= \frac{\text{kg} \cdot \text{m}^2 \cdot \text{sec}^2}{\text{sec}^2 \cdot \text{kg} \cdot \text{m}} = \text{m}$ = Head

The unit mass $\overline{m}$ of water is given by

$$\overline{m} = \overline{v} \cdot \rho_w \tag{A.1}$$

where $\overline{v}$ = specific volume $\left[\frac{m^3}{kg}\right]$ and ρ_w = density of water $\left[\frac{kg}{m^3}\right]$.

Since for water $\rho_w \sim 1$ and $\overline{v} \sim 1$, specific and volumetric potentials are numberically equal, i.e.:

$$\psi_{\left[\frac{\text{energy}}{\text{mass}}\right]} = \frac{1}{\rho_w} \cdot \psi_{\left[\frac{\text{energy}}{\text{volume}}\right]}$$

Usually the symbol ψ stands for a potential expressed in energy per unit mass, but often it is also used for a potential expressed in energy per unit volume. (Note that the quantities in Equations (2.4) through (2.6) are expressed in energy/mass, whereas the quantities in Equation (3.4) are expressed in energy/volume.)

In order to convert ψ in energy/mass into hydraulic head, one has to divide by the acceleration of gravity g.

Hence:

$$\frac{\psi}{g} = \frac{\left[\frac{\text{energy}}{\text{unit mass}}\right]}{g} = \frac{\left[\frac{\text{energy}}{\text{unit volume}}\right]}{\rho_w \cdot g} = \frac{\text{pressure}}{\rho_w \cdot g} = \text{hydraulic head}$$

$$= \left[\frac{\text{energy}}{\text{unit weight}}\right] \qquad \text{(A. 2)}$$

Table A.1: Relation Between Pressure Units

	atmosphere	bar	$\frac{\text{pounds}}{\text{sq. ft.}}$	$\frac{\text{pounds}}{\text{sq. in.}}$	$\frac{\text{tons}}{\text{sq. ft.}}$	$\frac{\text{kg}^*}{\text{sq. cm.}}$	mm Hg	cm H_2O
atmosphere	1.0	1.0133	2116.22	14.696	1.058	1.03323	760	1029.50
bar	0.9869	1.0	2088.50	14.503	1.044	1.0197	750.04	1016.01
lbs/sq. ft.	$4.725 \cdot 10^{-4}$	$4.788 \cdot 10^{-4}$	1.0	$6.9445 \cdot 10^{-3}$	$5 \cdot 10^{-4}$	$4.882 \cdot 10^{-4}$	0.359	0.4863
lbs/sq. in.	$6.805 \cdot 10^{-2}$	$6.895 \cdot 10^{-2}$	144.0	1.0	$7.20 \cdot 10^{-2}$	$7.031 \cdot 10^{-2}$	51.71	70.31
tons/sq. ft.	0.9451	0.9579	2000	13.8889	1.0	0.9765	718.39	972.92
kg^*/sq. cm	0.96784	0.9807	2048.16	14.223	1.024	1.0	735.46	996.39
mm Hg	$1.316 \cdot 10^{-3}$	$1.334 \cdot 10^{-3}$	2.785	$1.934 \cdot 10^{-2}$	$1.392 \cdot 10^{-3}$	$1.360 \cdot 10^{-3}$	1.0	1.3548
cm H_2O	$0.9713 \cdot 10^{-3}$	$0.984 \cdot 10^{-3}$	2.056	$1.421 \cdot 10^{-2}$	$1.0278 \cdot 10^{-3}$	$1.0036 \cdot 10^{-3}$	0.7382	1.0



Note: Use of table → x

for example: 1 pound/sq. ft. = $6.9445 \cdot 10^{-3}$ pounds/sq. in.

APPENDIX B

FLOW THROUGH POROUS MEDIA

Isothermal Single-Phase Flow

1. Darcy's Law

$$\left.\begin{aligned} v_x &= -K_x(h)\cdot\frac{\partial H}{\partial x} \\ v_y &= -K_y(h)\cdot\frac{\partial H}{\partial y} \\ v_z &= -K_z(h)\cdot\frac{\partial H}{\partial z} \end{aligned}\right\} \quad \text{or if: } K_x = K_y = K_z \qquad \text{(B. 1)}$$

$$v = -K(h)\cdot\nabla H$$

where ∇ is the vector $\left(\frac{\partial}{\partial x}, \frac{\partial}{\partial y}, \frac{\partial}{\partial z}\right)$

$$H = h + z \qquad \text{(B. 2)}$$

H is the hydraulic head

h is the soil water head

x, y, z are the space coordinates, z is positive upwards

v is the volume flux = volume of water through unit cross-sectional area of soil in unit time

K is the hydraulic conductivity (cm/sec)

If Darcy's law is written in terms of volumetric potentials (pressures) ψ, i.e.,

$$v = -K_p(h)\cdot\nabla\psi \qquad \text{(B. 3)}$$

then $K_p(h) = \frac{k}{\upsilon}$ (B. 4)

where: k = permeability and is a property of the soil alone (k is expressed in cm^2 or in Darcy (1 Darcy = $9.869 \cdot 10^{-9}$ cm^2).

υ = viscosity of the water (υ is expressed in $\frac{dyne \cdot sec}{cm^2}$ or Poise)
(1 Poise = $1 \frac{dyne \cdot sec}{cm^2}$).

The coefficient in the Darcy equation is therefore different depending if one uses the hydraulic head potential or the soil water potential ψ.

K depends on the water content of the soil and decreases rapidly as the water content decreases from saturation. This is due to the fact that the cross-sectional area available for flow decreases when the pores fill with air. K is also subjected to hysteresis effects for the same reasons as the suction. For a number of soils, K is given by the empirical function

$$K(h) = \frac{a}{h^{n_1} + b}, \quad a,\ b,\ n_1 \text{ constants} \qquad \text{(B. 5)}$$

2. Equation of Continuity

The equation of continuity expresses the conservation of mass. Consider an elemental cube in space (Figure B. 1). The fluxes are indicated by arrows. We assume that fluxes in the direction of the coordinate axis are positive.

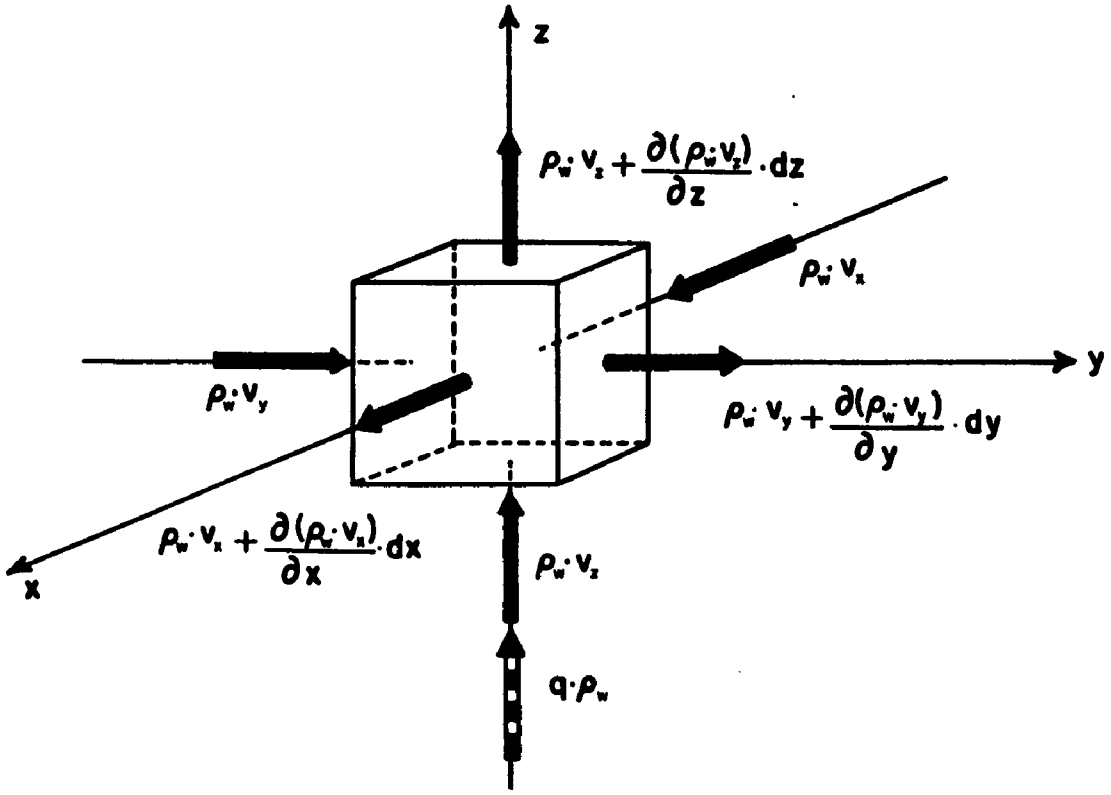


Figure B. 1. Derivation of the equation of Continuity

q denotes a possible source or sink term. If q points into the cube, one has a sink. If it comes out of the cube, one has a source term. In Figure B. 1 this q-term is shown only for the z-direction. One can now set up the mass balance:

$$\text{net inward mass flux: } -\left[\frac{\partial(\rho_w \cdot v_x)}{\partial x} + \frac{\partial(\rho_w \cdot v_y)}{\partial y} + \frac{\partial(\rho_w \cdot v_z)}{\partial z}\right] dx \cdot dy \cdot dz \qquad \text{(B. 6)}$$

source term contribution: $+ q(z)dx \cdot dy \cdot dz \cdot \rho_w$ (B.7)

The change of storage ΔSt which the elemental cube undergoes is

$$\Delta St = \Delta(\rho_w \cdot V_w) \tag{B.8}$$

where V_w is the volume of water in the elemental cube $dx \cdot dy \cdot dz$. The volumetric water content θ is defined by $\theta = \frac{V_w}{V_{tot}}$ where V_{tot} is the bulk volume of the cube.

Hence:

$$V_w = \theta \cdot V_{tot} = \theta \cdot dx \cdot dy \cdot dz \tag{B.9}$$

The rate of change of storage ΔSt is then (using Equation B.8)

$$\frac{\partial(\Delta St)}{\partial t} = \frac{\partial(\rho_w \cdot \theta)}{\partial t} dx \cdot dy \cdot dz \tag{B.10}$$

The rate of change of storage is equal to the net inward flux (Equation B.6).

Hence:
$$\frac{\partial(\rho_w \cdot \theta)}{\partial t} dx \cdot dy \cdot dz = -\left[\frac{\partial(\rho_w \cdot v_x)}{\partial x} + \frac{\partial(\rho_w \cdot v_y)}{\partial y} + \frac{\partial(\rho_w \cdot v_z)}{\partial z}\right] dx \cdot dy \cdot dz + q \cdot dx \cdot dy \cdot dz \cdot \rho_w \tag{B.11}$$

If the density of the water ρ_w is considered to be constant, which is a reasonable assumption, one obtains:

$$\frac{\partial \theta}{\partial t} = -\left[\frac{\partial v_x}{\partial x} + \frac{\partial v_y}{\partial y} + \frac{\partial v_z}{\partial z}\right] + q = -\nabla v + q \tag{B.12}$$

3. The Flow Equation

Combining Equation (B. 1) with Equation (B. 12) yields at once:

$$\nabla v = -\nabla [K(h) \cdot \nabla H] = q - \frac{\partial \theta}{\partial t}$$

or

$$\frac{\partial \theta}{\partial t} = \nabla [K(h) \cdot \nabla H] + q \qquad \text{(B. 13)}$$

(The source term q is omitted in the following discussion. It may be added any time, for example, to express the water uptake by plant roots.) Equation (B. 13) can be written as

$$\frac{\partial \theta}{\partial t} = \frac{\partial}{\partial x} [K(h) \cdot \frac{\partial H}{\partial x}] + \frac{\partial}{\partial y} [K(h) \cdot \frac{\partial H}{\partial y}] + \frac{\partial}{\partial z} [K(h) \cdot \frac{\partial H}{\partial z}] \qquad \text{(B. 14)}$$

In order to express everything in terms of hydraulic head H, one has to assume that the relation between θ and h is single-valued, i.e., no hysteresis effect. Then one may write:

$$\frac{\partial \theta}{\partial t} = \frac{\partial \theta}{\partial h} \cdot \frac{\partial h}{\partial t} = C(h) \cdot \frac{\partial h}{\partial t} \qquad \text{(B. 15)}$$

$$C(h) = \frac{\partial \theta}{\partial h}$$

C(h) is the slope of the soil water retention curve, and is called soil moisture capacity.

Now, since $\frac{\partial h}{\partial t} = \frac{\partial H}{\partial t}$, Equation (B. 14)takes the form

$$C(h)\cdot\frac{\partial H}{\partial t} = \frac{\partial}{\partial x}\left[K(h)\cdot\frac{\partial H}{\partial t}\right] + \frac{\partial}{\partial y}\left[K(h)\cdot\frac{\partial H}{\partial y}\right] + \frac{\partial}{\partial z}\left[K(h)\cdot\frac{\partial H}{\partial z}\right] \qquad (B.16)$$

One may also write this equation in terms of h:

$$C(h)\cdot\frac{\partial h}{\partial t} = \frac{\partial}{\partial x}\left[K(h)\cdot\frac{\partial h}{\partial x}\right] + \frac{\partial}{\partial y}\left[K(h)\cdot\frac{\partial h}{\partial y}\right] +$$

$$\frac{\partial}{\partial z}\left[K(h)\cdot\frac{\partial h}{\partial z} + K(h)\right] \qquad (B.17)$$

or in vector notation:

$$C(h)\cdot\frac{\partial h}{\partial t} = \nabla\left[K(h)\cdot\nabla h\right] + \frac{\partial K(h)}{\partial z} \qquad (B.18)$$

The flow equation can also be written in terms of the volumetric water content θ:

$$\frac{\partial\theta}{\partial t} = \frac{\partial}{\partial x}\left[K\frac{\partial h}{\partial\theta}\cdot\frac{\partial\theta}{\partial x}\right] + \frac{\partial}{\partial y}\left[K\frac{\partial h}{\partial\theta}\cdot\frac{\partial\theta}{\partial y}\right] + \frac{\partial}{\partial z}\left[K\frac{\partial h}{\partial\theta}\cdot\frac{\partial\theta}{\partial z}\right] + \frac{\partial K}{\partial\theta}\cdot\frac{\partial\theta}{\partial z}$$

$$\frac{\partial\theta}{\partial t} = \frac{\partial}{\partial x}\left[D(\theta)\cdot\frac{\partial\theta}{\partial x}\right] + \frac{\partial}{\partial y}\left[D(\theta)\cdot\frac{\partial\theta}{\partial y}\right] + \frac{\partial}{\partial z}\left[D(\theta)\cdot\frac{\partial\theta}{\partial z}\right] + \frac{\partial K}{\partial\theta}\cdot\frac{\partial\theta}{\partial z} \qquad (B.19)$$

or:

$$\frac{\partial\theta}{\partial t} = \nabla\left[D(\theta)\cdot\nabla\theta\right] + \frac{\partial K}{\partial\theta}\cdot\frac{\partial\theta}{\partial z} \qquad (B.20)$$

$$D = K\cdot\frac{\partial h}{\partial\theta} = \frac{K(h)}{C(h)} \qquad (B.21)$$

D is called the soil water diffusivity, since for horizontal flow where the gravity term $\frac{\partial K}{\partial z}$ is omitted, Equation (B. 19) becomes identical with the diffusion equation.

The diffusivity is also dependent on the soil water content, but it varies much less than the hydraulic conductivity does. For many soils the diffusivity can be related to the moisture content by an exponential function

$$D = D_o \cdot e^{\beta(\theta - \theta_o)} \tag{B. 22}$$

where D_o is the diffusivity when $\theta = \theta_o$ (initial condition) and β is a constant.

In cylindrical coordinates, for a system with cylindrical radial symmetry about a vertical axis, the flow equation becomes:

$$\frac{\partial \theta}{\partial t} = \frac{1}{r} \cdot \frac{\partial}{\partial r} \left(r \cdot D \cdot \frac{\partial \theta}{\partial r} \right) + \frac{\partial}{\partial z} \left(D \cdot \frac{\partial \theta}{\partial z} \right) - \frac{dK}{d\theta} \cdot \frac{\partial \theta}{\partial z} \tag{B. 23}$$

and for the special case of symmetrical radial flow

$$\frac{\partial \theta}{\partial t} = \frac{1}{r} \cdot \frac{\partial}{\partial r} \left(r \cdot D \cdot \frac{\partial \theta}{\partial r} \right) \tag{B. 24}$$

For saturated conditions $\frac{d\theta}{dt} = 0$, or C = 0 and $K = K_s$ = constant, hence Equation (B. 16) degenerates to the Laplace equation

$$\nabla^2 H = 0 \qquad \text{or:} \quad \frac{\partial^2 H}{\partial x^2} + \frac{\partial^2 H}{\partial y^2} + \frac{\partial^2 H}{\partial z^2} = 0 \tag{B. 25}$$

APPENDIX C

WATER CONTENT – DENSITY RELATIONS

1. Relation between Water Content by Weight and Water Content by Volume

Notation:

γ_{dry}	Bulk density or unit dry weight of soil
W_s	Weight of solids
W_w	Weight of soil water
V_s	Volume of solids
V_w	Volume of water in soil
V_a	Volume of air in soil
V_v	Volume of voids
e'	Void ratio
G_s	Specific gravity of soil material
γ_w	Density of water = 1 kg/dm^3 = 62.4 lbs/ft^3
w	Water content by weight
θ	Water content by volume
s	Degree of saturation

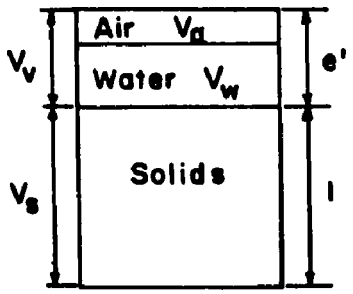


Figure C.1
Idealized three-phase soil system

$$e' = \frac{V_v}{V_s} \; ; \quad s = \frac{V_w}{V_v} \tag{C.1}$$

$$\gamma_{dry} = \frac{W_s}{V_s + V_v} = \frac{G_s \cdot \gamma_w}{1 + e'} \tag{C.2}$$

$$w = \frac{W_w}{W_s} \tag{C.3}$$

$$\theta = \frac{V_w}{V_s + V_v} = \frac{\frac{W_w}{\gamma_w}}{\frac{W_s}{\gamma_{dry}}} = \frac{W_w}{W_s} \cdot \frac{\gamma_{dry}}{\gamma_w} = w \cdot \frac{\gamma_{dry}}{\gamma_w} \tag{C.4}$$

(in metric units: $\theta = w \cdot \gamma_{dry}$)

2. Water Content – Density Relationships

$$w = \frac{e' \cdot s}{G_s} \tag{C.5}$$

$$\gamma_{dry} = \frac{G_s \cdot \gamma_w}{1 + \frac{G_s \cdot w}{s}} \tag{C.6}$$

For saturated soils: $s = 100\%$, hence $\gamma_{dry} = \frac{G_s \cdot \gamma_w}{1 + \frac{G_s \cdot w}{100}}$

(w in percent)

If Equation (C. 6) is solved in terms of w, one obtains

$$w = s \cdot \left(\frac{\gamma_w}{\gamma_{dry}} - \frac{1}{G_s} \right) \tag{C.7}$$

Using Equations (C. 4) and (C. 6) one can derive an expression for θ in terms of γ_{dry}

$$\theta = w \cdot \frac{\gamma_{dry}}{\gamma_w}; \qquad w = \frac{\theta}{\gamma_{dry}} \cdot \gamma_w$$

$$\gamma_{dry} = \frac{G_s \cdot \gamma_w}{1 + \frac{G_s \cdot \theta \cdot \gamma_w}{\gamma_{dry} \cdot s}} = \frac{G_s \cdot \gamma_w \cdot \gamma_{dry} \cdot s}{\gamma_{dry} \cdot s + G_s \cdot \theta \cdot \gamma_w}$$

$$\theta = (1 - \frac{\gamma_{dry}}{G_s \cdot \gamma_w}) \qquad \text{(C.8)}$$

APPENDIX D

SOIL MOISTURE MEASUREMENTS WITH TENSIOMETERS

1. Hydraulic Head Measurements with Tensiometers

The essential parts of a tensiometer with a mercury manometer are shown in Figure D.1. The form, size and arrangement of tensiometer parts can be varied considerably to suit individual requirements. Essential elements consist of a porous cup, a vacuum gage (Bourdon dial gage or mercury manometer), and a combined means for water filling and air removal. The walls of the porous cup should be as permeable as possible and still have an air entry value greater than 1 bar. This means that when the walls of the cup are saturated with deaired water, the cup should withstand an air pressure difference of more than 1 bar without leaking air.

Tensiometers are used to measure negative soil water heads, but they can also be used to measure small positive heads by adjusting the scale of the mercury manometer accordingly.

The hydraulic head is defined as (see Equation B.2):

$$H = h + z \qquad (D.1)$$

where h is the soil water head and z is the elevation head above a reference elevation.

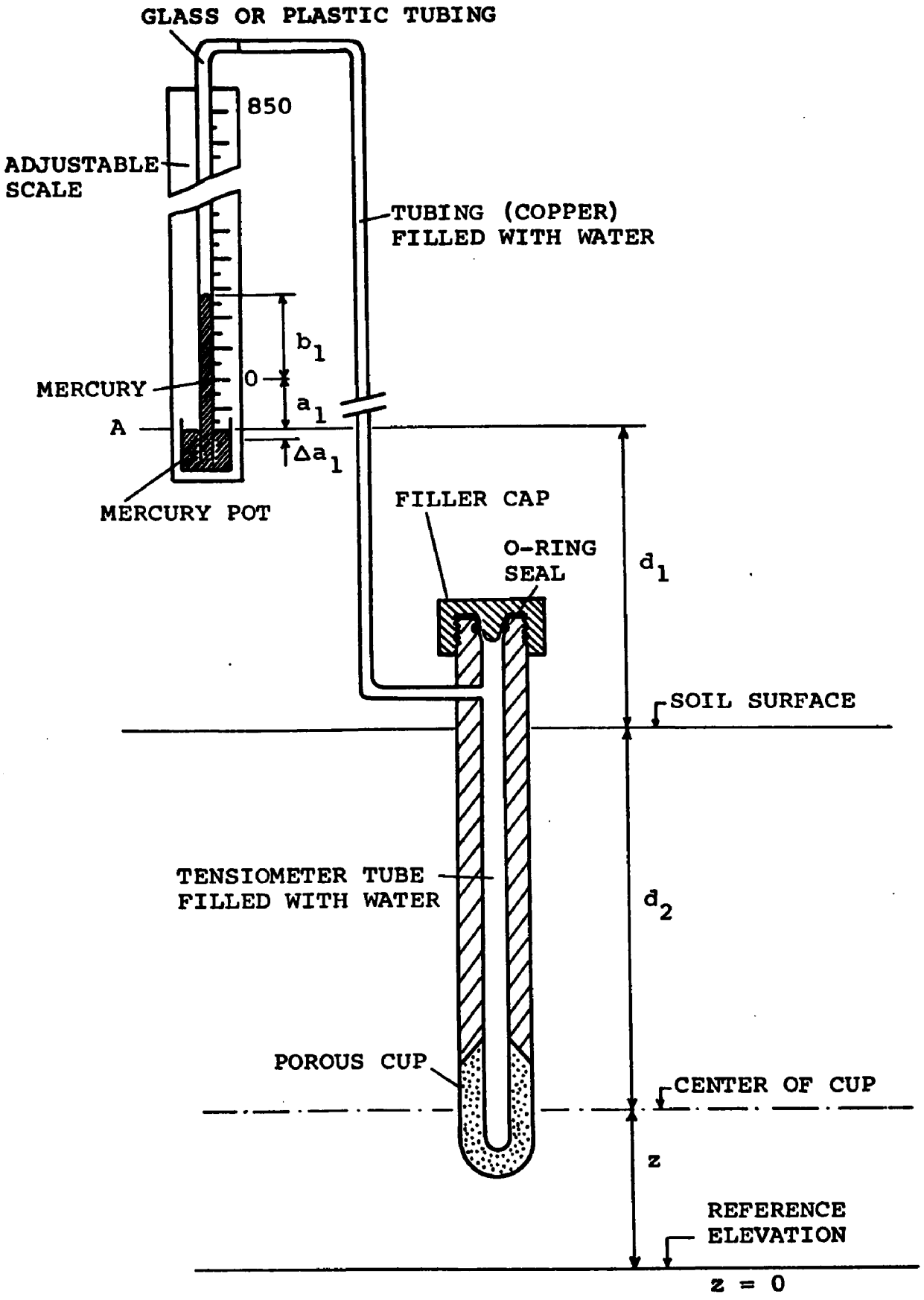


Figure D.1 Essential parts of a tensiometer and principles of measuring hydraulic heads.

Depending on how one positions initially the tensiometer scale, one can measure either hydraulic heads H or soil water heads h. The scale may be positioned to read zero opposite the mercury level of the manometer when any desired reference pressure or hydraulic head occurs at the cup. To read only the soil water head component (which is usually negative and then called suction), the reference elevation must be taken at the center of the cup. For hydraulic head readings, the scale zero is set to correspond to zero hydraulic head at some convenient elevation (such as the soil surface or the toe of a slope), and all tensiometers in a given system are zeroed to the same elevation.

Referring to Figure D. 1, we take the reference elevation at a distance z below the center of the porous cup.

The pressure at the surface of the mercury pot is atmospheric and hence zero, since atmospheric pressure is taken as the reference pressure. Assume that the system is in equilibrium and the hydraulic head H at the center of the cup is zero. Then by adding pressure increments through the system starting at point A (surface of the mercury pot) down to the reference elevation where z = 0, one obtains

$$\rho_{Hg} \cdot a'_1 + \Delta p'_{Hg\text{-}H_2O} - (a'_1 + d_1 + d_2 + z)\,\rho_w + 0 = 0$$

pressure

where ρ_{Hg} = density of mercury

ρ_w = density of water

$\Delta p'_{Hg\text{-}H_2O}$ = pressure difference across the mercury-water interface

Hence: $$a'_1 = \frac{(d_1 + d_2 + z)\ \rho_w - \Delta p'_{Hg\text{-}H_2O}}{(\rho_{Hg} - \rho_w)} \qquad (D.2)$$

(The prime for a_1 and later for b_1 is used when hydraulic heads with respect to a reference level not passing through the center of the cup should be measured.)

Now, if the reference elevation is to be set at the center of the porous cup, $z = 0$ and $H = h$, i.e., the scale can be set for suction measurements, Equation (D.2) becomes

$$a_1 = \frac{(d_1 + d_2)\ \rho_w - \Delta p'_{Hg\text{-}H_2O}}{(\rho_{Hg} - \rho_w)} \qquad (D.3)$$

(Note that $(d_1 + d_2)$ is a fixed distance for a given tensiometer.) $\Delta p'_{Hg\text{-}H_2O}$ is small and for practical purposes can be neglected. With $\rho_{Hg} = 13.55$ and $\rho_w = 1.0\ g/cm^3$, one obtains then

$$a_1 = \frac{(d_1 + d_2)}{12.55} \qquad (D.4)$$

If we want to measure now hydraulic heads with the scale zeroed for the reference elevation $z = 0$, we may proceed as previously by summing up pressure increments starting at the mercury surface which has been lowered by Δa_1 corresponding to a column rise equal to b_1:

$$(\Delta a'_1+a'_1+b'_1)\cdot\rho_{Hg}+\Delta p'_{Hg-H_2O}-(b'_1+a'_1+d_1+d_2+z)\cdot\rho_w+H\cdot\rho_w=0$$

since the hydraulic head at the center of the cup with respect to the reference elevation is H

Substituting Equation (D. 2) into the above relation, one obtains

$$(\Delta a'_1+b'_1)\cdot\rho_{Hg}-b'\cdot\rho_w=-H\cdot\rho_w$$

and

$$-H=\Delta a'_1\cdot\frac{\rho_{Hg}}{\rho_w}+b'_1\frac{(\rho_{Hg}-\rho_w)}{\rho_w} \qquad (D.5)$$

Δa_1 can be neglected usually, since if the pot diameter is 10 or more times the diameter of the mercury column, then Δa_1 is less than 1 percent of a_1 (Richards 1949). Equation (D. 5) then becomes

$$H_{(cm)}=-\frac{b'_1(\rho_{Hg}-\rho_w)}{\rho_w}=-b'_{(cm)}\cdot 12.55 \qquad (D.6)$$

A positive b'_1 means therefore a negative hydraulic head with respect to the reference elevation.

Again, if the center of the cup is taken as the reference elevation, Equation (D. 6) reads soil water heads ($z = 0$ and $H = h$). Equation (D. 6) is then

$$h=-\frac{b_1(\rho_{Hg}-\rho_w)}{\rho_w}=-b_1\cdot 12.55 \qquad (D.7)$$

If h is negative (suction), then b_1 is positive and vice versa. If a scale 8 cm = 100 mbar is chosen, one reads directly the soil water head in millibars.

For the case of the bin, all tensiometers were zeroed with respect to the center of the cup. This was done by putting the tensiometer into water with the porous cup immersed one-half way up. After the mercury column had assumed a stable position above the reservoir, the zero mark of the scale was set in line with the meniscus of the mercury in the manometer tubing. If during a rainstorm the meniscus fell below zero, it meant that positive pressures were present. Theoretically, the maximum possible positive pressure occurs when the whole profile is saturated.

Hence: Soil depth $\sim$ 25 cm

and

$1 \text{ cm } H_2O \sim 1$ millibar

$h_{max} = +25$ millibar, which would mean 2 cm below the zero mark.

2. Response Time

Tensiometers have a response time that is not zero because of the volume of water that must move into or out of the tensiometer to register a pressure change that occurs in the soil water. The response time depends primarily upon the gage sensitivity, the conductance of the porous cup and the hydraulic conductivity of the soil in which the tensiometer is placed (Klute and Gardner, 1962).

The cup conductance K_c has been defined (Richards, 1949) as the volume of water passing through the cup wall per unit time and per unit of pressure difference. It is usually in the range between 0.1 to 10 $cm^3/min \cdot bar$.

Hence one may write for K_c

$$K_c = \frac{1}{\tau} \cdot \frac{d\bar{q}}{dt} \qquad (D.8)$$

where $\frac{d\bar{q}}{dt}$ is the number of cm^3 of water per minute passing through a tensiometer cup submerged in water and τ is the gage reading in bars (suction).

The gage sensitivity has been defined as the change in gage reading per unit volume change by fluid transferred to or from the tensiometer

$$S_g = \frac{d\tau}{d\bar{q}} \qquad (D.9)$$

and may be expressed in bars per cm^3.

The response-time constant

$$t_R = \frac{1}{K_c \cdot S_g}$$

is a measure of the over-all responsiveness of the instrument to a change of soil moisture tension at the cup surface. Combining Equation (D.8) with Equation (D.9) gives

$$\frac{d\tau}{\tau} = -K_c \cdot S_g \cdot dt \qquad (D.10)$$

Integration of Equation (D. 10) yields

$$\tau = \tau_o \cdot e^{-K_c \cdot S_g \cdot t} \qquad \text{(D. 11)}$$

If a tensiometer is completely filled with water and evaporation from the porous cup has brought the gage to a reading of τ_o bars, then the gage reading after submergence of the cup in water is given by Equation (D. 11) (Richards, 1949), where t is the time of submergence in minutes.

If the tensiometer cup is brought into contact with soil, we may write instead of Equation (D. 8)

$$\frac{d\bar{q}}{dt} = K_c (\tau_{soil} - \tau_{cup}) \qquad \text{(D. 12)}$$

where τ_{soil} is the soil suction just outside the cup in the soil water and τ_{cup} is the suction in the tensiometer.

One may write Equation (D. 12) as

$$\frac{1}{K_c} \cdot \frac{d\bar{q}}{d\tau_{cup}} \cdot \frac{d\tau_{cup}}{dt} = \tau_{soil} - \tau_{cup} \qquad \text{(D. 13)}$$

From Equation (D. 9)

$$\frac{d\tau_{cup}}{d\bar{q}} = S_g \quad \text{and} \quad \frac{1}{K_c \cdot S_g} = t_R$$

Hence Equation (D. 13) becomes

$$t_R \cdot \frac{d\tau_{cup}}{dt} = \tau_{soil} - \tau_{cup} \qquad (D.14)$$

Klute and Gardner (1962) have solved Equation (D. 14) in terms of τ_{cup} for a periodically fluctuating suction τ_{soil} (just outside the tensiometer cup) and found that the difference between τ_{cup} and τ_{soil} is very small compared to the suction values measured. However, when the soil suction is in the upper part of the tensiometer range, the rate of transfer of water in the soil (i. e., the hydraulic conductivity) will tend to determine the overall response of a tensiometer, which might become quite large.

If the soil is not limiting, then Equation (D. 14) can also be used to compute the time for a tensiometer to come to equilibrium with the soil when it is flushed out, or is otherwise initially at some suction τ_i other than that in the surrounding soil. Integration of Equation (D. 14) gives:

$$\frac{d\,\tau_{cup}}{\tau_{cup} - \tau_{soil}} = \frac{dt}{t_R}$$

$$\ln (\tau_{cup} - \tau_{soil}) = -\frac{t}{t_R} + \text{const.}$$

For $t = 0$: $\tau_{cup} = \tau_i$

hence: $\ln(\tau_i - \tau_{soil}) = 0 + \text{const.} \longrightarrow \text{const.} = \ln(\tau_i - \tau_{soil})$

$$\ln\left(\frac{\tau_{cup} - \tau_{soil}}{\tau_i - \tau_{soil}}\right) = \frac{-t}{t_R}$$

$$t = t_R \cdot \ln\left(\frac{\tau_i - \tau_{soil}}{\tau_{cup} - \tau_{soil}}\right) \qquad \text{(D.15)}$$

REFERENCES

Aitchison, G. D. (Statement of The Review Panel), (1965), "Engineering Concepts of Moisture Equilibria and Moisture Changes in Soils," Moisture Equilibria and Moisture Changes in Soils Beneath Covered Areas, a Symposium in Print, G. D. Aitchison, ed., Butterworths, Australia, pp. 7-21.

Ashcroft, G. et al. (1962), "Numerical Method for Solving the Diffusion Equation: I. Horizontal Flow in Semi-Infinite Media," Proceedings, Soil Science Society of America, Vol. 26, No. 6, pp. 522-525.

Babcock, K. L. (1963), "Theory of the Chemical Properties of Soil Colloidal Systems at Equilibrium," Hilgardia, Vol. 34, No. 11, August, pp. 417-542.

Bethlahmy, N. (1962), "First Year Effects of Timber Removal on Soil Moisture," Int. Association of Scientific Hydrology, Bulletin, Vol. 7, No. 2, pp. 34-38.

Bishop, D. M. and Stevens, M. E. (1964), "Landslides on Logged Areas in Southeast Alaska, U. S. Forest Service Research Paper NOR-1, U. S. Department of Agriculture, Juneau, Alaska, 17 pp.

Biswas, T. D., Nielsen, D. R., and Biggar, J. W. (1966), "Redistribution of Soil Water after Infiltration," Water Resources Research, Vol. 2, No. 3, pp. 513-524.

Bolt, G. H. and Miller, R. D. (1958), "Calculation of Total and Component Potentials of Water in Soil," Transactions, American Geophysical Union, Vol. 39, No. 5, pp. 917-928.

Bormann, F. H. et al. (1968), "Nutrient Loss Accelerated by Clear-Cutting of a Forest Ecosystem," Science, Vol. 159, No. 3817, pp. 882-884.

Boyer, J. S. (1967), "Leaf Water Potentials Measured with a Pressure Chamber," Plant Physiology, Vol. 42, No. 1, pp. 133-137.

Bresler, E., Kemper, W. D., and Hanks, R. J. (1969), "Infiltration, Redistribution, and Subsequent Evaporation of Water from Soil as Affected by Wetting Rate and Hysteresis," Proceedings, Soil Science Society of America, Vol. 33, No. 6, pp. 832-840.

Brown, G. W. and Krygier, J. T. (1970), "Effects of Clear-Cutting on Stream Temperature," Water Resources Research, Vol. 6, No. 4, pp. 1133-1139.

Bybordi, M. (1969), "The Vertical Movement of Water in Stratified Porous Material, 2. Transient Stages of Drainage to a Water Table," Water Resources Research, Vol. 5, No. 3, pp. 694-697.

Childs, E. C. (1967), "Soil Moisture Theory," Advances in Hydroscience, Ven Te Chow, ed., Vol. 4, Academic Press Inc., New York, pp. 73-117.

Childs, E. C. (1969), An Introduction to The Physical Basis of Soil Water Phenomena, a Wiley-Interscience Publication, John Wiley & Sons, Ltd., 493 pp.

Childs, E. C. and Bybordi, M. (1969), "The Vertieal Movement of Water in Stratified Porous Material, 1. Infiltration," Water Resources Research, Vol. 5, No. 2, pp. 446-459.

Cowan, I. R. (1965), "Transport of Water in the Soil-Plant-Atmosphere System," The Journal of Applied Ecology, Vol. 2, No. 1, pp. 221-239.

Day, P. R. and Luthin, J.N. (1956), "A Numerical Solution of the Differential Equation of Flow for a Vertical Drainage Problem," Proceedings, Soil Science Society of America, Vol. 20, No. 4, pp. 443-447.

Dyrness, C. T. (1967), "Mass-Soil Movements in the H.J. Andrews Experimental Forest," U.S. Forest Service, Research Paper PNW-42, U.S. Department of Agriculture, Portland, Oregon, 12 pp.

Ehlig, C. F. and Gardner, W. R. (1964), "Relationship Between Transpiration and the Internal Water Relations of Plants," Agronomy Journal, Vol. 56, No. 2, pp. 127-130.

Esau, K. (1953), Plant Anatomy, John Wiley & Sons, Inc., New York, 735 pp.

Freeze, R. A. (1969), "The Mechanism of Natural Groundwater Recharge and Discharge, Part 1, One-Dimensional, Vertical, Unsteady, Unsaturated Flow above a Recharging or Discharging Groundwater Flow System," Water Resources Research, Vol. 5, No. 1, pp. 153-171.

Freeze, R. A. and Banner, J. (1970), "The Mechanism of Natural Ground-Water Recharge and Discharge, 2. Laboratory Column Experiments and Field Measurements," Water Resources Research, Vol. 6, No. 1, pp. 138-155.

Gardner, W. R. (1958a), "Some Steady-State Solutions of the Unsaturated Moisture Flow Equation with Application to Evaporation from a Water Table," Soil Science, Vol. 85, pp. 228-232.

Gardner, W. R. (1958b), "Mathematics of Isothermal Water Conduction in Unsaturated Soil," Highway Research Board, Special Report 40, Water and Its Conduction in Soils, Washington D. C., pp. 78-87.

Gardner, W. R. (1959), "Solutions of the Flow Equation for the Drying of Soils and Other Porous Media," Proceedings, Soil Science Society of America, Vol. 23, No. 3, pp. 183-187.

Gardner, W. R. (1960), "Dynamic Aspects of Water Availability to Plants," Soil Science, Vol. 89, No. 2, pp. 63-73.

Gardner, W. R. (1961), "Soil Suction and Water Movement," Conference on Pore Pressure and Suction in Soils, London, 1960, Butterworths, London, pp. 137-140.

Gardner, W. R. (1962a) "Approximate Solution of a Non-Steady-State Drainage Problem," Proceedings, Soil Science Society of America, Vol. 26, No. 2, pp. 129-132.

Gardner, W.R. (1962b), "Note on the Separation and Solution of Diffusion Type Equations," Proceedings, Soil Science Society of America, Vol. 26, No. 4, p. 404.

Gardner, W.R. (1964), "Relation of Root Distribution to Water Uptake and Availablity," Agronomy Journal, Vol. 56, No. 1, pp. 41-45.

Gardner, W.R. (1968), "Availability and Measurement of Soil Water," Water Deficits and Plant Growth, T.T. Kozlowski, ed., Vol. 1, Academic Press Inc., New York, pp. 107-135.

Gardner, W.R. and Mayhugh, M.S. (1958), "Solutions and Tests of the Diffusion Equation for the Movement of Water in Soil," Proceedings, Soil Science Society of America, Vol. 22, No. 3, pp. 197-201.

Gardner, W.R. and Ehlig, C.F. (1962a), "Some Observations on the Movement of Water to Plant Roots," Agronomy Journal, Vol. 54, No. 5, pp. 453-456.

Gardner, W.R. and Ehlig, C.F. (1962b), "Impedance to Water Movement in Soil and Plant," Science, Vol. 138, No. 3539, pp. 522-523.

Gardner, W.R. and Hillel, D.I. (1962), "The Relation of External Evaporative Conditions to the Drying of Soils," Journal of Geophysical Research, Vol. 67, No. 11, pp. 4319-4325.

Gardner, W.R. and Ehlig, C.F. (1963), "The Influence of Soil Water on Transpiration by Plants," Journal of Geophysical Research, Vol. 68, No. 20, pp. 5719-5724.

Gardner, W.R., Hillel, D.I., and Benyamini, Y. (1970a), "Post-Irrigation Movement of Soil Water, 1. Redistribution," Water Resources Research, Vol. 6, No. 3, pp. 851-861.

Gardner, W.R., Hillel, D.I., and Benyamini, Y. (1970b), "Post-Irrigation Movement of Soil Water, 2. Simultaneous Redistribution and Evaporation," Water Resources Research, Vol. 6, No. 4, pp. 1148-1153.

Gray, D.H. (1971), "Effect of Forest Clear-Cutting on the Stability of Natural Slopes," Bulletin of Assoc. of Engineering Geologists, Vol. 2, No. 1 (in press).

Green, D. et al. (1970), "Numerical Modeling of Unsaturated Groundwater Flow and Comparison of the Model to a Field Experiment," Water Resources Research, Vol. 6, No. 3, pp. 862-874.

Green, W.H. and Ampt, G.A. (1911), "Studies in Soil Physics, I. The Flow of Air and Water Through Soils," The Journal of Agricultural Science, Vol. 4, Part 1, pp. 1-24.

Guymon, G.L. (1970), "A Finite Element Solution of the One-Dimensional Diffusion-Convection Equation," Water Resources Research, Vol. 6, No. 1, pp. 204-210.

Hanks, R.J. and Bowers, S.A. (1962), "Numerical Solution of the Moisture Flow Equation for Infiltration into Layered Soil," Proceedings, Soil Science Society of America, Vol. 26, No. 6, pp. 530-534.

Hanks, R.J., Klute, A., and Bresler, E. (1969), "A Numeric Method for Estimating Infiltration, Redistribution, Drainage, and Evaporation of Water from Soil," Water Resources Research, Vol. 5, No. 5, pp. 1064-1069.

Hewlett, J.D. (1961a), "Soil Moisture as a Source of Base Flow from Steep Mountain Watersheds," Station Paper No. 132, Southeastern Forest Experiment Station, U.S. Department of Agriculture, Asheville, North Carolina, 11 pp.

Hewlett, J.D. (1961b), "Some Ideas about Storm Runoff and Baseflow," Report for 1961, U.S. Department of Agriculture, Forest Service, Southeastern Forest Experiment Station, Asheville, North Carolina, pp. 61-66.

Hewlett, J.D. and Hibbert, A.R. (1961), "Increases in Water Yield after Several Types of Forest Cutting," Int. Association of Scientific Hydrology, Bulletin, Vol. 6, No. 3, pp. 5-17.

Hewlett, J.D. and Hibbert, A.R. (1963), "Moisture and Energy Conditions within a Sloping Soil Mass during Drainage." Journal of Geophysical Research, Vol. 68, No. 4, pp. 1081-1087.

Hewlett, J.D. and Hibbert, A.R. (1967), "Factors Affecting the Response of Small Watersheds to Precipitation in Humid Areas," International Symposium on Forest Hydrology, W.E. Sopper and H.W. Lull, ed., Pergamon Press Ltd., pp. 275-290.

Hewlett, J. D. and Nutter, W. L. (1969), An Outline of Forest Hydrology, University of Georgia Press, Athens, Georgia, 137 pp.

Hewlett, J. D. and Helvey, J. D. (1970), "Effects of Forest Clear-Felling on the Storm Hydrograph," Water Resources Research, Vol. 6, No. 3, pp. 768-782.

Hibbert, A. R. (1969), "Water Yield Changes after Converting a Forested Catchment to Grass," Water Resources Research, Vol. 5, No. 3, pp. 634-640.

van den Honert, T. H. (1948), "Water Transport in Plants as a Catenary Process," Discussions of the Faraday Society, No. 3, pp. 146-153.

Hoover, M. D., Olson, D. F., and Greene, G. E. (1953), "Soil Moisture under a Young Loblolly Pine Plantation," Proceedings, Soil Science Society of America, Vol. 17, No. 2, pp. 147-150.

Hoover, M. D., Olson, D. F., Jr., and Metz, L. J. (1954), "Soil Sampling for Pore Space and Percolation," Station Paper No. 42, U. S. Department of Agriculture, Forest Service, Southeastern Forest Experiment Station, Asheville, North Carolina, 29 pp.

Hornbeck, J. W., Pierce, R. S., and Federer, C. A. (1970), "Streamflow Changes after Forest Clearing in New England," Water Resources Research, Vol. 6, No. 4, pp. 1124-1132.

Hornberger, G. M., Remson, I., and Fungaroli, A. A. (1969), "Numeric Studies of a Composite Soil Moisture Ground-Water System," Water Resources Research, Vol. 5, No. 4, pp. 797-802.

Homberger, G. M. and Remson, I. (1970), "A Moving Boundary Model of a One-Dimensional Saturated-Unsaturated, Transient Porous Flow System," Water Resources Research, Vol. 6, No. 3, pp. 898-905.

Ibrahim, H. A. and Brutsaert, W. (1968), "Intermittent Infiltration into Soils with Hysteresis," Journal of the Hydraulics Division, American Society of Civil Engineers, Vol. 94, No. HY1, pp. 113-137.

Kaufmann, M. R. (1968), "Evaluation of the Pressure Chamber Technique for Estimating Plant Water Potential of Forest Tree Species," Forest Science, Vol. 14, No. 4, pp. 369-374.

Klute, A. (1952a), "A Numerical Method for Solving the Flow Equation for Water in Unsaturated Materials," Soil Science, Vol. 73, No. 2, pp. 105-116.

Klute, A. (1952b), "Some Theoretical Aspects of the Flow of Water in Unsaturated Soils," Proceedings, Soil Science Society of America, Vol. 16, No. 2, pp. 144-148.

Klute, A. (1965), "Laboratory Measurement of Hydraulic Conductivity of Saturated Soil," Methods of Soil Analysis, C.A. Black, ed., Part 1, No. 9 in the series Agronomy American Society of Agronomy, Inc., Madison, Wisconsin, pp. 210-221.

Klute, A. and Gardner, W. R. (1962), "Tensiometer Response Time," Soil Science, Vol. 93, No. 3, pp. 204-207.

Klute, A., Whisler, F. D., and Scott, E.J. (1965), "Numerical Solution of the Nonlinear Diffusion Equation for Water Flow in a Horizontal Soil Column of Finite Length," Proceedings, Soil Science Society of America, Vol. 29, No. 4, pp. 353-358.

Klute, A., Scott, E.J., and Whisler, F. D. (1965), "Steady State Water Flow in a Saturated Inclined Soil Slab," Water Resources Research, Vol. 1, No. 2, pp. 287-294.

Kramer, P.J. (1952), "Plant and Soil Water Relations on the Watershed," Journal of Forestry, Vol. 50, No. 2, pp. 92-95.

Kramer, P.J. (1969), Plant and Soil Water Relationships, McGraw-Hill Book Co., 482 pp.

Lewis, D.C. (1968), "Annual Hydrologic Response to Watershed Conversion from Oak Woodland to Annual Grassland," Water Resources Research, Vol. 4, No. 1, pp. 59-72.

Liakopoulos, A.C. (1965a), "Theoretical Solution of the Unsteady Unsaturated Flow Problems in Soils," Int. Association of Scientific Hydrology, Bulletin, Vol. 10, No. 1, pp. 5-39.

Liakopoulos, A.C. (1965b), "Retention and Distribution of Moisture in Soils after Infiltration has Ceased," Int. Association of Scientific Hydrology, Bulletin, Vol. 10, No. 2, pp. 58-69.

Luthin, J.N. and Day, P.R. (1955), "Lateral Flow Above a Sloping Water Table," Proceedings, Soil Science Society of America, Vol. 19, No. 4, pp. 406-410.

Metz, L.J. and Douglass, J. E. (1959), "Soil Moisture Depletion under Several Piedmont Cover Types," Technical Bulletin No. 1207, U.S. Department of Agriculture, Forest Service, September, 23 pp.

Meyer, B.S., Anderson, D.B., and Böhning, R.H. (1960), Introduction to Plant Physiology, D. Van Nostrand Co., Inc., Princeton, N.J., 541 pp.

Molz, F.J. et al. (1968), "Soil Moisture Availability for Transpiration," Water Resources Research, Vol. 4, No. 6, pp. 1161-1169.

Molz, F.J. and Remson, I. (1970), "Extraction Term Models of Soil Moisture Use by Transpiring Plants," Water Resources Research, Vol. 6, No. 5, pp. 1346-1356.

Monteith, J. L. (1965), "Evaporation and Environment," Symposia of the Society for Experimental Biology, No. 19, The State and Movement of Water in Living Organisms, Academic Press Inc., New York, pp. 205-234.

Northen, H.T. (1968), Introductory Plant Science, 3rd ed., The Ronald Press Company, 586 pp.

Patric, J. H., Douglas, J. E., and Hewlett, J. D. (1965), "Soil Water Absorption by Mountain and Piedmont Forests," Proceedings, Soil Science Society of America, Vol. 29, No. 3, pp. 303-308.

Penman, H.L. (1948), "Natural Evaporation from Open Water, Bare Soil and Grass," Proceedings of the Royal Society, Series A, Vol. 193, No. 1032, pp. 120-145.

Philip, J. R. (1957a), "The Theory of Infiltration: 1. The Infiltration Equation and Its Solution," Soil Science, Vol. 83, pp. 345-357.

Philip, J. R. (1957b), "The Theory of Infiltration: 2. The Profile of Infinity," Soil Science, Vol. 83, pp. 435-448.

Philip, J. R. (1957c), "The Theory of Infiltration: 3. Moisture Profiles and Relation to Experiment," Soil Science, Vol. 84, pp. 163-178.

Philip, J. R. (1957d), "The Theory of Infiltration: 4. Sorptivity and Algebraic Infiltration Equations," Soil Science, Vol. 84, pp. 257-264.

Philip, J. R. (1957e), "The Theory of Infiltration: 5. The Influence of the Initial Moisture Content," Soil Science, Vol. 84, pp. 329-339.

Philip, J. R. (1957f), "Remarks on the Analytical Derivation of the Darcy Equation," Transactions, Americal Geophysical Union, Vol. 38, No. 5, pp. 782-784.

Philip, J. R. (1958a), "The Theory of Infiltration: 6. Effect of Water Depth Over Soil," Soil Science, Vol. 85, pp. 278-286.

Philip, J. R. (1958b), "The Theory of Infiltration: 7," Soil Science, Vol. 85, pp. 333-337.

Philip, J. R. (1958c), "Physics of Water Movement in Porous Solids," Highway Research Board, Special Report 40, Water and Its Conduction in Soils, Washington, D. C., pp. 147-163.

Philip, J. R. (1969), "Theory of Infiltration," Advances in Hydroscience, Ven Te Chow, ed., Vol. 5, Academic Press Inc., New York, pp. 215-296.

Rabinowicz, E. (1970), An Introduction to Experimentation, Addison-Wesley Publishing Company, 124 pp.

Ray, P. M. (1963), The Living Plant, Modern Biology Series, Holt, Rinehart and Winston, New York, 127 pp.

Reeve, R. C. (1965), "Hydraulic Head," Methods of Soil Analysis, C. A. Black, ed., Part 1, No. 9 in the series Agronomy, American Society of Agronomy, Inc., Madison, Wisconsin, pp. 180-196.

Reinhart, K.G. (1964), "Effect of a Commercial Clearcutting in West Virginia on Overland Flow and Storm Runoff," Journal of Forestry, Vol. 62, No. 3, pp. 167-171.

Reisenauer, A.E. (1963), "Methods for Solving Problems of Multidimensional, Partially Saturated Steady Flow in Soils," Journal of Geophysical Research, Vol. 68, No. 20, pp. 5725-5733.

Remson, I., Drake, R.L., McNeary, S.S., and Wallo, E.M. (1965), "Vertical Drainage of an Unsaturated Soil," Journal of the Hydraulics Division, American Society of Civil Engineers, Vol. 91, No. HY1, pp. 55-74.

Remson, I., Fungaroli, A.A., and Hornberger, G.M. (1967), "Numerical Analysis of Soil-Moisture Systems," Journal of the Irrigation and Drainage Division, American Society of Civil Engineers, Vol. 93, No. IR3, pp. 153-166.

Richards, L.A. (1949), "Methods of Measuring Soil Moisture Tension," Soil Science, Vol. 68, No. 1, pp. 95-110.

Richards, L.A. (1965), "Physical Conditions of Water in Soil," Methods of Soil Analysis, C.A. Black, ed., Part 1, No. 9 in the series Agronomy, American Society of Agronomy, Inc., Madison, Wisconsin, pp. 128-152.

Richards, S.J. (1965), "Soil Suction Measurements with Tensiometers," Methods of Soil Analysis, C.A. Black, ed., Part 1, No. 9 in the series Agronomy, American Society of Agronomy, Inc., Madison, Wisconsin, pp. 153-163.

Rubin, J. (1966), "Theory of Rainfall Uptake by Soils Initially Drier Than Their Field Capacity and Its Applications," Water Resources Research, Vol. 2, No. 4, pp. 739-749.

Rubin, J. (1967), "Numerical Method for Analyzing Hysteresis-Affected, Post-Infiltration Redistribution of Soil Moisture," Proceedings, Soil Science Society of America, Vol. 31, No. 1, pp. 13-20.

Rubin, J. (1968), "Theoretical Analysis of Two-Dimensional, Transient Flow of Water in Unsaturated and Partly Unsaturated Soils," Proceedings, Soil Science Society of America, Vol. 32. No. 5, pp. 607-615.

Rubin, J., and Steinhardt, R. (1963), "Soil Water Relations During Rain Infiltration: I. Theory," Proceedings, Soil Science Society of America, Vol. 27, No. 3, pp. 246-251.

Rubin, J., Steinhardt, R., and Reiniger, P. (1964), "Soil Water Relations During Rain Infiltration: II. Moisture Content Profiles During Rains of Low Intensities," Proceedings, Soil Science Society of America, Vol. 28, No. 1, pp. 1-5.

Rubin, J. and Steinhardt, R. (1964), "Soil Water Relations During Rain Infiltration: III. Water Uptake at Incipient Ponding," Proceedings, Soil Science Society of America, Vol. 28, No. 5, pp. 614-619.

Rutter, A.J. (1968), "Water Consumption by Forests," Water Deficits and Plant Growth, T.T. Kozlowski, ed., Vol. 2, Academic Press Inc., New York, pp. 23-84.

Scholander, P. F. et al. (1965), "Sap Pressure in Vascular Plants," Science, Vol. 148, No. 3668, pp. 339-346.

Scott, E.J. and Hanks, R.J. (1962), "Solution of the One-Dimensional Diffusion Equation for Exponential and Linear Diffusivity Functions by Power Series Applied to Moisture Flow in Soils," Soil Science, Vol. 94, No. 5, pp. 314-322.

Sellers, W.D. (1965), Physical Climatology, University of Chicago Press, Chicago, Illinois, 272 pp.

Slatyer, R.O. (1967), Plant-Water Relationships, Academic Press, Ltd., London, 366 pp.

Slatyer, R.O. and Gardner, W.R. (1965), "Overall Aspects of Water Movement in Plants and Soils," Symposia of the Society for Experimental Biology, No. 19, The State and Movement of Water in Living Organisms, Academic Press Inc., New York, pp. 113-129.

Staple, W.J. (1966), "Infiltration and Redistribution of Water in Vertical Columns of Loam Soil," Proceedings, Soil Science Society of America, Vol. 30, No. 5, pp. 553-558.

Staple, W.J. (1969), "Comparison of Computed and Measured Moisture Redistribution Following Infiltration," Proceedings, Soil Science Society of America, Vol. 33, No. 6, pp. 840-847.

Sutcliffe, J. (1968), Plants and Water, The Institute of Biology's Studies in Biology No. 14, Edward Arnold, Ltd., London, 81 pp.

Tanner, C. B. (1968), "Evaporation of Water from Plants and Soil," Water Deficits and Plant Growth, T. T. Kozlowski, ed., Vol. 1, Academic Press Inc., New York, pp. 73-106.

Taylor, S. A. (1968), "Terminology in Plant and Soil Water Relations," Water Deficits and Plant Growth, T. T. Kozlowski, ed., Vol. 1, Academic Press Inc., New York, pp. 49-72.

Ter Stepanian, G. (1963), "On the Long-Term Stability of Slopes," Publication No. 52, Norwegian Geotechnical Institute, Oslo, Norway, 27 pp.

Vasquez, R. and Taylor, S. A. (1958), "Simulated Root Distribution and Water Removal Rates from Moist Soil," Proceedings, Soil Science Society of America, Vol. 22, No. 2, pp. 106-110.

Visser, W. C. (1966), "Progress in the Knowledge About the Effect of Soil Moisture Content on Plant Production," Inst. Land Water Management, Wageningen, Netherlands, Techn. Bulletin, 45.

Wang, F. C., Hassan, N. A., and Franzini, J. B. (1964), "A Method of Analyzing Unsteady, Unsaturated Flow in Soils," Journal of Geophysical Research, Vol. 69, No. 12, pp. 2569-2577.

Wang, F. C. and Lakshminarayana, V. (1968), "Mathematical Simulation of Water Movement Through Unsaturated Nonhomogeneous Soils," Proceedings, Soil Science Society of America, Vol. 32, No. 3, pp. 329-334.

Waring, R. H. and Cleary B. D. (1967), "Plant Moisture Stress: Evaluation by Pressure Bomb," Science, Vol. 155, No. 3767, pp. 1248-1254.

Whisler, F. D. (1969), "Analyzing Steady-State Flow in an Inclined Soil Slab with an Electric Analog," Proceedings, Soil Science Society of America, Vol. 33, No. 1, pp. 19-25.

Whisler, F.D. and Klute, A. (1965), "The Numerical Analysis of Infiltration, Considering Hysteresis, Into a Vertical Soil Column at Equilibrium Under Gravity," Proceedings, Soil Science Society of America, Vol. 29, No. 5, pp. 489-494.

Whisler, F.D., Klute, A., and Millington, R.J. (1968), "Analysis of Steady-State Evapotranspiration from a Soil Column," Proceedings, Soil Science Society of America, Vol. 32, No. 2, pp. 167-174.

Whisler, F.D. and Bouwer, H. (1970), "Comparison of Methods for Calculating Vertical Drainage and Infiltration for Soils," Journal of Hydrology, Vol. 10, No. 1, pp. 1-19.

Whisler, F.D., Klute, A., and Millington, R.J. (1970), "Analysis of Steady-State Solution and Solute Flow," Proceedings, Soil Science Society of America, Vol. 34, No. 3, pp. 382-386.

Wisler, C.O. and Brater, E.F. (1959), Hydrology, 2nd ed., John Wiley & Sons, Inc., 408 pp.

Woo, K.B., Boersma, L., and Stone, L.N. (1966), "Dynamic Simulation Model of the Transpiration Process," Water Resources Research, Vol. 2, No. 1, pp. 85-97.

Youngs, E.G. (1957), "Moisture Profiles During Vertical Infiltration," Soil Science, Vol. 84, pp. 283-290.

Youngs, E.G. (1958a), "Redistribution of Moisture in Porous Materials After Infiltration: 1," Soil Science, Vol. 86, pp. 117-125.

Youngs, E.G. (1958b), "Redistribution of Moisture in Porous Materials After Infiltration: 2," Soil Science, Vol. 86, pp. 202-207.

Zahner, R. (1967), "Refinement in Empirical Functions for Realistic Soil-Moisture Regimes Under Forest Cover," International Symposium on Forest Hydrology, W.E. Sopper and H.W. Lull, eds., Pergamon Press, Ltd., pp. 261-274.

Zimmermann, M.H. (1964), "Sap Movements in Trees," Biorheology, Vol. 2, No. 1, pp. 15-27.

Zinke, P.J. (1959), "The Influence of a Stand of Pinus Coulteri on the Soil Moisture Regime of a Large San Dimas Lysimeter in Southern California," Int. Association of Scientific Hydrology, Publication No. 49, Symposium of Hannoversch-Münden, Vol. 2, Lysimeters, pp. 126-138.